Doctoral Program in Molecular and Cellular Biology

In vitro methods of biopharmaceutical evaluation in the blood-brain barrier

---

Bárbara Sánchez Dengra

Thesis supervisor

Dr. María del Val Bermejo Sanz

Thesis cosupervisor

Dr. Marta González Álvarez

Universidad Miguel Hernández de Elche

2022

According to the Regulations for Doctoral Studies approved by virtue of the Royal Decree 99/2011 of January 28, this doctoral thesis entitled "*In vitro* methods of biopharmaceutical evaluation in the blood-brain barrier" is presented under the modality of **thesis by compendium** of the following **publications**:

Type of publication	Chapter of book
Title	Nanomedicine in the Treatment of Pathologies of the Central Nervous System
Authors	Bárbara Sánchez-Dengra, Isabel González-Álvarez, Marival Bermejo and Marta González-Álvarez
Book	Advances in Nanomedicine
Publisher	OPEN ACCESS EBOOKS
Year of publication	2020
Web	https://www.openaccessebooks.com/advances-in-nanomedicine.html

Type of publication	Chapter of book
Title	Marine based biopolymers for central nervous system drug delivery
Authors	Bárbara Sánchez-Dengra, Isabel González-Álvarez, Marival Bermejo and Marta González-Álvarez
Book	Marine Biomaterials
Publisher	SpringerNature
Year of publication	2022 *(Accepted for publication)*
Web	https://link.springer.com/book/9789811647864

Type of publication	Article
Title	*In vitro* model for predicting the access and distribution of drugs in the brain using hCMEC/D3 cells
Authors	Bárbara Sánchez-Dengra, Isabel González-Álvarez, Flavia Sousa, Marival Bermejo, Marta González-Álvarez and Bruno Sarmento
Journal	European Journal of Pharmaceutics and Biopharmaceutics
Impact factor	5.571 (Q1 - Pharmacology and Pharmacy)
Year of publication	2021
DOI	doi.org/10.1016/j.ejpb.2021.04.002

Type of publication	Article
Title	New *in vitro* methodology for kinetics distribution prediction in the brain. An additional step towards an animal-free approach.
Authors	Bárbara Sánchez-Dengra, Isabel González-Álvarez, Marta González-Álvarez and Marival Bermejo
Journal	Animals
Impact factor	2.752 (Q1 - Veterinary Sciences)
Year of publication	2021
DOI	doi.org/10.3390/ani11123521

Type of publication	Article
Title	Physiologically Based Pharmacokinetic (PBPK) Modeling for Predicting Brain Levels of Drug in Rat
Authors	Bárbara Sánchez-Dengra, Isabel González-Álvarez, Marival Bermejo and Marta González-Álvarez
Journal	Pharmaceutics
Impact factor	6.321 (Q1 - Pharmacology and Pharmacy)
Year of publication	2021
DOI	doi.org/10.3390/pharmaceutics13091402

In addition to the already published or accepted publications mentioned above, the following publications which are **submitted or under preparation** are also part of this doctoral thesis

Type of publication	Review article
Title	Access to the CNS: Strategies to overcome the BBB
Authors	Bárbara Sánchez-Dengra, Isabel González-Álvarez, Marival Bermejo and Marta González-Álvarez
Journal	Expert Opinion on Drug Delivery
Impact factor	6.648 (Q1 - Pharmacology and Pharmacy)
Year of publication	
DOI	Under preparation

Type of publication	Article
Title	New nanotechnology strategy to increase ponatinib delivery to the brain
Authors	Bárbara Sánchez-Dengra, María Alfonso, Isabel González-Álvarez, Marival Bermejo, Marta González-Álvarez and Ramón Martínez-Máñez
Journal	Journal of Controlled Release
Impact factor	9.776 (Q1 - Pharmacology and Pharmacy)
Year of publication	
DOI	Under preparation

Dr. María del Val Bermejo Sanz, supervisor, and Dr. Marta González Álvarez, cosupervisor of the doctoral thesis entitled "*In vitro* methods of biopharmaceutical evaluation in the blood-brain barrier"

INFORM

That Ms. Bárbara Sánchez Dengra has developed under our supervision the project entitled "*In vitro* methods of biopharmaceutical evaluation in the blood-brain barrier" in accordance with the terms and conditions defined in its Research Plan and in accordance with the Code of Good Practices of the Miguel Hernández University of Elche, fulfilling satisfactorily the set objectives for its public defence as a doctoral thesis.

So, we sign for the appropriate purposes, in Elche at 27 January of 2022.

Supervisor	Cosupervisor
Dr. María del Val Bermejo Sanz	Dr. Marta González Álvarez

Dr. Asia Fernández Carvajal, coordinator of the Doctoral Program in Molecular and Cellular Biology

INFORMS

That Ms. Bárbara Sánchez Dengra has developed under the supervision of our Doctoral Program the project entitled "*In vitro* methods of biopharmaceutical evaluation in the blood-brain barrier" in accordance with the terms and conditions defined in its Research Plan and in accordance with the Code of Good Practices of the Miguel Hernández University of Elche, fulfilling satisfactorily the set objectives for its public defence as a doctoral thesis.

So, we sign for the appropriate purposes, in Elche at 27 January of 2022.

Dr. Asia Fernández Carvajal

Coordinator of the Doctoral Program in Molecular and Cellular Biology

For developing this doctoral thesis, Bárbara Sánchez Dengra has received the following funding:

- A grant for the training of university teachers (FPU) [FPU17/00530] from the Ministry of Science, Innovation and Universities of Spain.
- An international mobility grant [0762/19] from Miguel Hernández University of Elche.
- A complementary grant for FPU recipients: Short stays and Temporary Transfers [EST19/00010] from Ministry of Education and Vocational Training.

In addition, this work was, mainly, supported by the project: "Modelos *in vitro* de evaluación biofarmacéutica" [SAF2016-78756 (AEI/FEDER, EU)] funded by Agencia Estatal Investigación and European Union, through FEDER (Fondo Europeo de Desarrollo Regional).

To everyone who loves me

INDEX

RESUMEN

RESUMEN

El acceso y la distribución de fármacos en el sistema nervioso central (SNC) es uno de los pasos limitantes a la hora de tratar patologías que afectan tanto al cerebro como a la médula espinal por la presencia de la barrera hematoencefálica (BHE). Además, la prevalencia de estas patologías aumenta año tras año en todo el mundo y la mayoría de los ensayos clínicos que se realizan con nuevas moléculas para tratarlas fracasan tras una gran inversión de dinero.

Así, en esta tesis, se ha optimizado la metodología *in vitro* para la determinación de la permeabilidad de la BHE, se han obtenido varias correlaciones *in vitro*/*in vivo* (IVIVCs) que pueden relacionar los resultados obtenidos mediante la metodología *in vitro* con datos *in vivo* procedentes de ratas, se ha desarrollado un nuevo modelo matemático que es capaz de predecir la distribución de fármacos en el cerebro y se han conseguido dos nuevas nanoestructuras que aumentan el acceso de ponatinib al SNC.

Primero, se optimizó un modelo de BHE propuesto previamente, en el que se utilizaban dos monocapas celulares diferentes (MDCK y MDCK-MDR1) para simular la barrera y se llevaban a cabo 4 tipos diferentes de experimentos (estándar de A a B, estándar de B a A, albúmina de A a B y homogeneizado de cerebro de B a A) para evaluar el acceso y distribución de fármacos en el cerebro, mediante: **a)** la sustitución de la monocapa celular por una más compleja (hCMEC/D3) y **b)** la sustitución del homogeneizado cerebral por una nueva formulación " libre de animales ". Ambas estrategias demostraron ser capaces de predecir los siguientes parámetros: el coeficiente de reparto plasma-cerebro libre ($Kp_{uu,brain}$), la fracción libre de fármaco en plasma ($f_{u,\ plasma}$), la fracción libre de fármaco en cerebro ($f_{u,brain}$) y el volumen aparente de distribución en cerebro ($V_{u,brain}$) y constituir herramientas de cribado de alto rendimiento que contribuyen a la reducción, el refinamiento y el remplazo de animales en la investigación.

A continuación, los datos *in vitro* obtenidos con la metodología mencionada anteriormente se combinaron con información *in silico* e *in vivo* para obtener un nuevo modelo semifisiológico que, mediante el uso de ecuaciones diferenciales y varias relaciones cuantitativas estructura-propiedad (QSPRs) fue capaz de predecir los perfiles cerebrales completos de varios fármacos en ratas.

Finalmente, se elaboraron dos nanopartículas diferentes, nanopartículas de sílice mesoporosa (MSN) y nanopartículas magnéticas de sílice mesoporosa (M-MSN), cargadas con ponatinib, un inhibidor de la tirosina quinasa indicado para el tratamiento del glioblastoma. Ambos tipos de partículas se caracterizaron y testaron *in vitro* e *in vivo*, demostrando que no son tóxicas para las células BHE y que pueden incrementar la cantidad de fármaco que llega al cerebro cuando se administran por vía intranasal en comparación con los resultados obtenidos para el fármaco libre.

ABSTRACT

ABSTRACT

The access and distribution of drugs in the central nervous system (CNS) is one of the limiting steps when treating pathologies that affect both the brain and/or the spinal cord due to the presence of the blood-brain barrier (BBB). In addition, the prevalence of these pathologies increases worldwide year after year and most of the clinical trials carried out with new molecules to treat them fail after huge amounts of money have been invested.

So, in this thesis, **(1)** the *in vitro* methodology for determining the permeability of the BBB has been optimized, **(2)** several *in vitro*/*in vivo* correlations (IVIVCs) have been obtained which can relate the results obtained using the *in vitro* methodology with *in vivo* data coming from rats, **(3)** a new mathematical model which is able to predict the distribution of drugs in the brain has been developed and **(4)** a couple of new nanostructures which increase the access of ponatinib to the CNS have been succeed.

First, a previously proposed BBB model, in which two different monolayers (MDCK and MDCK-MDR1) were used to simulate the BBB and 4 different types of experiments (Standard A to B, standard B to A, albumin A to B and brain homogenate B to A) were carried out to evaluate the access and distribution of drugs in the brain, was optimized by means of: **a)** substituting the cell monolayer by a more complex one (hCMEC/D3) and **b)** substituting the brain homogenate by a new "animal-free" formulation. Both approaches proved to be able to predict the following parameters: the unbound plasma–brain partition coefficient ($Kp_{uu,brain}$), the unbound fraction of drug in plasma ($f_{u,plasma}$), the unbound fraction of drug in brain ($f_{u,brain}$) and the apparent volume of distribution in brain ($V_{u,brain}$) and constitute high-throughput screening tools which contribute to the reduction, refinement and replacement of animals in research.

Then, the *in vitro* data obtained with the methodology mentioned above were combined with *in silico* and *in vivo* information to obtain a new semi-physiological model which, by means of using differential equations and several Quantitative Structure–Property Relationships (QSPRs) was able to predict the complete brain profiles of several drugs in rats.

Finally, two different nanoparticles, mesoporous silica nanoparticles (MSNs) and magnetic mesoporous silica nanoparticles (M-MSNs), loaded with ponatinib, a tyrosine kinase inhibitor indicated for the treatment of glioblastoma, were prepared. Both types of particles were characterized and tested *in vitro* an *in vivo*, proving that they are not toxic for BBB cells and that they can increase the amount of drug that reaches the brain when they are administered intranasally in comparison with the results obtained by the free drug.

INTRODUCTION

INTRODUCTION

The brain and the spinal cord comprise the central nervous system (CNS). Both organs are responsible for the integration of all the sensations that peripheral nerves detect and for the coordination of responses to those sensations [1]. These responsibilities make the brain and the spinal cord the most important organs of human beings and, for this reason, they are protected by several structures: bones, meninges, cerebrospinal fluid (CSF) and blood-brain barrier (BBB) [2–4]. Bones, such as the skull or the vertebra, are the most external protection and they act as an armor; meninges and CSF, which are the second level of protection act as a cushion that avoids strong blows between organs and bones; and the BBB, the third level of protection, surrounds the circulatory vessels present in the CNS and limits the access of microorganisms and toxic substances to it [5,6]. Figure 1 shows a scheme of the CNS protective structures.

Classically, meninges were thought to be just "wrappers" of the CNS. These wrappers are divided in 3 different membranes, from the outer one to the inner one, dura mater, arachnoid and pia mater. More recent studies have shown that meninges are also important in CNS development during embryogenesis and in CNS homeostasis during the adult life, as they contain several cell types able to produce trophic factors, such as FGF-2, EGF or retinoic acid, which promote the proliferation and differentiation of stem cells [7]. In fact, it has been proved that there is a stem cell niche in the leptomeningeal compartment (arachnoid and pia mater) which, when properly cultured *in vitro*, can form neurospheres that are able to differentiate to neurons or to oligodendrocytes [7,8].

Between the arachnoid and the pia mater, the subarachnoid space can be found, which is filled with CSF, a colourless and protein-free liquid produced by the choroid plexus at a rate of approximately 600 mL/day [5,9]. In an adult human, the volume of CSF present in the CNS is about 150 mL, so its rate of production allows a complete renewal of the CSF several times each day [5]. CSF flows from the lateral, third and fourth ventricles where it is produced to the subarachnoid space and, finally, it is reabsorbed into the circulatory system (figure 1). During its journey, CSF is responsible for distributing nutrients and removing waste from the CNS [10].

Blood is separated from the brain and the spinal cord tissues by the BBB. It is constituted by endothelial cells, pericytes and astrocytes [11]. These endothelial cells have a high number of proteins, such as claudins, occludins and junctional adhesion molecules, which form the tight junctions, give a high electrical resistance to the BBB (1500-2000 $\Omega \cdot cm^2$) and limit the paracellular access of substances to the CNS [12,13]. Pericytes are thought to stabilize the microvessel walls, regulate angiogenesis and neuroimmune functions in the CNS [14]. Astrocytes have a foot like shape at the end and they cover the endothelial cells, nonetheless, it is thought that they do not contribute in the barrier functions of the BBB, but in the differentiation and maintenance of those vessels [15].

In addition to the BBB, the blood-CSF barrier (BCSFB) and the blood-arachnoid barrier (BAB) can be defined [9,16,17]. The BCSFB separates the blood in the vessels that reach the ventricles from the CSF present inside them. In this barrier, unlike in the BBB, the endothelial cells are fenestrated and tight junctions can be found in between the choroid plexus epithelial cells [17]. Finally, the BAB isolates the CSF present in the subarachnoid space from the blood that reaches the subdural spaces, tight junctions are found in between the arachnoid cells [9].

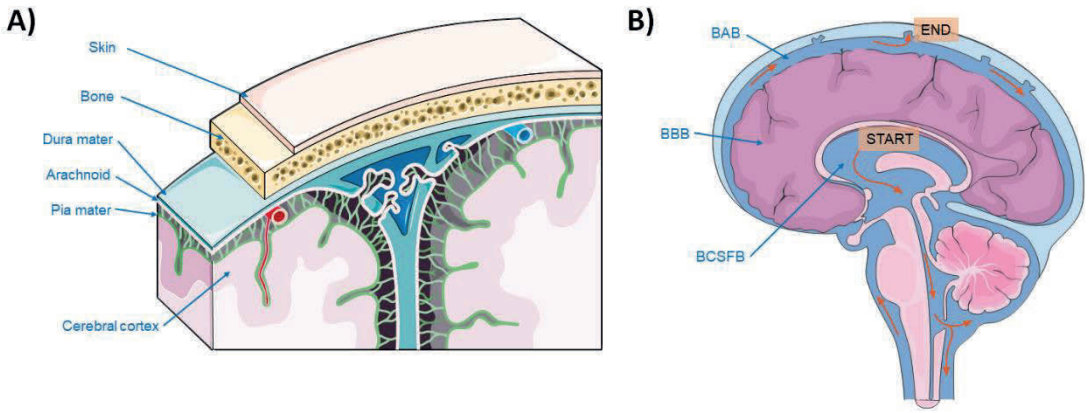

Figure 1. Scheme of the CNS protective structures. **A)** Scheme showing meninges structure. **B)** Scheme showing the CSF flow route and where the different brain barriers (BBB, BCSFB and BAB) can be found. Vectors downloaded from Servier Medical Art [18].

1. Pathologies that require drug access to the CNS

Pathologies that affect the CNS can be classified in 7 groups:

1) Infectious diseases, such as meningitis or encephalitis.

2) Brain and CNS cancers.

3) Stroke, including ischemic stroke, intracerebral haemorrhage and subarachnoid haemorrhage.

4) Neurological disorders, such as Alzheimer's disease and other dementias, Parkinson's disease, idiopathic epilepsy, multiple sclerosis, motor neuron disease, headache disorders (migraine or tension-type headache) and other neurological disorders.

5) Mental disorders, like schizophrenia, depressive disorders (major depressive disorder or dysthymia), bipolar disorder, anxiety disorders, eating disorders (anorexia nervosa, bulimia nervosa), autism spectrum disorders, attention-deficit/hyperactivity disorder, conduct disorder, idiopathic developmental intellectual disability and other mental disorders.

6) Substance use disorders, such as alcohol use disorders and drug use disorders (opioid use disorders, cocaine use disorders, amphetamine use disorders, cannabis use disorders and other drug use disorders).

All the pathologies mentioned above have increased their global prevalence in the last two decades with the exception of meningitis, whose prevalence has decreased by 29%. Specifically, from 2000 to 2019, the prevalence of brain and CNS cancers has increased by 46%, the prevalence of stroke by 36%, neurological disorders by 24%, mental disorders by 20%, substance disorders by 17% and encephalitis by 2% [19]. This generalized increment can be explained by the aging of global population and the globalisation process which has made easier the access to abuse substances. On the other hand, the decrease in the prevalence of meningitis can be explained by a better control of the cases in those countries in which meningitis is more frequent (the meningitis belt of sub-Saharan Africa) and the implementation of vaccination in those countries [20]. Figure 2 summarizes the variation in the prevalence of the different diseases that affect the CNS.

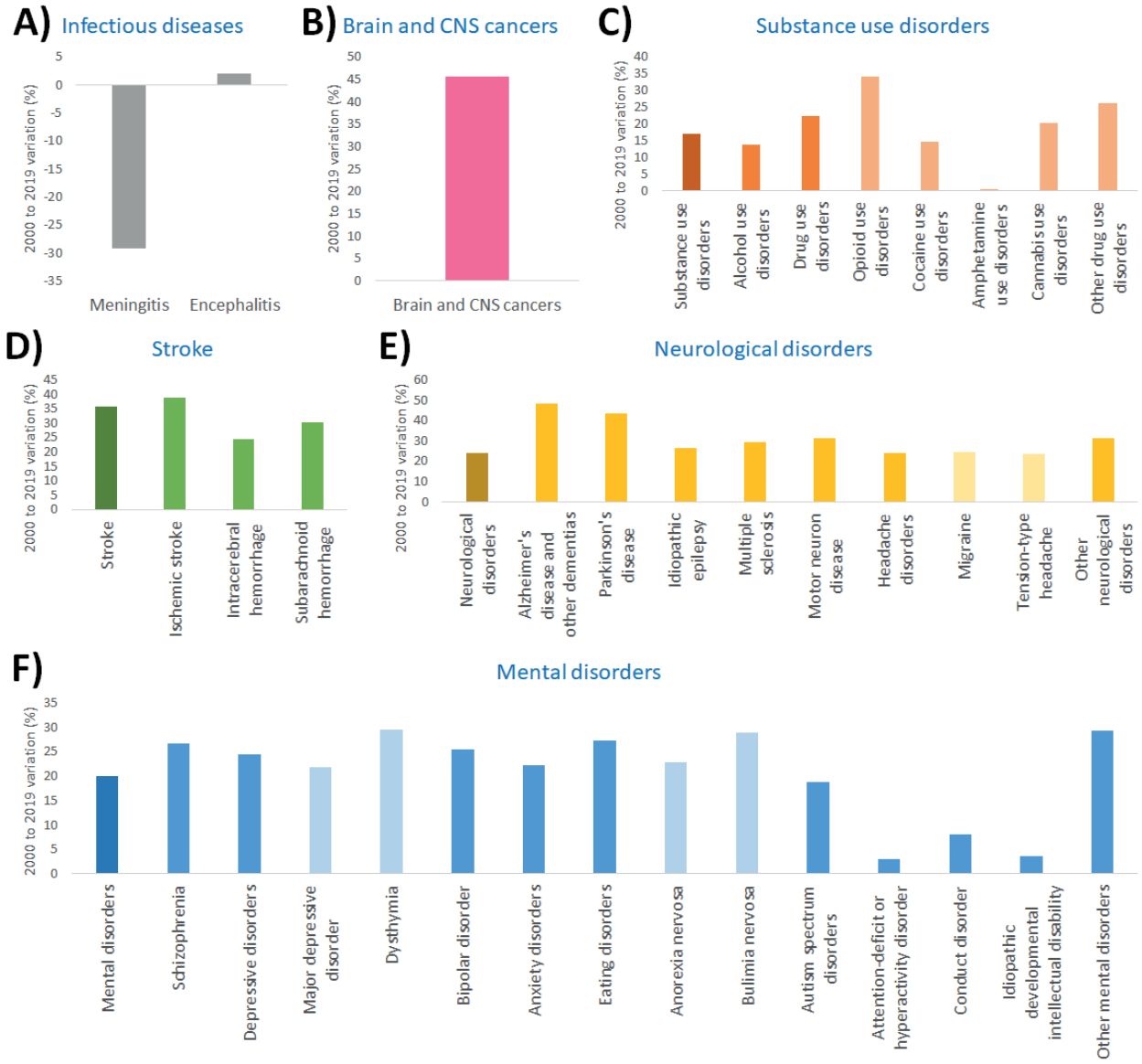

Figure 2. Variation in the prevalence of the different diseases that affect the CNS between 2000 and 2019 (subgroups marked in a lighter tone): **A)** Infectious diseases, **B)** Brain and CNS cancers, **C)** Substance use disorders, **D)** Stroke, **E)** Neurological disorders, **F)** Mental disorders [19].

The considerable increase in the prevalence of most diseases that affect CNS highlights the need for new treatments to combat them. Nonetheless, about 85% of CNS trials fail, which is the second highest failure rate just after the oncology trials [21]. Some studies have tried to collect the main reasons for explaining these failures [22–24], which can be summarized as follows:

1) Problems with the target: Sometimes clinical trials at phase II fail to demonstrate the engagement of the drug and its target and once it arrives to phase III they

cannot confirm the effectivity of the molecule [22]. This fact is quite common in CNS trials as in a lot of the pathologies affecting the brain, such as in neurological disorders, the diagnosis is made by means of information that the patient gives to the physician, but a physio-pathological mechanism of the disease is not clearly defined [24].

2) Lack of biomarkers: Together to the absence of a clear target the lack of biomarkers to make a correct diagnosis or to evaluate the outcome of the drug is a big drawback when a drug for the CNS is developed [22,24].

3) Problems with the design of the study: Normally, CNS trials require thousands of patients to obtain significant results, which is translated to huge studies that are carried out in different areas of the world. The size of the trials has provoked the inclusion of larger groups of patients who receive placebo and whose characteristics differ depending on the area where they live, giving, therefore, different results. Because of that some authors consider that is crucial to develop the trials in areas with similar characteristics, such as North America and Western Europe [22], or to carry out some "fast fail" trials as a proof of concept before moving into the big ones [24,25].

4) Issues with the transition from animals to human because animal models tend not to be as complex as human beings. For instance, the forced swim test use to evaluate antidepressants or the genetically modified mice used in Alzheimer's disease just show a characteristic of the illness they represent but not the whole of it [22,24].

5) Drugs not crossing the BBB is a big problem because without crossing the BBB molecules cannot reach their targets in the CNS. An oversized molecule, the influence of an expulsion transporter or a not appropriate preclinical model are some of the causes for this problem. The last one was the case for Tarenflurbil, a drug designed for treating Alzheimer's disease, which was effective in the animal model for this pathology but in humans did not cross the BBB in sufficient amounts [22].

Trying to overcome these failures some industries have opted for a repositioning strategy, a more cost-effective and time-saving alternative also known as drug repurposing or drug reprofiling [26]. Although having been used as interchangeable terms, there is a subtle difference between repurposing and repositioning. In repurposing, a drug already

approved and without suffering any molecular modification is reapproved for a different indication, while in repositioning, the drug suffers some change in its structure before being approved for another indication [26]. Historically, reposition has happened unintentionally, but, recently, researchers and industries have realized its benefits and used it with those drugs which have proved to be safe, but not effective, in their clinical trials. This is the reason why, year after year, the number of articles including on their keywords "drug repositioning" increases [26].

In the field of CNS treatments, approximately 30% of the drugs have been repurposed two or more times [26], mainly because once the drug crosses the BBB it is easier to find a new target for it. In fact, drugs used for treating epilepsy, schizophrenia or depressive disorders are the richest source of drugs in CNS repurposing (74%) [27]. Table 1 shows four examples of drugs that have been successfully repurposed for the treatment of CNS diseases [26,28].

Table 1. Examples of drugs that have been successfully repurposed for the treatment of CNS diseases.

Drug	Original indication (year of approval)	New indication (year of approval)
Amantadine	Influenza (1976)	Parkinson's disease (2017)
Edaravone	Stroke (2001)	Amyotrophic lateral sclerosis (2017)
Valproic acid	Epilepsy (1967)	Migraine (2011)
Zonisamide	Epilepsy (1989)	Parkinson's disease (2009)

2. The blood-brain barrier (BBB)

As said before, the BBB constitutes the third level of protection of the CNS and limits the access of substances to it, due to the presence of tight junctions, efflux transporters, pericytes and astrocytes. Nonetheless, 6 different access routes through the BBB can be defined, as seen in figure 3:

1) Paracellular diffusion: This term refers to the passive transport that happens between cells moving molecules from the side in which they are more concentrated to the side in which the concentration is lower. It is strictly regulated by the presence of tight junctions between the endothelial cells [29]. So, only extremely small hydrophilic molecules can use this route, such as erythropoietin and antibodies [16].

2) Transcellular diffusion: Also refers to a passive transport which moves molecules from the side of the BBB with the greater concentration to the side with the lower one, but, in this case, the transport takes place across the cells and not between them. Because of that, it is only possible for small lipophilic drugs (i.e. steroids), which meet the following characteristics: low molecular weight ≤500 Da, neutral charge, not too high or too low lipophilicity (logP ≈ 2) and a limited number of potential H-bonds (<10) [30].

3) Carrier-mediated transport: This pathway is responsible for the transport of essential molecules such as glucose and amino acids to the brain, but, any molecule similar to the glucose or to those amino acids could benefit from this route [16]. System L (LAT1 + 4F2hc) is a sodium-independent neutral amino acid transporter and it is one of the most important transporters involved in this route together with GLUT1. GLUT1 is a sodium-independent glucose transporter which contribute to the homeostasis of glucose and L-ascorbic acid in the CNS. Other influx transporters are responsible for the transport of monocarboxlic acids, such as lactate and pyruvate (MCT1), basic amino acids, like L-lysine and L-arginine (CAT1), nucleosides (CNT1) and organic anions and opioids (Oatp2) [31].

4) Receptor-mediated transport: It is also known as receptor-mediated transcytosis and moves molecules from one side of the BBB to the other using vesicles that are formed after they join a specific receptor. This is the case for big macromolecules such as insulin, transferrin or lipoproteins [16,32].

5) Adsorptive-mediated transport: This pathway conforms a non-specific way of transcytosis which can be used by polycationic substances, such as albumin or other peptides, which, after interacting with the negative surface of endothelial cells, are embedded into vesicles [16].

6) Cell-mediated transport: Finally, in this route, cells, normally from the immune system, move directly across the BBB by means of transcytosis. In some cases, as in virus infections, these cells are used as "trojan horses" to introduce molecules into the brain [16].

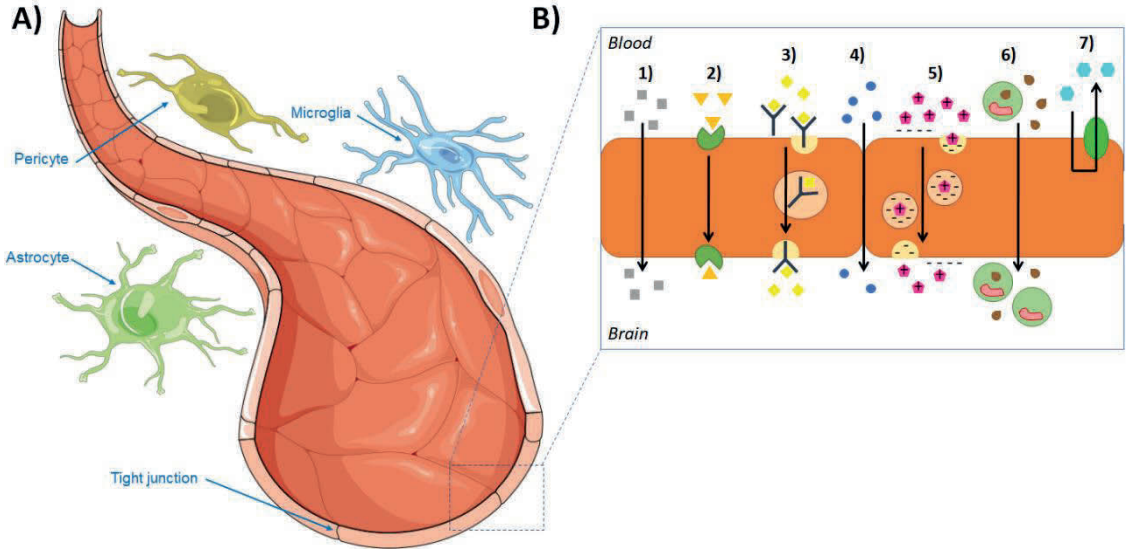

Figure 3. Scheme of the BBB structure **(A)** and the different mechanisms of transport that can be found on it **(B)**: **1)** Transcellular diffusion, **2)** Carrier-mediated transport, **3)** Receptor-mediated transport, **4)** Paracellular diffusion, **5)** Adsorptive-mediated transport, **6)** Cell-mediated transport and **7)** Efflux transport. Vectors downloaded from Servier Medical Art [18].

In addition to those 6 routes, which would allow molecules to reach the brain or the spinal cord, the BBB has several efflux transporters whose mission is to expel from the CNS those toxic or potentially dangerous substances that manage to reach it. Some examples of efflux transporters present in the BBB are the ATP-binding cassette (ABC) transporters: P-glycoprotein (Pgp - MDR1), the multidrug resistance protein (MRP) family and the breast cancer resistance protein (BCRP) [33].

Pgp was first detected in human endothelial cells in 1989 and since then several studies to evaluate its function and location have been carried out. In fact, it is the most studied efflux transporter of the BBB. It has been seen that, in mammals, Pgp can be found in the

apical side of endothelial cells, so those molecules that enter these cells are directly pushed back to the blood. Furthermore, Pgp has also been detected in parenchymal and perivascular astrocytes and in neurons, specially when the animal models suffer seizures [33–35].

The access routes (tight junctions, influx transporters and carriers) and the efflux transporters work together to maintain brain and spinal cord homeostasis, but some diseases can alter the functioning of the BBB.

Some *in vitro* studies have shown that glioblastoma, the most aggressive brain cancer, is able to reduce the transepithelial electrical resistance (TEER) of healthy BBB models [36] and it secretes the chemokine IL-8 which has pro-angiogenic and pro-permeability effects [37,38]. In addition, the study of serum samples from patients with glioblastoma has shown an increase in other pro-inflammatory factors and cytokines (IL-6, IL-1β, TNF-α, VEGF, FGF-2, IL-8, IL-2, and GM-CSF) [39]. Nonetheless, the generalized disruption of the BBB in patients with glioblastoma has become controversial during the last years, due to the lack of effectivity of the drugs directed to treat this pathology and the inability to completely eliminate the tumor when it is surgically removed. It is because image techniques using gadolinium-based contrast agents can mark some areas of the brain in which the BBB is disrupted and the tumor is present, but after the resection of those areas, cancer tends to reappear. This can be explained by the fact that the contrast cannot reach all the tumor cells because not all its BBB is disrupted [40,41].

In multiple sclerosis (MS), gadolinium can be also used to check the BBB disruption. Nonetheless, in this pathology, it is thought that the BBB breakdown is transitory and it is not clear if it is responsible of MS lesions or just a consequence of them [42]. MS is an autoimmune condition in which an excess of immune cells provoke demyelination, axonal loss and neurodegeneration. The lack of tightness between the BBB endothelial cells accounts for the excess of immune cells extravasation from the blood to the CNS, which, at the same time, promotes a greater lack of tightness as the immune cells produce pro-inflammatory chemokines that disrupt the BBB [43,44].

BBB dysfunction has also been confirmed in Alzheimer's disease patients by means of image techniques (gadolinium contrast) and post-mortem analysis of CNS tissues. It is

thought that the vascular damage, which is related with genetic (ε4 allele of apolipoprotein E - APOE4), environmental (i.e. pollution) and vascular risk factors (hypertension, diabetes, dyslipidemia…), is responsible for the accumulation of amyloid β (Aβ) in the brain [45]. In fact, studies with transgenic animals have shown that APOE4 carriers develop BBB leakage prior to Aβ accumulation [44,46,47], but more studies are needed to move from correlational findings to causal explanation.

MS and Alzheimer's disease are a couple of examples of neurological disorders in which BBB is altered. Nonetheless, BBB can also be affected in stroke or mental disorders, such as schizophrenia [11,46]. After a stroke, BBB leakage happens in two phases. First, there is an increase in transcytosis and, later on, a weakening of the tight junctions [46], both contributing to the cell damage, edema and bad prognosis of this disease [48,49]. On the other hand, some tight junctions protein levels (claudin-5) have been found to be reduced in psychiatric diseases and this decrease have been correlated with the disease duration and age of onset bipolar disease and schizophrenia [50].

3. Methodologies to evaluate the access of drugs to the CNS

3.1. *In vivo and in situ monitoring techniques*

Animal models are considered to be the best ones to study the access of molecules to the CNS. However, the cost of these models and their time consumption have promoted the progress of *in vitro* and *in silico* alternatives. Because of its similarity to human beings, the nonhuman primate models, such as *Macaca Mulatta/fascicularis*, are considered the best models for drug development, but they are difficult to manage [51]. Rodents models (mice and rats) are easier to manipulate, which makes them the most used *in vivo* models to study the access of molecules to the CNS. In addition to that, the BBB of rodents have proved to be quite similar to the human BBB, in terms of tight junctions (claudin-3 and -5, ZO-1 and occludins) and transporters (Pgp and GLUT1) [51]. When a large number of molecules want to be evaluated, the zebrafish model or *Drosophila melanogaster* can be used, although only the first one maintains a BBB physiology similar to the human one [51].

Regarding the techniques that can be used in these models, they can be divided in: invasive techniques (CSF sampling, brain microdialysis, *in situ* brain perfusion, brain uptake index, intravenous injection) and non-invasive image techniques (magnetic resonance and positron emission tomography) [51].

Invasive techniques

- CSF sampling: Due to its easier accessibility and its closeness to the brain tissue, the concentration of drug in CSF has been frequently used as a substitute for evaluating the amount of unbound drug that there is in the brain [51]. This technique has the advantage that the animal can be freely moving and serial samples can be taken by means of a cannula placed in the Cisterna Magna [52]. However, despite that, the serial sampling of CSF can alter the pressure equilibrium between the extracellular fluid (ECF) on the brain and the CSF. Furthermore, the concentrations measure in the CSF does not give information about the distribution of the drug in the different areas of the brain [52]. In addition to that, several studies have proved that the concentration of drug in CSF

tends to be higher than in ECF, especially in those drugs which are substrates of Pgp [53].

- Brain microdialysis: Intracerebral microdialysis is considered the gold standard technique for evaluating the unbound concentration of drug in the brain [53]. From a pharmacokinetic point of view, knowing the unbound concentration of drug in the brain is much more interesting than knowing the total concentration, as only the free fraction of drug is able to join its target and provoke a response. In this technique, a microdialysis probe with a semipermeable membrane is inserted into a specific area of the brain and at different times samples are taken from it. The semipermeable membrane, whose composition can vary depending on the drug that needs to be studied, allows the free drug to diffuse from the most concentrated solution (ECF) to the less concentrated (dialysate) until equilibration [52]. Intracerebral microdyalisis can be used to evaluate regional distribution in the brain, the influence of disease in drug permeability or the influence of influx and efflux transporters [54–56]. A relevant issue to take into account when planning to use this technique is that high lipophilic and very big macromolecules can shut off the probe, so, selecting the best composition of the semipermeable membrane in *in vitro* studies is recommended before starting the *in vivo* studies [53]. Table 2 summarizes the most important aspects that need to be considered when using brain microdialysis [52].

Table 2. Most important aspects to be considered when applying intracerebral microdialysis.

Important aspect	If not taken into account
Make some adsorption test *in vitro* to select the most appropriate membrane for the probe.	The microdialysis probe can shut off.
Use a perfusion solution with an ion composition as physiological as possible.	The concentration of ions in the brain can be altered and thus the permeability of drugs.
Avoid a too high flow rate when introducing the perfusate solution through the probe.	High flow rates alter the pressure equilibrium between the brain and the probe and reduce the recovery of drug.
Minimize tissue trauma by using a probe with an appropriate shape and dimensions and waiting 24 hours after implantation to carry out the experiment.	Tissue trauma can disrupt the BBB and permeability results would not be valid.
Implant a guide cannula at least a week before the experiment to minimize the effect of anaesthesia.	Anaesthesia can alter the basal conditions of the animal (i.e. dopamine basal levels)

- *In situ* brain perfusion: This technique was first developed in 1984 by Takasato *et al*. and it has been used to study the brain uptake of drug without having the influence of plasma or other organs metabolism [51,57]. Briefly, the drug is administered directly to the common carotid artery during 5 to 30 minutes after the ligation of the external carotid artery and the pterygopalatine artery. At the end of the perfusion, the animal is decapitated and the total amount of drug in the brain is measured after brain homogenisation [51,58].
- Brain uptake index (BUI): In a similar way to the previous technique, for calculating the BUI, a drug is directly injected in the carotid artery. Nonetheless, in this case, a rapid bolus injection is administered and animals are sacrificed after 5-15 seconds. The high speed of the experiment allows researchers to consider metabolism depreciable, but as a drawback, the concentrations reached in the brain are extremely low, which can give sensitivity problems [51,59].
- Intravenous injection: This constitutes a quite simple and informative technique, with which both plasma and brain profiles can be obtained. Although, it measures total concentrations and not unbound concentrations. In this case, the drug is administered in an IV bolus injection and blood samples are taken at different times. When a brain sample wants to be taken, the animal is euthanized, its brain homogenized and drug amounts measured [51].

Non-invasive techniques

Non-invasive techniques such as, positron emission tomography (PET) or magnetic resonance, have the advantage of allowing real-time evaluation of BBB permeability without sacrificing any animal and showing the distribution of the molecule evaluated within the different areas of the brain. Nevertheless, both techniques need expensive equipment and radiolabelled compounds [51]. These techniques can also be used in humans, for instance, to evaluate BBB disruption in different pathologies and obtained personalized permeabilities [59].

3.2. *In vitro models*

An ideal *in vitro* BBB model to study the access of drugs to the CNS, whose characteristics would be those summarized in table 3, does not exist [60], but these models constitute a quite useful and informative tool when developing new drugs. According to its basis, *in vitro* BBB models can be divided in two big groups: noncell-based *in vitro* models and cell-based *in vitro* models.

Table 3. Summary of the characteristics for an ideal *in vitro* BBB model [60].

	Characteristics of the ideal *in vitro* BBB model
1	High selectivity and electrical resistance due to the presence of tight junctions.
2	Presence of a polarized structure and influx and efflux transporters, the same ones that are in an alive BBB.
3	Ability to discriminate substances in accordance to its permeability.
4	Ability to response to aggressions and to regulate its morphology according to the shear stress from blood flow.
5	Cost-effectiveness, availability, convenience, predictability and reproducibility.

Noncell-based *in vitro* models

Noncell-based *in vitro* models are built on the important role of lipophilicity in the access of substances to the CNS.

- Immobilized-artificial-membrane chromatography (IAM): In this case, HPLC columns modified with phospholipid molecules are used as surrogates to evaluate permeability. It is because the retention times of the molecules have been correlated to cell permeabilities [61]. Nonetheless, the reliability is debatable and its use is decreasing [51,59].
- Parallel artificial membrane permeability assays (PAMPA): The first PAMPA model was developed in 1998 by Kansy *et al*. for evaluating gastrointestinal permeability [62]. In PAMPA models, a mixture of phospholipids, an organic solvent or a mixture of solvents are placed over an artificial membrane and the amount of drug that is able to pass from one side of the membrane to the other one is evaluated [26,59]. The PAMPA-BBB model, which was first employed in 2003 and used porcine brain lipids to cover the membrane, was able to classify 25

compounds out of 30 in CNS+, CNS- and CNS+/- and those drugs which were not correctly classified were substrates of efflux and influx transporters [63–65]. Later on, some studies have tried to optimize the conditions of PAMPA-BBB model and have obtained good correlations (r^2 = 0.839, n = 27) between the *in vivo* total brain-plasma coefficient of partition (logBB) and the PAMPA one [66].

Both methods, IAM and PAMPA, fail to simulate BBB influx and efflux transporters and also the metabolism that happens in the BBB, but, due to their low cost, they can be used as an initial high throughput approach to evaluate BBB permeability when a new drug is developed [51].

Cell-based *in vitro* models

Cell-based *in vitro* models can counteract the main disadvantages from the previous models (lack of transporters and lack of tight junctions) and, by means of the combination of different cell lines, can be used to study BBB permeability under pathological circumstances. The different cell lines that have been used to construct these types of models can be distinguish among them through their transendothelial electrical resistance (TEER), their permeability coefficient for paracellular markers (i.e. sucrose) and their transporters and BBB biomarkers expression [59]. Cell-based *in vitro* models can be divided in three big groups: monolayers, cocultures and dynamic BBB models (figure 4).

1) Cell monolayers are obtained after seeding the cells over a semipermeable membrane and leaving them to grow during several days (more or less days depending on the cell type). Ideally, the closer the TEER value of these monolayers is to 1000-2000 $\Omega \cdot cm^2$, the better, as that value is considered to be the resistance of brain microvessels [59]. Primary culture endothelial cells from humans and mammals (BCECs), which are obtained from brain biopsies and directly used to evaluate permeability, retain many *in vivo* properties, but they are not considered to be the best option for obtaining BBB monocultures, as, firstly, they are quite difficult to isolate without contamination (only 0.1% of brain are endothelial cells), secondly, their results have a big variability intra and inter-laboratory and, finally, they lose their BBB properties (tight junctions and transporters) quite rapidly [26,59,67]. Immortalized cells can solve some of the problems from

primary cell cultures, such as their difficult handling, because of that researchers have developed several mouse, rat, bovine and human immortalized cells. These types of cell cultures, tend to form less tighten monolayers, but they are considered interesting as they express BBB transporters. In fact, the immortalized cell line with human origin hCMEC/D3, whose TEER value is around 30-50 $\Omega \cdot cm^2$, is considered to be the gold standard in *in vitro* modelling [51,68]. Other non-cerebral cell lines, like MDCK and MDCK-MDR1, which come from a dog's kidney, can also be used to simulate the BBB [60,69]. In this case, non-cerebral cell lines are used because of their higher TEER, but their differences in terms of morphology, tight junctions proteins, and transporters with brain endothelial cells must be taken into account [26].

2) Cocultures: It has been seen that combining primary endothelial cells or cell lines with other types of cells, such as astrocytes or pericytes, improves the properties of BBB *in vitro* models (increase of TEER value, tight junctions expression and upregulation of efflux transporters) [51]. That's why, several researchers have proposed the use of cocultures to evaluate the access of substances to the CNS [26,59,67,70]. Depending on their organization, cocultures can be divided in two groups: noncontact coculture models (where endothelial cells are seeded in a semipermeable membrane and the additional cell in the other compartment of the system, but not touching the semipermeable membrane) or contact coculture models (in which both cell types, the endothelial one and the extra one are touching the semipermeable membrane, but each one on different sides of the system) [51]. When endothelial cells are cultured with two others supplemental cell lines (astrocytes and pericytes) the best reproduction of the *in vivo* environment is obtained. In 2009, Nakagawa *et al*. stablished a triple culture model, in which primary endothelial cells from rat were seeded on the apical side of a semipermeable membrane, astrocytes were cocultured in the basolateral chamber with no contact with the membrane and pericytes were cocultured in contact with the membrane at the basolateral side [71]. Researchers observed an increase in tight junctions expression by western blot and electron microscopy, an increase in TEER values which went from $\approx$90 $\Omega \cdot cm^2$ in cell monolayers to $\approx$350 $\Omega \cdot cm^2$ in the triple culture, a decrease in paracellular marker permeability (fluorescein) and a greater expression of several BBB transporters (Pgp, GLUT1 and ABCC1) [71]. In addition to the models mentioned before, cocultures have

also been used to simulate the BBB under pathological conditions. For instance, in 2015, Mendes *et al*. proposed a new *in vitro* model for studying BBB permeability with glioblastoma. They established a noncontact coculture of hCMEC/D3 and U87-MG cell lines and they observed a decrease in TEER values and an increment in the permeability of fluorescein, as it would happen in an *in vivo* glioblastoma due to the disruption of BBB [37].

3) Dynamic models: These models try to replicate the shear stress from blood flow at which BBB endothelial cells are subject. Within this group of models, microfluidics models (μBBB) are becoming increasingly popular [72]. In its simplest design, the dispositive has a couple of small electrodes which allow continuous TEER measurements and two types of cells can grow at both sides of a membrane that is placed at the interface of two microchannels. Then, a pump and a gas-permeable tubing system are used to move liquid through the system, generate shear stress and allow O_2-CO_2 exchange [67,72]. The presence of shear stress increases the tightness of endothelial cells, as was seen with hCMEC/D3 cell line, whose TEER value moves from ≈40 Ω·cm^2 to ≈120 Ω·cm^2 after just 18 hours in a microfluidic system [73]. Nonetheless, the system has some drawbacks like the lack of cell-cell contact, the possibility to incorporate only two cell types or the inability to replicate the dimensions of microvasculature *in vivo* [70].

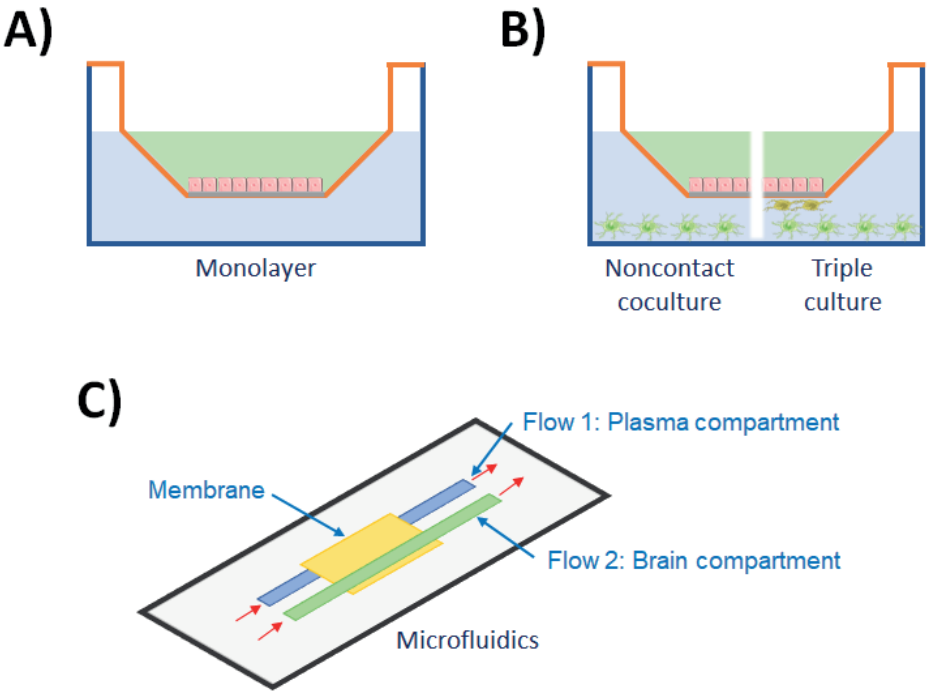

Figure 4. Scheme of different *in vitro* BBB models: cell monolayer **(A)**, coculture modes **(B)** and dynamic model **(C)**. Vectors downloaded from Servier Medical Art [18].

3.3. In silico methods

In silico models use available *in vitro* and *in vivo* data, the physicochemical properties of the drugs to be studied and computational techniques to predict BBB permeability. Once they are ready to be used, these methods constitute a quite cheap and fast tool to rapidly select a few candidates that may successfully cross the BBB from a batch of thousands of new molecules [59,70]. According to Lipinski's "rule of five", there are five key physiochemical properties which exert great control over drug access to the CNS: the molecular weight, the lipophilicity, the polar surface area, the hydrogen bonding, and the charge [74]. For having a good BBB permeability, the following characteristics in a molecule are recommended:

- Molecular weight ≤ 400 Da [70].
- Lipophilicity (logP) ≤ 5 [70].
- Polar surface area < 90 $Å^2$ [70].
- H-bond donors ≤ 3 and H-bond acceptors ≤ 7 [70].
- Charge (pKa = 7.5 - 10.5) [70].

Quantitative structure-activity relationships (QSARs) and physiologically based pharmacokinetic modelling (PBPK) are two computational strategies that are used, not only for obtaining penetrability parameter, such as logBB, but also for predicting brain distribution and complete concentration profiles in the brain. Because of that, investigation is moving towards this type of methodologies and several studies talking about QSARs and PBPK modelling for CNS can be found [75–83].

4. Strategies to allow the access of substances to the CNS

When trying to overcome the BBB, several strategies can be attempted which can be divided in: invasive strategies and non-invasive strategies. The invasive techniques include the direct injection into the brain parenchyma or the CSF and the therapeutic opening of the BBB, while the non-invasive techniques include the use of alternative routes of administration (nose-to-brain route), the inhibition of efflux transporters, the chemical modification of the molecules (prodrugs and chemical drug delivery systems (CDDS)) and the use of nanocarriers [16,59].

4.1. Invasive strategies

Invasive strategies tend to be the least used ones because of the inconveniences and discomfort that they cause to the patient. Nonetheless, in some pathologies they are the only feasible option.

Direct injection

The direct injection of drugs or the implantation of controlled release systems into the brain parenchyma have been studied for the treatment of different pathologies: cancers, stroke, neurological disorders or mental disorders [84]. The implantation of controlled release systems requires the opening of the skull, but allows long-term treatments, as drugs can be released during even several months [85]. In the following bullet point list, some examples of brain implants studied in different diseases are summarized:

- Glioblastoma: In 1996, the FDA approved a carmustine implant (Gliadel® wafer) for the treatment of glioblastoma. Currently, it is indicated for the treatment of recurrent glioblastoma and newly-diagnosed high-grade glioma as an adjunct to surgery and radiation. It has the advantage that it can be implanted during the same surgery in which the tumor is resected and it helps to eliminate the tumor cells that are not removed during the surgery, avoiding the adverse effects of a systemic administration of carmustine [86]. Studies have proved that carmustine is released by diffusion during several days and significant levels of drug can be measured within 5 cm of the implant for 30 days after implantation. Besides that,

these implants are able to increase the survival rate of glioblastoma patients by 2–3 months [84] and, according to a post-marketing study carried out in Japan, the risk of toxicity with the wafers is tolerable as, only 35.7% of the patients studied suffered adverse effects (22.2% cerebral edema, 9.9% convulsions, 4.8% impaired healing and 3.4% infection) [87].

- Epilepsy: The direct injection of antiepileptic drugs to the seizure focus has proved to be well tolerated and effective in terms of anticonvulsant activity in several animal studies [84,88]. For instance, the direct injection of phenytoin into the cortical focus of an epilepsy animal model was able to control the seizures better than a systemic administration of a higher dose of the same drug [88]. More sophisticated devices which are able to measure the electrical activity of the brain and release drug according to this activity have also been proposed for the management of epilepsy [84]. The device proposed in 2012 by Salam *et al*. was able to release drug just 16 seconds after the beginning of the electographical detection of a seizure onset [89].
- Schizophrenia: A long-term (5 months) delivery system has been also tested for the treatment of schizophrenia in animal models [84,90]. The reason for studying this kind of systems is that they would improve patient autonomy as they solve the problem of lack of adherence to the treatment normally associated to mental disorders [91].
- Stroke: Solid implants to prevent neurological damage after stroke have been studied during years [84]. For instance, since 1999, nicardipine prolonged-release implants have been tested with success for the prevention of vasospasm in patients with subarachnoid hemorrhage (SAH) [92]. In fact, nowadays, we can find a phase 2 clinical trial, that is currently recruiting participants, in which rod-shaped implants loaded with 4 mg of nicardipine (NicaPlant®) will be administered to patients with SAH to test if they are able to reduce neurological complications associated to this pathology [93].

On the other hand, the direct injection into the CSF is more accessible, but it is not really efficient because of the lack of diffusion between CSF and ECF [59]. Furthermore, it must be considered that only if the drug is injected into the ventricles, it will be distributed in the whole CSF. Nonetheless, this type of injection is indicated in some infectious diseases, such as meningitis [94].

Therapeutic opening of the BBB

The other invasive technique that can be used to increase the access of substances to the CNS is the therapeutic opening of the tight junctions in the BBB, which can be obtained by either administering hyperosmolar solutions or using ultrasounds [16].

The administration of hyperosmolar solutions typically prepared with mannitol or other aromatic substances makes endothelial cells to release water and reduce their size, resulting in an increase in the space between them [59]. This type of treatment is only used for treating life-threatening diseases, as the shrinkage of endothelial cells derives in a non-selective opening of the BBB and both, drugs and toxic substances, could reach the CNS provoking neurological complications (aphasia and hemiparesis) [95]. In addition to that, the administration of mannitol with several penetration markers has shown that the mannitol derived BBB disruption is not homogenously distributed and different permeability rates can be detected depending on the region of the brain analysed [96].

A more selective opening of the BBB can be obtained by means of combining the use of ultrasounds with the administration of microbubbles (small particles of 1-10 µm which contain heavy gases). When using this technique, microbubbles are directed towards a specific area of the brain, moving them with ultrasounds, and once in the correct place they interact with the endothelial cells and disrupt the tight junctions, leaving a free way for drugs to access the BBB [16]. Besides that, microbubbles can also be loaded or externally modified to carry some drugs on them. This technique has the advantage of safely opening just a desired area of the BBB without requiring a high ultrasound energy [85].

4.2. Non-invasive strategies

As said before, the non-invasive strategies to increase the access of substances to the CNS include the nose-to-brain route of administration, the inhibition of efflux transporters, the development of prodrugs and CDDS and the use of nanocarriers [16,59].

Nose-to-brain route

The olfactory area of the nasal cavity can be used as an alternative route for the delivery of molecules to the CNS. It is not clearly defined how drugs can reach the brain by means of this route, but what is clear is that olfactory nerves connect directly the nasal cavity with the CNS without having any BBB around them. It is thought that drugs administered into the nasal cavity can use two different pathways to travel until the brain: a) the olfactory nerves transportation or b) the trigeminal nerves transportation. The second one can only happen after the drug has been absorbed from nasal mucosa [97]. The main advantages and limitations of this route of administration are summarized in table 4.

Table 4. Summary of the main advantages and limitations of the nasal route of administration for the treatment of pathologies affecting the CNS [97,98].

	Advantages
1	Avoidance of plasma exposure, peripheral metabolism and peripheral side-effects, as the amount of drug that can reach general circulation through the nasal vasculature is depreciable (bioavailability = 0.01% - 0.1%).
2	Reduced risk of infection due to the lack of invasiveness of the administration technique.
3	Ease of administration for the patient, because drugs can be formulated in nasal sprays.
	Limitations
1	Only a small volume (100-250 µL) and a small amount of powder (20-50 mg) can be directly administered to the nasal cavity. So, this route is only feasible for very potent drugs which do not need high doses.
2	Enzymes present in nasal mucosa may metabolize the drugs administered into nasal cavity.
3	Drugs and formulations designed to be administered by this route should not irritate the nasal cavity.
4	The presence of an upper respiratory infection may alter the nasal environment and hinder the drug delivery to the brain.

For example, the intranasal administration of insulin has been considered a promising option for the treatment of Alzheimer's disease. In fact, several studies have proved that after administering insulin via intranasal, it can be detected in CSF and not in plasma and it can improve the cognitive response of Alzheimer's disease patients [97,99]. Nonetheless, a recent clinical trial with 289 patients concludes that no cognitive or functional benefits of intranasal insulin administration could be observed after 12 months

and it proposes that more efforts need to be done in the development of intranasal delivery devices [100].

Migraine is another pathology in which intranasal administration has been deeply studied [101–105]. The last device approved by FDA for the treatment of this pathology, Trudhesa®, was allowed to be commercialized in the USA in September 2021. This product contains dihydroergotamine mesylate, a well-known anti-migraine drug, that is directly delivered to the upper part of the nasal cavity. A phase 3, open-label safety study has shown that pain can start disappearing just 15 minutes after administration and relief can last 2 days after just one dose [106,107].

Inhibition of efflux transporters

As already said, efflux transporters such as Pgp, MRP family and BCRP, are responsible for expelling potentially toxic substances from the CNS. Because of that, when the drug of choice is a substrate of this type of transporter, they hinder the treatment of pathologies affecting the brain or the spinal cord. The coadministration of the drug in question with an inhibitor of the efflux transporter for which it is substrate is another strategy for overcoming the BBB, but it must be used with care as the inhibition of efflux transporters can lead to the massive entrance of xenobiotics to the CNS and, subsequent, unwanted side effects [59,85].

Industries have worked in the development of efflux transporters during several years, specially, in the development of inhibitors for Pgp, for which three generations of molecules can be distinguished [33]:

- 1st generation: This generation of Pgp inhibitors includes several molecules, i.e. verapamil, quinidine or cyclosporin A, which, having been developed for the treatment of different pathologies, showed to have some cytotoxicity as they competed for the efflux transporter with other molecules. Nonetheless, these molecules, which were not specifically designed for inhibiting Pgp and have low affinity for it, can interact with other transporters and enzymes provoking unexpected adverse effects and need a too higher dose to induce a proper inhibition of the efflux transporter [108].

- 2nd generation: Trying to reduce the pharmacological effect and increase the inhibition power of the molecules from first generation, several chemical modifications were performed to the original drugs. Following this basis, dexverapamil, the R-enantiomer of verapamil, or valspodar, derivative of cyclosporin A, were discovered. However, the inhibitors from this second generation are not selective of Pgp and interact with metabolic enzymes, causing undesirable adverse effects. This is the case of valspodar which competes with other molecules for cytochrome P450 leading to an increase in the concentration of other xenobiotics [108].
- 3rd generation: Finally, in this last generation, new molecules, such as zosuquidar, tariquidar or laniquidar, have been directly designed making use of computational tools and QSARs. So, they are able to specifically inhibit Pgp without interacting with other transporters or metabolic enzymes. Nevertheless, not everything is ideal, as some unexpected adverse effects have been observed when testing these molecules in clinical trials [108].

HIV can reach the brain using the infected immune cells as "trojan horses" to cross the BBB. Once there, the virus can multiply and use the CNS as a reservoir, as the drugs designed for their elimination fail to cross this barrier [109]. In this regard, the use of Pgp inhibitors have proved to be effective in the treatment of HIV CNS infections [59]. In 2017, Namanja-Magliano *et al.* developed a homodimer of azidothymidine, an antiretroviral drug also known as zidovudine, which was able to inhibit both, the Pgp and the ABCG2 efflux transporter. Researchers concluded that this type of homodimer has potential to enhance the delivery of antiretrovirals across the BBB, as they block two transporters at the same time allowing the free drug to stay in the brain [110].

Chemical strategies: prodrugs and chemical drug delivery systems (CDDS)

The chemical modification of molecules is a strategy that has been used not only for obtaining more powerful inhibitors of the efflux transporters present in the BBB, but also for obtaining new drug candidates with more chances to cross this barrier.

On the one hand, the development of prodrugs consists in the chemical modification of an active molecule with the aim of increasing its lipophilicity. Once it has crossed the BBB,

the prodrug loses its "extra" portion and becomes an active molecule ready to perform its mission. When talking about prodrugs for the treatment of pathologies affecting the CNS, the typical example is L-Dopa, an inactive prodrug of dopamine used in the treatment of Parkinson's disease [16,59].

On the other hand, when a chemical modification is used for appending a bioremovable targeting structure to a drug, then, a chemical drug delivery system (CDDS) is obtained [16]. The route for obtaining the active drug from a CDDS is more complex than when using prodrugs, which allows researchers to obtain intermediary molecules that once cross the BBB are trapped in brain parenchyma where they are not active yet but where they can be accumulated, this is known as the "lock-in" strategy [95,111]. For instance, linking dihydrotrigonelline to a drug forms a CDDS which works in three phases [112], as shown in figure 5:

1) Dihydrotrigonelline increases the lipophilicty of the drug enabling it to cross the BBB.

2) When the CDDS crosses the BBB it is oxidized and a positively charge molecule is obtained. The positive charge prevents the intermediary molecule from crossing the BBB back to plasma.

3) Finally, esterases hydrolyse the intermediate molecule and slowly release the active drug.

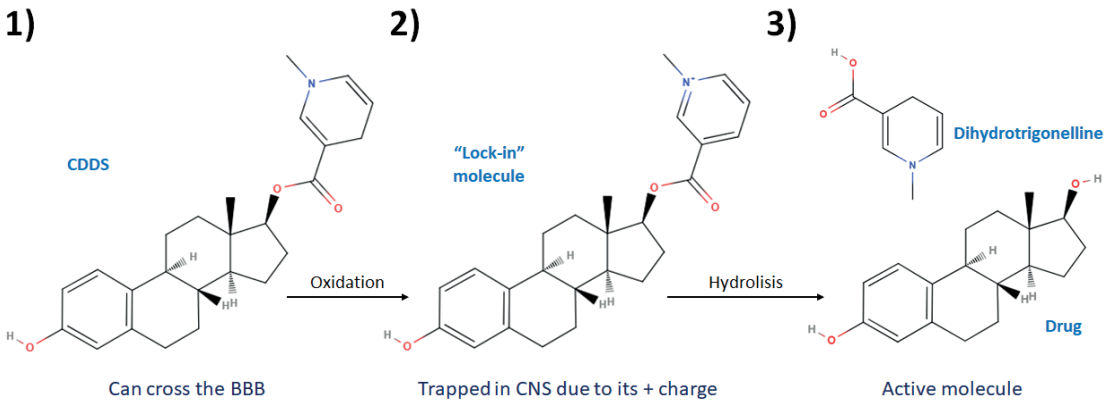

Figure 5. Mechanism of action of a dihydrotrigonelline CDDS.

Nanocarriers

The use of nanocarriers, small particles ranging from 1 to 100 nm, has proved to facilitate the delivery of drugs to the CNS. It is because they are able to protect the drug from enzymatic degradation and they can improve plasma stability and solubility. Furthermore, they can be designed to be directed towards a specific targeting, thus, minimizing non-desired side effects [113]. Nonetheless, it is important to remark that for all this to happen the nanocarrier must not release its content prematurely, so, the ideal nanocarriers for CNS delivery have: **A)** two different ligands, a first one which contributes to BBB passage and a second one, whose aim is to target the carrier to a specific area of the brain and **B)** a responsive (pH or enzymatic triggered) system which quickly releases the drug once it has reached its target but prevents it from leaving the carrier while it is on its way to it [114].

A) Liposomes

Liposomes a are small vesicles, first discovered in the 1960s, formed by a phospholipid bilayer which entraps a small volume of aqueous phase inside them. Because of that, they can incorporate both lipophilic drugs, among the lipids of the bilayer, and hydrophilic drugs, on the inside core [59,115]. Depending on their complexity, liposomes can be classified in three different generations:

- 1st generation: These are the simplest model of liposomes. They are constituted just by the lipid bilayer and, because of that, they tend to aggregate and be eliminated by the reticuloendothelial system [59].
- 2nd generation: In this second group, the phospholipid bilayer is surrounded by polyethylene glycol, which makes liposomes less recognisable as foreign bodies and increases their stability. Liposomes from this group are also known as stealth liposomes [59].
- 3rd generation: The most complex liposomes are included in this group. They are PEGylated like in the 2nd generation, but they also have other moieties linked around them which help in targeting [59].

Liposomes from third generation have been widely studied for the treatment of different pathologies affecting to the CNS [115]. For instance, multifunctionalized liposomes, with apolipoprotein-E (ApoE) and phosphatidic acid (PA), have been tested for the treatment of Alzheimer's disease. ApoE acts as a first ligand helping the particle to cross the BBB and PA targets the liposome towards β-amyloid plaques and is able to break them [116–118]. *In vitro* tests with hCMEC/D3 monolayers show an increase in BBB permeability after the functionalization of PA-liposomes with ApoE. This increase in permeability was confirmed later on with a biodistribuiton assay in healthy mice in which researchers observed that after 24 horas the brain/blood ratio was 5-fold higher with dual liposomes than with PA ones [117].

On the other hand, in 2019, Xiao *et al*. designed ascorbic acid-thiamine disulfide system liposomes loaded with docetaxel which may be an interesting tool for the treatment of glioblastoma. These liposomes followed a "lock-in" behaviour similar to that presented above when talking about CDDS: once the liposomes cross the BBB, the thiamine disulphide system is reduced gaining a positive charge which entrap them in the brain. The pharmacokinectic parameters obtained after the administration of the liposomes and free docetaxel to adult mice show a 3.24-fold and a 5.61-fold increase in the area under the curve (AUC) and the maximum concentration (Cmax) in the brain [119].

B) Solid lipid nanoparticles

Solid lipid nanoparticles (SLNs) are constituted by a matrix of lipids, because of that they are useful for the delivery of hydrophobic drugs [16]. In 2019, He *et al*. studied SLNs, composed of glyceryl monostearate and glycerol tristearate and loaded with β-elemene, for the treatment of glioblastoma. β-elemene is a natural essential oil with anti-tumor activity. The SLNs loaded with this drug proved to reach a greater concentration in plasma and in the brain, both in mice and rats, which would propose this formulation to improve BBB permeability of β-elemene [120].

The previous study together with others in which plain SLNs are administered *in vivo* prove that this type of nanocarrier can inherently increase the penetration of drugs across the BBB [121]. Nonetheless, in other studies the SLNs have been functionalized and they have obtained very promising results too, for instance:

- SLNs loaded with quinine dihydrochloride and conjugated with transferrin, which were designed for the management of cerebral malaria, showed an enhanced uptake in the brain than the free drug in solution [122]. This can be explained by the fact that transferrin promotes the receptor mediated transport of the SLNs.
- The use of cationic bovine serum albumin (CBSA) as a ligand for the functionalization of SLNs have also proved to be a promising strategy for bypassing the BBB [123]. Nonetheless, in this case, the mechanism for this enhancement in the penetration is not due to the use of receptor mediated mechanisms, but adsorptive transcytosis, as the positive charge of the albumin can interact with the negative charge of the surface of the endothelial cells.

C) Lipid nanocapsules

Finally, lipid nanocapsules can be found as the last type of lipid-based nanocarriers. They have the advantages of being more stable than liposomes and being able to encapsulate greater amounts of lipophilic drug. It is because they have a lipoprotein-like structure, with an oily core surrounded by a rigid membrane of polymer or tensioactive [124].

In 2020, Elhesaisy and Swidan proved that they were able to reduce the immobility time of mice when they forced them to swim in a beaker, a stressful situation in which animals tend to desperate, resign and stop moving, after the administration of lipid core nanoparticles loaded with trazodone hydrochloride. In fact, the immobility time for the group without treatment was 158 ± 15 seconds, for the group which received a solution of free trazodone was 128 ± 12 seconds, but in the group treated with the nanocapsules the immobility time dropped until 88 ± 8 seconds (1.8-fold lower than the control group). So, researchers conclude that these carriers were a promising alternative for controlling depression [125].

From May 2018 to April 2020, the project BIONICS founded by Horizon 2020 worked in the development of lipid nanoparticles with anti-oxidant effects for the treatment and prevention of post-stroke side effects [126]. The reason for this is that the current treatment for ischeamic stroke, the administration of tissue plasminogen activator or the physical removal of the thrombo, can restore the blood flow in the affected area, but it cannot avoid the damage of brain tissue due to the release of reactive oxygen and reactive

nitrogen species. Preliminary results show that the new carrier was able to target both BBB and neuronal cells and, now, the group is working to prove its antioxidant and neuroprotective effect [126].

D) Polymeric nanoparticles

Polymeric nanoparticles can be divided in two groups depending on their structure: nanospheres (a solid polymeric matrix) or nanocapsules (an inner core surrounded by polymer). Several biodegradable and biocompatible polymers have been studied for the development of CNS nanocarriers, i.e. polylactic acid (PLA), polylactic-co-glycolic acid (PLGA), chitosan and polycaprolactone (PCL), among others [16,114]. The next bullet points show examples of polymeric nanocarriers developed with the polymers mentioned above:

- Polylactic acid (PLA): PEGylated PLA nanoparticles modified with an anti-transferrin receptor antibody and loaded with amphotericin B were developed in 2015 for the treatment of fungal meningitis. The PEG modification increases the stability of the particles in the blood and the anti-transferrin receptor antibody promotes the receptor-mediated transport through the BBB. The studies carried out with this formulation showed that the particles were able to significantly reduce the necrosis of brain tissue after 15 days of infection and increase the survival rate of mice whose lethality rate dropped from 100% in day 16 post-infection in the untreated group to 50% after 24 days [127].
- Polylactic-co-glycolic acid (PLGA): In the prospect of treating Alzheimer's disease, PLGA nanoparticles loaded with curcumin were prepared by Barbara and co-workers in 2017. Curcumin has proved to be able to inhibit the formation of Aβ plaques and disaggregate those already formed, but, as many other drugs, it has a low ability to cross the BBB. The new particles, which were modified with a peptide ligand (g7) for BBB crossing, showed to be able to reduce the number of Aβ aggregates in an *in vitro* model with hippocampal cells. Besides that, they seemed to reduce the inflammatory process associated to Alzheimer's disease. Nonetheless, further studies in in vivo models are needed to obtain further conclusions [128].

- Chitosan: Chitosan is a natural polysaccharide, which can be obtained after the deacetylation of chitin extracted from crustacean shells and has been studied for the treatment of many conditions, mainly Alzheimer's disease and Parkinson's disease [129]. Nanoparticles of chitosan loaded with rotigotine have proved that, after being administered intranasally, are able to reduce catalepsy, akinesia and improve the swimming ability in a Parkinson-induced animal model. Furthermore, pharmacokinetics studies showed a greater accumulation of rotigotine in the brain in comparison with the intranasal administration of the free drug or the administration of the particles by other ways [130].
- Polycaprolactone (PCL): *In vitro* studies carried out in three different cell lines with PCL nanoparticles loaded with clozapine, an antipsychotic drug used in the treatment of schizophrenia, show that this type of formulation may be a valuable alternative for the management of this pathology. The PEGylated particles were not toxic nor immunogenic and increased the permeability of clozapine in hCMEC/D3 monolayers [131].

E) Inorganic nanoparticles

Inorganic nanoparticles prepared with metals, metal oxides or silica are useful for, both, diagnosis and treatment of pathologies affecting the CNS, this is, they can act as theragnostic devices. Nonetheless, they have the big drawback that, in contrast to those nanoparticles mentioned previously, they are not biodegradable and they can be toxic [114].

Due to their surface plasmon property, gold nanoparticles can absorb and emit light at different wavelengths according to their size, shape and aggregate status [16]. Besides that, the surface plasmon property also makes this kind of particle ideal for photothermal therapy as the light they absorb can be converted into heat [132]. The photothermal therapy with gold nanoparticles has been tested in several *in vitro* and *in vivo* models of glioblastoma, but, for translating the findings obtained in those models to the treatment of human beings several challenges must be faced, such as: the several barriers that the irradiating light needs to cross until it reachs the particles in the tumor without damaging any other cerebral structures [133].

Magnetic nanoparticles prepared from iron oxides have also been studied as a thermal therapy for the treatment of glioblastoma or as contrast agents for imaging techniques [121]. In addition, these nanoparticles can be used as a driving force for promoting the passage of other types of nanocarriers through the BBB [16]. For instance, magneto-liposomes entrap a magnetic core in its inner part, which facilitates the delivery of drugs across the BBB, as proved by Saiyed *et al*. and Ding *et al*. in 2010 and 2014, respectively [134–136].

Mesoporous silica nanoparticles (MSNs) have a high surface area, can load big amounts of cargo, are biocompatible and are easy to functionalize. Because of that, a lot of researchers try to use this system for the development of new nanocarriers [114]. In 2016, an *in vitro* study carried out in two different monolayers, which are able to simulate the BBB (MDCK and RBE4 cells), showed that bare MSNs had low permeability and external functionalization was necessary to improve BBB penetration [137]. After that, several studies with functionalized MSNs have been carried out. For instance, lactoferrin-MSNs proved to reach the brain due to the use of the receptor-mediated pathway in a triculture *in vitro* model [138]. Also, Ri7 antibody-MSNs increased the drug delivery to the brain by means of binding to the transferrin receptor [137].

F) Dendrimers

Dendrimers are three-dimensional and regular polymeric macromolecules with three different areas, as shown in figure 6: **A)** a central core, **B)** branches and **C)** surface groups. The number of ramifications in a dendrimer defines its generation and the spaces that there are in between the branches can be used to transport other molecules [16,85].

The most studied dendrimer is poly-amidoamine (PAMAM) [85]. In 2016, Xu and collaborators loaded PAMAM with doxorubicin and did several *in vitro* and *in vivo* studies to prove its efficacy against glioblastoma. As surface groups, they selected two molecules: borneol, whose mission is to open the tight junctions in between the endothelial cells of the BBB, and, folic acid, to target the dendrimers to cancer cells, as they overexpressed the folic acid receptor. The *in vitro* studies showed that the nanocarriers prepared by Xu and collaborators were not toxic for BBB cells, but they were able to kill the glioblastoma cells. Besides that, a sustained released of doxorubicin was observed when the

dendrimers were placed in pH 5.5 buffer and the permeability of the drug in HBMEC monolayers was enhanced. Once in the *in vivo* studies, dendrimers showed a greater accumulation in brain and tumor than the free drug, a significant reduction of tumor volume and an increase in the survival of the animals tested [139].

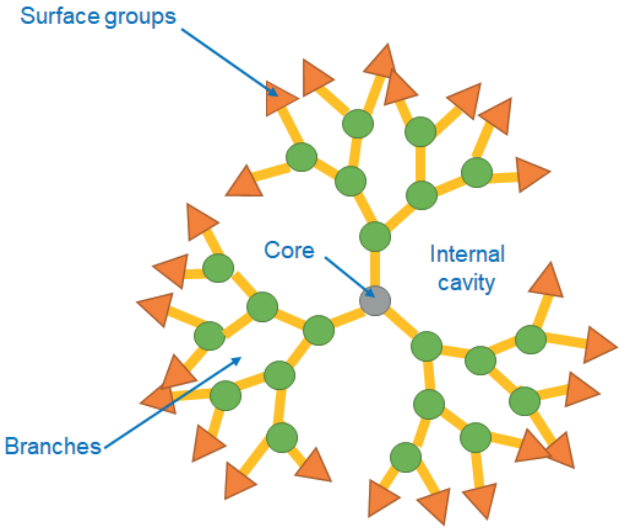

Figure 6. Schematic representation of a dendrimer.

G) Cyclodextrins

Cyclodextrins are cyclic polysaccharides used for delivering lipophilic drugs in an aqueous environment, as they are highly hydrophilic in their surface, but more hydrophobic in their inner part. Furthermore, cyclodextrins are able to interact with lipid membranes, so, they can be used to increase BBB permeability by means of altering its membrane fluidity [85,140].

Recently, a new complex of crocetin and γ-cyclodextrin was proposed for the treatment of Alzheimer's disease. The *in vitro* evaluation of the new complex showed that it was nontoxic and it was able to reduce the levels of Aβ in 7PA2 cell line. The pharmacokinetic evaluation in rats showed that, after an intraperitoneal injection, the maximum concentration in plasma of crocetin was 43.5 times higher when it was administered in the cyclodextrin complex than when it was administered on its own and the AUC was also 13.1 times higher. In terms of biodistribution, it was seen that the crocetin-γ-cyclodextrin complex was able to penetrate the BBB and reach the brain after its administration [141].

H) Quantum dots

Quantum dots (QDs) are small nanosystems ranging from 2 to 10 nm with semiconductor properties. In a similar way that gold nanoparticles, QDs can emit light in different wavelengths depending on their size, shape, and composition, because of that they have been proposed as theragnostic tools [142].

In the treatment of CNS pathologies, QDs have been explored to target and identify brain tumors, to detected areas affected by ischemia after a stroke or to treat HIV-associated encephalopathy [114,143]. In the last case, quantum dots conjugated with transferrin, as a targeting ligand to BBB, and saquinavir, as an antiretroviral drug, have proved to efficiently cross the BBB and inhibit HIV replication in infected PBMC cells, using a triculture *in vitro* model [143].

I) Nanogels

Nanogels can be defined as nanoparticles composed of a cross-linked hydrophilic polymer network [144]. Its capacity to retain water promotes nanogels biocompatibility and facilitates drug release. Nonetheless, this type of nanocarrier have been less studied for the treatment of pathologies affecting the CNS [114]. In June 2021, Ribovski *et al*. published an article in which they discuss the influence of nanogel' stiffness in BBB permeability. Briefly, they prepared 4 types of nanogels with different percentages of polymer and different polymerization times. Once obtained, they analysed the permeability of the different particles in a hCMEC/D3 BBB *in vitro* model. They saw that the low stiffness promotes intracellular trafficking and exocytosis through the cell monolayers [144]. So, soft nanogels would be the most promising ones for developing drugs directed towards the CNS.

J) Nanoemulsions

Nanoemulsions (NEs) are composed of kinetically stable dispersions of two immiscible liquids [145]. They can transport both hydrophilic and hydrophobic drugs and the smaller are the droplets of the emulsion, the greater is its stability. The mechanisms by which this type of nanocarrier can promote BBB permeability are:

- Lipid exchange, because of the interactions between the lipid phase of the NEs and the lipids of the endothelial cell's membranes [145].
- Carrier-mediated or receptor-mediated transport, which can occur if the external phase of the NE is decorated with a specific ligand [145].
- Adsorptive-mediated transcytosis, if the hydrophilic head of the lipids forming the droplets of the NE are positively charged [145].
- Efflux transport inhibition, as the droplets of the NEs can mask the drug from its efflux transporter and some surfactants present in the NE, i.e. polysobate 80, are well-known Pgp inhibitors [145].

NEs have been studied for the treatment of: brain tumors, neurodegenerative disorders, HIV-associated CNS disorders, ischemic stroke and schizophrenia [145]. Several examples of NEs intended for the treatment of those pathologies is shown in table 5.

Table 5. Examples of nanoemulsions intended for the treatment of CNS diseases [145].

Disease	Nanocarrier	Outcomes
Brain tumors	Kaempferol mucodhesive NE	Increased brain levels after intranasal administration.
		Reduced glioma (C6 cell line) viability.
	Chloroaluminun phtalocyanine NE	Reduced glioma (U87 cell line) viability.
	Paclitaxel ClinOleic®	Reduced glioma (U87 cell line) viability.
		Selectivity towards cancerous cells.
	Honokiol NE	Inhibition of tumor growth *in vivo*.
Neurodegenerative disorders	Oridonin NE	Less Aβ plaques and Aβ deposition.
		Restored construction behaviour.
	Rivastigmine NE	Increased brain levels after intranasal administration.
	Thymoquinone-rich fraction NE	Less Aβ generation and more Aβ degradation.
		Increased antioxidant levels.
	Selegiline NE	Increased antioxidant enzymes.
		Higher dopamine levels in Parkinson's disease rats.
	Riluzole NE	Increased brain levels after intranasal administration.
HIV-associated CNS disorders	Saquinavir mesylate NE	Increased brain levels after intranasal administration.
	Indinavir NE	Increased brain levels after intravenous administration.
	Atovaquone NE	Increased bioavailability after oral administration.
		Reduced parasitemia and less brain cysts in a toxoplasmosis.
Ischemic stroke	Thymoquinone mucoadhesive NE	Increased brain levels after intranasal administration.
		Better motor skills.
	Olmesartan NE	Increased brain levels after oral administration.
	Quercetin mucoadhesive NE	Better motor skills.
		Lower infarction volume and less hematoma.
		Increased antioxidant capacity.
Schizophrenia	Quetiapine NE	Increased brain levels after intranasal administration.
	Risperidone NE	Increased bioavailability and brain levels after intraperitoneal administration.
		Early onset of antipsychotic action.
		Less locomotor side symptoms.

K) Viral vectors

Finally, in terms of gene therapy, viral vectors have become extremely popular for the treatment of neurological disorders due to its high transfection efficiency and its long-term expression [113]. The adeno-associated virus serotype 9 (AAV9) is the most promising vector for CNS gene therapy as it has proved to be able to cross the endothelial cells by active transport without disrupting the BBB [85,146].

AVV9 has been tested for the treatment of spinal muscular atrophy (SMA) in several clinical trials [147]. SMA is a genetic disease affecting the alpha motor neurons of the spinal cord and brainstem. The degeneration of these neurons causes several difficulties in speaking, walking, breathing, and swallowing; it can lead to paralysis and death too, being the leading cause of mortality in infants [148]. Early-diagnosed patients treated with AAV9 showed a better motor behaviour and an increase in its rate of survival. Nonetheless, more efforts are needed before obtaining the final vector for treating this disease, as there were patients who developed antibodies against the vector and this may cause severe side effects [148].

OBJECTIVES

OBJECTIVES

The title of this thesis project is "*In vitro* methods of biopharmaceutical evaluation in the blood-brain barrier" and it has 4 different objectives:

1. Optimizing an *in vitro* methodology for determining the permeability of the BBB.

2. Developing *in vitro*/*in vivo* correlations (IVIVCs) with the purpose of validating the results obtained using the *in vitro* methodology with *in vivo* data coming from rats.

3. Performing the mathematical modelling of the data to predict distribution of drugs in the brain.

4. Developing new formulation strategies, such as nanostructures, to increase the access of drugs to the CNS.

In the following sections ("Materials and methods" and "Results and discussion") information will be divided into two different subsections: the first one for objectives 1, 2 and 3 and, the second one, for the last objective.

MATERIALS & METHODS

MATERIALS AND METHODS

1. *In vitro* BBB model: objectives 1, 2 and 3

1.1. Drugs, cells and products

The drugs (amitriptyline, atenolol, caffeine, carbamazepine, fleroxacin, genistein, loperamide, norfloxacin, pefloxacin, propranolol and zolpidem) and the HPLC grade solvents (water, acetonitrile and methanol), used for completing the objectives 1, 2 and 3 of this thesis, were acquired from Sigma-Aldrich (Barcelona, Spain). The molecular properties of the drugs mentioned above are summarized in table 6.

Table 6. Molecular properties of the drugs employed for completing the first three objectives of this thesis [149,150].

Drug	**MW** (g/mol)	**Solubility log S** (pH 7)	**logP**	**SA pKa**	**SB pKa**	**Charge** (pH 7.4)	**Transporters** (substrates)
Amitriptyline	277.41	-1.63	4.81		9.76	+	ABCB1 (Pgp)
Atenolol	266.34	0.43	0.43	14.08	9.67	+	ABCB11
Caffeine	194.19	-0.44	-0.55		-1.16	0	
Carbamazepine	236.27	-3.79	2.77	15.96		0	ABCC2 RALBP1
Fleroxacin	369.34	-1.33	0.98	5.32	5.99	-	
Genistein	270.24	-2.78	3.08	6.55		-	
Loperamide	477.05	-2.23	4.77	13.96	9.41	+	ABCB1 (Pgp)
Norfloxacin	319.34	-2.06	-0.97	5.58	8.77	0	ABCB1 (Pgp)
Pefloxacin	333.36	-1.21	0.75	5.50	6.44	-	ABCB1 (Pgp)
Propranolol	259.35	-1.03	2.58	14.09	9.67	+	ABCB1 (Pgp)
Zolpidem	307.40	-4.27	3.02		5.39	0	

MW = molecular weight, SA pKa = Strongest acidic pKa, SB pKa = Strongest basic pKa

The MDCK cells were acquired from ATCC (USA), the MDCK-MDR1 cell line was kindly provided by Dr. Gottesman, MM (National Institutes of Health, Bethesda) and the hCMEC/D3 cell line was acquired from Cedarlane (Burlington, ON, Canada). Pig brains were obtained from a local slaughterhouse and fresh chicken eggs were bought in a local supermarket.

The products for the cell culture of the MDCK and MDCK-MDR1 cell lines were obtained from Sigma-Aldrich (Barcelona, Spain): Dulbecco's modified Eagle's medium (DMEM) with high content of glucose, fetal bovine serum (FBS), MEM Non-Essential aminoacids, penicillin–streptomycin, L-glutamine, HEPES, phosphate buffer solution (PBS), trypsin-EDTA and Hank's balanced salt solution (HBSS).

The products required for culturing the hCMEC/D3 cell line were bought in different places: Sigma-Aldrich (Barcelona, Spain) (ascorbic acid, bFGF, HEPES, hydrocortisone and Triton X-100), Gibco (Barcelona, Spain) (chemically defined lipid concentrate, collagen I rat protein, HBSS, FBS, penicillin–streptomycin, and trypsin-EDTA) and Lona (Barcelona, Spain) (EBM-2 medium).

1.2. Cell culture

In this thesis, three different cell lines were used for the optimization of an *in vitro* methodology for determining the permeability of the BBB, the development of *in vitro/in vivo* correlations (IVIVCs) and the prediction of the distribution of drugs in the brain. These cells were: MDCK, MDCK-MDR1 and hCMEC/D3.

MDCK and MDCK-MDR1 cells were maintained in DMEM with a high content of glucose completed with FBS (10% (v/v)), MEM Non-Essential aminoacids (1% (v/v)), penicillin–streptomycin (1% (v/v)), L-glutamine (1% (v/v)) and HEPES (1% (v/v)). Whereas, the hCMEC/D3 cell line was cultured in EBM-2 medium complemented with FBS (5% (v/v)), lipid concentrate (1% (v/v)), penicillin–streptomycin (1% (v/v)), HEPES (1% (v/v)), ascorbic acid (5 µg/mL), hydrocortisone (0.5 µg/mL) and bFGF (1 ng/mL - added directly to the flasks when cells were cultured).

All cells were kept in flasks of 75 cm^2 in an incubator at 37 °C with 5% CO_2 and 90% humidity. When they reached 80% confluence, they were split and sub-cultured in new flasks. For detaching the cells and allowing the sub-culturing procedure a trypsin-EDTA:PBS (2:8) solution was used. The day after sub-culturing the medium of the flasks was replaced with new fresh medium to remove all the dead cells.

1.3. Permeability studies

Permeability studies were performed with three different BBB monolayers: MDCK, MDCK-MDR1 and hCMEC/D3. Cells were seeded in 6-transwell plates with a pore size of 0.4 micron, an effective area of 4.2 cm^2 and a pore density of (100 ± 10) x 10^6 pores/cm^2 and they were maintained, changing the culture medium every 2 days, for 8 days until confluence.

After 8 days, cells were washed with HBSS and the integrity of the monolayers was checked by means of measuring the TEER, the values expected were: 30-40 kΩ/cm^2 for hCMEC/D3 cells monolayers, 120-140 kΩ/cm^2 for MDCK-MDR1 monolayers and 130-150 kΩ/cm^2 for MDCK monolayers [151]. Later on, five types of experiments were carried out, in non-sterile conditions, assuming that the apical chamber of the transwell (A) acts as a substitute for the plasma and the basolateral chamber of the transwell (B) acts as a substitute for the brain, as seen in figure 7:

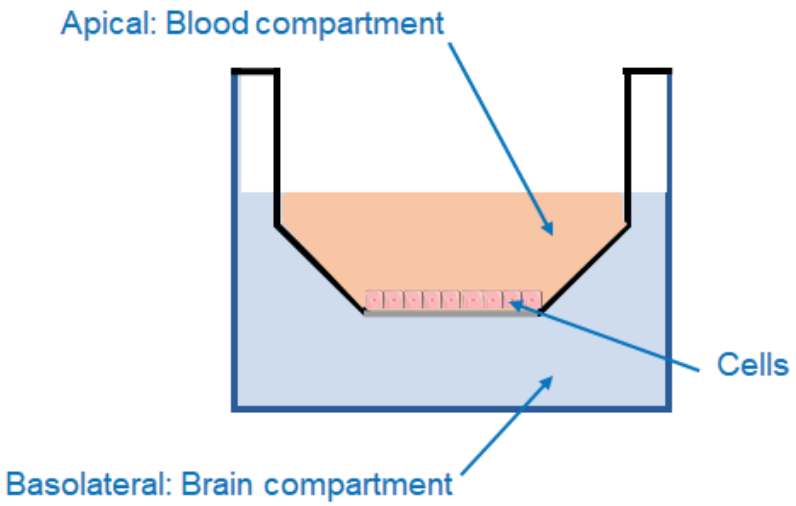

Figure 7. Representation of the transwell system used for evaluating *in vitro* BBB permeability.

- Standard A to B: This experiment was done for obtaining the apparent influx clearance (Cl_{in} = $P_{app\ A\rightarrow B}$). The drug dissolved in HBSS was placed in the apical chamber and samples were taken from basolateral.
- Standard B to A: In this experiment the apparent efflux clearance (Cl_{out} = $P_{app\ B\rightarrow A}$) was obtained. The drug dissolved in HBSS was placed in the basolateral chamber and samples were taken from apical, the opposite to what was done first.

- Albumin A to B: In this case, the drug was dissolved in a solution of 4% (w/v) albumin and placed in the apical chamber. So, the content of albumin present in human plasma was mimicked and the influx clearance of the free fraction of drug was obtained ($P_{app\ ALB}$).
- Brain homogenate B to A: The aim of this experiment was to simulate the binding of the drug to the brain tissue and obtain the efflux clearance of the free fraction of drug ($P_{app\ HOM}$). The drug was dissolved in a mixture of pig brain homogenate and phosphate buffer (180 mM, pH 7.4) in a ratio 1:3, then the solution was placed in the basolateral chamber and samples were taken from apical.
- Emulsion B to A: This last experiment was equivalent to the previous one, but the drug was dissolved in a new formulation to substitute the brain homogenate of the model and reduce the use of animals in experimentation. As before, the efflux clearance of the free fraction of drug ($P_{app\ EMUL}$) was obtained.

In all cases, cells were kept at 37 °C in an orbital shaker (100 rpm). Samples were taken from the chamber opposite to the one where the drug was administered. In addition, to check the mass balance, samples from the donor compartment (where the drug was placed) were taken at time 0 and at the end of the experiment and cells were disrupted with methanol of triton X-100 (1%) to measure the content of drug inside the monolayers. Three replicates for each experiment and drug (the concentrations used are shown in table 7) were performed and all samples were frozen and kept at -20 °C until their analysis.

The combination of the permeability values obtained in these experiments gives the main parameters which describe the access and distribution of drugs in the brain ($Kp_{uu,brain}$, $f_{u,plasma}$, $f_{u,brain}$ and $V_{u,brain}$).This will be explained in the section: *1.6. Parameters calculation: P_{app}, $Kp_{uu,brain}$, $f_{u,plasma}$, $f_{u,brain}$ and $V_{u,brain}$*.

1.4. Preparation of brain homogenate and the new substitute formulation

The pig brains, which were kindly supplied by a local slaughterhouse, were grinded and mixed with phosphate buffer (180 mM, pH 7.4) solution (brain:buffer, ratio 1:3) to obtain the brain homogenate. The ratio 1:3 was selected as appropriate because it gave a not too textured liquid to allow samples to be taken.

The new formulation for replacing the brain homogenate in the permeability studies was prepared from unfertilized chicken eggs. For obtaining 100 g of the new formulation, first, 15.35 g of whites were mixed with 67.73 mL of water and 16.92 g of yolk were weighed separately. Finally, the yolk was poured into the white-water mixture and stirred vigorously until obtaining an emulsion with a texture similar to that of the brain homogenate and a composition in proteins and lipids equal to the one of this organ (12% lipids and 8% proteins).

1.5. HPLC analysis of the samples

The equipment used for HPLC analysis was a Waters 2695 separation module, a Waters 2487 UV detector and a XBridge C18 column (3.5 µM, 4.6 x 100 mm) (Barcelona, Spain).

Samples from the albumin, the brain homogenate and the emulsion experiment were diluted (50:50) with cold methanol to precipitate the proteins. Then, all the samples were centrifuged (10 min; 10000 rpm - Eppendorf Centrifuge 5424, Rotor FA-45-24-11).

The analytical methods are summarized in table 7. All of them were validated in terms of linearity, accuracy, precision, selectivity and specificity. In addition to the conditions shown in table 7, a flow rate of 1 mL/min, a run temperature of 30 °C and an injection volume of 90 µL were fixed for all the drugs.

Table 7. Chromatographic conditions and validation parameters [60,69,83,152,153].

Drug	C (µM)	λ (nm)	Mobile phase	RT (min)	r^2	LLQ (µM)	ACC (%)	PRC (%)
Amitriptyline	250	240	40% AW 60% ACN	1.020	0.996	8.20	6.1	3.2
Atenolol	150	231	20% MeOH 60% AW 20% ACN	1.330	0.996	1.49	6.3	5.1
Caffeine	2.14	273	35% MeOH 65% AW	1.200	0.999	0.05	3.1	4.3
Carbamazepine	18 150	280	65% AW 35% ACN	1.926	0.994	0.76	3.9	3.6
Fleroxacin	1.39 150	285	70% AW 30% ACN	1.348	0.997	0.05	6.0	5.2
Genistein	3.81	254	60% MeOH 15% AW 25% ACN	1.334	0.996	0.28	5.0	5.9
Loperamide	241	260	60% MeOH 40% AW	3.199	0.995	2.65	4.0	4.5
Norfloxacin	150	285	70% AW 30% ACN	1.730	0.991	2.42	3.9	4.9
Pefloxacin	8.91	285	65% AW 35% ACN	0.721	0.998	0.61	3.9	3.7
Propranolol	150	291	30% MeOH 40% AW 30% ACN	1.950	0.999	5.74	3.9	3.4
Zolpidem	158	231	20% MeOH 60% H_2O 20% ACN	4.624	0.997	4.30	6.3	4.8

RT = Retention time, LLQ = Lower limit of quantification, ACC = Accuracy, PRC = Precision, ACN = Acetonitrile, MeOH = Methanol, AW = Acid water (Trifluoroacetic acid 0.05% (v/v))

1.6. Parameters calculation: P_{app}, $Kp_{uu,brain}$, $f_{u,plasma}$, $f_{u,brain}$ and $V_{u,brain}$

The apparent permeability (P_{app}) across the BBB of the drugs tested under the different conditions mentioned in the section *1.3. Permeability studies* was calculated using 4 different equations: Sink, Sink Corrected, Non-Sink and Modified Non-Sink [154]. Nonetheless, due to its better ability to capture the permeation rate in both sink and no

sink conditions and when the initial clearance differs from the clearance of the rest of the profile, the values obtained with the Modified Non-Sink equation were the ones used for the calculation of the rest of the parameters. The Modified Non-Sink equation is shown in equation 1:

$$C_{r,t} = \frac{Q_t}{V_r + V_d} + \left(\left(C_{r,t-1} \cdot f \right) - \frac{Q_t}{V_r + V_d} \right) \cdot e^{-\boldsymbol{P_{eff0,1}} \cdot S \cdot \left(\frac{1}{V_r} + \frac{1}{V_d} \right) \cdot \Delta t} \quad (1)$$

In which $C_{r,t}$ and $C_{r,t-1}$ are the concentrations in the receiver compartment (apical or basolateral depending on the experiment) at time t and time t-1, V_r and V_d are the volumes of the receiver and donor compartments, Q_t is the total amount of drug in both chambers at time t, f is the sample replacement dilution factor, S is the surface area of the monolayer and Δt is the time interval. $P_{eff,0}$ and $P_{eff,1}$ are the apparent permeability values, which can differ if the permeation rate is different at the beginning of the experiment with regard to the rest of the transport profile.

Equation 2 shows the formula for obtaining the unbound plasma–brain partition coefficient ($Kp_{uu,brain}$). This neuropharmacokinetic (neuroPK) parameter is defined as the relationship between the concentration of free drug in plasma ($C_{u,p}$) and the concentration of free drug in the brain ($C_{u,b}$) at a steady state. It can be obtained from the combination of the permeabilities of both standard experiments A to B and B to A.

$$Kp_{uu,brain} = \frac{Cl_{in}}{Cl_{out}} = \frac{P_{app\ A \to B} \cdot S}{P_{app\ B \to A} \cdot S} = \frac{P_{app\ A \to B}}{P_{app\ B \to A}} \quad (2)$$

Combining the results from the standard A to B and the albumin A to B experiments the unbound fraction of drug in plasma ($f_{u,plasma}$) can be obtained. This parameter can be considered essential when evaluating if a drug would access to the CNS as only the fraction that is not bound to proteins is able to cross the BBB. Equation 3 shows how this parameter can be calculated.

$$P_{app\ ALB} \cdot C_D = P_{app\ A \to B} \cdot f_{u,plasma} \cdot C_D \quad \rightarrow \quad f_{u,plasma} = \frac{P_{app\ ALB}}{P_{app\ A \to B}} \quad (3)$$

The unbound fraction of drug in brain ($f_{u,brain}$) can be calculated in a similar way to $f_{u,plasma}$, but, in this case, combining the permeability values from the B to A experiments. This parameter is also essential as once it has crossed the BBB, the fraction of drug that does not bind the brain tissue will be the only one able to return to the blood. Equation 4 shows how this parameter can be calculated.

$$P_{app\ HOM} \cdot C_D = P_{app\ B\to A} \cdot f_{u,brain} \cdot C_D \quad \rightarrow \quad f_{u,brain} = \frac{P_{app\ HOM}}{P_{app\ B\to A}}$$
$$P_{app\ EMUL} \cdot C_D = P_{app\ B\to A} \cdot f_{u,brain} \cdot C_D \quad \rightarrow \quad f_{u,brain} = \frac{P_{app\ EMUL}}{P_{app\ B\to A}} \qquad (4)$$

In equation 5, the formula for obtaining the apparent volume of distribution in the brain ($V_{u,brain}$) is shown, where V_{ECF} is the volume of the brain extracellular fluid (0.2 mL/g brain) and V_{ICF} is the volume of the brain intracellular fluid (0.6 mL/ g brain). This neuroPK parameter reflects the distribution of the drug once it has crossed the BBB, and can be defined as a relationship between the total amount of drug present in the brain (C_b) and the concentration of free drug in the brain ($C_{u,b}$). When the $f_{u,brain}$ gets lower, the $V_{u,brain}$ gets greater and the retention time of the drug in the CNS gets longer with independence of its transport through the BBB or its plasma concentration. The $V_{u,brain}$ can be directly compared with the physiological volumes of the CNS to evaluate the drug affinity to the brain tissue.

$$V_{u,brain} = V_{ECF} + \frac{1}{f_{u,brain}} \cdot V_{ICF} = 0.2 + \frac{1}{f_{u,brain}} \cdot 0.6 \quad (mL/g\ brain) \qquad (5)$$

1.7. *In Vitro-In Vivo Correlations (IVIVCs): Linear Regression*

For optimizing the *in vitro* methodology proposed by Mangas-Sanjuan *et al*. [69] for obtaining the neuroPK from 4 different *in vitro* tests two approaches were followed:

1) The methodology was tested in a more physiological cell line, hCMEC/D3 [60].

2) A novel preparation obtained from unfertilized chicken eggs was tested as a surrogate of brain homogenate [153].

In both cases, *in vitro-in vivo* correlations (IVIVCs) between the predicted and experimental parameters obtained in rats [155,156] were established. The IVIVCs were adjusted to a linear model with the following structure: y = a + bx and their 95% confidence intervals were also calculated.

1.8. PBPK model construction

The information from the permeability studies carried out in the MDCK, MDCK-MDR1 and hCMEC/D3 cells was used to develop a semi-physiological model (figure 8) to predict the concentration profile of different drugs in the brain of rats [83].

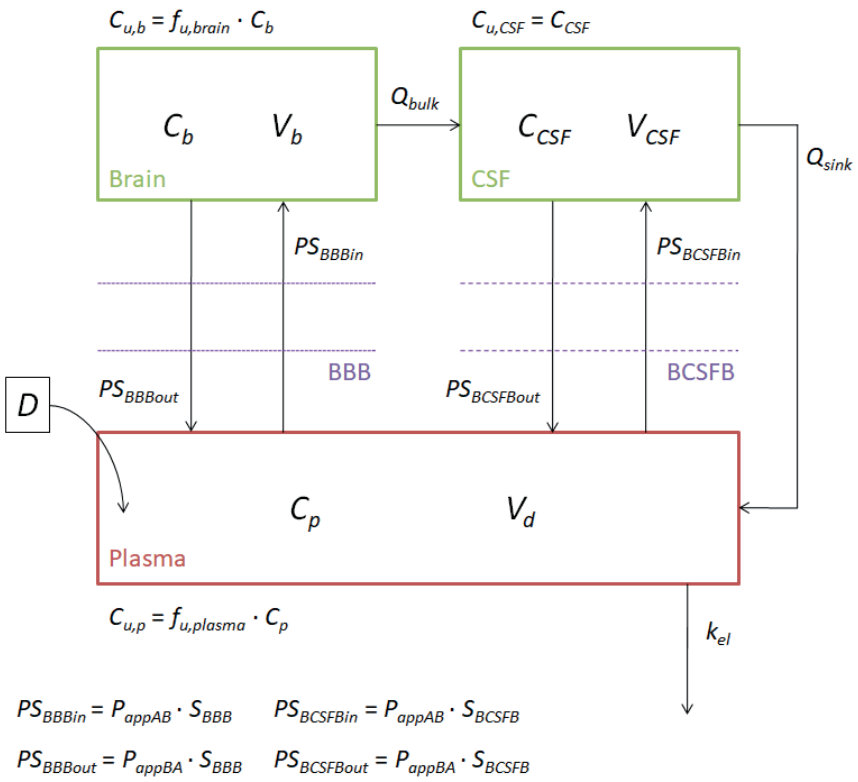

Figure 8. Scheme of the PBPK model.

$$V_d \cdot \frac{dC_p}{dt} = -PS_{BBBin} \cdot C_{u,p} + PS_{BBBout} \cdot C_{u,b} - PS_{BCSFBin} \cdot C_{u,p} + PS_{BCSFBout} \cdot C_{CSF} + Q_{sink} \cdot C_{CSF} - k_{el} \cdot C_p \cdot V_d \quad (6)$$

$$V_b \cdot \frac{dC_b}{dt} = PS_{BBBin} \cdot C_{u,p} - PS_{BBBout} \cdot C_{u,b} - Q_{bulk} \cdot C_{u,b} \quad (7)$$

$$V_{CSF} \cdot \frac{dC_{CSF}}{dt} = PS_{BCSFBin} \cdot C_{u,p} - PS_{BCSFBout} \cdot C_{CSF} - Q_{sink} \cdot C_{CSF} + Q_{bulk} \cdot C_{u,b} \quad (8)$$

Equations 6, 7 and 8 describe the processes shown in figure 8. Specifically:

- Equation 6 describes how the concentration in plasma can vary with time. On the one hand, the unbound concentration of drug in plasma ($C_{u,p}$), which was defined as the total concentration of drug in that compartment multiplied by the $f_{u,plasma}$, can leave the plasma compartment because it crosses the BBB and it accesses the brain tissue, because it crosses the BCSFB and it accesses to the CSF or because it is eliminated. On the other hand, the drug can return to the plasma compartment, because the unbound concentration of drug in brain ($C_{u,b}$), which was defined as the total concentration of drug in that compartment multiplied by the $f_{u,brain}$, crosses back the BBB, because the drug in the CSF, which was considered all unbound, as the CSF is a clear liquid without proteins, crosses back the BCSFB or because of the drainage of the CSF to plasma (Q_{sink}).
- The variation of the concentration of drug in the brain is described with the equation 7. The concentration of drugs in this compartment increases with the $C_{u,p}$ that crosses the BBB and decreases due to the ability of the $C_{u,b}$ to cross back the BBB and the flow of the extracellular fluid (ECF) to the CSF (Q_{bulk}).
- Equation 8 describes how the concentration in the CSF varies with time. As said before, all the concentration in this compartment is considered unbound concentration as the CSF has no proteins. The concentration of drug in this compartment increases due to the amount of drug that arrives from plasma crossing the BCSFB and the amount of drug that comes from brain tissue (Q_{bulk}) and decreases due to the drainage of CSF to plasma (Q_{sink}) and the drug that can cross the BCSFB back to plasma.

When it was necessary, due to the nature of the *in vivo* data found, the differential equations of the model were modified and an extra compartment for absorption was added to the model or an intravenous infusion was assumed instead of a single injection.

Table 8 summarizes the value of the physiological parameters in rats that were considered equal and fixed for all the drugs. Other parameters that were different depending on the drug studied are summarized in table 9.

Table 8. Fixed physiological parameters used in the model [82,157].

V_b (cm^3)	V_{CSF} (cm^3)	Q_{bulk} (cm^3/s)	Q_{sink} (cm^3/s)	S_{BBB} (cm^2)	S_{BCSFB} (cm^2)
1.28	0.25	0.012	0.132	187.5	0.0375

V_b = Brain volume, V_{CSF} = CSF volume, S_{BBB} = BBB surface area, S_{BCSFB} = BCSFB surface area

Table 9. PK parameters used in the model as initial estimates and were different for each drug.

Drug	Fixed estimates				Nonfixed estimates			REF
	RW (g)	D (mg)	k_0 (ng/s)	$f_{u,plasma}$	V_d (cm^3)	k_{el} ($\cdot 10^{-5}$ s^{-1})	k_a ($\cdot 10^{-5}$ s^{-1})	
Amitriptyline	250	5		0.090	4000	7.70	15.4	[150,155,158]
Caffeine	300		833.3	0.917	180	3.55		[150,156,159]
Carbamazepine	300	3.6		0.385	1490.5	4.50	8.99	[156,160,161]
Fleroxacin	285	1.1	83.13	0.793	427.5	7.13		[156,162–164]
Pefloxacin	285	3.7	214.5	0.860	361.1	5.83		[156,163–165]
Zolpidem	190	0.5		0.267	304	15.6		[156,166]

RW = Rat weight, k_0 = Infusion rate constant, k_a = Absorption rate constant, k_{el} = Elimination rate constant, V_d = Volume of distribution

The profiles were adjusted with the software Berkeley-Madonna® (Berkeley, USA). With this aim, three scaling factors were assumed as seen in equations 9 to 13. The adjustment of the *in vitro* apparent permeabilities to the physiological permeability was done with the first and second scaling factors (SC1 and SC2), as Ball *et al*. did before [82]. The differences between the *in vitro* and the *in vivo* $f_{u,brain}$ values, because of the different composition and behaviour of the pig brain homogenate and a healthy rat brain, were corrected with the third scaling factor (SC3).

$$PS_{BBBin} = SC_1 \cdot P_{app\ A\to B} \cdot S_{BBB} \quad (9)$$

$$PS_{BCSFBin} = SC_1 \cdot P_{app\ A\to B} \cdot S_{BCSFB} \quad (10)$$

$$PS_{BBBout} = SC_2 \cdot P_{app\ B\to A} \cdot S_{BBB} \quad (11)$$

$$PS_{BCSFBout} = SC_2 \cdot P_{app\ B\to A} \cdot S_{BCSFB} \quad (12)$$

$$C_{u,b} = SC_3 \cdot f_{u,brain} \cdot C_b \quad (13)$$

1.9. QSPRs and internal validation of the model

To make the PBPK model useful for the prediction of brain profiles without the use of animals, several Quantitative Structure–Property Relationships (QSPRs) were defined for each scaling factor and cell line. The scaling factors were related with the lipophilicity of the drugs (logP) and non-linear QSPRs were obtained. These QSPRs give an equation that would allow researchers to calculate the scaling factors for a drug depending on the cell line where they study the *in vitro* permeability.

The predictability of the model in combination with the QSPRs was evaluated by internal validation, comparing the brain C_{max} and the brain AUC obtained with the adjusted scaling factors and with the scaling factors estimated with the QSPRs. Equation 14 shows how the prediction error percentages were calculated.

$$PE\% = \left|\frac{Experimental\ value - Predicted\ value}{Experimental\ value}\right| \cdot 100 \qquad (14)$$

2. New strategies to cross the BBB: objective 4

2.1. Drugs, cells and products

Ponatinib was purchased from Enamine (Riga, Latvia). Trypan blue, borneol, succinic anhydride and folic acid were acquired from Sigma-Aldrich (Barcelona, Spain). (3-aminopropyl)triethoxysilane (APTES), anhydrous acetonitrile (ACN), cetyltrimethylammonium bromide (CTAB), diethanolamine (DEA), 4-dimethylaminopiridine (DMAP), N-(3-dimethylaminopropyl)-N'-ethylcarbodiimide (EDC), $FeCl_3 \cdot 6H_2O$, $FeCl_2 \cdot 4H_2O$, N-hydroxysuccinimide (NHS), oleic acid and tetraethylorthosilicate (TEOS) were acquired from Sigma-Aldrich (Madrid, Spain). Chloroform, dimethylformamide (DMF), and anhydrous methylene chloride (DCM) were acquired from Acros Organics (Spain). Ammonia (32% v/v), ethanol, dimethyl sulfoxide (DMSO) and ethyl acetate were acquired from Scharlab (Barcelona, Spain).

Lysosomal extract was given by Dr. Martinez-Mañez (Valencia, Spain). The MDCK-MDR1 cell line was kindly provided by Dr. Gottesman, MM (National Institutes of Health, Bethesda) and the U87 cell line was purchased from Sigma-Aldrich (Barcelona, Spain).

Dulbecco's modified Eagle's medium (DMEM) with high content of glucose, fetal bovine serum (FBS), MEM Non-Essential aminoacids, penicillin–streptomycin, L-glutamine, HEPES, phosphate buffer solution (PBS), trypsin-EDTA, Hank's balanced salt solution (HBSS), tween 80 and the cell proliferation kit I (MTT) were purchased from Sigma-Aldrich (Barcelona, Spain). DMEM with high content of glucose and high content of pyruvate used with the U87-MG cell line was obtained from Gibco (Barcelona, Spain).

2.2. Synthesis of mesoporous nanoparticles

Nonmagnetic mesoporous silica nanoparticles (MSNs)

Nonmagnetic mesoporous silica nanoparticles (MSNs) were prepared using as a basis the protocol described in [167]. Briefly, 1 g of CTAB and 20 mL of deionized water were placed in a two neck round bottom flask and stirred for 30 minutes at 500 rpm with a rugby shape magnet. Then, 160 µL of DEA were added and temperature was increased to 95 °C,

temperature at which the mixture was stirred with reflux for 1 hour. After that time, 1.5 mL of TEOS were added dropwise and everything was again stirred for 1 hour, but at 950 rpm. Finally, the particles were recovered and washed with water at 13400 *g* (20 min) until reaching a neutral pH. The particles were then dried and calcined in the presence of air at 550 °C.

Ultrasmall superparamagnetic iron oxide nanoparticles (USPIONs)

Ultrasmall superparamagnetic iron oxide nanoparticles (USPIONs), which were used later on, as seeds for preparing magnetic mesoporous silica nanoparticles (M-MSNs), were prepared according to the protocol described in [168]. First, 50 mL of deionized water were placed under Argon atmosphere for 30 minutes. Then, 12 g of $FeCl_3 \cdot 6H_2O$, 4.9 g of $FeCl_2 \cdot 4H_2O$ and 19.53 mL of ammonia 32% (v/v) were added at 80 °C. After 30 minutes, 2.13 mL of oleic acid was added to the flask and the reaction was left stirring for 90 minutes at 80 °C. Finally, the particles were cooled at room temperature and recovered after washing 3 times with deionized water and 3 times with ethanol (12108 *g*, 10 min). The material was dried overnight under vacuum and the next day it was resuspended in chloroform to be kept it in the fridge until its use.

Magnetic mesoporous silica nanoparticles (M-MSNs)

M-MSNs were prepared following a slightly modified protocol already described in [168]. 100 mg of CTAB and 10 mL of deionized water were placed in a vial and the mixture was stirred until the CTAB was dissolved. Then, 580 µL of a previously prepared suspension of USPIONs in chloroform (Fe concentration = 3.6 mg/mL) was added to the vial and it was sonicated with a probe sonicator (Branson 450 Sonifier) for 3 minutes. After sonication, chloroform was evaporated at 70 °C with manual agitation and 30 mL of deionized water, 0.547 mL of ammonia 32% (v/v) and the particles were placed in a two neck round bottom flask where the mixture was stirred at 400 rpm with reflux and a rugby shape magnet until the temperature reached 75 °C. Later on, 0.5 mL of TEOS and 3 ml of ethyl acetate were added to the flask (TEOS, dropwise) and the reaction was stirred for 2 minutes at 850 rpm and for 3 hours at 350 rpm. At the end of that time, the particles were cooled in an ice bath and they were washed 3 times with ethanol (13400 *g*, 10 min). Finally, the magnetic

particles were separated from the non-magnetic ones with a magnet, they were dried and calcined in the presence of air at 550 °C.

2.3. Drug loading and functionalization of the nanoparticles

MSNs and M-MSNs were loaded following the immersion protocol, in which the particles are left stirring overnight in a solution of drug ((0.8 mmol of drug + 30 mL of solvent)/1 g nanoparticle)). Two different molecules were loaded in the particles: trypan blue and ponatinib, as trypan blue is soluble in water the solvent used for loading the particles was deionized water and as ponatinib is not soluble in water, but soluble in DMSO, this one was the solvent used for dissolving ponatinib. The day after loading, the particles were filtered and dried under vacuum.

Once loaded, both MSNs and M-MSNs were functionalized following the same protocol with the aim of obtaining double gated nanoparticles with: borneol and folic acid.

First, for allowing borneol to attach to the nanoparticles it was modified with succinic acid as done in [139]. Once this component was prepared, particles were reacted with APTES for 5.5 hours in anhydrous ACN ((6 mmol APTES + 30 mL of solvent)/1 g nanoparticles). Then, the particles were vacuum filtered and dried and they were made to react with gate components overnight. So, the following compounds were placed in a vial and left stirred overnight: modified borneol (0.3 mmol/100 mg nanoparticles), folic acid (0.3 mmol/100 mg nanoparticles), EDC (3 mmol/100 mg nanoparticles), NHS (3 mmol/100 mg nanoparticles), DMF (3 mL/100 mg nanoparticles) and DMSO (1 mL/100 mg nanoparticles). Finally, the particles were washed 4 times with DMF and 4 times with deionized water and dried at 37 °C.

2.4. Characterization of the nanoparticles

Dynamic light scattering (DLS)

Dynamic light scattering (DLS) experiments were conducted with a Zetasizer Nano ZS (Malvern Instruments). This technique was used for measuring the hydrodynamic size, the polydispersity index (PDI) and the Z potential of the particles. Suspensions of 1 mg/mL

of nanoparticles were prepared in water and the characteristics mentioned above were measured thrice.

Transmission electron microscopy (TEM)

The proper size and shape of the MSNs and M-MSNs were checked in a 100 kV JEOL JEM-1010 transmission electronic microscope operated with AMT image capture engine software.

X-ray Powder Diffraction Analysis

The X-ray diffractograms of the USPIONS, the MSNs and the M-MSNs (as-made, calcined, calcined and functionalized with borneol and folic acid and loaded with trypan blue and functionalized with borneol and folic acid) were obtained with a Bruker D8 Advance diffractometer (Bruker, Coventry, UK).

Porosimetry

A Micromeritics TriStar II Plus automated analyser (Micromeritics Instrument Corporation, Norcross, GA, USA) was used for recording the N_2 adsorption–desorption isotherms of the MSNs and the M-MSNs. The samples were degassed at 120 °C in vacuum overnight. A BET model was used for calculating the specific surface areas from the adsorption data in the low-pressure range. On the other hand, the BJH method was used to determine the size and volume of the pores present in the particles.

Thermogravimetry

A TGA/SDTA 851e thermobalance from Mettler Toledo (Mettler Toledo Inc., Schwarzenbach, Switzerland) was used to obtain thermograms for different solid samples and evaluate the organic content in loaded and functionalized nanoparticles. So, the % of drug loaded in the MSNs and the M-MSNs could be obtained. Briefly, samples were heated in a dynamic step at 10 °C/min, from 25 °C to 100 °C. Then temperature was maintained at 100 °C for 60 mins and temperature was increased again until 1000 °C at 10 °C/min. Samples were kept at 1000 °C for 30 minutes. Total organic content was evaluated in the range between 100 and 800 °C.

2.5. In vitro drug release

Release studies were carried out at 37 °C for both types of nanoparticles, MSNs and M-MSNs, loaded with trypan blue and ponatinib. First, a suspension of each type of particles, with a particle concentration of 10 µg/µL was prepared in PBS and it was divided into two eppendorfs. Then, PBS or lysosomal extract were added until reach a final concentration of particles of 1 µg/µL. Samples were taken at different times (2', 30', 1h, 2.5h, 4h and 5.5h). They were diluted with cold methanol, centrifuged (5 mins; 10000 rpm - Eppendorf Centrifuge 5424, Rotor FA-45-24-11) and kept in the freezer at -20 °C until their analysis.

2.6. Cytotoxicity assay in vitro

The cytotoxicity of the MSNs and the M-MSNs functionalized with borneol and folic acid and loaded with ponatinib and functionalized with borneol and folic acid was evaluated in two different cell types (U87-MG, glioblastoma cells and MDCK-MDR1, BBB cells) using an MTT kit.

MDCK-MDR1 cells were maintained as explained in section *1.2. Cell culture* of "Materials and methods" and U87-MG cells were kept using the same protocol as MDCK-MDR1, but with a cell culture medium with a higher concentration of pyruvate. The protocol for carrying out the cytotoxicity assay is explained below:

1. 100 µL of cells were seeded in each well of a 96-well plate (2.5 x 10^4 cells/well).
2. After 24 hours at 37 °C, the medium was removed and replaced with 100 µL of a ponatinib solution or a particle suspension with ponatinib concentration ranging from 0.002 to 200 µM.
3. After 72 hours, the solutions/suspensions were aspirated and replaced with 100 µL of fresh culture medium. Then, 10 µL of the MTT labelling reagent were added to the wells and cells were kept in the incubator for 4 hours.
4. 100 µL of solubilization solution was added to the plates and incubated overnight.
5. Finally, the absorbance of the plate was measured at 570 and 630 nm using a microplate reader (Microplate Reader MB-850, Heales®).

2.7. BBB permeability

The penetrability of the formulations (MSN and M-MSN) was evaluated in MDCK-MDR1 monolayers. Cells were seeded in 6-transwell plates with a pore size of 0.4 micron, an effective area of 4.2 cm^2 and a pore density of (100 ± 10) x 10^6 pores/cm^2 and they were maintained, changing the culture medium every 2 days, during 8 days until confluence. Once, the cells were confluent (TEER = 120-140 kΩ/cm^2), the permeability study was carried out using an orbital shaker at 37 °C and 100 rpm.

Standard experiments from apical to basolateral were developed using an initial concentration of trypan blue of 10 and 30 µM and an initial concentration of ponatinib of 10 and 20 µM. In the experiments with the M-MSNs, circular neodymium magnets were placed under each well. Samples were taken from basolateral at 15, 30, 60, 90, 120, 180 and 240 minutes and the mass balance was checked by means of taking two samples from apical at time 0 and 240 minutes, a sample of the particles adhered to the cells and a sample after disrupting the cells with methanol. Samples were kept at -20 °C until their analysis.

2.8. Biodistribution in vivo

The biodistribution of the particles was evaluated in rats. The *in vivo* experiments were approved by the ethical committee of Miguel Hernández University (2021/VSC/PEA/0133 type 2).

After intraperitoneal anaesthesia, healthy wistar rats (≈ 300 g) were administered intravenously or intranasally with a solution of ponatinib or a suspension of MSNs or M-MSNs loaded with ponatinib with a concentration of drug of 3 mg/kg. The rats were previously cannulated at the jugular vein to allow intravenous administration and blood sampling. In addition, the skull of the rats which received the M-MSNs was shaved and a neodymium magnet was attached in between the ears and the eyes. In the intravenous pathway, 5 mL/kg of solvent (DMSO:Tween 80:PBS; 2:1:7) were used to administer the drug as done in [169]; and in the intranasal administration, 20 µL/nostril of the same solvent mixture were used [170]. At different times, blood samples were taken by the cannula. In addition, when the animals were euthanized, its blood was removed with

physiological serum and their brains and other organs were extracted to evaluate the amount of drug present on them. Proteins were precipitated using cold methanol and in the half of the samples, particles were forced to be opened with sodium hydroxide with DMSO (1 %, v/v) and the other half did not receive sodium hydroxide with DMSO (1 %, v/v). All the samples were kept at -20 °C until their analysis.

2.9. Analysis of the samples

Trypan blue was analysed by HPLC using a Waters 2695 separation module, a Waters 2487 UV detector and a XBridge C18 column (3.5 µM, 4.6 x 100 mm) (Barcelona, Spain). The method used was previously validated its characteristics are summarized in table 10.

Table 10. HPLC method for detecting Trypan Blue.

Molecule	**λ** (nm)	**Mobile phase**	**Retention time** (min)	**Flow rate** (mL/min)	**T** (°C)	**Injection volume** (µL)	r^2
Trypan blue	300	20% H_2O 80% ACN	0.750	1	30	90	0.998

Ponatinib samples were sent to Valencia University to be analysed using a QTRAP 6500+ LC-MS/MS System.

RESULTS & DISCUSSION

RESULTS AND DISCUSSION

1. *In vitro* BBB model: objectives 1, 2 and 3

As already mentioned in the introduction of this thesis, about 85% of CNS trials fail, an extremely high percentage which is just below the % for the oncology trials [21]. One of the main reasons for these failures is the inability of the drugs to cross the BBB [22]. So, to avoid the economic losses and the ethical problems derived from the animal and human studies, the use of robust *in vitro* BBB models to evaluate the passage of drugs through the BBB is a good alternative before starting the *in vivo* tests.

The model suggested in 2013 by Mangas Sanjuan *et al*. was the starting point of this thesis. In that model, the researchers used two different monolayers (MDCK and MDCK-MDR1) to simulate the BBB and did 4 different types of experiments (Standard A to B, standard B to A, albumin A to B and brain homogenate B to A). So, they could evaluate not only the drug permeability, but also the access and distribution of drugs in the brain with the following parameters: $Kp_{uu,brain}$, $f_{u,plasma}$, $f_{u,brain}$ and $V_{u,brain}$ [69]. The development of the four experiments and how these parameters are obtained have already been explained in the sections *1.3. Permeability studies* and *1.6. Parameters calculation: P_{app}, $Kp_{uu,brain}$, $f_{u,plasma}$, $f_{u,brain}$ and $V_{u,brain}$* of "Materials and methods".

Substituting the MDCK and MDCK-MDR1 cell lines by another more physiological type of cells (hCMEC/D3) was the first approach tested to optimize the *in vitro* methodology for determining the permeability of drugs through the BBB.

MDCK and MDCK-MDR1 epithelial cells constitute simple BBB models, which are considered appropriate because of their strong tight junctions (TEER = 120-150 kΩ/cm^2) [151,171]. Nonetheless, the MDCK cell type does not express any BBB transporter in significant levels and the MDCK-MDR1 only incorporates the Pgp. On the other hand, the hCMEC/D3 endothelial cell type forms less tightened monolayers (TEER = 30-40 kΩ/cm^2) [151], but it expresses more BBB transporters, which makes it ideal for the study of complex drugs or formulations directed towards the CNS and it could overcome the main disadvantages of using the MDCK and MDCK-MDR1 cell lines (differences in transporters, growth, metabolism and morphology with the endothelial cells of human BBB) [172,173].

Figure 9 shows the permeability rates obtained for seven different drugs when the methodology suggested in 2013 by Mangas Sanjuan *et al*. is tested in the hCMEC/D3 cell line. It can be seen that for those drugs with a high affinity for plasma proteins or brain tissue, whose $f_{u,plasma}$ or $f_{u,brain}$ are lower than 0.5, there is a considerable reduction in permeability when the albumin or the brain homogenate are added to the plasma or the brain compartment of the transwell system. The values of the *in vitro* and *in vivo* neuroPK for each drug, such as the $f_{u,plasma}$ or the $f_{u,brain}$, can be checked in table 11.

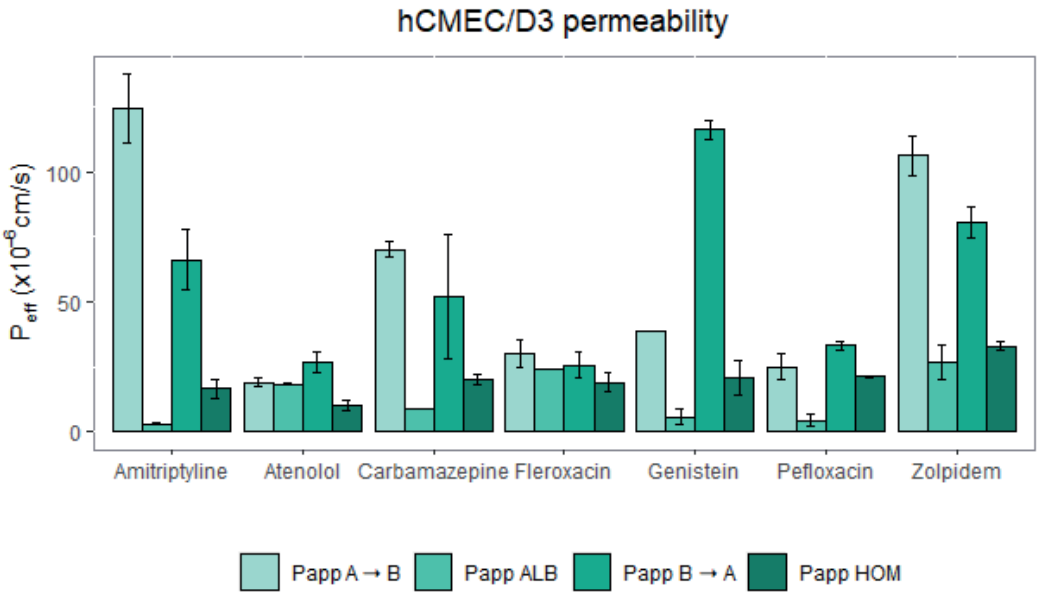

Figure 9. Permeability values ± SD obtained under different experimental conditions with the hCMEC/D3 cell line.

Table 11. Comparison of the *in vitro* and the *in vivo* [155,156] neuroPK parameters.

Drug	$Kp_{uu,brain}$		$f_{u,plasma}$		$f_{u,brain}$		$V_{u,brain}$ (mL/g brain)	
	In vitro	***In vivo***	***In vitro***	***In vivo***	***In vitro***	***In vivo***	***In vitro***	***In vivo***
Amitriptyline	1.876	0.730	0.024	0.090	0.252	0.002	2.577	310.00
Atenolol	0.707	0.030	0.964	1.000	0.379	0.261	1.784	2.500
Carbamazepine	1.351	0.771	0.123	0.385	0.386	0.170	1.755	3.729
Fleroxacin	1.164	0.250	0.814	0.793	0.743	0.555	1.007	1.281
Genistein	0.330	0.181	0.150	0.010	0.177	0.053	3.584	11.499
Pefloxacin	0.753	0.199	0.171	0.860	0.642	0.514	1.134	1.367
Zolpidem	1.314	0.447	0.253	0.267	0.408	0.265	1.671	2.464

After representing together the *in vitro* and the *in vivo* values from table 11, linear IVIVCs can be obtained for each parameter (figure 10). IVIVCs are useful tools which allow researchers to predict the *in vivo* behaviour of a substance without testing it in animals or humans.

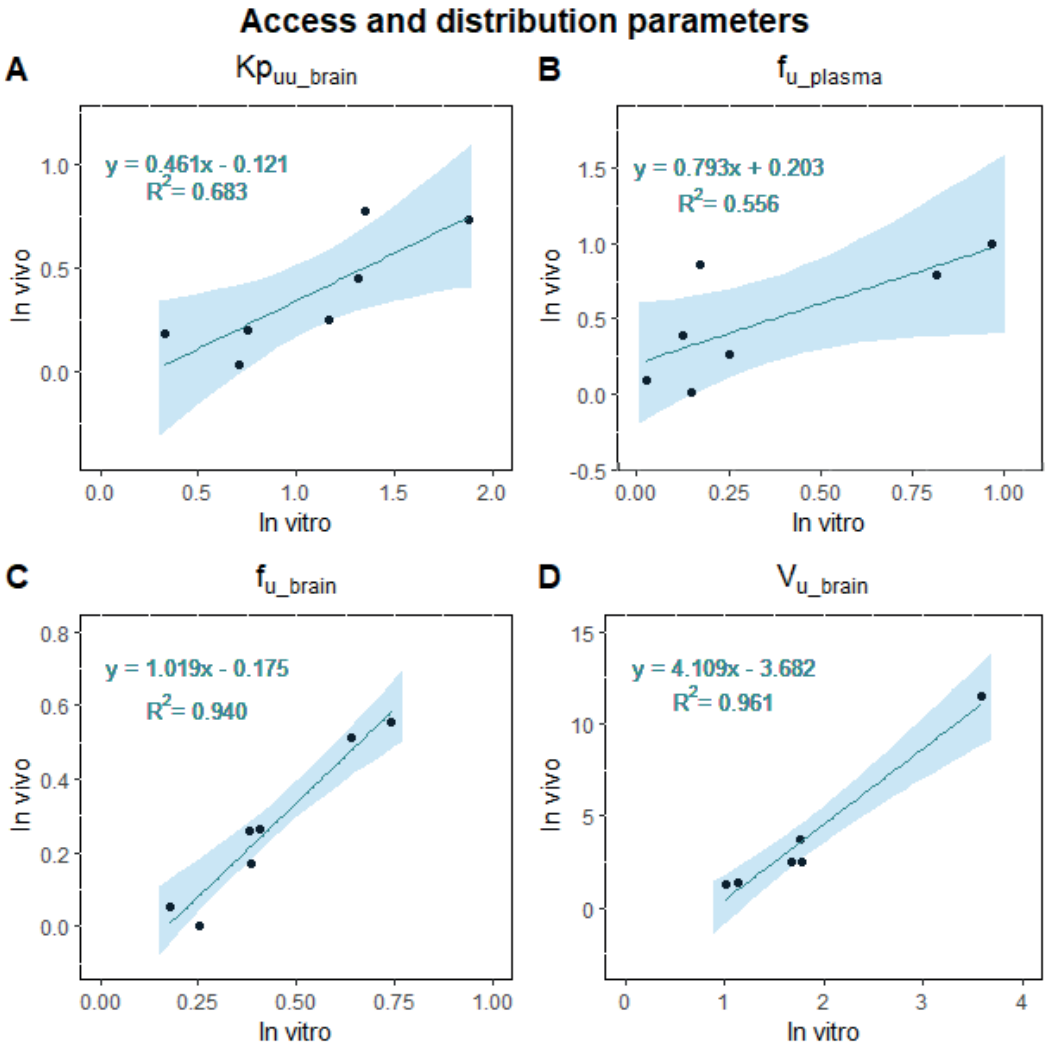

Figure 10. IVIVCs for the different neuroPK parameters (**A)** $Kp_{uu,brain}$, **B)** $f_{u,plasma}$, **C)** $f_{u,brain}$ and **D)** $V_{u,brain}$) with their 95% confidence interval.

From figure 10, it can be extracted that the *in vitro* parameters that are better correlated with their *in vivo* equivalents are the $f_{u,brain}$ and the $V_{u,brain}$ as their coefficients of determination (r^2) are the ones closer to the highest value, one (figure 10C and 10D). This fact highlights the usefulness of the brain homogenate for evaluating the distribution of drugs in the brain. On the other hand, when talking about the $Kp_{uu,brain}$ and the $f_{u,plasma}$, r^2 are not as good as the ones for the previous parameters, but a clear tendency among the values can be observed (figure 10A and 10B).

From these results, it can be concluded that the methodology proposed in 2013 by Mangas Sanjuan *et al*. can be successfully used in another cell line, but, for evaluating which cell line gives the best IVIVCs, the current r^2 and those obtained by Mangas Sanjuan *et al*. are compared in table 12. According to this table, there is not a cell type which could be considered the best one to evaluate the access and distribution of drugs in the brain, as, depending on the parameter, the higher r^2 varies from one cell type to another.

Table 12. Coefficients of determination (r^2) for the IVIVCs obtained for each neuroPK parameter in hCMEC/D3, MDCK [69] and MDCK-MDR1 [69] cell lines.

IVIVC	MDCK	MDCK-MDR1	hCMEC/D3
$Kp_{uu,brain}$	0.063	0.401	0.683
$f_{u,plasma}$	0.846	0.452	0.556
$f_{u,brain}$	0.616	0.624	0.940
$V_{u,brain}$	0.985	0.839	0.961

It is important to remark, that the r^2 = 0.961 for the $V_{u,brain}$ parameter in hCMEC/D3 cells was obtained after discarding the point of amitryptiline, whose *in vivo* value was 310 mL/g brain, but this point was not removed for obtaining the IVIVC for the $f_{u,brain}$ parameter. The discordance between the $f_{u,brain}$ and the $V_{u,brain}$ IVIVCs, which was also observed by Mangas Sanjuan *et al.* as the r^2 from one parameter to the other varies at least 25%, reflects that utility of the system to evaluate the drug distribution in the brain is limited by the fraction of drug that joins the brain tissue. In fact, the $f_{u,brain}$ should not be lower than 0.05 (percentage bound ≥ 95%) to properly use this methodology.

The lack of *in vivo* data from human beings makes necessary the development of the previous IVIVCs with data from rats [155,156] and the mixture of data coming from animals with the *in vitro* data from a cell line of human origin (hCMEC/D3) may be considered a limitation of the study and the main reason for the most complex cell line not showing the best IVIVCs. Nevertheless, the prediction of the permeability values of several drugs with endothelial cells from different species (porcine, bovine, rodent and human) was previously evaluated in 2011 by Avdeef and it was seen that there were not significant differences between species [174]. So, the methodology can be considered appropriate for the early stages of drug development with the three cell lines. Although, if the drug tested is a substrate of several BBB transporters hCMEC/D3 monolayers would be the recommended ones.

The second approach tested in this thesis to optimize the *in vitro* methodology for determining the permeability of drugs through the BBB, relied in the development of a new formulation to act as a surrogate of the brain homogenate used by Mangas Sanjuan *et al*. to evaluate the distribution of drugs in the brain and, thus, obtain an "animal-free" *in vitro* test that would improve the accomplishment of the 3Rs principles (reduction, refinement and replacement). Figure 11 shows a scheme of the idea that guided this approach.

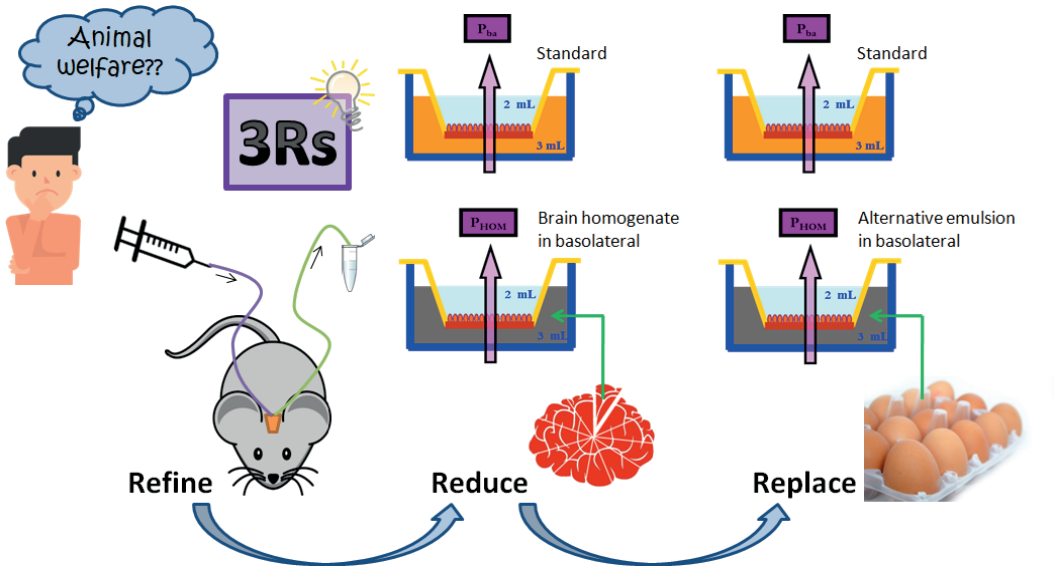

Figure 11. Scheme that shows how the fulfilment of the 3Rs principles can be obtained with the replacement of the brain homogenate by an alternative formulation [153].

A new preparation made of unfertilized chicken eggs was prepared with the same proportion of lipids and proteins than a human brain (12% lipids, from the yolk, and 8% proteins, 5.1% from the yolk and 2.9% from the whites) [175–177]. This formulation was placed in the brain compartment of the transwell system and experiments from the basolateral side to the apical side were carried out with MDCK and MDCK-MDR1 cell lines. Figures 12 and 13 show the IVIVCs obtained for the parameters $f_{u,brain}$ and $V_{u,brain}$ with several drugs when using the MDCK or the MDCK-MDR1 cell line, respectively. The observation of the upper and the middle panels of the figure gives an idea of how the r^2 of the IVIVCs changes when the brain homogenate is replaced with the new emulsion. In addition, the lower panels show the relationship between the *in vitro* values obtained with brain homogenate and the *in vitro* values obtained with the new emulsion.

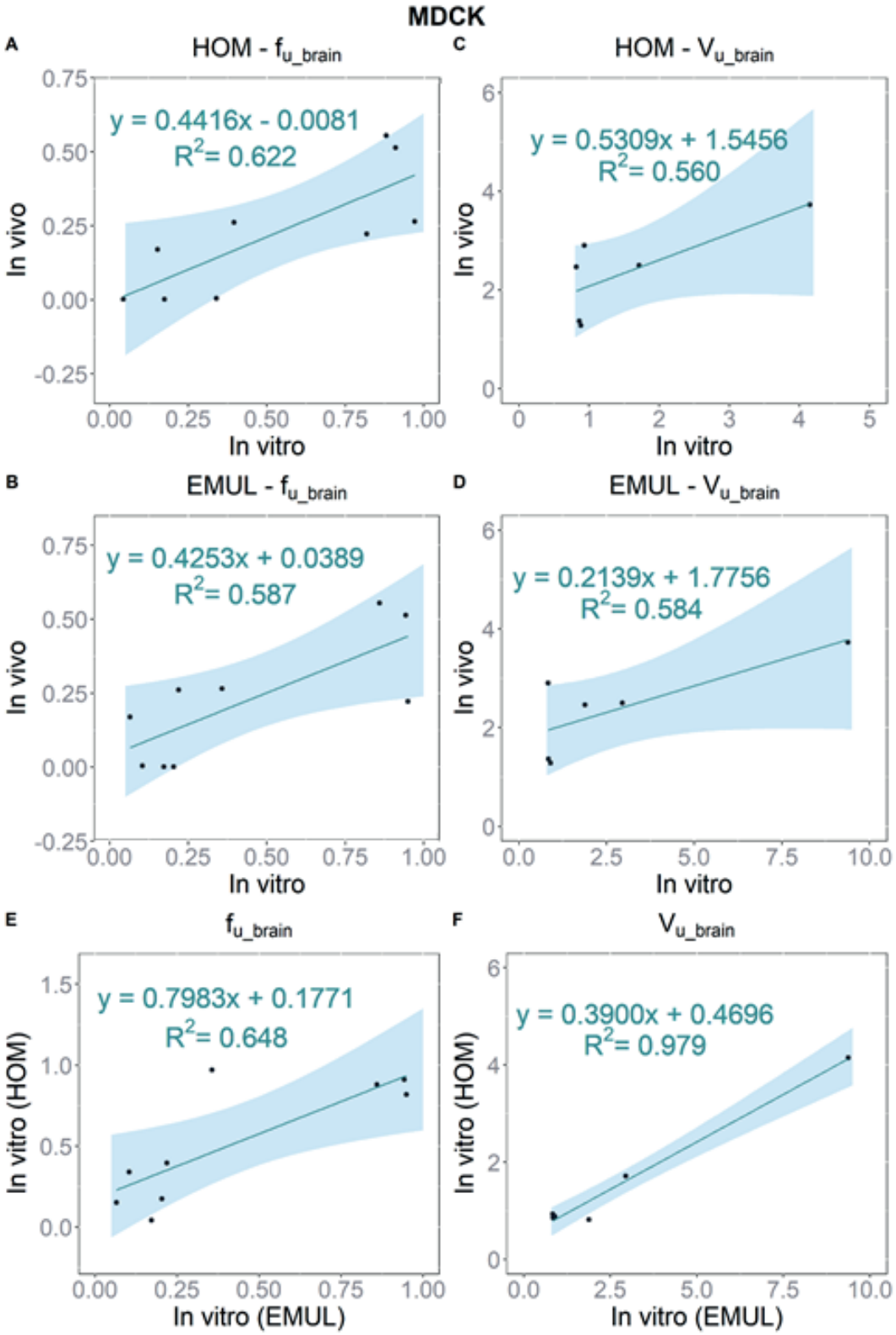

Figure 12. IVIVCs for the parameters $f_{u,brain}$ and $V_{u,brain}$ obtained in the MDCK cell line. **A)** IVIVC for the $f_{u,brain}$ parameter using brain homogenate, **B)** IVIVC for the $f_{u,brain}$ parameter using the alternative formulation, **C)** IVIVC for the $V_{u,brain}$ parameter using brain homogenate, **D)** IVIVC for the $V_{u,brain}$ parameter using the alternative formulation, **E)** Relationship between the $f_{u,brain}$ *in vitro* values and **F)** Relationship between the $V_{u,brain}$ *in vitro* values.

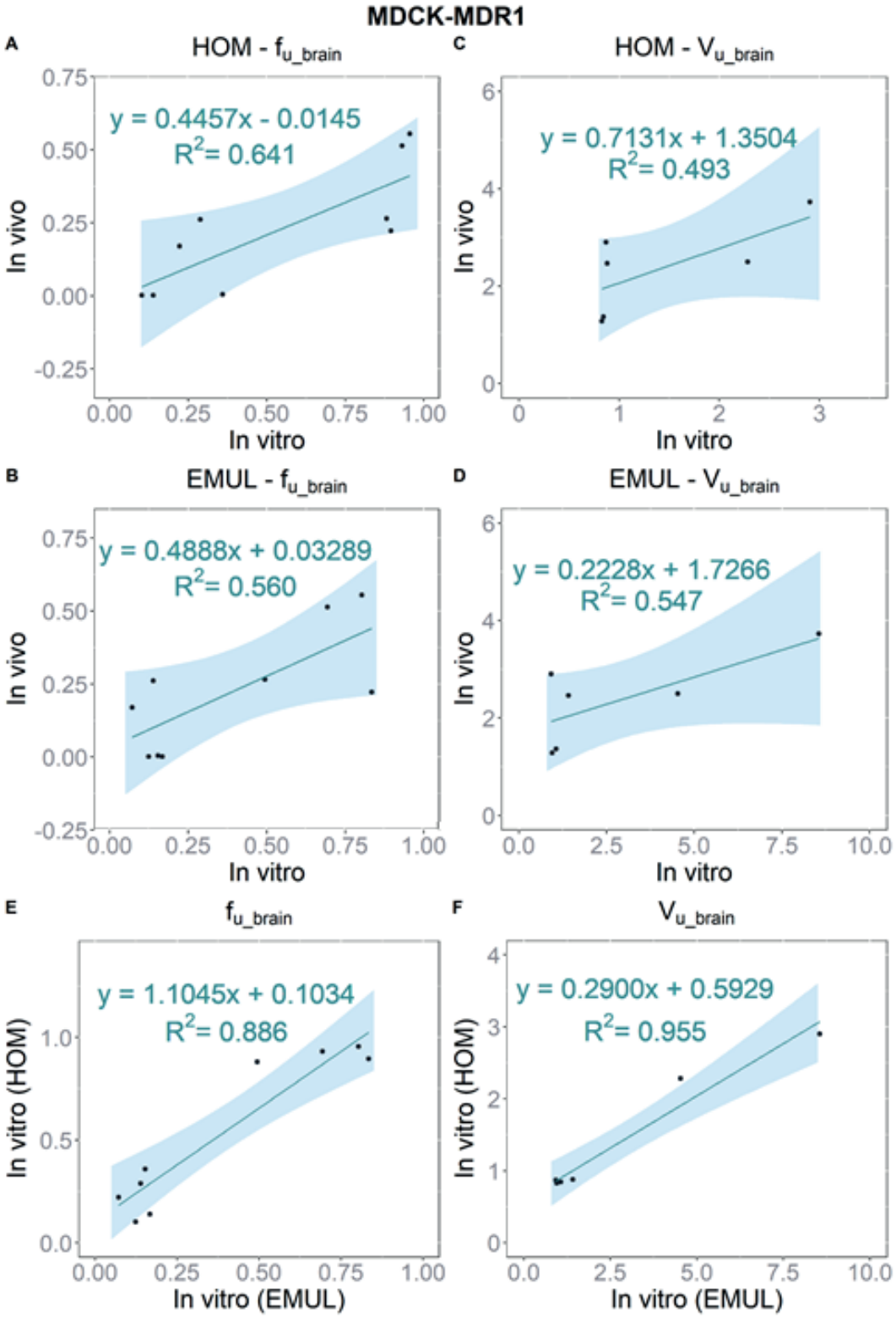

Figure 13. IVIVCs for the parameters $f_{u,brain}$ and $V_{u,brain}$ obtained in the MDCK-MDR1 cell line. **A)** IVIVC for the $f_{u,brain}$ parameter using brain homogenate, **B)** IVIVC for the $f_{u,brain}$ parameter using the alternative formulation, **C)** IVIVC for the $V_{u,brain}$ parameter using brain homogenate, **D)** IVIVC for the $V_{u,brain}$ parameter using the alternative formulation, **E)** Relationship between the $f_{u,brain}$ *in vitro* values and **F)** Relationship between the $V_{u,brain}$ *in vitro* values.

Talking about the $f_{u,brain}$ parameter, it can be seen that there is not a big difference between the r^2 for the IVIVCs obtained with brain homogenate (figures 12A and 13A) and the IVIVCs obtained with the new emulsion (figures 12B and 13B). In fact, those values are quite similar to the ones that Mangas Sanjuan *et al*. obtained in 2013 for that parameter (table 12). Additionally, when the $f_{u,brain}$ values obtained with both *in vitro* methodologies are represented in the same plot (figures 12E and 13E), it can be observed that with the MDCK-MDR1 the values are more similar (r^2 = 0.886) which could be attributed to the presence of Pgp in these cells, as the fraction of drug that binds the transporter does not contribute to the $f_{u,brain}$.

In terms of the $V_{u,brain}$ parameter, similar conclusions can be extracted, as when the IVIVCs for the brain homogenate (figures 12C and 13C) are compared with the IVIVCs for the new emulsion (figures 12D and 13D), there is not a great difference in their r^2. In this case, when both *in vitro* methods are represented together the r^2 are greater than 0.950 for both cell lines (figures 12F and 13F) which may be considered reasonable as the volume of distribution represents what happens to the drug once it is in the brain, with independence of the BBB equilibrium and, thus, with independence of the BBB transporters.

None of the r^2 for any IVIVC is greater than 0.650, this reflects that, also a clear trend can be observed among the points, the IVIVCs are not really good. The main reason for this is the lack of order in both the brain homogenate, whose proteins can be denaturalized and the lipidic structures damaged, and the new emulsion in comparison with an alive *in vivo* brain. Because of that, future investigations may move towards the development of a new organized “animal-free” slice with proteins and lipids placed in a fixed structure so it may predict $f_{u,brain}$ and $V_{u,brain}$ in a better way. Although, previous to that development, the system should be tested using brain slices from animal, instead of brain homogenate, to check how it works.

If a simplification of the system want to be done, the use of the new emulsion could be tested in a non-cell based *in vitro* model, such as the PAMPA-BBB model, which has proved to correctly classify substances in CNS+, CNS- and CNS+/- according to their logBB [63–66], but it may be useful to evaluate the distribution of drugs in the brain too.

As it is, this *in vitro* model will not be used in place of the brain microdialysis technique to evaluate brain distribution, since it cannot reproduce all the physiological properties of an alive CNS. Despite that, it is a useful and rapid screening tool which can be used, on its own or with information from *in silico* [178–180] and PBPK [82,83,181] models, in the early stages of development of new drugs to decide which molecules should be evaluated *in vivo*.

The new formulation developed in this thesis project has advantages in the fields of ethics, economy and industry, i.e.: it speeds up the ethical procedures, as the use of an egg emulsion does not need the approval of a committee, while for obtaining pig brain homogenate an ethical evaluation is necessary and it reduces costs for industry as the maintenance of a cell culture room is cheaper than the maintenance of a stable with animals and staff to take care of them.

With the previous studies, the two first objectives of this thesis were covered, but as being able to predict a complete brain profile for a drug would be more interesting than being able to just obtain its neuroPK parameters, once both approaches were tested, the apparent standard A to B and B to A permeability values and the $f_{u,brain}$ (obtained with brain homogenate) from MDCK, MDCK-MDR1 and hCMEC/D3 cells were used to construct a semi-physiological model to predict concentration levels of drugs in the brain.

Table 13 shows the $P_{app\ A\rightarrow B}$, $P_{app\ B\rightarrow A}$ and $f_{u,brain}$ values used to construct the model for the three cell lines mentioned before. These values can be transformed into the three main neuroPK parameters that can be used to describe the rate and the extent of drug delivery to the brain: the influx clearance (Cl_{in} = $P_{app\ A\rightarrow B}$), the unbound plasma-brain partition coefficient ($Kp_{uu,brain}$, equation 2) and the apparent volume of distribution in the brain ($V_{u,brain}$, equation 5). The $P_{app\ A\rightarrow B}$, $P_{app\ B\rightarrow A}$ and $f_{u,brain}$ values differ from one cell type to another, which can be explained by the differences in terms of morphology, transporters and tight junctions among the different cell monolayers [172,182,183].

Table 13. *In vitro* values obtained in the MDCK, MDCK-MDR1 and hCMEC/D3 cell lines used in the development of a new PBPK model.

Drug	MDCK			MDCK-MDR1			hCMEC/D3		
	AB	BA	$f_{u,brain}$	AB	BA	$f_{u,brain}$	AB	BA	$f_{u,brain}$
Amitriptyline	74.77	178.48	0.037	17.95	16.91	0.104	124.24	66.21	0.252
Caffeine	26.10	35.31	0.857	33.57	30.59	0.613	63.93	194.70	0.095
Carbamazepine	114.64	78.66	0.673	142.96	75.64	0.238	70.14	51.93	0.386
Fleroxacin	88.48	63.44	0.471	67.40	42.57	0.813	29.96	25.73	0.743
Pefloxacin	41.21	37.49	0.910	30.82	35.39	0.931	24.95	33.14	0.642
Zolpidem	21.32	36.48	0.971	8.92	33.43	0.881	106.16	80.76	0.408

AB = $P_{app\ A\rightarrow B}$ ($\cdot 10^{-6}$ cm/s), BA = $P_{app\ B\rightarrow A}$ ($\cdot 10^{-6}$ cm/s)

Scaling factors can be used to correct the differences between an *in vitro* and an *in vivo* system. This strategy was previously followed by Ball *et al*. when developing a PBPK model of the CNS using permeability values coming from *in vitro* tests with Caco-2 cells [82]. In the PBPK model developed in this thesis, which uses *in vitro* data to predict brain profiles in rats, three different scaling factors were defined (SC1, SC2 and SC3), they are summarized in table 14.

Table 14. Summary of the scaling factors used in this PBPK model for each drug and cell line.

Drug	MDCK			MDCK-MDR1			hCMEC/D3		
	SC1	SC2	SC3	SC1	SC2	SC3	SC1	SC2	SC3
Amitriptyline	220.59	224.82	0.05	920.39	2377.06	0.02	132.89	606.69	0.01
Caffeine	3.85	1.00	0.22	2.85	1.00	0.31	4.09	1.00	2.15
Carbamazepine	25.71	81.01	1.16	95.00	391.22	0.71	193.66	569.98	0.44
Fleroxacin	3.18	12.96	1.07	1.59	6.43	0.68	3.58	10.65	0.74
Pefloxacin	4.88	13.32	0.55	6.15	13.19	0.56	7.59	14.09	0.81
Zolpidem	16.53	26.79	0.27	20.59	14.51	0.30	10.26	38.70	0.65

The first and second scaling factors (SC1 and SC2) were used, as Ball *et al*. already did, to estimate the rat influx and efflux clearances from the apparent permeability values from MDCK, MDCK-MDR1 and hCMEC/D3 cells. In an *in vivo* system, such as the rat BBB, the access of drugs to the CNS is limited by the neuro-glial-vascular unit (NGVU), a combination of endothelial cells, neurons, pericytes, astrocytes and smooth muscle cells

[184]. Whereas in cells monolayers, the permeability of a drug, depends on the transporters and tight junctions of just the endothelial cells. The most abundant proteins responsible of tight junctions present in primary rat brain endothelial cells are occludin, the endothelial cell-specific adhesion molecule and claudin-5, in MDCK and MDCK-MDR1 cells the most abundant proteins are claudin-1 and claudin-2 and, in hCMEC/D3, claudin-11 [172].

The third scaling factor (SC3) affects the $f_{u,brain}$ parameter and its use is justified by the homogenization process that destroys the structures of a healthy brain and by the possible differences in composition between a pig brain (animal used to obtain the brain homogenate) and a rat brain (animal for which brain levels want to be predicted).

In figure 14, it can be observed how the use of the scaling factors correct the differences among cell lines, as, once fitted, all the plasma (figure 14.1) and brain (figure 14.2) profiles are overlapping. Nonetheless, for fitting the curves and obtain the scaling factors, both *in vitro* and *in vivo* data are necessary and, as the idea was to use this model to predict the *in vivo* profiles, several QSPRs were developed to allow the prediction of the scaling factors of any drug from its lipophilicity (logP), a descriptor that is frequently used to calculate *in silico* the BBB permeability and the unbound fractions of drug in plasma or brain [185–187]. The QSPRs for each scaling factor and cell line are shown in figure 15.

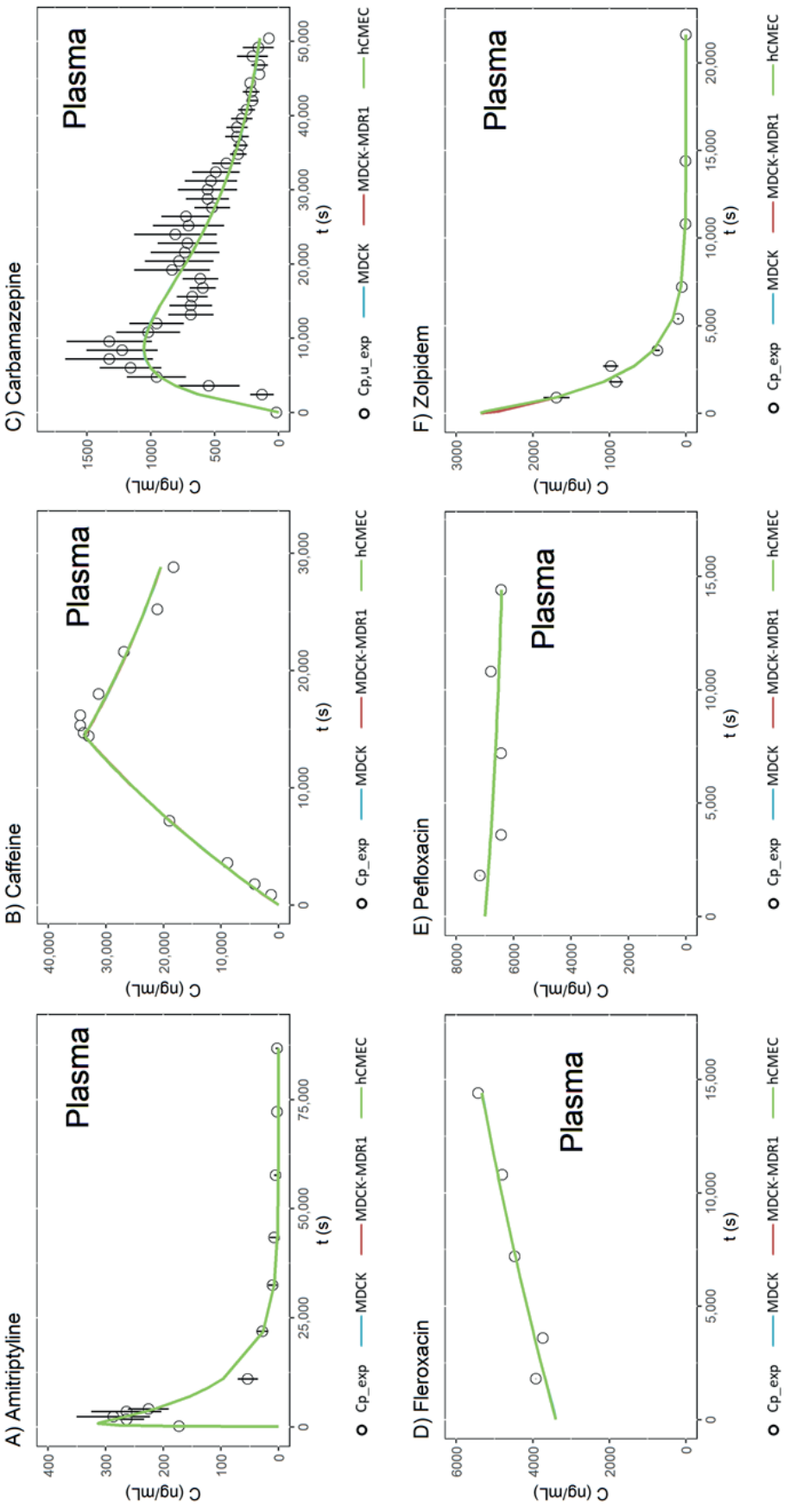

Figure 14.1. Experimental and fitted plasma profiles for amitriptyline, caffeine, carbamazepine, fleroxacin, pefloxacin, zolpidem. Cp_exp = Experimental total plasma concentration, Cp,u_exp = Experimental unbound plasma concentration.

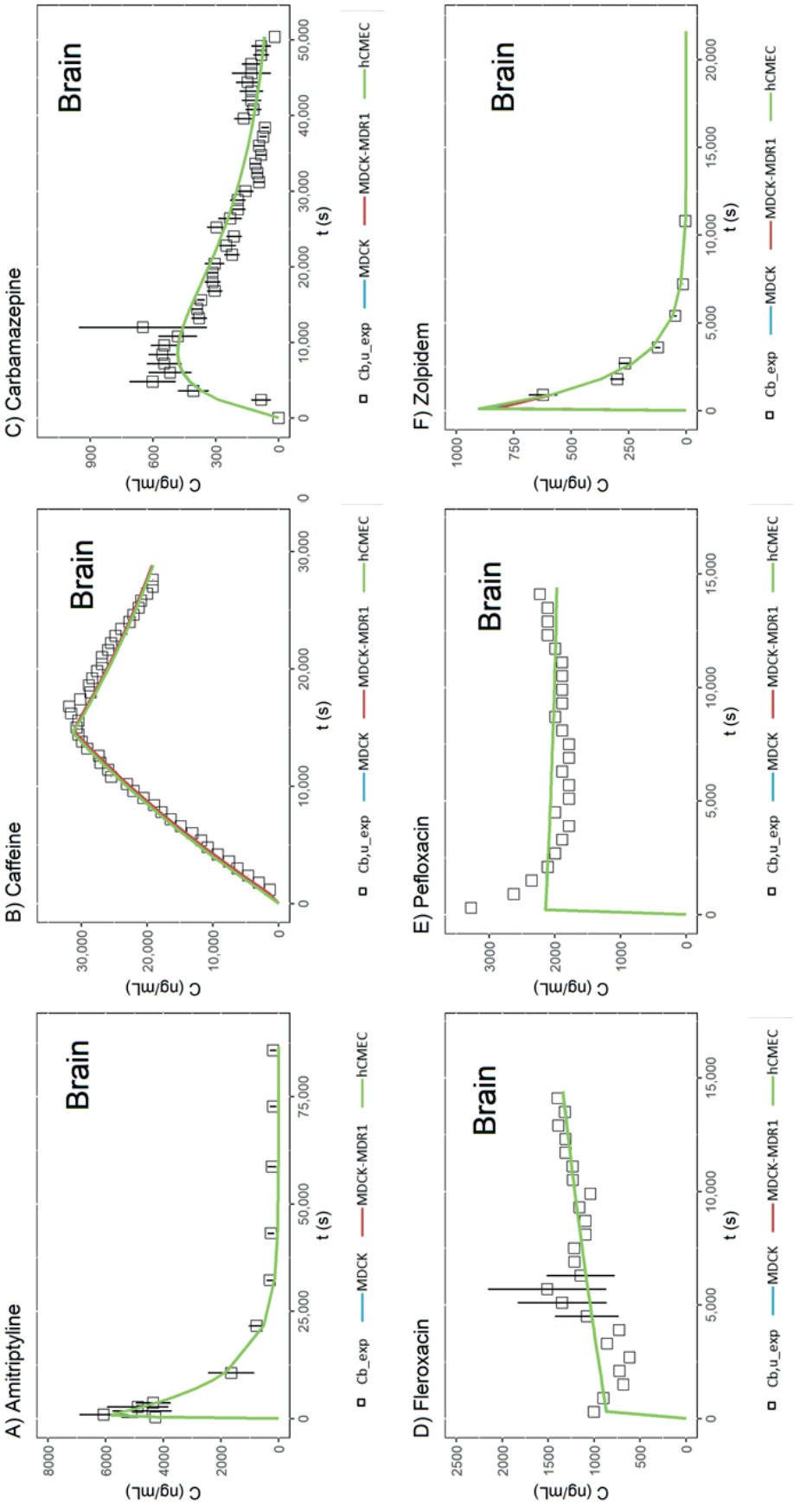

Figure 14.2. Experimental and fitted brain profiles for amitriptyline, caffeine, carbamazepine, fleroxacin, pefloxacin, zolpidem. Cb_exp = Experimental total brain concentration, Cb,u_exp = Experimental unbound brain concentration.

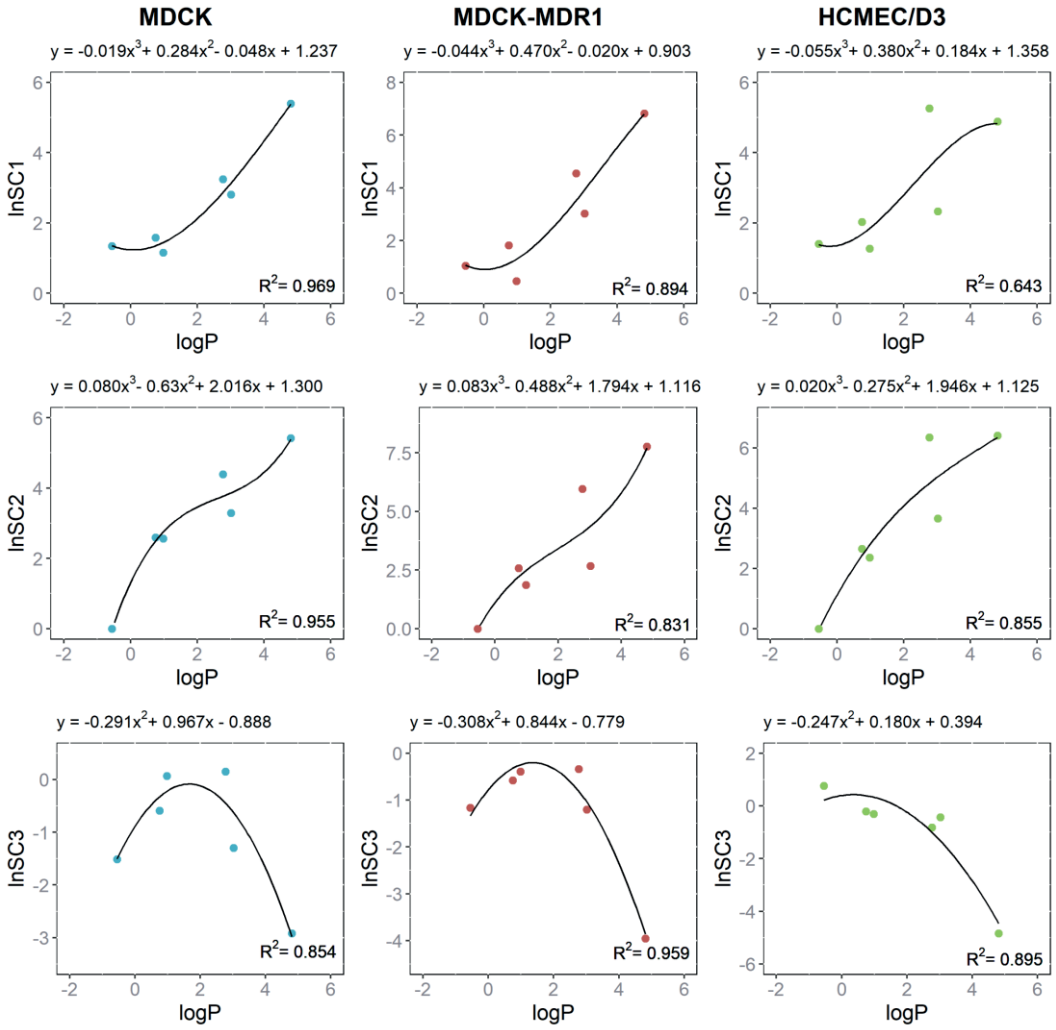

Figure 15. QSPRs between the logP and the natural logarithm of each scaling factor

The QSPRs for SC1 and SC2 have a sigmoidal form while the QSPRs for SC3 are parabolic, these types of trends have been previously observed when relating intestinal and gastric permeability values with lipophilicity [188–190]. Sigmoidal plots obtained with the intestinal barrier were explained by its lipophilic nature, which allows lipidic drugs to cross up, but to a limit, due to the unstirred water layer diffusion. In the gastric barrier, parabolic relationships are obtained because of the presence of alternate lipophilic and hydrophilic layers, which would correspond with the balance of hydrophilic and lipophilic components of the brain homogenate.

To evaluate the predictability of the model, an internal validation was carried out, and the scaling factors obtained for each drug with the QSPRs were used to obtain the simulated brain profiles. Figure 16 shows these profiles with their 95% confidence intervals.

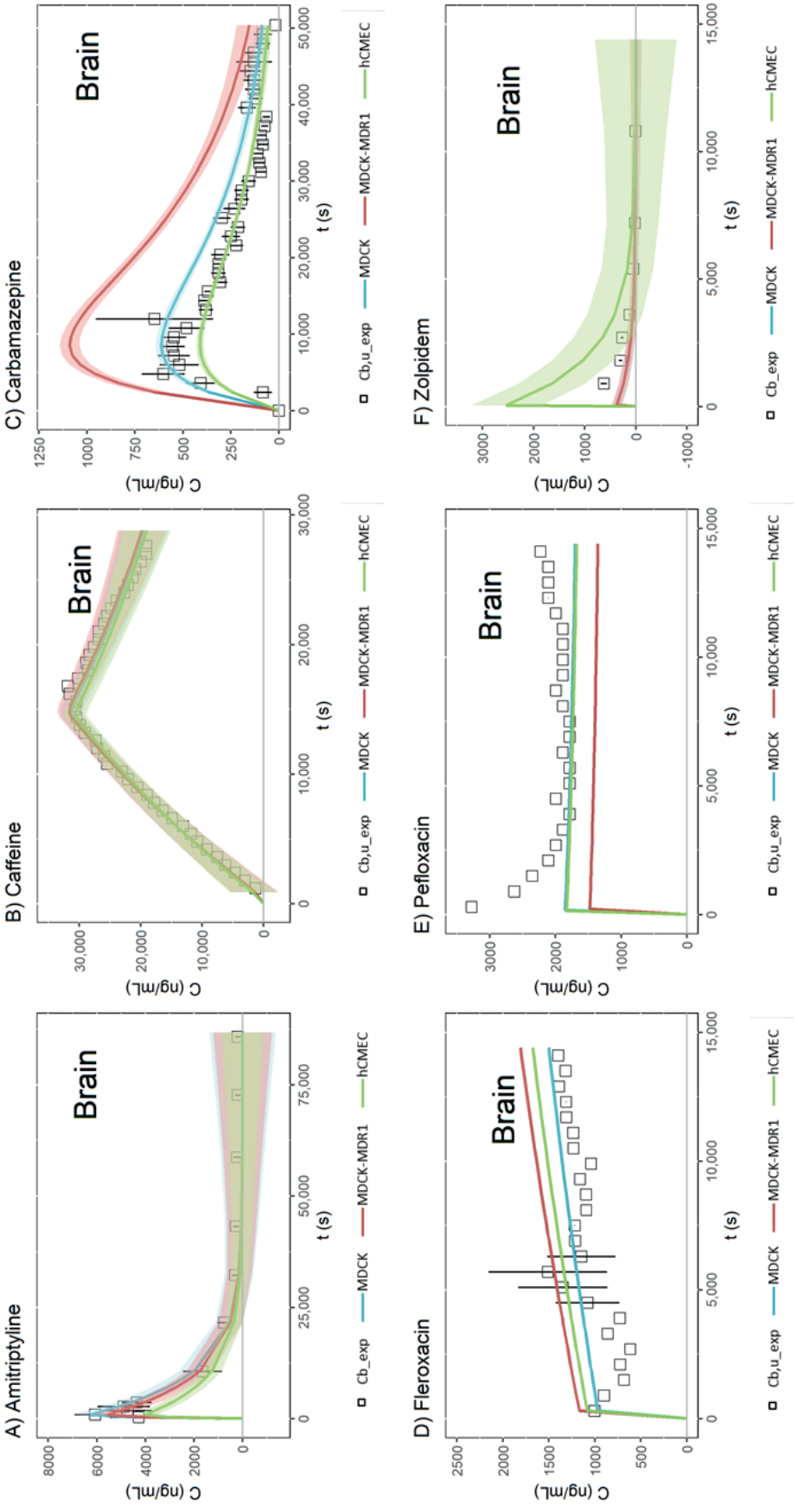

Figure 16. Experimental and simulated brain profiles for amitriptyline, caffeine, carbamazepine, fleroxacin, pefloxacin, zolpidem. Cb_exp = Experimental total brain concentration, Cb,u_exp = Experimental unbound brain concentration.

The %PEs for both fitted and simulated profiles were calculated for the maximum concentration in the brain and the brain AUC for each drug and cell line and the difference between them was evaluated (table 15).

Table 15. Mean %PE for the fitted and simulated brain profiles.

Profile	MDCK		MDCK-MDR1		$f_{u,brain}$	
	%PE C_{max}	%PE AUC	%PE C_{max}	%PE AUC	%PE C_{max}	%PE AUC
Fitted	14.34	5.28	15.05	5.45	13.56	5.16
Simulated	19.23	22.34	35.71	48.21	49.77	46.69

%PE = prediction error percentage, C_{max} = maximum concentration, AUC = area under the curve

In table 15, it can be seen that the simulated profiles adjust worse to the experimental points than the fitted profiles. Nonetheless, all the %PEs are below 50% which can be considered appropriate due to the complexity of this model which mixes *in silico*, *in vitro* and *in vivo* data. The best predictions are obtained for the MDCK cell line (%PEs < 25%), whose simulated profiles are all close to the experimental points, and the %PEs increase with the complexity of the cell line (MDCK-MDR1 < hCMEC/D3). It is thought that this occurs because the equations of the model only include the passive movement of drugs from one compartment to another, but the drugs used to construct the QSPRs and check the predictability of it use both passive and active routes to reach the CNS (table 6) [150]. So, in the MDCK cell line, which has no transporters, all the scaling factors have only a passive component on them, while in the other cell lines, the scaling factor will include only a passive or both, passive and active, components, depending on the route of access of each drug to the brain. In addition, in the hCMEC/D3 cell line, as it has different transporters, the active component of the scaling factors will be more variable than in the MDCK-MDR1 cell line where there is only an efflux transporter (Pgp). Therefore, this model will be appropriate for predicting brain profiles for any kind of drug (with passive or active access to the CNS) when using the MDCK cell line and it could be further improved to be used with the others type of cell in two different ways:

a) Including the active component in the differential equations of the model, for which different concentrations of each drug should be tested *in vitro*.
b) Studying more drugs and developing different QSPRs dividing them in groups depending on the transporter they are substrate of.

2. New strategies to cross the BBB: objective 4

Developing new formulation strategies, such as nanostructures, to increase the access of drugs to the CNS was the last objective of this thesis. So, two different types of nanoparticles were prepared: MSNs and M-MSNs. Figure 17 shows TEM images of both types of particles. It can be observed that MSNs (figure 17A) have a grape form and a particle size which corresponds with the one obtained in the article from which the synthesis method was extracted [167]. In figure 17B, a core-shell structure can be observed in which the magnetic core is surrounded by mesoporous material which creates wormhole-like channels as reported in literature [168].

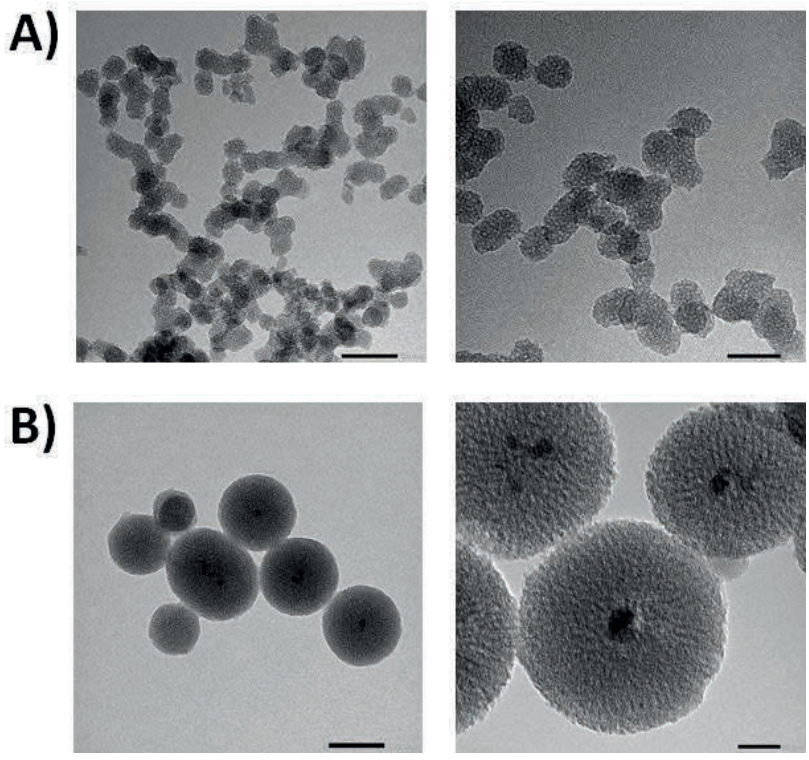

Figure 17. TEM images of **A)** MSNs and **B)** M-MSNs.

The hydrodynamic diameter, the surface charge and the polydispersity of the particles were analysed in a Zetasizer (Figure 18). Both types of particles have a negative charge on their surface once they are prepared and calcined, but once they are functionalized with borneol and folic acid, the charge becomes positive with independence of the loading. In terms of side, the MSNs are smaller than the M-MSNs, but they have a greater polydispersion index, so the batch is less homogeneous. In any case, the real particle size, measured by TEM, is below 100 nm, which allows the particles to cross the BBB [191].

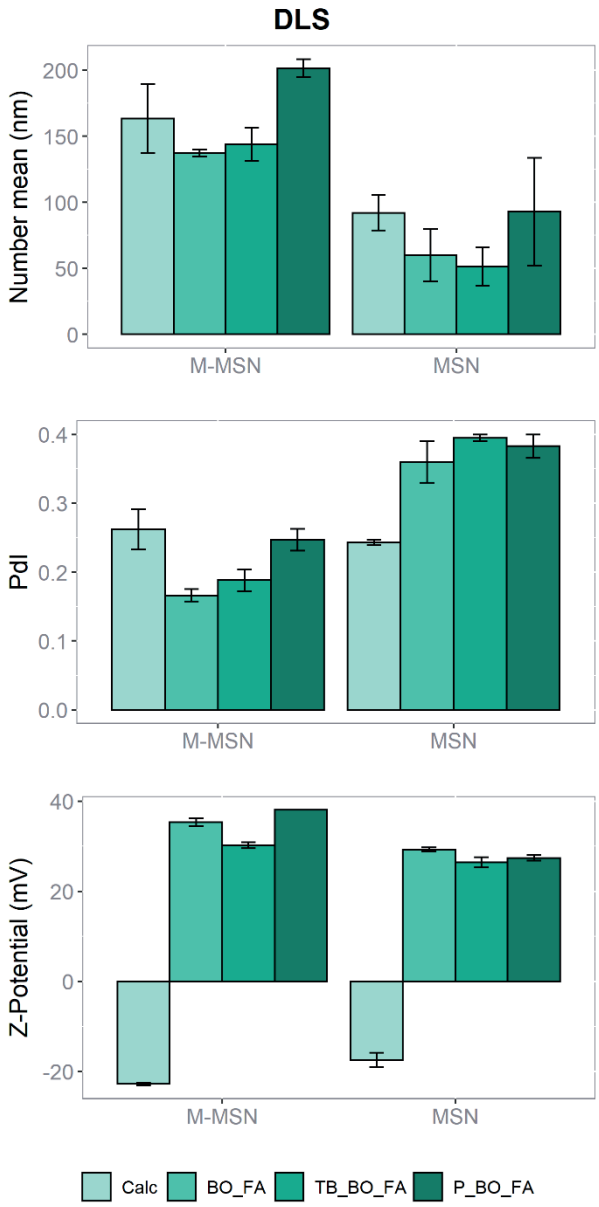

Figure 18. Dynamic light scattering (DLS) results of MSNs and M-MSNs. Calc = calcined, BO_FA = calcined and functionalized with borneol and folic, TB_BO_FA = calcined, loaded with trypan blue and functionalized with borneol and folic and P_BO_FA = calcined, loaded with ponatinib and functionalized with borneol and folic

Figure 19 shows the X-ray diffractograms (XRDs) for the USPIONS, the MSNs and the M-MSNs (as-made, calcined, calcined and functionalized with borneol and folic acid and loaded with trypan blue and functionalized with borneol and folic acid). The magnetic seeds have 6 different peaks whose position and intensity agree with the Bragg reflections of magnetite [168]. On the other hand, the MSNs and the M-MSNs show just one clear peak, which is due to the non-ordered structure of the MSNs and the radial growth of the shell in the M-MSNs [168].

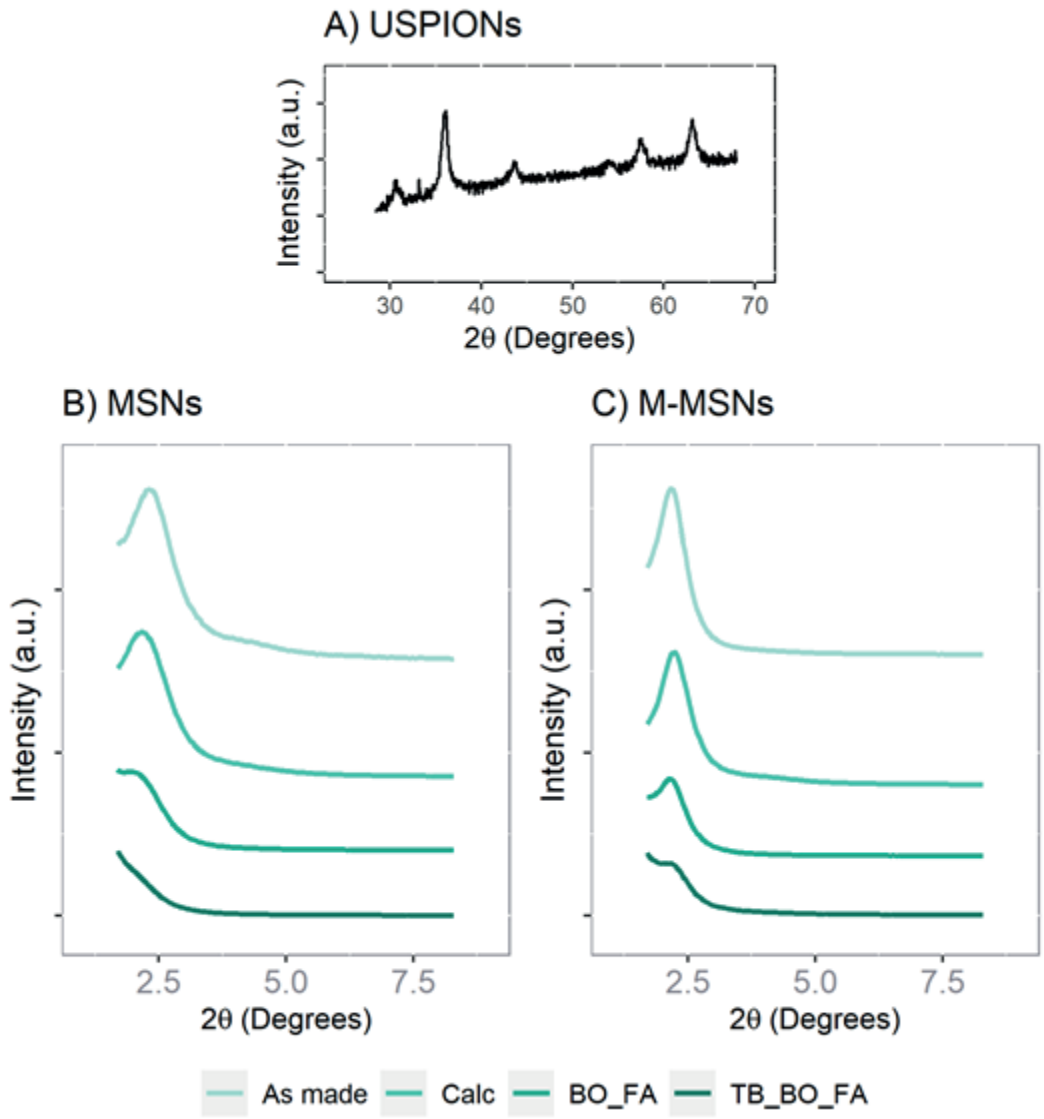

Figure 19. XRDs for **A)** USPIONs, **B)** MSNs and **C)** M-MSNs. Calc = calcined, BO_FA = calcined and functionalized with borneol and folic and TB_BO_FA = calcined, loaded with trypan blue and functionalized with borneol and folic.

The porosimetry analysis showed that, after being prepared and calcined, both types of particles (MSNs and M-MSNs) have similar surface area, pore volume, and pore size (table 16). In addition, as seen in figure 20, the adsorption and desorption isotherms are also very similar and are type IV, which corresponds to mesoporous material [192]. Furthermore, when doing the porosimetry of the nanoparticles with the borneol and folic acid gate, it can be seen that it covers the pores since the adsorption and desorption isotherms decrease and the peak of the pores disappears in the volume-size distribution (figure 20).

Table 16. Mean %PE for the fitted and simulated brain profiles.

Nanoparticle	BET surface area (m^2/g)	BJH Adsorption pore volume (cm^3/g)	BJH Adsorption pore size (nm)
Calcined MSNs	989.317	0.858	2.919
Calcined M-MSNs	896.343	0.802	2.871

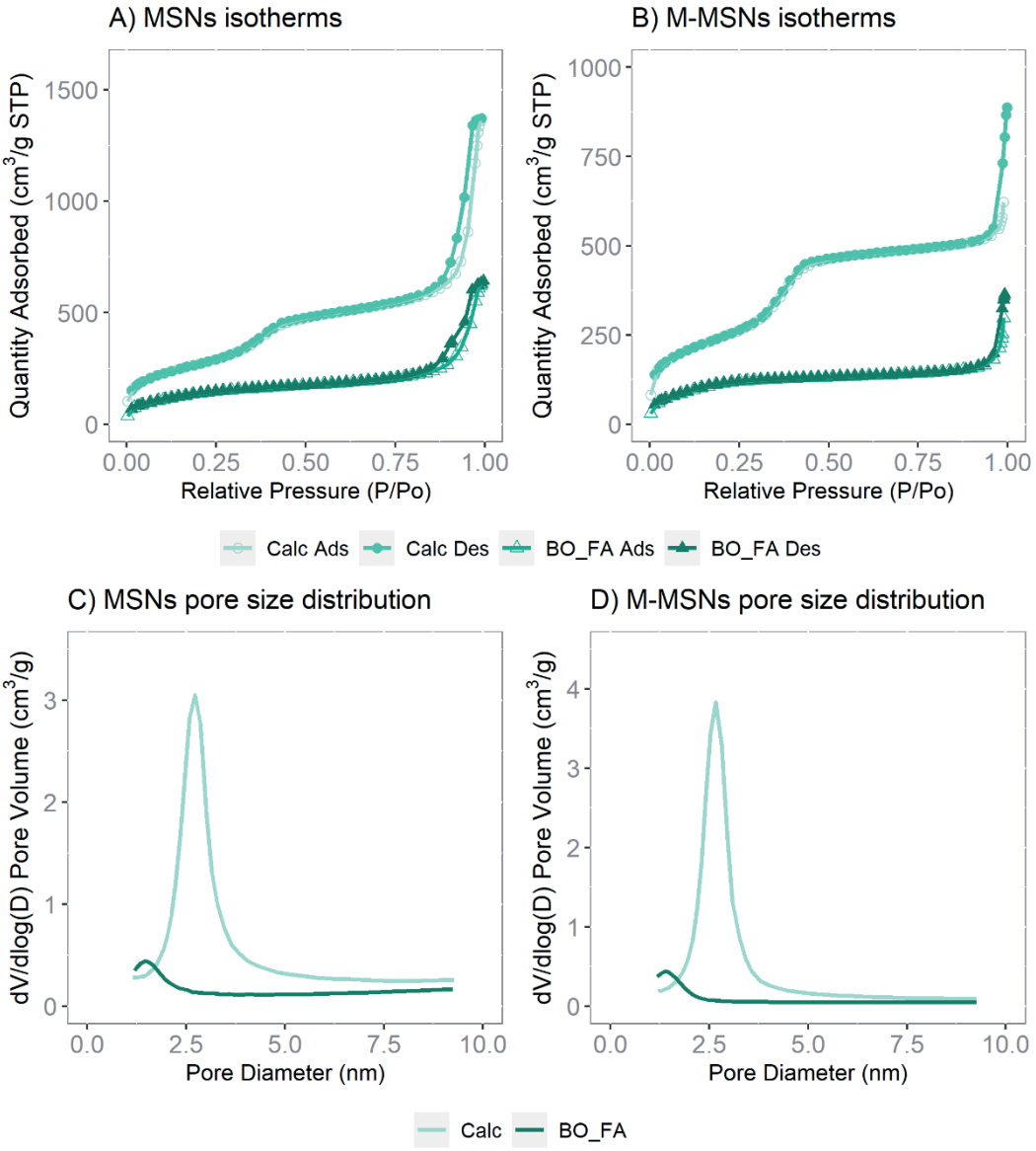

Figure 20. Porosimetry characterization for MSNs and M-MSNs. Calc = calcined, BO_FA = calcined and functionalized with borneol and folic, Ads = adsorption and Des = desorption.

Finally, the last characterization was done by thermogravimetry and gave as a result the organic content of the particles, that is the content of drug loaded in each type of nanoparticle. This result is summarized in table 17.

Table 17. Content of trypan blue and ponatinib in each type of nanoparticle, once calcined and functionalized with borneol and folic acid.

	Trypan Blue (%)	Ponatinib (%)
Final MSNs	11.43	19.04
Final M-MSNs	13.86	14.84

Once the particles were prepared and characterized, the ability of the gate to keep the drug inside them and release it when they are in contact with the correct stimulus was evaluated with an *in vitro* release test. Figure 21 shows the release profiles for both the MSNs and the M-MSNs loaded with trypan blue (figure 21A) or with ponatinib (figure 21B). It can be seen that, when the particles are resuspended in PBS, there is not any released drug, but when they are in touch with an excess of lysozymes, from lysosomal extract, the content of the particles is rapidly released. Profiles were described with a Weibull kinetics model.

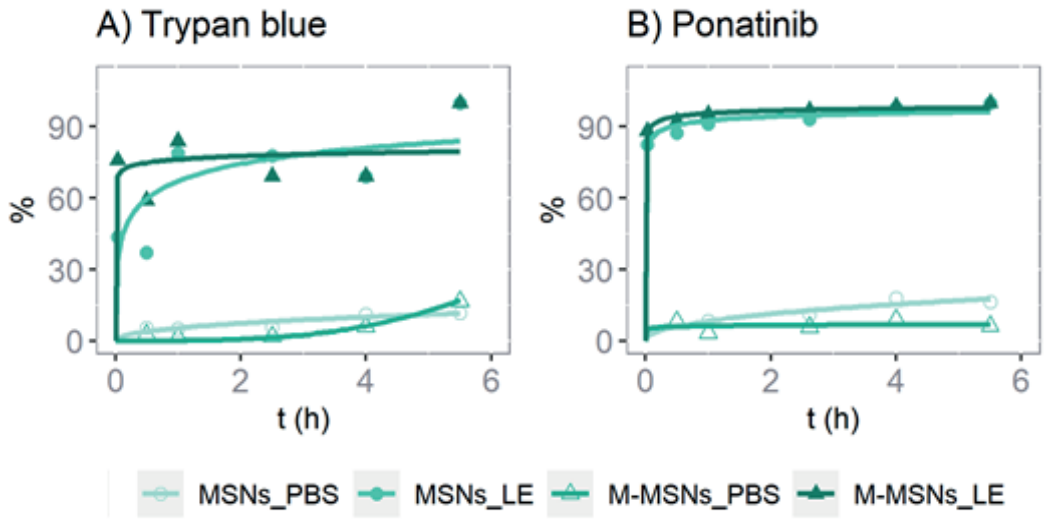

Figure 21. Release profiles for the different nanoparticles with and without stimulus to open the borneol and folic acid gate. LE = lysosomal extract.

In terms of cytotoxicity, two types of study were carried out. First, as it can be seen in figures 22A and 22B, the lack of toxicity of the empty nanoparticles functionalized with borneol and folic acid was evaluated in an *in vitro* BBB model (MDCK-MDR1) and in an *in vitro* glioblastoma model (U87-MG). In figures 22A and 22B, it can be observed that at the highest concentrations tested, 20 and 200 µM, the free Ponatinib is able to kill both types of cells, as it was previously observed by Zhang *et al*. in 2014 [193]. Nonetheless, neither

the empty nanoparticles nor the loaded ones, reduce the viability of the cells at any concentration after 72 hours. This fact confirms that both, the case and the gate of the particles, are not toxic. Besides that, the lack of toxicity of the particles loaded with ponatinib may be explained by the presence of low levels of lysosomes in the *in vitro* culture. So, an extra assay was carried out in the U87-MG cell line after resuspending the particles in lysosomal extract (figure 22C). In this second case, MSNs and M-MSNs with lysozymes are able to kill the glioblastoma cells at the highest concentration tested and, although, the levels of toxicity are not as high as the ones obtained with the free drug, this can be explained by the difficulties of the drug in getting out of the nanoparticle.

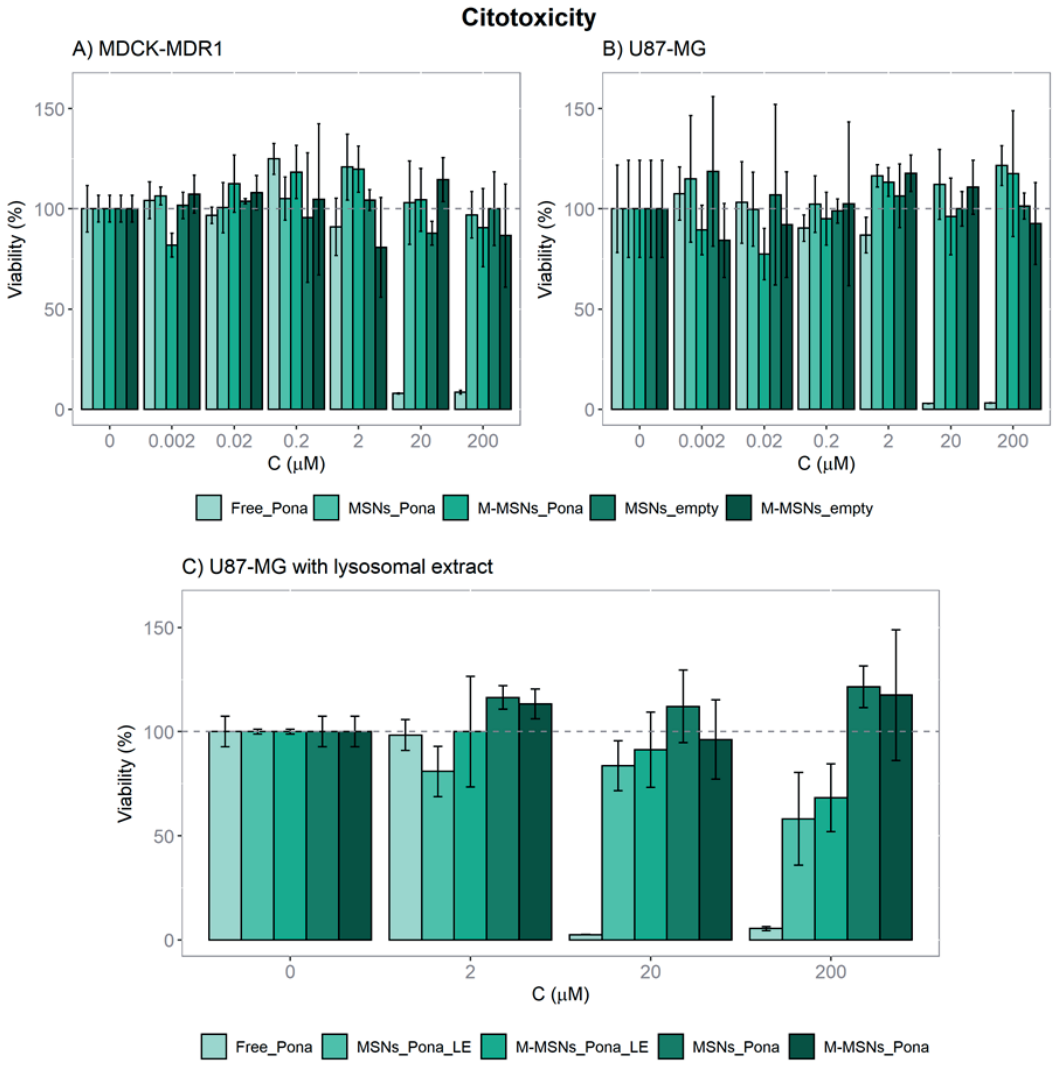

Figure 22. Cytotoxicity results obtained with an MTT assay in **A)** an *in vitro* BBB model and **B)** an *in vitro* glioblastoma model after administering different concentrations of free drug, empty nanoparticles and loaded nanoparticles. **C)** Cytotoxicity results when adding lysosomal extract with the loaded nanoparticles. Pona = ponatinib, LE = lysosomal extract.

When evaluating the *in vitro* BBB permeability of the nanoparticles, it was observed that just in the case of the ones loaded with ponatinib there is a slight increment of the influx clearance (figure 23). Theoretically, both molecules, trypan blue and ponatinib have low access to the CNS. In fact, trypan blue was used in the 20th century when the BBB was discovered as it was observed that after an intravenous injection of this dye, the brain and the spinal cord were not stained [194]. Nonetheless, the toxicity of trypan blue in cell cultures has also been described [195–197], so it is considered that the high permeability rates obtained with both the free trypan blue and the trypan blue loaded in the nanoparticles are due to that toxicity which may alter the tight junctions in the monolayers. Ponatinib is substrate of efflux transporters and it has a low $f_{u,plasma}$ [169]. In this *in vitro* test, the particles increase the permeability rate of this drug, because they prevent the drug from binding to the efflux transporters and they open the tight junctions due to the presence of borneol [95].

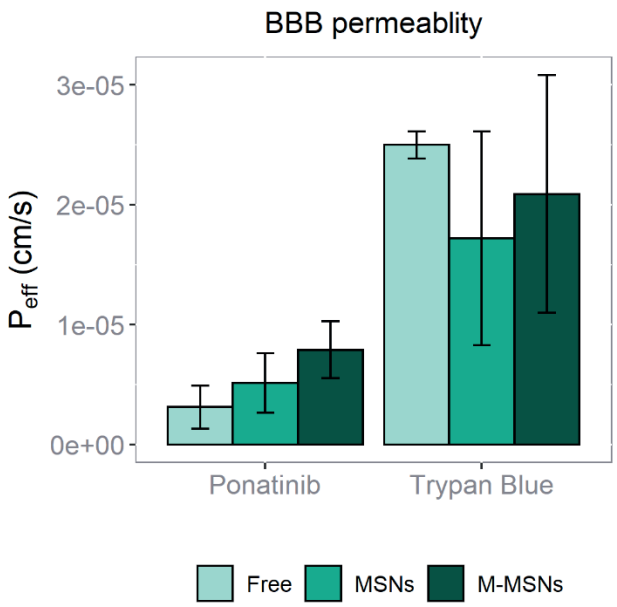

Figure 23. *In vitro* BBB permeability of ponatinib and trypan blue tested in MDCK-MDR1 monolayers as free drug or in MSNs and M-MSNs.

The MSNs and the M-MSNs loaded with ponatinib were selected to evaluate the *in vivo* biodistribution in rats. These studies revealed that the particles were not able to cross the BBB after being administered intravenously. Nonetheless, when the administration was done via intranasal a clear increase in the accumulation of drug in the brain was observed with both, the MSNs and the M-MSNs, in comparison to the free ponatinib (figure 24) and no drug was detected in the rest of the organs.

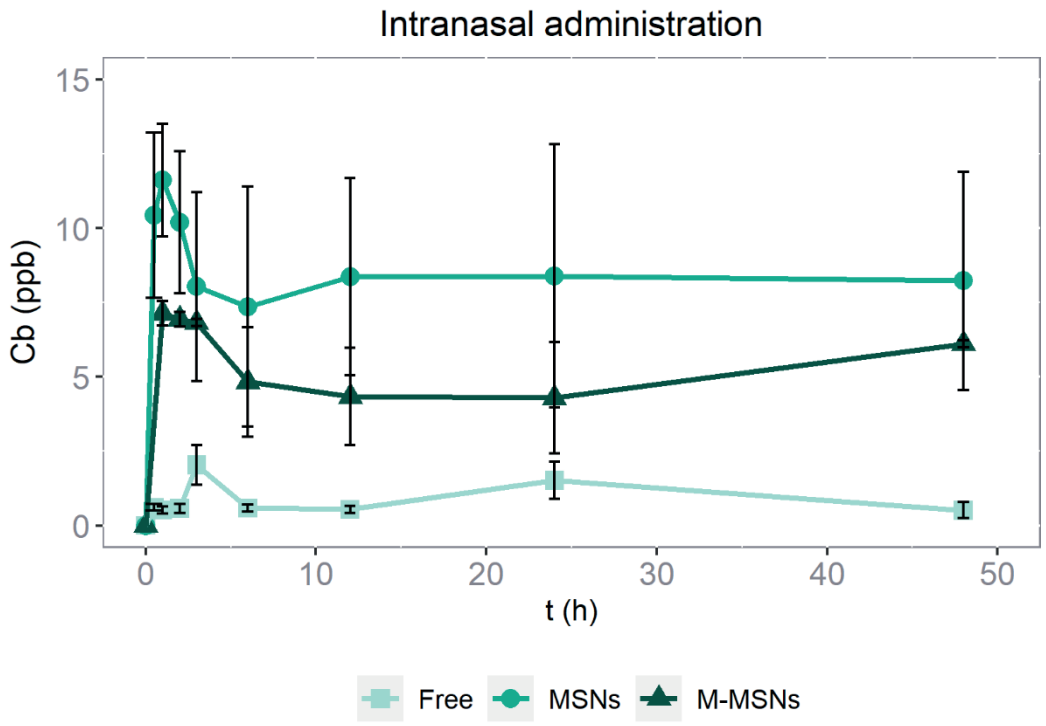

Figure 24. Brain profiles obtained after the intranasal administration of a free ponatinib solution or MSNs and M-MSNs loaded with ponatinib suspensions (Dose = 3 mg/kg).

In figure 24, it can be observed how the use of the nanoparticles increases both the penetration and the retention of ponatinib in the brain of the rats after a single intranasal administration. Probably, it is because the particles are better adhered to the nasal mucosa than the free drug, which may be expelled out of the nostrils or moved down to the respiratory system. Specifically, it can be observed that, after 48 hours, the concentration of ponatinib after the administration of MSNs is 8.9 times the concentration of free ponatinib and after the administration of M-MSNs it is 4.1 times the concentration of free ponatinib. One could expect a greater accumulation when the M-MSNs are used, due to the additional force of the magnet, but it is also true that this type of particle was bigger than the MSNs (figure 17 and 18). In fact, in 2020, a study carried out with a "nose-brain" *in vitro* cell model, showed that the cut-off point for silver nanoparticles to have good access to the brain through the nasal epithelium was 60 nm [198] and, according to the TEM images, the MSNs prepared in this thesis were below 60 nm, but the M-MSNs were above this limit. In addition, the presence of the USPIONs in the core of the M-MSNs can promote its aggregation, increasing even more the final size of the particles present in the administered suspension and hindering the passage to the CNS.

CONCLUSIONES

CONCLUSIONES

De este proyecto de tesis ("Métodos *in vitro* de evaluación biofarmacéutica en la barrera hematoencefálica") se pueden extraer varias conclusiones que responden a los objetivos inicialmente planteados:

1. La metodología *in vitro* para determinar la permeabilidad de la BHE se ha optimizado de dos formas diferentes:

   a. Se ha confirmado que el sistema de 4 experimentos propuesto por Mangas-Sanjuan *et al*. también se puede usar con una línea celular más compleja (hCMEC/D3), que expresa más transportadores de la BHE, y constituye una herramienta de detección de alto rendimiento en el desarrollo farmacéutico.

   b. Se ha desarrollado un nuevo medio artificial, a base de huevos de gallina sin fertilizar, que puede predecir la distribución de fármacos en el SNC de la misma forma que el homogeneizado de cerebro, contribuyendo al refinamiento, la reducción y el remplazo de los animales en investigación.

2. Todos los resultados obtenidos mediante las metodologías *in vitro* optimizadas se han validado mediante el desarrollo de varias correlaciones *in vitro*/*in vivo* (IVIVC) con datos *in vivo* procedentes de ratas.

3. Se ha desarrollado un nuevo modelo semifisiológico, que es capaz de predecir la concentración de varios fármacos en el cerebro de ratas, utilizando datos *in silico* e *in vitro*, provenientes de experimentos con células MDCK, MDCK-MDR1 y hCMEC/D3, como información inicial.

4. Se han desarrollado, caracterizado y evaluado adecuadamente *in vitro* e *in vivo* dos nuevas nanoestructuras mesoporosas, una magnética y otra no magnética, que aumentan el acceso de ponatinib al SNC por vía intranasal.

CONCLUSIONS

CONCLUSIONS

From this thesis project ("*In vitro* methods of biopharmaceutical evaluation in the blood-brain barrier") several conclusions can be extracted which answer the initial objectives:

1. The *in vitro* methodology for determining the permeability of the BBB has been optimized in two different ways:

a. It has been confirmed that the 4 experiments system proposed by Mangas-Sanjuan *et al*. can also be used with a more complex cell line (hCMEC/D3), which expresses more BBB transporters, and it can be used as a high-throughput screening tool in drug development.

b. A new artificial preparation, based on unfertilized chicken eggs, has been developed and it has been able to predict the distribution of drugs in the CNS in the same way that brain homogenate, contributing to the refinement, reduction and replacement of animals in research.

2. All results obtained using the optimized *in vitro* methodologies have been validated by means of the development of several *in vitro*/*in vivo* correlations (IVIVCs) with *in vivo* data coming from rats.

3. A novel semi-physiological model has been developed, which is able to predict the concentration of several drugs in the brain of rats, using *in silico* and *in vitro* data, coming from experiments with MDCK, MDCK-MDR1 and hCMEC/D3 cell lines, as initial information.

4. Two new mesoporous nanostructures, a magnetic and a non-magnetic one, which increase the access of ponatinib to the CNS via intranasal have been developed, characterized and adequately evaluated *in vitro* and *in vivo*.

REFERENCES

REFERENCES

[1] Biga LM, Dawson S, Harwell A, Hopkins R, Kaufmann J, LeMaster M, et al. The Nervous System and Nervous Tissue. Anat. Physiol., OpenStax/Oregon State University; n.d.

[2] Tortora GJ, Derrickson B. Chapter 12: Nervous Tissue. Princ. Anat. Physiol. 11th ed., John Wiley and Sons, Inc.; 2011, p. 407–42.

[3] Tortora GJ, Derrickson B. Chapter 13: The Spinal Cord and Spinal Nerves. Princ. Anat. Physiol. 11th ed., John Wiley and Sons, Inc.; 2011, p. 443–76.

[4] Tortora GJ, Derrickson B. Chapter 14: The Brain and Cranial Nerves. Princ. Anat. Physiol. 11th ed., John Wiley and Sons, Inc.; 2011, p. 477–527.

[5] Telano LN, Baker S. Physiology, Cerebral Spinal Fluid (CSF). StatPearls Publishing; 2018.

[6] Abbot NJ, Patabendige AAK, Dolman DEM, Yusof SR, Begley DJ. Structure and function of the blood-brain barrier. Neurobiol Dis 2010;37:13–25. https://doi.org/10.1016/j.nbd.2009.07.030.

[7] Decimo I, Fumagalli G, Berton V, Krampera M, Bifari F. Meninges: from protective membrane to stem cell niche. Am J Stem Cells 2012;1:92.

[8] Bifari F, Decimo I, Chiamulera C, Bersan E, Malpeli G, Johansson J, et al. Novel stem/progenitor cells with neuronal differentiation potential reside in the leptomeningeal niche. J Cell Mol Med 2009;13:3195. https://doi.org/10.1111/J.1582-4934.2009.00706.X.

[9] Cipolla MJ. Barriers of the CNS. Cereb. Circ., San Rafael: Morgan & Claypool Life Sciences; 2009.

[10] Gordana S. Cerebrospinal fluid flow: Anatomy and functions. Kenhub 2021. https://www.kenhub.com/en/library/anatomy/circulation-of-the-cerebrospinal-fluid (accessed September 8, 2021).

[11] Palmer AM. The role of the blood–CNS barrier in CNS disorders and their treatment. Neurobiol Dis 2010;37:3–12. https://doi.org/10.1016/J.NBD.2009.07.029.

[12] Lochhead JJ, Yang J, Ronaldson PT, Davis TP. Structure, Function, and Regulation of the Blood-Brain Barrier Tight Junction in Central Nervous System Disorders. Front Physiol 2020;0:914. https://doi.org/10.3389/FPHYS.2020.00914.

[13] Kniesel U, Wolburg H. Tight Junctions of the Blood–Brain Barrier. Cell Mol Neurobiol 2000;20:57–76. https://doi.org/10.1023/A:1006995910836.

[14] Armulik A, Genové G, Mäe M, Nisancioglu MH, Wallgard E, Niaudet C, et al. Pericytes regulate the blood–brain barrier. Nature 2010;468:557–61. https://doi.org/10.1038/nature09522.

[15] Abbott NJ, Rönnbäck L, Hansson E. Astrocyte–endothelial interactions at the blood–brain barrier. Nat Rev Neurosci 2006;7:41–53. https://doi.org/10.1038/nrn1824.

[16] Sánchez-Dengra B, González-Álvarez I, Bermejo M, González-Álvarez M. Nanomedicine in

the Treatment of Pathologies of the Central Nervous System Advances in Nanomedicine. Adv. Nanomedicine, 2020.

[17] Laterra J, Keep R, Betz LA, Goldstein GW. Blood—Cerebrospinal Fluid Barrier. In: Siegel G, Agranoff B, Albers R, editors. Basic Neurochem. Mol. Cell. Med. Asp. 6th ed., Philadelphia: Lippincott-Raven; 1999.

[18] SMART - Servier Medical ART n.d. https://smart.servier.com/ (accessed September 8, 2021).

[19] Global Burden of Disease Collaborative Network. Global Burden of Disease Study 2019 (GBD 2019) Results. 2020. http://ghdx.healthdata.org/gbd-results-tool (accessed September 9, 2021).

[20] WHO. Meningococcal meningitis 2018. https://www.who.int/news-room/fact-sheets/detail/meningococcal-meningitis (accessed September 9, 2021).

[21] WCG Institute. CNS Trial Failures Problematic But Fixable, Experts Agree n.d. https://www.wcgclinical.com/insights/institute/cns-trial-failures-problematic-but-fixable-experts-agree (accessed September 9, 2021).

[22] Cummings J. Lessons Learned from Alzheimer Disease: Clinical Trials with Negative Outcomes. Clin Transl Sci 2018;11:147–52. https://doi.org/10.1111/cts.12491.

[23] Savitz SI, Fisher M. Future of neuroprotection for acute stroke: In the aftermath of the SAINT trials. Ann Neurol 2007;61:396–402. https://doi.org/10.1002/ana.21127.

[24] Wegener G, Rujescu D. The current development of CNS drug research. Int J Neuropsychopharmacol 2013;16:1687–93. https://doi.org/10.1017/S1461145713000345.

[25] Paul SM, Mytelka DS, Dunwiddie CT, Persinger CC, Munos BH, Lindborg SR, et al. How to improve R&D productivity: the pharmaceutical industry's grand challenge. Nat Rev Drug Discov 2010;9:203–14. https://doi.org/10.1038/nrd3078.

[26] Morofuji Y, Nakagawa S. Drug Development for Central Nervous System Diseases Using In vitro Blood-brain Barrier Models and Drug Repositioning. Curr Pharm Des 2020;26:1466–85. https://doi.org/10.2174/1381612826666200224112534.

[27] Caban A, Pisarczyk K, Kopacz K, Kapuśniak A, Toumi M, Rémuzat C, et al. Filling the gap in CNS drug development: evaluation of the role of drug repurposing. J Mark Access Heal Policy 2017;5:1299833. https://doi.org/10.1080/20016689.2017.1299833.

[28] Mao X-Y. Drug Repurposing in Neurological Diseases: Opportunities and Challenges. Drug Repurposing - Hypothesis, Mol. Asp. Ther. Appl., IntechOpen; 2020. https://doi.org/10.5772/intechopen.93093.

[29] Wong AD, Ye M, Levy AF, Rothstein JD, Bergles DE, Searson PC. The blood-brain barrier: An engineering perspective. Front Neuroeng 2013;6. https://doi.org/10.3389/fneng.2013.00007.

[30] Teleanu DM, Negut I, Grumezescu V, Grumezescu AM, Teleanu RI. Nanomaterials for drug delivery to the central nervous system. Nanomaterials 2019;9.

https://doi.org/10.3390/nano9030371.

[31] Ohtsuki S, Terasaki T. Contribution of Carrier-Mediated Transport Systems to the Blood–Brain Barrier as a Supporting and Protecting Interface for the Brain; Importance for CNS Drug Discovery and Development. Pharm Res 2007;24:1745–58. https://doi.org/10.1007/s11095-007-9374-5.

[32] Pulgar VM. Transcytosis to cross the blood brain barrier, new advancements and challenges. Front Neurosci 2019;13. https://doi.org/10.3389/fnins.2018.01019.

[33] Löscher W, Potschka H. Blood-brain barrier active efflux transporters: ATP-binding cassette gene family. NeuroRx 2005;2:86–98. https://doi.org/10.1602/neurorx.2.1.86.

[34] Volk H., Burkhardt K, Potschka H, Chen J, Becker A, Löscher W. Neuronal expression of the drug efflux transporter P-glycoprotein in the rat hippocampus after limbic seizures. Neuroscience 2004;123:751–9. https://doi.org/10.1016/j.neuroscience.2003.10.012.

[35] Volk H, Potschka H, Löscher W. Immunohistochemical Localization of P-glycoprotein in Rat Brain and Detection of Its Increased Expression by Seizures Are Sensitive to Fixation and Staining Variables. J Histochem Cytochem 2005;53:517–31. https://doi.org/10.1369/jhc.4A6451.2005.

[36] Schneider SW, Ludwig T, Tatenhorst L, Braune S, Oberleithner H, Senner V, et al. Glioblastoma cells release factors that disrupt blood-brain barrier features. Acta Neuropathol 2004;107:272–6. https://doi.org/10.1007/s00401-003-0810-2.

[37] Mendes B, Marques C, Carvalho I, Costa P, Martins S, Ferreira D, et al. Influence of glioma cells on a new co-culture in vitro blood–brain barrier model for characterization and validation of permeability. Int J Pharm 2015;490:94–101. https://doi.org/10.1016/J.IJPHARM.2015.05.027.

[38] Dwyer J, Hebda JK, Le Guelte A, Galan-Moya E-M, Smith SS, Azzi S, et al. Glioblastoma Cell-Secreted Interleukin-8 Induces Brain Endothelial Cell Permeability via CXCR2. PLoS One 2012;7:e45562. https://doi.org/10.1371/journal.pone.0045562.

[39] Albulescu R, Codrici E, Popescu ID, Mihai S, Necula LG, Petrescu D, et al. Cytokine Patterns in Brain Tumour Progression. Mediators Inflamm 2013;2013:1–7. https://doi.org/10.1155/2013/979748.

[40] Karmur BS, Philteos J, Abbasian A, Zacharia BE, Lipsman N, Levin V, et al. Blood-Brain Barrier Disruption in Neuro-Oncology: Strategies, Failures, and Challenges to Overcome. Front Oncol 2020;10:1811. https://doi.org/10.3389/fonc.2020.563840.

[41] Sarkaria JN, Hu LS, Parney IF, Pafundi DH, Brinkmann DH, Laack NN, et al. Is the blood–brain barrier really disrupted in all glioblastomas? A critical assessment of existing clinical data. Neuro Oncol 2018;20:184–91. https://doi.org/10.1093/neuonc/nox175.

[42] Waubant E. Biomarkers indicative of blood-brain barrier disruption in multiple sclerosis. Dis Markers 2006;22:235–44.

[43] Ortiz GG, Pacheco-Moisés FP, Macías-Islas MÁ, Flores-Alvarado LJ, Mireles-Ramírez MA,

González-Renovato ED, et al. Role of the Blood–Brain Barrier in Multiple Sclerosis. Arch Med Res 2014;45:687–97. https://doi.org/10.1016/j.arcmed.2014.11.013.

[44] Xiao M, Xiao ZJ, Yang B, Lan Z, Fang F. Blood-Brain Barrier: More Contributor to Disruption of Central Nervous System Homeostasis Than Victim in Neurological Disorders. Front Neurosci 2020;14:764. https://doi.org/10.3389/fnins.2020.00764.

[45] Sweeney MD, Sagare AP, Zlokovic B V. Blood–brain barrier breakdown in Alzheimer's disease and other neurodegenerative disorders. Nat Rev Neurol 2018;14:133. https://doi.org/10.1038/NRNEUROL.2017.188.

[46] Profaci CP, Munji RN, Pulido RS, Daneman R. The blood–brain barrier in health and disease: Important unanswered questions. J Exp Med 2020;217. https://doi.org/10.1084/jem.20190062.

[47] Rosenberg GA. Neurological Diseases in Relation to the Blood–Brain Barrier. J Cereb Blood Flow Metab 2012;32:1139–51. https://doi.org/10.1038/jcbfm.2011.197.

[48] Abdullahi W, Tripathi D, Ronaldson PT. Blood-brain barrier dysfunction in ischemic stroke: targeting tight junctions and transporters for vascular protection. Am J Physiol Physiol 2018;315:C343–56. https://doi.org/10.1152/ajpcell.00095.2018.

[49] Yang C, Hawkins KE, Doré S, Candelario-Jalil E. Neuroinflammatory mechanisms of blood-brain barrier damage in ischemic stroke. Am J Physiol Physiol 2019;316:C135–53. https://doi.org/10.1152/ajpcell.00136.2018.

[50] Greene C, Hanley N, Campbell M. Blood-brain barrier associated tight junction disruption is a hallmark feature of major psychiatric disorders. Transl Psychiatry 2020;10:373. https://doi.org/10.1038/s41398-020-01054-3.

[51] Sharma B, Luhach K, Kulkarni GT. In vitro and in vivo models of BBB to evaluate brain targeting drug delivery. Brain Target. Drug Deliv. Syst., Elsevier; 2019, p. 53–101. https://doi.org/10.1016/B978-0-12-814001-7.00004-4.

[52] de Lange E. Methodological considerations of intracerebral microdialysis in pharmacokinetic studies on drug transport across the blood–brain barrier. Brain Res Rev 1997;25:27–49. https://doi.org/10.1016/S0165-0173(97)00014-3.

[53] Syvänen S, Hammarlund-Udenaes M, Loryan I. In Vivo Studies of Drug BBB Transport: Translational Challenges and the Role of Brain Imaging, Springer, Berlin, Heidelberg; 2020, p. 1–22. https://doi.org/10.1007/164_2020_425.

[54] de Lange ECM, Danhof M, de Boer AG, Breimer DD. Critical factors of intracerebral microdialysis as a technique to determined the pharmacokinetics of drugs in rat brain. Brain Res 1994;666:1–8. https://doi.org/10.1016/0006-8993(94)90276-3.

[55] Xie R, Hammarlund-Udenaes M, De Boer AG, De Lange ECM. The role of P-glycoprotein in blood-brain barrier transport of morphine: transcortical microdialysis studies in mdr1a (−/−) and mdr1a (+/+) mice. Br J Pharmacol 1999;128:563–8. https://doi.org/10.1038/sj.bjp.0702804.

[56] Ravenstijn PGM, Merlini M, Hameetman M, Murray TK, Ward MA, Lewis H, et al. The exploration of rotenone as a toxin for inducing Parkinson's disease in rats, for application in BBB transport and PK–PD experiments. J Pharmacol Toxicol Methods 2008;57:114–30. https://doi.org/10.1016/j.vascn.2007.10.003.

[57] Takasato Y, Rapoport SI, Smith QR. An in situ brain perfusion technique to study cerebrovascular transport in the rat. Am J Physiol Circ Physiol 1984;247:H484–93. https://doi.org/10.1152/ajpheart.1984.247.3.H484.

[58] Smith QR, Allen DD. In Situ Brain Perfusion Technique. Blood-Brain Barrier, vol. 89, New Jersey: Humana Press; 2003, p. 209–18. https://doi.org/10.1385/1-59259-419-0:209.

[59] Passeleu-Le Bourdonnec C, Carrupt P-A, Scherrmann JM, Martel S. Methodologies to Assess Drug Permeation Through the Blood–Brain Barrier for Pharmaceutical Research. Pharm Res 2013;30:2729–56. https://doi.org/10.1007/s11095-013-1119-z.

[60] Sánchez-Dengra B, González-Álvarez I, Sousa F, Bermejo M, González-Álvarez M, Sarmento B. In vitro model for predicting the access and distribution of drugs in the brain using hCMEC/D3 cells. Eur J Pharm Biopharm 2021;163:120–6. https://doi.org/10.1016/j.ejpb.2021.04.002.

[61] Pidgeon C, Ong S, Liu H, Qiu X, Pidgeon M, Dantzig AH, et al. IAM chromatography: an in vitro screen for predicting drug membrane permeability. J Med Chem 1995;38:590–4. https://doi.org/10.1021/jm00004a004.

[62] Kansy M, Senner F, Gubernator K. Physicochemical High Throughput Screening: Parallel Artificial Membrane Permeation Assay in the Description of Passive Absorption Processes. J Med Chem 1998;41:1007–10. https://doi.org/10.1021/jm970530e.

[63] Di L, Kerns EH, Fan K, McConnell OJ, Carter GT. High throughput artificial membrane permeability assay for blood–brain barrier. Eur J Med Chem 2003;38:223–32. https://doi.org/10.1016/S0223-5234(03)00012-6.

[64] Di L, Kerns E, Ma X, Huang Y, Carter G. Applications of High Throughput Microsomal Stability Assay in Drug Discovery. Comb Chem High Throughput Screen 2008;11:469–76. https://doi.org/10.2174/138620708784911429.

[65] Di L, Kerns EH, Bezar IF, Petusky SL, Huang Y. Comparison of blood–brain barrier permeability assays: in situ brain perfusion, MDR1-MDCKII and PAMPA-BBB. J Pharm Sci 2009;98:1980–91. https://doi.org/10.1002/jps.21580.

[66] Müller J, Esso K, Dargó G, Könczöl Á, Balogh GT. Tuning the predictive capacity of the PAMPA-BBB model. Eur J Pharm Sci 2015;79:53–60. https://doi.org/10.1016/J.EJPS.2015.08.019.

[67] He Y, Yao Y, Tsirka SE, Cao Y. Cell-Culture Models of the Blood–Brain Barrier. Stroke 2014;45:2514. https://doi.org/10.1161/STROKEAHA.114.005427.

[68] Weksler B, Romero IA, Couraud PO. The hCMEC/D3 cell line as a model of the human blood brain barrier. Fluids Barriers CNS 2013;10. https://doi.org/10.1186/2045-8118-10-

16.

[69] Mangas-Sanjuan V, González-Álvarez I, González-Álvarez M, Casabó VG, Bermejo M. Innovative in vitro method to predict rate and extent of drug delivery to the brain across the blood-brain barrier. Mol Pharm 2013;10:3822–31. https://doi.org/10.1021/mp400294x.

[70] Bagchi S, Chhibber T, Lahooti B, Verma A, Borse V, Jayant RD. In-vitro blood-brain barrier models for drug screening and permeation studies: an overview. Drug Des Devel Ther 2019;13:3591–605. https://doi.org/10.2147/DDDT.S218708.

[71] Nakagawa S, Deli MA, Kawaguchi H, Shimizudani T, Shimono T, Kittel Á, et al. A new blood–brain barrier model using primary rat brain endothelial cells, pericytes and astrocytes. Neurochem Int 2009;54:253–63. https://doi.org/10.1016/J.NEUINT.2008.12.002.

[72] Jiang L, Li S, Zheng J, Li Y, Huang H. Recent Progress in Microfluidic Models of the Blood-Brain Barrier. Micromachines 2019;10:375. https://doi.org/10.3390/mi10060375.

[73] Griep LM, Wolbers F, de Wagenaar B, ter Braak PM, Weksler BB, Romero IA, et al. BBB ON CHIP: microfluidic platform to mechanically and biochemically modulate blood-brain barrier function. Biomed Microdevices 2013;15:145–50. https://doi.org/10.1007/s10544-012-9699-7.

[74] Li G, Shao K, Umeshappa CS. Recent progress in blood-brain barrier transportation research. Brain Target. Drug Deliv. Syst., Elsevier; 2019, p. 33–51. https://doi.org/10.1016/B978-0-12-814001-7.00003-2.

[75] Yamamoto Y, Välitalo PA, Huntjens DR, Proost JH, Vermeulen A, Krauwinkel W, et al. Predicting Drug Concentration-Time Profiles in Multiple CNS Compartments Using a Comprehensive Physiologically-Based Pharmacokinetic Model. CPT Pharmacometrics Syst Pharmacol 2017;6:765–77. https://doi.org/10.1002/psp4.12250.

[76] Vendel E, Rottschäfer V, de Lange ECM. Improving the Prediction of Local Drug Distribution Profiles in the Brain with a New 2D Mathematical Model. Bull Math Biol 2019;81:3477–507. https://doi.org/10.1007/s11538-018-0469-4.

[77] Spreafico M, Jacobson MP. In Silico Prediction of Brain Exposure: Drug Free Fraction, Unbound Brain to Plasma Concentration Ratio and Equilibrium Half-Life. Curr Top Med Chem 2013;13:813–20. https://doi.org/10.2174/1568026611313070004.

[78] Gaohua L, Neuhoff S, Johnson TN, Rostami-Hodjegan A, Jamei M. Development of a permeability-limited model of the human brain and cerebrospinal fluid (CSF) to integrate known physiological and biological knowledge: Estimating time varying CSF drug concentrations and their variability using in vitro data. Drug Metab Pharmacokinet 2016;31:224–33. https://doi.org/10.1016/j.dmpk.2016.03.005.

[79] Yamamoto Y, Välitalo PA, van den Berg D-J, Hartman R, van den Brink W, Wong YC, et al. A Generic Multi-Compartmental CNS Distribution Model Structure for 9 Drugs Allows

Prediction of Human Brain Target Site Concentrations. Pharm Res 2017;34:333–51. https://doi.org/10.1007/s11095-016-2065-3.

[80] Vendel E, Rottschäfer V, de Lange ECM. The need for mathematical modelling of spatial drug distribution within the brain. Fluids Barriers CNS 2019;16:12. https://doi.org/10.1186/s12987-019-0133-x.

[81] Verscheijden LFM, Koenderink JB, de Wildt SN, Russel FGM. Development of a physiologically-based pharmacokinetic pediatric brain model for prediction of cerebrospinal fluid drug concentrations and the influence of meningitis. PLOS Comput Biol 2019;15:e1007117. https://doi.org/10.1371/journal.pcbi.1007117.

[82] Ball K, Bouzom F, Scherrmann JM, Walther B, Declèves X. A physiologically based modeling strategy during preclinical CNS drug development. Mol Pharm 2014;11:836–48. https://doi.org/10.1021/mp400533q.

[83] Sánchez-Dengra B, Gonzalez-Alvarez I, Bermejo M, Gonzalez-Alvarez M. Physiologically Based Pharmacokinetic (PBPK) Modeling for Predicting Brain Levels of Drug in Rat. Pharmaceutics 2021;13:1402. https://doi.org/10.3390/pharmaceutics13091402.

[84] Kaurav H, Kapoor DN. Implantable systems for drug delivery to the brain. Ther Deliv 2017;8:1097–107. https://doi.org/10.4155/tde-2017-0082.

[85] Bors L, Erdő F. Overcoming the Blood–Brain Barrier. Challenges and Tricks for CNS Drug Delivery. Sci Pharm 2019;87:6. https://doi.org/10.3390/scipharm87010006.

[86] Arbor Pharmaceuticals LLC. Gliadel 2021. https://www.gliadel.com/hcp/index.php (accessed November 3, 2021).

[87] Nishikawa R, Iwata H, Sakata Y, Muramoto K, Matsuoka T. Safety of Gliadel Implant for Malignant Glioma: Report of Postmarketing Surveillance in Japan. Neurol Med Chir (Tokyo) 2021;61:oa.2021-0024. https://doi.org/10.2176/nmc.oa.2021-0024.

[88] Gernert M, Feja M. Bypassing the Blood–Brain Barrier: Direct Intracranial Drug Delivery in Epilepsies. Pharmaceutics 2020;12:1134. https://doi.org/10.3390/pharmaceutics12121134.

[89] Salam MT, Mirzaei M, Ly MS, Nguyen DK, Sawan M. An Implantable Closedloop Asynchronous Drug Delivery System for the Treatment of Refractory Epilepsy. IEEE Trans Neural Syst Rehabil Eng 2012;20:432–42. https://doi.org/10.1109/TNSRE.2012.2189020.

[90] Siegel S, Winey K, Gur R, Lenox R, Bilker W, Ikeda D, et al. Surgically Implantable Long-term Antipsychotic Delivery Systems for the Treatment of Schizophrenia. Neuropsychopharmacology 2002;26:817–23. https://doi.org/10.1016/S0893-133X(01)00426-2.

[91] Siegel SJ. Increased patient autonomy through long-term antipsychotic delivery systems for the treatment of schizophrenia. Expert Rev Neurother 2002;2:771–3. https://doi.org/10.1586/14737175.2.6.771.

[92] Krischek B, Kasuya H, Onda H, Hori T. Nicardipine prolonged-release implants for

preventing cerebral vasospasm after subarachnoid hemorrhage: effect and outcome in the first 100 patients. Neurol Med Chir (Tokyo) 2007;47:389–94; discussion 394-6. https://doi.org/10.2176/nmc.47.389.

[93] US National Library of Medicines. A Safety and Efficacy Study of NicaPlant® in Aneurysmal Subarachnoid Haemorrhage Patients Undergoing Aneurysm Clipping - Full Text View - ClinicalTrials.gov 2021. https://clinicaltrials.gov/ct2/show/NCT04269408 (accessed November 4, 2021).

[94] Nau R, Sörgel F, Eiffert H. Penetration of Drugs through the Blood-Cerebrospinal Fluid/Blood-Brain Barrier for Treatment of Central Nervous System Infections. Clin Microbiol Rev 2010;23:858–83. https://doi.org/10.1128/CMR.00007-10.

[95] He Q, Liu J, Liang J, Liu X, Li W, Liu Z, et al. Towards Improvements for Penetrating the Blood–Brain Barrier—Recent Progress from a Material and Pharmaceutical Perspective. Cells 2018;7:24. https://doi.org/10.3390/cells7040024.

[96] Brown RC, Egleton RD, Davis TP. Mannitol opening of the blood–brain barrier: regional variation in the permeability of sucrose, but not 86Rb+ or albumin. Brain Res 2004;1014:221–7. https://doi.org/10.1016/j.brainres.2004.04.034.

[97] Wang Z, Xiong G, Tsang WC, Schätzlein AG, Uchegbu IF. Nose-to-Brain Delivery. J Pharmacol Exp Ther 2019;370:593–601. https://doi.org/10.1124/jpet.119.258152.

[98] Veronesi MC, Alhamami M, Miedema SB, Yun Y, Ruiz-Cardozo M, Vannier MW. Imaging of intranasal drug delivery to the brain. Am J Nucl Med Mol Imaging 2020;10:1–31.

[99] Freiherr J, Hallschmid M, Frey WH, Brünner YF, Chapman CD, Hölscher C, et al. Intranasal Insulin as a Treatment for Alzheimer's Disease: A Review of Basic Research and Clinical Evidence. CNS Drugs 2013;27:505–14. https://doi.org/10.1007/s40263-013-0076-8.

[100] Craft S, Raman R, Chow TW, Rafii MS, Sun C-K, Rissman RA, et al. Safety, Efficacy, and Feasibility of Intranasal Insulin for the Treatment of Mild Cognitive Impairment and Alzheimer Disease Dementia. JAMA Neurol 2020;77:1099. https://doi.org/10.1001/jamaneurol.2020.1840.

[101] Logemann CD, Rankin LM. Newer Intranasal Migraine Medications. Am Fam Physician 2000;61:180–6.

[102] Chi P-W, Hsieh K-Y, Chen K-Y, Hsu C-W, Bai C-H, Chen C, et al. Intranasal lidocaine for acute migraine: A meta-analysis of randomized controlled trials. PLoS One 2019;14:e0224285. https://doi.org/10.1371/journal.pone.0224285.

[103] Menshawy A, Ahmed H, Ismail A, Abushouk AI, Ghanem E, Pallanti R, et al. Intranasal sumatriptan for acute migraine attacks: a systematic review and meta-analysis. Neurol Sci 2018;39:31–44. https://doi.org/10.1007/s10072-017-3119-y.

[104] Rapoport AM, Bigal ME, Tepper SJ, Sheftell FD. Intranasal Medications for the Treatment of Migraine and Cluster Headache. CNS Drugs 2004;18:671–85. https://doi.org/10.2165/00023210-200418100-00004.

[105] Dodick D, Brandes J, Elkind A, Mathew N, Rodichok L. Speed of Onset, Efficacy and Tolerability of Zolmitriptan Nasal Spray in the Acute Treatment of Migraine. CNS Drugs 2005;19:125–36. https://doi.org/10.2165/00023210-200519020-00003.

[106] NeuroPharma® I. Trudhesa™ (dihydroergotamine mesylate) nasal spray | Official Website 2021. https://www.trudhesa.com/ (accessed November 5, 2021).

[107] Drugs.com. Trudhesa (dihydroergotamine mesylate) FDA Approval History 2021. https://www.drugs.com/history/trudhesa.html (accessed November 5, 2021).

[108] Palmeira A, Sousa E, H. Vasconcelos M, M. Pinto M. Three Decades of P-gp Inhibitors: Skimming Through Several Generations and Scaffolds. Curr Med Chem 2012;19:1946–2025. https://doi.org/10.2174/092986712800167392.

[109] Osborne O, Peyravian N, Nair M, Daunert S, Toborek M. The Paradox of HIV Blood–Brain Barrier Penetrance and Antiretroviral Drug Delivery Deficiencies. Trends Neurosci 2020;43:695–708. https://doi.org/10.1016/j.tins.2020.06.007.

[110] Namanja-Magliano HA, Bohn K, Agrawal N, Willoughby ME, Hrycyna CA, Chmielewski J. Dual inhibitors of the human blood-brain barrier drug efflux transporters P-glycoprotein and ABCG2 based on the antiviral azidothymidine. Bioorg Med Chem 2017;25:5128–32. https://doi.org/10.1016/j.bmc.2017.07.001.

[111] Grabrucker AM, Chhabra R, Belletti D, Forni F, Vandelli MA, Ruozi B, et al. Nanoparticles as Blood–Brain Barrier Permeable CNS Targeted Drug Delivery Systems. Top. Med. Chem., vol. 10, Springer, Berlin, Heidelberg; 2013, p. 71–89. https://doi.org/10.1007/7355_2013_22.

[112] Rautio J, Laine K, Gynther M, Savolainen J. Prodrug Approaches for CNS Delivery. AAPS J 2008;10:92–102. https://doi.org/10.1208/s12248-008-9009-8.

[113] Ahlawat J, Guillama Barroso G, Masoudi Asil S, Alvarado M, Armendariz I, Bernal J, et al. Nanocarriers as Potential Drug Delivery Candidates for Overcoming the Blood–Brain Barrier: Challenges and Possibilities. ACS Omega 2020;5:12583–95. https://doi.org/10.1021/acsomega.0c01592.

[114] Alexander A, Agrawal M, Uddin A, Siddique S, Shehata AM, Shaker MA, et al. Recent expansions of novel strategies towards the drug targeting into the brain . Int J Nanomedicine 2019;Volume 14:5895–909. https://doi.org/10.2147/ijn.s210876.

[115] Vieira D, Gamarra L. Getting into the brain: liposome-based strategies for effective drug delivery across the blood–brain barrier. Int J Nanomedicine 2016;Volume 11:5381–414. https://doi.org/10.2147/IJN.S117210.

[116] Ross C, Taylor M, Fullwood N, Allsop D. Liposome delivery systems for the treatment of Alzheimer's disease. Int J Nanomedicine 2018;Volume 13:8507–22. https://doi.org/10.2147/IJN.S183117.

[117] Bana L, Minniti S, Salvati E, Sesana S, Zambelli V, Cagnotto A, et al. Liposomes bi-functionalized with phosphatidic acid and an ApoE-derived peptide affect Aβ aggregation

features and cross the blood–brain-barrier: Implications for therapy of Alzheimer disease. Nanomedicine Nanotechnology, Biol Med 2014;10:1583–90. https://doi.org/10.1016/j.nano.2013.12.001.

[118] Agrawal M, Ajazuddin, Tripathi DK, Saraf S, Saraf S, Antimisiaris SG, et al. Recent advancements in liposomes targeting strategies to cross blood-brain barrier (BBB) for the treatment of Alzheimer's disease. J Control Release 2017;260:61–77. https://doi.org/10.1016/j.jconrel.2017.05.019.

[119] Xiao W, Fu Q, Zhao Y, Zhang L, Yue Q, Hai L, et al. Ascorbic acid-modified brain-specific liposomes drug delivery system with "lock-in" function. Chem Phys Lipids 2019;224:104727. https://doi.org/10.1016/j.chemphyslip.2019.01.005.

[120] He H, Yao J, Zhang Y, Chen Y, Wang K, Lee RJ, et al. Solid lipid nanoparticles as a drug delivery system to across the blood-brain barrier. Biochem Biophys Res Commun 2019;519:385–90. https://doi.org/10.1016/j.bbrc.2019.09.017.

[121] Lombardo SM, Schneider M, Türeli AE, Günday Türeli N. Key for crossing the BBB with nanoparticles: the rational design. Beilstein J Nanotechnol 2020;11:866–83. https://doi.org/10.3762/bjnano.11.72.

[122] Gupta Y, Jain A, Jain SK. Transferrin-conjugated solid lipid nanoparticles for enhanced delivery of quinine dihydrochloride to the brain. J Pharm Pharmacol 2010;59:935–40. https://doi.org/10.1211/jpp.59.7.0004.

[123] Agarwal A, Majumder S, Agrawal H, Majumdar S, P. Agrawal G. Cationized Albumin Conjugated Solid Lipid Nanoparticles as Vectors for Brain Delivery of an Anti-Cancer Drug. Curr Nanosci 2011;7:71–80. https://doi.org/10.2174/157341311794480291.

[124] Huynh NT, Passirani C, Saulnier P, Benoit JP. Lipid nanocapsules: A new platform for nanomedicine. Int J Pharm 2009;379:201–9. https://doi.org/10.1016/j.ijpharm.2009.04.026.

[125] Elhesaisy N, Swidan S. Trazodone Loaded Lipid Core Poly (ε-caprolactone) Nanocapsules: Development, Characterization and in Vivo Antidepressant Effect Evaluation. Sci Rep 2020;10:1964. https://doi.org/10.1038/s41598-020-58803-z.

[126] EU Publications Office. A biomimetic and neuroprotective delivery nanocapsule for the targeted treatment of post-ischemic stroke effects | BIONICS Project | Fact Sheet | H2020 | CORDIS | European Commission 2020. https://cordis.europa.eu/project/id/793644 (accessed November 10, 2021).

[127] Tang X, Zhu Y, Dai J, Ni W, Qian Y, Wei J, et al. Anti-transferrin receptor-modified amphotericin B-loaded PLA-PEG nanoparticles cure Candidal meningitis and reduce drug toxicity. Int J Nanomedicine 2015;10:6227. https://doi.org/10.2147/IJN.S84656.

[128] Barbara R, Belletti D, Pederzoli F, Masoni M, Keller J, Ballestrazzi A, et al. Novel Curcumin loaded nanoparticles engineered for Blood-Brain Barrier crossing and able to disrupt Abeta aggregates. Int J Pharm 2017;526:413–24.

https://doi.org/10.1016/j.ijpharm.2017.05.015.

[129] Ojeda-Hernández DD, Canales-Aguirre AA, Matias-Guiu J, Gomez-Pinedo U, Mateos-Díaz JC. Potential of Chitosan and Its Derivatives for Biomedical Applications in the Central Nervous System. Front Bioeng Biotechnol 2020;8. https://doi.org/10.3389/fbioe.2020.00389.

[130] Bhattamisra SK, Shak AT, Xi LW, Safian NH, Choudhury H, Lim WM, et al. Nose to brain delivery of rotigotine loaded chitosan nanoparticles in human SH-SY5Y neuroblastoma cells and animal model of Parkinson's disease. Int J Pharm 2020;579:119148. https://doi.org/10.1016/j.ijpharm.2020.119148.

[131] Łukasiewicz S, Mikołajczyk A, Szczęch M, Szczepanowicz K, Warszyński P, Dziedzicka-Wasylewska M. Encapsulation of clozapine into polycaprolactone nanoparticles as a promising strategy of the novel nanoformulation of the active compound. J Nanoparticle Res 2019;21:1–16. https://doi.org/10.1007/S11051-019-4587-1/FIGURES/8.

[132] Pissuwan D. Monitoring and tracking metallic nanobiomaterials in vivo. Monit. Eval. Biomater. their Perform. Vivo, Elsevier; 2017, p. 135–49. https://doi.org/10.1016/B978-0-08-100603-0.00007-9.

[133] Bastiancich C, Da Silva A, Estève M-A. Photothermal Therapy for the Treatment of Glioblastoma: Potential and Preclinical Challenges. Front Oncol 2021;10. https://doi.org/10.3389/fonc.2020.610356.

[134] Thomsen LB, Thomsen MS, Moos T. Targeted drug delivery to the brain using magnetic nanoparticles. Ther Deliv 2015;6:1145–55. https://doi.org/10.4155/tde.15.56.

[135] Ding H, Sagar V, Agudelo M, Pilakka-Kanthikeel S, Atluri VSR, Raymond A, et al. Enhanced blood–brain barrier transmigration using a novel transferrin embedded fluorescent magneto-liposome nanoformulation. Nanotechnology 2014;25:055101. https://doi.org/10.1088/0957-4484/25/5/055101.

[136] Saiyed Z, Gandhi N, Nair M. Magnetic nanoformulation of azidothymidine 5’-triphosphate for targeted delivery across the blood–brain barrier. Int J Nanomedicine 2010;5:157. https://doi.org/10.2147/IJN.S8905.

[137] Mendiratta S, Hussein M, Nasser HA, Ali AAA. Multidisciplinary Role of Mesoporous Silica Nanoparticles in Brain Regeneration and Cancers: From Crossing the Blood–Brain Barrier to Treatment. Part Part Syst Charact 2019;36:1900195. https://doi.org/10.1002/ppsc.201900195.

[138] Song Y, Du D, Li L, Xu J, Dutta P, Lin Y. In Vitro Study of Receptor-Mediated Silica Nanoparticles Delivery across Blood–Brain Barrier. ACS Appl Mater Interfaces 2017;9:20410–6. https://doi.org/10.1021/acsami.7b03504.

[139] Xu X, Li J, Han S, Tao C, Fang L, Sun Y, et al. A novel doxorubicin loaded folic acid conjugated PAMAM modified with borneol, a nature dual-functional product of reducing PAMAM toxicity and boosting BBB penetration. Eur J Pharm Sci 2016;88:178–90.

https://doi.org/10.1016/j.ejps.2016.02.015.

[140] Vecsernyés M, Fenyvesi F, Bácskay I, Deli MA, Szente L, Fenyvesi É. Cyclodextrins, Blood–Brain Barrier, and Treatment of Neurological Diseases. Arch Med Res 2014;45:711–29. https://doi.org/10.1016/j.arcmed.2014.11.020.

[141] Wong KH, Xie Y, Huang X, Kadota K, Yao X-S, Yu Y, et al. Delivering Crocetin across the Blood-Brain Barrier by Using γ-Cyclodextrin to Treat Alzheimer's Disease. Sci Rep 2020;10:3654. https://doi.org/10.1038/s41598-020-60293-y.

[142] Badıllı U, Mollarasouli F, Bakirhan NK, Ozkan Y, Ozkan SA. Role of quantum dots in pharmaceutical and biomedical analysis, and its application in drug delivery. TrAC Trends Anal Chem 2020;131:116013. https://doi.org/10.1016/J.TRAC.2020.116013.

[143] Xu G, Mahajan S, Roy I, Yong KT. Theranostic quantum dots for crossing blood–brain barrier in vitro and providing therapy of HIV-associated encephalopathy. Front Pharmacol 2013;4. https://doi.org/10.3389/FPHAR.2013.00140.

[144] Ribovski L, de Jong E, Mergel O, Zu G, Keskin D, van Rijn P, et al. Low nanogel stiffness favors nanogel transcytosis across an in vitro blood–brain barrier. Nanomedicine Nanotechnology, Biol Med 2021;34:102377. https://doi.org/10.1016/j.nano.2021.102377.

[145] Karami Z, Saghatchi Zanjani MR, Hamidi M. Nanoemulsions in CNS drug delivery: recent developments, impacts and challenges. Drug Discov Today 2019;24:1104–15. https://doi.org/10.1016/j.drudis.2019.03.021.

[146] Fu H, McCarty DM. Crossing the blood–brain-barrier with viral vectors. Curr Opin Virol 2016;21:87–92. https://doi.org/10.1016/j.coviro.2016.08.006.

[147] Chen W, Yao S, Wan J, Tian Y, Huang L, Wang S, et al. BBB-crossing adeno-associated virus vector: An excellent gene delivery tool for CNS disease treatment. J Control Release 2021;333:129–38. https://doi.org/10.1016/j.jconrel.2021.03.029.

[148] Pattali R, Mou Y, Li X-J. AAV9 Vector: a Novel modality in gene therapy for spinal muscular atrophy. Gene Ther 2019;26:287–95. https://doi.org/10.1038/s41434-019-0085-4.

[149] Chemicalize. Chemicalize - Instant Cheminformatics Solutions n.d. https://chemicalize.com/welcome (accessed May 3, 2020).

[150] DrugBank. DrugBank n.d. https://www.drugbank.ca/ (accessed May 14, 2020).

[151] Mangas-Sanjuan V, Gonzalez-Alvarez M, Gonzalez-Alvarez I, Bermejo M. In vitro methods for assessing drug access to the brain. Adv. Non-Invasive Drug Deliv. to Brain, Marshall University, USA: Future Science Ltd; 2015, p. 44–61. https://doi.org/10.4155/9781909453937.FSEB2013.13.61.

[152] del Moral-Sanchez J, Ruiz-Picazo A, Gonzalez-Alvarez M, Navarro A, Gonzalez-Alvarez I, Bermejo M. Impact on intestinal permeability of pediatric hyperosmolar formulations after dilution: Studies with rat perfusion method. Int J Pharm 2019;557:154–61.

https://doi.org/10.1016/J.IJPHARM.2018.12.047.

[153] Sánchez-Dengra B, González-Álvarez I, González-Álvarez M, Bermejo M. New In Vitro Methodology for Kinetics Distribution Prediction in the Brain. An Additional Step towards an Animal-Free Approach. Animals 2021;11:3521. https://doi.org/10.3390/ani11123521.

[154] Mangas-Sanjuan V, González-Álvarez I, González-Álvarez M, Casabó VG, Bermejo M. Modified nonsink equation for permeability estimation in cell monolayers: Comparison with standard methods. Mol Pharm 2014;11:1403–14. https://doi.org/10.1021/mp400555e.

[155] Fridén M, Gupta A, Antonsson M, Bredberg U, Hammarlund-Udenaes M. In vitro methods for estimating unbound drug concentrations in the brain interstitial and intracellular fluids. Drug Metab Dispos 2007;35:1711–9. https://doi.org/10.1124/dmd.107.015222.

[156] Kodaira H, Kusuhara H, Fujita T, Ushiki J, Fuse E, Sugiyama Y. Quantitative evaluation of the impact of active efflux by P-glycoprotein and breast cancer resistance protein at the blood-brain barrier on the predictability of the unbound concentrations of drugs in the brain using cerebrospinal fluid concentration as a. J Pharmacol Exp Ther 2011;339:935–44. https://doi.org/10.1124/jpet.111.180398.

[157] Engelhard HH, Arnone GD, Mehta AI, Nicholas MK. Biology of the Blood-Brain and Blood-Brain Tumor Barriers. Handb. Brain Tumor Chemother. Mol. Ther. Immunother. Second Ed., Elsevier Inc.; 2018, p. 113–25. https://doi.org/10.1016/B978-0-12-812100-9.00008-5.

[158] Coudore F, Besson A, Eschalier A, Lavarenne J, Fialip J. Plasma and brain pharmacokinetics of amitriptyline and its demethylated and hydroxylated metabolites after one and six half-life repeated administrations to rats. Gen Pharmacol 1996;27:215–9. https://doi.org/10.1016/0306-3623(95)02008-x.

[159] Hansen DK, Scott DO, Otis KW, Lunte SM. Comparison of in vitro BBMEC permeability and in vivo CNS uptake by microdialysis sampling. J Pharm Biomed Anal 2002;27:945–58. https://doi.org/10.1016/s0731-7085(01)00542-8.

[160] Remmel RP, Sinz MW, Cloyd JC. Dose-Dependent Pharmacokinetics of Carbamazepine in Rats: Determination of the Formation Clearance of Carbamazepine-10,11-epoxide. Pharm Res An Off J Am Assoc Pharm Sci 1990;7:513–7. https://doi.org/10.1023/A:1015872901523.

[161] Graumlich JF, McLaughlin RG, Birkhahn D, Shah N, Burk A, Jobe PC, et al. Subcutaneous microdialysis in rats correlates with carbamazepine concentrations in plasma and brain. Epilepsy Res 2000;40:25–32. https://doi.org/10.1016/s0920-1211(00)00110-8.

[162] Weidekamm E, Portmann R, Suter K, Partos C, Dell D, Lucker PW. Single- and multiple-dose pharmacokinetics of fleroxacin, a trifluorinated quinolone, in humans. Antimicrob Agents Chemother 1987;31:1909–14. https://doi.org/10.1128/AAC.31.12.1909.

[163] Chartrand SA. Quinolones in Animal Models of Infection. In: Siporin C, Heifetz C, Domagala J, editors. New Gener. Quinolones, New York: Marcel Dekker; 1990.

[164] Ooie T, Terasaki T, Suzuki H, Sugiyama Y. Quantitative brain microdialysis study on the mechanism of quinolones distribution in the central nervous system. Drug Metab Dispos 1997;25:784–9.

[165] Bulitta JB, Jiao Y, Landersdorfer CB, Sutaria DS, Tao X, Shin E, et al. Comparable bioavailability and disposition of pefloxacin in patients with cystic fibrosis and healthy volunteers assessed via population pharmacokinetics. Pharmaceutics 2019;11. https://doi.org/10.3390/pharmaceutics11070323.

[166] Garrigou-Gadenne D, Burke JT, Durand A, Depoortere H, Thénot JP, Morselli PL. Pharmacokinetics, brain distribution and pharmaco-electrocorticographic profile of zolpidem, a new hypnotic, in the rat. J Pharmacol Exp Ther 1989;248:1283–8.

[167] Mo J, He L, Ma B, Chen T. Tailoring Particle Size of Mesoporous Silica Nanosystem to Antagonize Glioblastoma and Overcome Blood-Brain Barrier. ACS Appl Mater Interfaces 2016;8:6811–25. https://doi.org/10.1021/ACSAMI.5B11730/SUPPL_FILE/AM5B11730_SI_001.PDF.

[168] Sánchez-Cabezas S. Development of a reproducible and optimized synthetic protocol for the preparation of monodisperse core-shell-type magnetic mesoporous silica nanoparticles. Universidad Politécnica de Valencia, 2019.

[169] Laramy JK, Kim M, Parrish KE, Sarkaria JN, Elmquist WF. Pharmacokinetic assessment of cooperative efflux of the multitargeted kinase inhibitor ponatinib across the blood-brain barrier. J Pharmacol Exp Ther 2018;365:249–61. https://doi.org/10.1124/jpet.117.246116.

[170] Sousa F, Dhaliwal HK, Gattacceca F, Sarmento B, Amiji MM. Enhanced anti-angiogenic effects of bevacizumab in glioblastoma treatment upon intranasal administration in polymeric nanoparticles. J Control Release 2019;309:37–47. https://doi.org/10.1016/j.jconrel.2019.07.033.

[171] Mangas-Sanjuan V, González-Alvarez M, Gonzalez-Alvarez I, Bermejo M. Drug penetration across the blood-brain barrier: An overview. Ther Deliv 2010;1:535–62. https://doi.org/10.4155/tde.10.37.

[172] Veszelka S, Tóth A, Walter FR, Tóth AE, Gróf I, Mészáros M, et al. Comparison of a rat primary cell-based blood-brain barrier model with epithelial and brain endothelial cell lines: Gene expression and drug transport. Front Mol Neurosci 2018;11. https://doi.org/10.3389/fnmol.2018.00166.

[173] Gomes MJ, Mendes B, Martins S, Sarmento B. Cell-based in vitro models for studying blood-brain barrier (BBB) permeability. Concepts Model. Drug Permeability Stud. Cell Tissue based Vitr. Cult. Model., Elsevier Inc.; 2015, p. 169–88. https://doi.org/10.1016/B978-0-08-100094-6.00011-0.

[174] Avdeef A. How well can in vitro brain microcapillary endothelial cell models predict rodent in vivo blood-brain barrier permeability? Eur J Pharm Sci 2011;43:109–24.

https://doi.org/10.1016/j.ejps.2011.04.001.

[175] McIlwain H, Bachelard H. Biochemistry and the Central Nervous System. 5th ed. Edingburg: Churchill Livingstone; 1985.

[176] Instituto de Estudios del Huevo. Composición nutricional del huevo n.d. https://www.institutohuevo.com/composicion-nutricional-del-huevo/#1501003984074-a5111b1a-4b63 (accessed July 3, 2020).

[177] Wikipedia. Huevo (alimento) n.d. https://es.wikipedia.org/wiki/Huevo_(alimento) (accessed July 19, 2020).

[178] Garg P, Jitender V. In Silico Prediction of Blood Brain Barrier Permeability: An Artificial Neural Network Model. J Chem Inf Model 2005;46:289–97. https://doi.org/10.1021/CI050303I.

[179] Pajouhesh H, Lenz GR. Medicinal Chemical Properties of Successful Central Nervous System Drugs. NeuroRx 2005;2:541. https://doi.org/10.1602/NEURORX.2.4.541.

[180] Carpenter TS, Kirshner DA, Lau EY, Wong SE, Nilmeier JP, Lightstone FC. A Method to Predict Blood-Brain Barrier Permeability of Drug-Like Compounds Using Molecular Dynamics Simulations. Biophys J 2014;107:630–41. https://doi.org/10.1016/j.bpj.2014.06.024.

[181] Loryan I, Sinha V, Mackie C, Van Peer A, Drinkenburg W, Vermeulen A, et al. Mechanistic understanding of brain drug disposition to optimize the selection of potential neurotherapeutics in drug discovery. Pharm Res 2014;31:2203–19. https://doi.org/10.1007/s11095-014-1319-1.

[182] Weksler B, Romero IA, Couraud PO. The hCMEC/D3 cell line as a model of the human blood brain barrier. Fluids Barriers CNS 2013;10:16. https://doi.org/10.1186/2045-8118-10-16.

[183] Garberg P, Ball M, Borg N, Cecchelli R, Fenart L, Hurst RD, et al. In vitro models for the blood-brain barrier. Toxicol Vitr 2005;19:299–334. https://doi.org/10.1016/j.tiv.2004.06.011.

[184] Kugler EC, Greenwood J, MacDonald RB. The “Neuro-Glial-Vascular” Unit: The Role of Glia in Neurovascular Unit Formation and Dysfunction. Front Cell Dev Biol 2021;9:2641. https://doi.org/10.3389/FCELL.2021.732820/BIBTEX.

[185] Geldenhuys WJ, Mohammad AS, Adkins CE, Lockman PR. Molecular determinants of blood-brain barrier permeation. Ther Deliv 2015;6:961–71. https://doi.org/10.4155/tde.15.32.

[186] Lanevskij K, Dapkunas J, Juska L, Japertas P, Didziapetris R. QSAR analysis of blood-brain distribution: The influence of plasma and brain tissue binding. J Pharm Sci 2011;100:2147–60. https://doi.org/10.1002/jps.22442.

[187] Watanabe R, Esaki T, Kawashima H, Natsume-Kitatani Y, Nagao C, Ohashi R, et al. Predicting Fraction Unbound in Human Plasma from Chemical Structure: Improved

Accuracy in the Low Value Ranges. Mol Pharm 2018;15:5302–11. https://doi.org/10.1021/acs.molpharmaceut.8b00785.

[188] Bermejo M, Avdeef A, Ruiz A, Nalda R, Ruell JA, Tsinman O, et al. PAMPA - A drug absorption in vitro model: 7. Comparing rat in situ, Caco-2, and PAMPA permeability of fluoroquinolones. Eur J Pharm Sci 2004;21:429–41. https://doi.org/10.1016/j.ejps.2003.10.009.

[189] Garrigues TM, Pérez-Varona AT, Climent E, Bermejo M V., Martín-Villodre A, Plá-Delfina JM. Gastric absorption of acidic xenobiotics in the rat: Biophysical interpretation of an apparently atypical behaviour. Int J Pharm 1990;64:127–38. https://doi.org/10.1016/0378-5173(90)90261-2.

[190] Sánchez-Castaño G, Ruíz-García A, Bañón N, Bermejo M, Merino V, Freixas J, et al. Intrinsic absolute bioavailability prediction in rats based on in situ absorption rate constants and/or in vitro partition coefficients: 6-Fluoroquinolones. J Pharm Sci 2000;89:1395–403. https://doi.org/10.1002/1520-6017(200011)89:11<1395::AID-JPS3>3.0.CO;2-U.

[191] Saraiva C, Praça C, Ferreira R, Santos T, Ferreira L, Bernardino L. Nanoparticle-mediated brain drug delivery: Overcoming blood-brain barrier to treat neurodegenerative diseases. J Control Release 2016;235:34–47. https://doi.org/10.1016/j.jconrel.2016.05.044.

[192] Thommes M, Kaneko K, Neimark A V., Olivier JP, Rodriguez-Reinoso F, Rouquerol J, et al. Physisorption of gases, with special reference to the evaluation of surface area and pore size distribution (IUPAC Technical Report). Pure Appl Chem 2015;87:1051–69. https://doi.org/10.1515/PAC-2014-1117/PDF.

[193] Kong L, Zhang J, Zhou Q, Fang Z, Wang Y, Gao G, et al. The effects of ponatinib, a multi-targeted tyrosine kinase inhibitor, against human U87 malignant glioblastoma cells. Onco Targets Ther 2014;7:2013. https://doi.org/10.2147/OTT.S67556.

[194] Saunders NR, Dreifuss J-J, Dziegielewska KM, Johansson PA, Habgood MD, MÃ¸llgÃ¥rd K, et al. The rights and wrongs of blood-brain barrier permeability studies: a walk through 100 years of history. Front Neurosci 2014;8. https://doi.org/10.3389/fnins.2014.00404.

[195] Kwok AKH. Effects of trypan blue on cell viability and gene expression in human retinal pigment epithelial cells. Br J Ophthalmol 2004;88:1590–4. https://doi.org/10.1136/bjo.2004.044537.

[196] Awad D, Schrader I, Bartok M, Mohr A, Gabel D. Comparative Toxicology of Trypan Blue, Brilliant Blue G, and Their Combination Together with Polyethylene Glycol on Human Pigment Epithelial Cells. Investig Opthalmology Vis Sci 2011;52:4085. https://doi.org/10.1167/iovs.10-6336.

[197] Chemometec. Why Trypan Blue is Not a Good Idea And How It Effects Your Cell Counting n.d. https://chemometec.com/resources/mini-reviews/why-working-with-trypan-blue-is-not-a-good-idea/ (accessed December 31, 2021).

[198] Yang B, Lu Y, Du SY, Li PY, Zhang Y. Influences of molecular weight and particle size to intranasal drug delivery based on cell model of “nose-brain.” Chinese Tradit Herb Drugs 2020;51:5748–53. https://doi.org/10.7501/J.ISSN.0253-2670.2020.22.011.

ANNEX: PUBLICATIONS

ANNEX: PUBLICATIONS

1. Nanomedicine in the Treatment of Pathologies of the Central Nervous System

Type of publication	Chapter of book
Title	Nanomedicine in the Treatment of Pathologies of the Central Nervous System
Authors	Bárbara Sánchez-Dengra, Isabel González-Álvarez, Marival Bermejo and Marta González-Álvarez
Book	Advances in Nanomedicine
Publisher	OPEN ACCESS EBOOKS
Year of publication	2020
Web	https://www.openaccessebooks.com/advances-in-nanomedicine.html

1. The blood-brain barrier (BBB)

Despite its small size, just 2 kg, 3% of the corporal weight, the nervous system is one of the most complex and crucial systems of human body. It is composed by millions of neurons and glial cells that are organized in central nervous system (CNS) and peripheral nervous system (PNS). The CNS processes the sensitive information and it is responsible of sending the instructions for muscles contractions and glandular secretions. Additionally, it is behind all the thoughts, emotions and memories. The CNS structure includes two parts: the brain and the spinal cord.(1,2)

Due to its importance and its several functions, the CNS consumes big amounts of oxygen and glucose that reach the brain by means of the circulatory system. Nevertheless, the capillaries present in CNS are distinct to those present in the rest of the body, their endothelial cells are “sealed cell-to-cell” by both, tight junctions and adherent junctions, and they are surrounded by a thick layer of glial cells (astrocytes and perycites). (1,3–6) These characteristics (figure 1) create a physical barrier between the CNS and the rest of the body, this barrier can be subdivided in three different barriers: the blood-brain barrier (BBB), which keeps the blood apart from brain tissue, the blood-cerebrospinal fluid barrier (BCSFB), which separates the blood from the CSF present in brain ventricles, and the blood-arachnoid barrier, which isolates the blood from the CSF present in the subarachnoid space (Figure 2). (7,8)

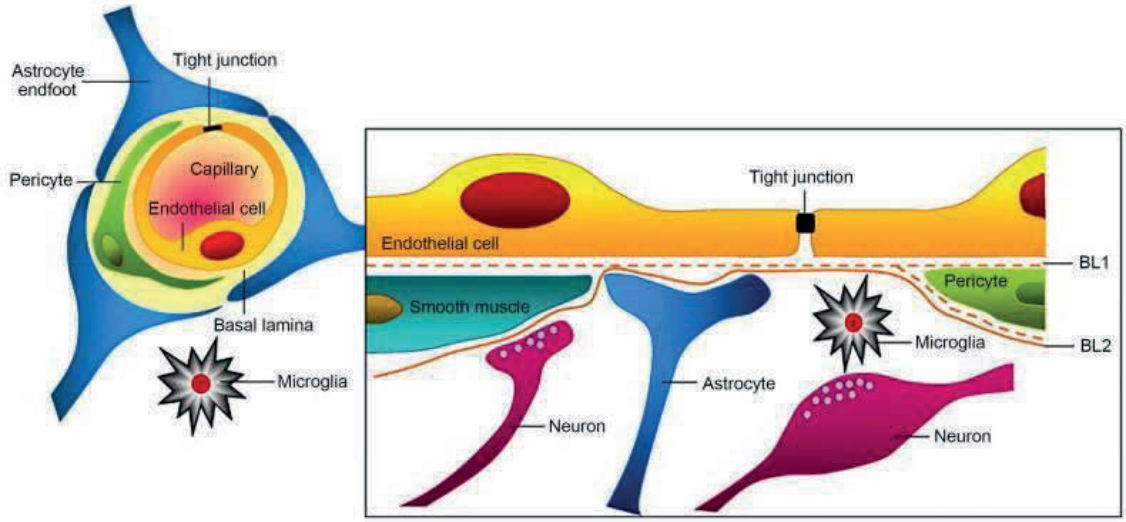

Figure 1. Scheme of the blood-brain barrier structure. Extracted from He *et al*. (6)

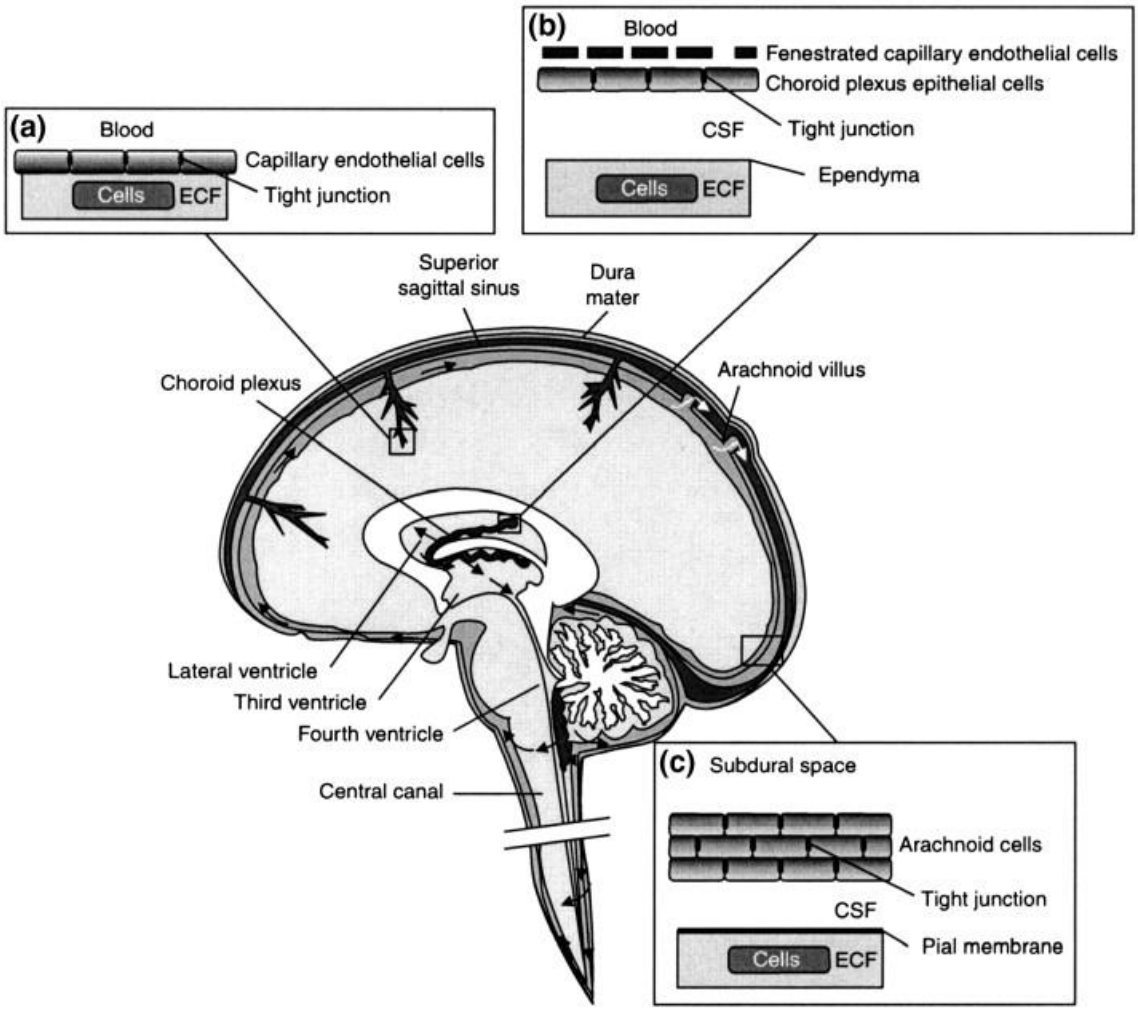

Figure 2. Brain barriers: A) The blood-brain barrier (BBB), B) The blood-cerebrospinal fluid barrier (BCSFB) and C) the blood-arachnoid barrier. Extracted from Abbot *et al*.(7)

From the perspective of nutrition and transport of substances the BBB is considered the main brain barrier, as it covers the biggest part of the brain and it has the largest surface area for exchanging substances (around 150-200 cm^2/g brain). (7)

In addition to the physical barrier built by the tight junctions and the glia cells, the BBB has also efflux transporters and metabolic enzymes that preserve the brain from strange substances and microorganisms. Nonetheless, these properties also hinder the delivery of drugs into the CNS when they are needed and, because of that, new strategies as nanomedicines need to be developed to overcome this barrier in case of brain disease. (9)

2. Blood-brain barrier permeability

There are several routes that allow some substances to be transported through the BBB (figure 3): paracellular diffusion, transcellular diffusion, carrier-mediated transport, receptor-mediated transport, adsorptive-mediated transport or cell-mediated transport. (5,10–12)

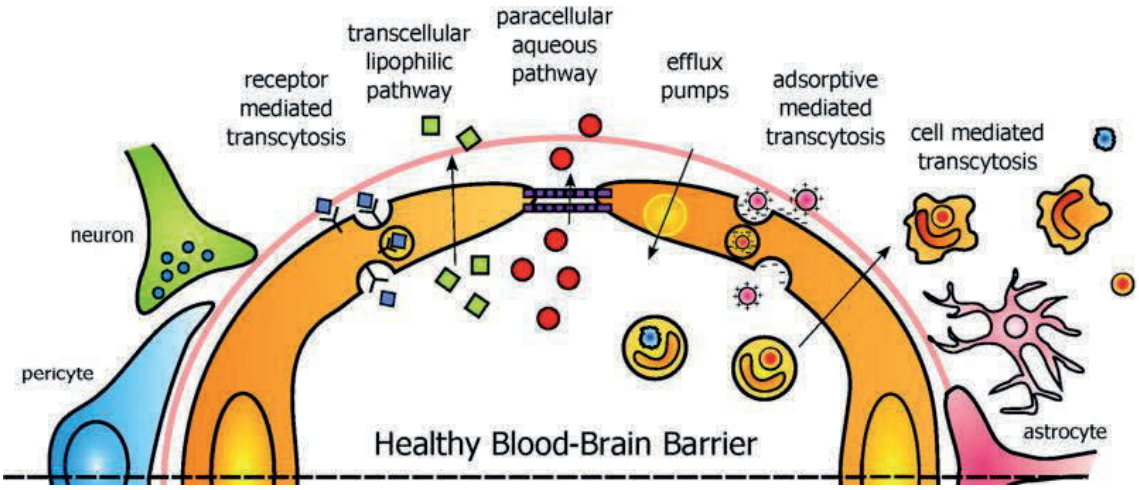

Figure 3. Transport routes across the blood–brain barrier. Modified from Chen *et al*. (5)

Paracellular diffusion and transcellular diffusion are routes in which substances cross passively the BBB depending on their concentration. Concretely, paracellular diffusion is available for a very few small hydrophilic molecules (i.e. erythropoietin) that can pass between the tight junctions, although the extent of pass of this pathway is always very low. On the other hand, transcellular diffusion is only available for small lipophilic molecules, like steroids, that can be dissolved in the cytoplasm of endothelial cells and fit the following characteristics: molecular weight less than 500 Da, neutral charge, log P approximately with a value of 2 and cumulative number of hydrogen bonds less than 10.

Carrier-mediated transport is a pathway used by essential molecules as glucose or amino acids to achieve the brain. In this pathway, that requires external energy, like ATP, molecules bind to a specific transporter that by mean of changing its conformation allows their access to the endothelial cell. Some of these specific transporters are: the glucose transporter (GLUT-1) that facilitates the access of glucose to the BBB or the system L-transporters (LAT1 and LAT2) that mediate the uptake of large, neutral amino acids.

For its part, larger molecules as insulin, transferrin, lactoferrin or lipoproteins use the receptor-mediated transport mechanism for reaching the brain. In this case of active transport, a molecule bind a receptor in the surface of the endothelial cells and so both, the molecule and the receptor are invaginated into the cytoplasm of the cell. Finally, endosomes are opened and the receptor returns to the surface of the cell and the free molecule reach the brain.

In adsorptive-mediated transport, molecules are also introduced in the brain by mean of creating invaginations from cell surface. However, these molecules do not interact with any membrane receptor; they have electrostatic interactions directly with the membrane of the endothelial cells. As cell surfaces have negative charge due to their proteoglycans, this mechanism can be used by molecules that are positively charged such as albumin or other peptides.

Finally, an alternative pathway is the cell-mediated transport mechanism, also known as the “Trojan horse”. Physiologically, this route is used by immune cells to access to the brain when the BBB is not damage. Nonetheless, it is also used by pathogens that infect immune cells, as VIH, to reach the CNS.

Beside all these input mechanisms, BBB also have several efflux transporter that return molecules to the blood. Some of these transporters are: the P-glycoprotein (P-gp), some Multidrug Resistance Proteins (MRP) or the Breast cancer Resistance Protein (BCRP). (12)

3. Pathologies of the CNS

An indisputable fact is that people worldwide are living longer. Conforming to the World Health Organization (WHO): in 35 years, from 2015 to 2050, the percentage of world's population over 60 years will pass from 12% to 22%, nearly the double and, by 2020, this group of people over 60 years will exceed by far the children younger than 5 years. (13)

This issue is causing an increment in the incidence and prevalence of several diseases, including pathologies of the CNS, and the main problem with these illnesses is that potentially active molecules are not able to arrive at their targets due to the BBB, making the development of new nanomedicine systems extremely necessary.

a) Glioblastoma

Glioblastoma is the most frequent and most lethal brain tumour. It comprises more than 50 % of total astrocytomas, it has an incidence of 1 per 33,330 adults per year, a median survival period of 1.16 and a 5-year survival of 2.7 %. It is formed by a mixture of altered glial cells (astrocytes and oligodendrocytes) that have acquired an extremely high capacity to invade the surrounding tissue, although extra-neural metastases are extremely rare. Normally, it progresses very quickly in just 2-3 months, unless it is developed within a pre-existing low grade astrocytoma (secondary glioblastoma). (14–17)

b) Alzheimer's disease

Alzheimer's disease is the most frequent type of dementia worldwide. It is a neurodegenerative disease, characterized by a progressive loss of memory which is caused by the accumulation of amyloid-beta peptides around the brain. (14)

Just in the United States, there are approximately 5.8 millions of people who are living with dementia in 2019, 5.6 millions of people being over 65 years and 200,000 of people being younger. In fact, the 10% of people older than 65 years has Alzheimer's dementia. The incidence of this disease in USA is around 500,000 cases in 2019, but because of population aging, it is projected that by 2050, Alzheimer and other dementias in people aged 65 and older will double. (18)

c) Parkinson's disease

The next most frequent neurodegenerative disease after Alzheimer's disease is Parkinson's disease which affects the substantia nigra. Parkinson's patients show a reduced level of dopamine transporters which triggers in a loss of neural functions due to the lack of dopamine available in the brain. The most characteristic symptoms of Parkinson's disease are bradykinesia and tremors. (14)

This pathology is more frequent in men than women and affects around 7-10 million of people all around the world. Its prevalence clearly increases with age, passing from 41 people per 100,000 among people who are 40 years old to 1,900 people per

100,000 when people are 80 or older. The same happens with its incidence, which grows with age until it becomes stable between people older than 80 years old. (19)

d) Depression

Depression is a common mental disorder that, at global level, affects at 4.4% of the world's population. It is characterized by long duration sadness, less interest or pleasure, feelings of guilt or low self-esteem, sleeping or appetite problems, tiredness, and low concentration which can interfere with or limit one's ability to carry out major life activities. At its most severe form, depression can lead to suicide. (20,21)

4. Strategies to increase the permeability through the BBB

Due to the strong opposition to the passage of substances exerted by the BBB, several strategies for increasing the amount of drug that arrives at the brain in CNS pathologies have been tried. Some of them try to use some of the transport pathways mentioned above or try to inhibit the efflux transporters, others try to momentarily modify the compact structure of the BBB and others just pass beyond the BBB by administrating the drug directly into the brain tissue or giving it intranasally. (22)

Strategies that go beyond the BBB include: invasive strategies such as, intraparenchymal, intraventricular or intrathecal drug delivery strategies and non-invasive strategies like the intranasal administration. When a drug is directly delivered into the brain by injection or intracerebral implants high local drug concentrations can be rapidly achieved, but, besides their invasiveness, these methods have the disadvantages of having several side effects and being hard to control and repeat. On the other hand, intranasal administration, which profits the lack of BBB in the neural pathways connecting the nasal mucosa and the brain, is a noninvasive strategy with low risk, easy to operate and repeat, but it has a smaller drug delivery volume and big interindividual differences.(6,11,22)

Alternatively, strategies that look for the delivery of drugs through the BBB try to overcome the limitations of the methodologies mentioned above. These strategies can be divided in three groups: chemical, physical and nanothecnological methods.

a) Chemical strategies

Chemical strategies are those that try to enhance drug permeability through the BBB by means of: (1) preparing a prodrug, adding a chemical modification to the original

drug to intensifies its lipophilicity, (2) constructing a chemical drug delivery system (CDDS), combining the original drug with a bioremovable targeting material or (3) coupling the administration of the drug with an agent that temporally opens the BBB, such as mannitol or some aromatic substances. (6)

The first chemical strategy, the synthesis of lipophilic prodrugs, can be fronted by several chemical modifications: glycol-sylation, methylation, esterification or pegylation between others. One example of prodrug that can cross the BBB, but its parental drug cannot, is L-Dopa. (6,23,24) By definition, prodrugs are pharmacologically inactive and they need to be transformed to their active form after administrations, and when treating pathologies of CNS, ideally after going through the BBB. (6,11) Figure 4 shows the chemical structure of L-Dopa and dopamine, prodrug and drug, for treating Parkinson disease.

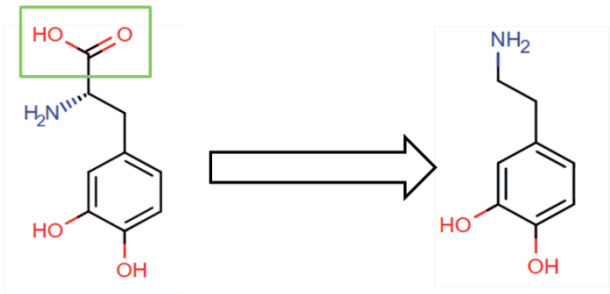

Figure 4. Chemical structures of L-Dopa (prodrug) and dopamine (active drug).(25)

It is considered that when a molecule has a log P value around 1.5 and 2.5, it will cross the BBB and it will arrive to the CNS. (11) Nevertheless, one of the most important problem of this procedure is that once the lipophilic molecule has crossed the first membrane of the endothelial cells it can be returned to the blood by efflux pumps, such as P-glycoprotein. (6)

CDDS are obtained when a drug is combined with a targeting molecule that after reaching its target can be removed enzymatically. Two examples of targeting molecules are dihydropyridine and dihydrotrigonelline. Generally, the difference between a prodrug and a CDDS is that in the second case the removal step is more complex. (6,11)

The last chemical strategy couples the administration of a drug with another substance that temporally opens the BBB. In this context, mannitol is known to create a hyperosmolar environment that makes endothelial cells to release water, reduce their size and consequently open their tight junctions. The disadvantage of using mannitol to increase BBB permeability is that the BBB opening is not selective and many substances,

not all of them beneficial, can reach the CNS. On the other hand, some aromatic substances can also open the BBB during a limited time and increase drug permeation through the BBB; it has been studied that borneol can increase permeability of substances by provoking the translocation of tight junctions proteins back to the cytoplasm of endothelial cells, by inhibiting some efflux pumps and by increasing the levels of excitatory amino acids (neurotransmisors) that modify the endothelial cells and promote permeation. (6)

b) Physical strategies

Physical, not invasive, strategies using ultrasounds for treating pathologies of the CNS have been studied since the 1940s. However, it has not been able to use it until recently because, initially, the transfer of energy through the skull caused an extremely high overheating. (4,26) Currently, ultrasounds strategies have been improved and they have been proved to be an alternative to temporally open the BBB. Although, there has not been proved a total lack of BBB damage when ultrasound are applied for increasing permeability through the BBB and more studies are needed to elucidate the exact mechanism by which this ultrasound waves increase the permeability.(26)

At the moment, the most secure strategy for applying ultrasounds to the BBB is combining them with the intravenous administration of microbubbles, particles made of lipids or albumin and filled with gas, that makes the effect of ultrasounds to be more localized. (6,22) This method has proved to have a good selectivity of opening position, which could be an advantage over using an hyperosmolar solution or aromatic substances to open the BBB. (6) Figure 5 shows a scheme of this method in which, briefly, the microbubbles are moved by the ultrasound wave near to endothelial cells and they oscillate, altering their environment and inducing mechanical stress that disrupts the tight junctions between the cells. (22)

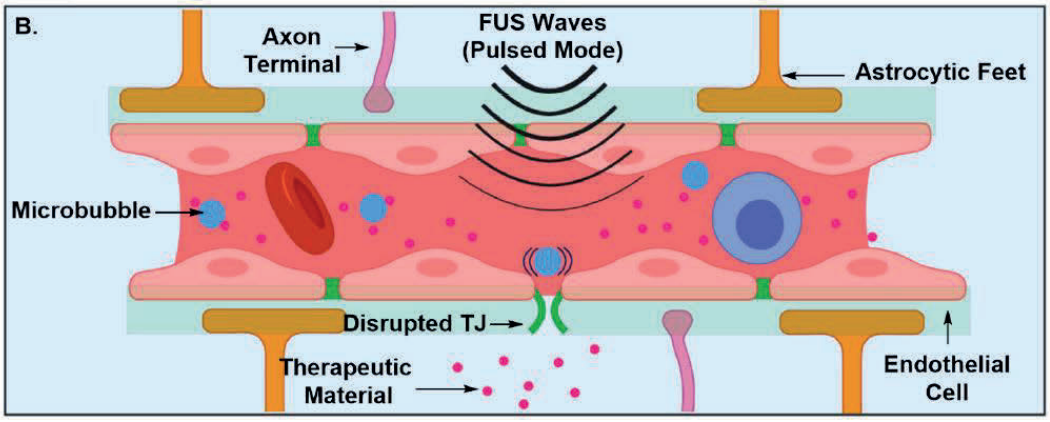

Figure 5. Scheme of the microbubble-assisted focused-ultrasound technique used for disrupting the BBB. Modified from Abdul *et al*(22).

c) Nanotechnological strategies

Nanotechnological strategies aid drugs to cross the BBB by means of the association of an unaltered therapeutic molecule with a nanoscale carrier made from lipids, polymers or metal. According to its composition, nanocarriers can be divided in 3 groups: lipid-based nanocarriers, polymer-based nanocarriers or metal-based nanocarriers. (14,27) Main types of nanocarriers that can be used as nanotechnological strategies for crossing the BBB are shown in table 1.

Table 1. Main types of nanocarriers that can be used as nanotechnological strategies for crossing the BBB. (27)

Lipid-based nanocarriers	Polymer-based nanocarriers	Metal-based nanocarriers
Liposomes	Polymeric conjugates	Magnetic nanoparticles
Solid lipid nanoparticles	Polymer nanoparticles	Non-magnetic nanoparticles
Lipid nanocapsules	Polymeric micelles	
	Dendrimers	

Nanocarriers can cross the BBB by different methods, the most important ones are: receptor-mediated and adsorption mediated transcytosis. Additionally, they can cross the barrier by paracellular diffusion when a surfactant is present in the nanocarrier and it provokes a non-permanent toxic effect in the tight junctions or the tight junctions

are opened by a pathological state of the CNS. As a last method, cell-mediated transcytosis has been also used with positive results for the delivery of antiretroviral drugs in liposomes. Furthermore, the mechanisms mentioned above could be combined by the same nanocarrier for crossing the BBB. (10,28,29)

Several aspects can influence the passage of nanocarriers through the BBB and they must be taken into account when they are prepared: its size, its shape, its charge and the presence of ligands.

- Size: For crossing the BBB through any of the transcytosis pathways, nanocarriers must measured around or less than 50 nm. (27) Nevertheless, in studies with non-healthy animal models, carriers with a diameter below 100 nm were able to cross the BBB. Although, as the carrier becomes bigger, its BBB penetration becomes smaller. (28)
- Shape: The most used nanocarriers for delivering drugs to the CNS are spherical nanoparticles as they are the easiest to prepare. Nonetheless, other shapes could be used with the same purpose, such as cubic particles or rod-like particles. In fact, some studies with nanorods have demonstrated promising results for this particle shape, having higher adhesion propensity and higher brain accumulations than their spherical nanoparticles counterpart. (28)
- Charge: For effectively crossing the BBB, nanocarriers must have negative to neutral surface charge (zeta potential). Otherwise, high positive charge can damage the BBB endothelial cells. (28)
- Ligands: Depending on the ligand added to the nanocarrier different properties can be reached. There are ligands that can adsorb proteins from the bloodstream that, then, can interplay with BBB receptors or transporters (i.e. tween 80 that adsorbs apolipoproteins). Other ligands can communicate directly with BBB receptors (transferrin receptor or insulin receptor) to promote BBB permeability. Amphiphilic peptides can actuate as ligands that increase hydrophobicity of the nanocarrier. Finally, ligands, such PEG, can be used to increase the circulation time of the nanocarrier in the bloodstream. In all the cases, it is important taking into account the affinity between the ligand and its receptor, as a too high affinity can hinder the carrier to be release to the brain after reaching the BBB. (28)

Lipid-based nanocarriers

Liposomes

Nanoliposomes are small vesicles constituted by lipid bilayers that can entrap both, hydrophilic and hydrophobic drugs in its core and in its surface structure, respectively. (30) Regarding the treatment of Alzheimer's disease several surface modified liposomal formulations have shown to successfully cross the BBB: stealth liposomes, transferrin modified liposomes, lactoferrin modified liposomes, glucose modified liposomes or glutathione modified liposomes.(31)

Stealth liposomes are covered with PEG which rises the blood circulation time of the liposomes and prevent phagocytes from uptaking them. (32) In a study carried out in mice with this type of liposomes targeted to the β amyloid plaque of Alzheimer's disease it was seen that they satisfactory increase drug concentration in brain and they were able to just bind the brain of sick mice, not the healthy ones. (33)

Also, liposomes have demonstrated to be an appropriate nanocarrier in the treatment of Parkinson's disease. Recently, Qu *et al* prepared pegylated nanoliposomes loaded with a dopamine derivative N-3,4-bis(pivaloyloxy)-dopamine (BPD) and functionalized with 29 amino-acid peptide (RVG29) derived from rabies virus glycoprotein as a targeting molecule towards acetylcholine receptor on both brain capillary endothelial cells and dopaminergic cells. They saw, *in vitro* and *in vivo*, that these liposomes were able to go through the BBB and reach the substantia nigra in a better way than the free BPD. Furthermore, they saw a limited distribution to off-target organs which ensures the biosafety of the carrier. (34)

Solid lipid nanoparticles

Solid lipid nanoparticles are solid colloid drug carriers which can entrap hydrophobic drugs with a high efficiency, as they are formed by a hydrophobic solid matrix covered with a monolayer of phospholipids. (35) Table 2 shows some examples of solid lipid nanoparticles prepared for the treatment of brain tumors, such as glioblastoma or brain methastasis.

Table 2. Solid lipid nanoparticles for the treatment of brain tumors.

Drug	Targeting molecule	Preparation technique	*In vitro* studies	*In vivo* studies	Ref
Camptothecin		High pressure homogenization	Porcine BCEC - Viability BCEC and RAW 264.7 - Uptake	Biodistribuition in rats	(36)
Camptothecin		High shear homogenization and ultrasonication technique	A172, U251, U87, U373 glioma cell lines and THP1 macrophage cell line - Viability	Biodistribuition in rats	(37)
Etoposide	5-HT moduline	Microemulsion	HBMECs - Uptake, permeability and viability		(38)
Etoposide	p-aminophenyl--D-manno-pyranoside and Folic Acid	Microemulsion	HBMECs, U87MG and HA - Viability HBMECs and U87MG - Uptake HBMECs and HA - permeability		(39)
Docetaxel Ketoconazole	Folic acid	Emulsification and solvent evaporation	bEnd.3 cells - Uptake and viability	Pharmacokinetis (plasma and brain) in rats	(40)
Docetaxel	β-Hydroxybutyric acid	Emulsification and solvent evaporation	bEnd.3 cells - Uptake and viability	Pharmacokinetis (plasma and brain) in rats	(41)

Additionally, these particles have been used to heal other pathologies of the central nervious system as depression. In 2015, Zhou and co-workers published an article in which they prepared solid lipid nanoparticles loaded with venlafaxin, an antidepressant drug substrate of the P-gp and inductor of its expression. According to their results after intravenous administration, they demonstrate that the brain uptake of venlafaxine was significantly higher when the drug was administered in the particles than when it was administered in solution, alone or combine with the empty nanoparticles or a P-gp inhibitor. Furthermore, the amount of P-gp present in the group of animals treated with the particles was the lowest one, indicating that entrapping venlafaxin in the particles prevents it from inducing the expression of P-gp. (42)

Lipid nanocapsules

The last type of lipid-based nanocarrier, the lipid nanocapsules are generally constituted by a liquid oil reservoir and a polymeric protective membrane. (43) In terms of treating pathologies of the central nervous system, lipid nanocapsules functionalized with cannabidiol have been succesfully prepared and tested in the human brain endothelial cell line hCMEC/D3 and in mice. Also, cannabidiol has proved to enhance the active targeting of lipid nanocapsules to glioma cells. (44)

Polymeric-based nanocarriers

Polymeric conjugates and dendrimers

Polymer conjugates and dendrimers are both nanoscopic molecules constituted by the combination of different monomers of polymers that can be used for transporting drugs to their targets.

The main difference between dendrimers and linear polymer conjugates is their structure, while dendrimers are globular compact molecules with a regular architecture and a spherical shape, linear polymer conjugates are not compat, irregular and they have a random-coil shape. Furthermore, there are two other important differences between these nanocarriers: on the one hand, due to its preparation methodology, dendrimers are monodisperse and they have a very high structural control, whereas linear polymer conjugates are completely the opposite (polydisperse and with low structural control); on the other hand, in terms of solubility, dendrimers are highly soluble in water and linear polymer conjugates have a low solubility.

An example of dendrimer for increasing the permeability of drugs in the treatment of glioblastoma was prepared by Liu and collaborators. (45) They constructed a poly(amidoamine) dendrimer functionalized twice with: a) angiopep-2, a peptide that can binds the less density lipoprotein receptor-relative protein-1 (LRP1) on the endothelial cells of BBB provoking a receptor mediated transcytosis and b) an epidermal growth factor receptor (EGFR)-targeting peptide (EP-1) which helps the dendrimer to reach the cancer cells once it has crossed the BBB. Results showed that this strategy was effective for increasing the penetrability of doxorubicin to the central nervous system and releasing the drug in the acidic microenvironment of tumor. These facts enhanced the therapeutic efficacy of doxorubicin and limited its systemic toxicity both in *in vitro* and *in vivo* tests. (45)

Dendrimers have also been tested in Alzheimer's disease, concretely, with the aim of protect synapses and memory. Poly(propylene imine) dendrimers with a histidine-maltose (G4HisMal) shell have shown to increase biocompatibility and brain accumulation after intranasal administration and to interfere with β-amyloid fibril formation *in vitro* and *in vivo*. In addition, the chronic treatment of APP/PS1 mice, Alzheimer's disease in animals, with G4HisMal protected mice from memory deterioration. (46)

Polymer nanoparticles

Polymer nanoparticles can be defined as drug carrying systems formed by one or more biocompatible polymers that are not water soluble. (6,11) Some examples of these synthetic polymers are: poly(alkyl cyanoacrylates), polyethylene glycol (PEG), polylactic acid (PLA) or poly (D,L-lactide-co-glycolate) (PLGA). (6) PLA and PLGA polymers have been accepted for human use by the Food and Drug Administration (FDA) as they have proved, besides being biocompatible, to be biodegradable and not induce any inflammatory response after its administration. (11)

Polymer nanoparticles can be divided in two big groups: nanocapsules or nanospheres, depending on if they have an empty core or they are solid entities and, in both cases, drugs can be loaded to the particles by adsorption to their surface or by entrapment within its matrix. (6) These particles can directly permeate the BBB, nevertheless, for obtaining a high enough transport efficiency of drugs into the brain to result in therapeutic effects, functionalization with molecules that can augment the circulation time of the particles (i.e. PEG) and stimulate their penetration into BBB endothelial cells is necessary.(11)

The Na^+-coupled carnitine transporter 2 (OCTN2) is expressed in both BBB endothelial cells and glioma cells (47,48), so it has been used as a target receptor to create new strategies for the treatment of glioblastoma. In this way, Kou and co-workers prepared PLGA nanoparticles conjugated with L-carnitine and modified with PEG (Figure 6).They saw, after carrying out *in vitro* and *in vivo* studies, that the particles increased anti-glioma efficacy. Furthermore, the ones with PEG1000 showed the maximum targeting efficiency and they explained that it is because it gives enough flexibility for improving the binding of L-Carnitine to its target. Also, they think that using a bigger PEG molecule provokes L-carnitine to be trapped between PEG tails hindering its binding to OCTN2 receptor. (49)

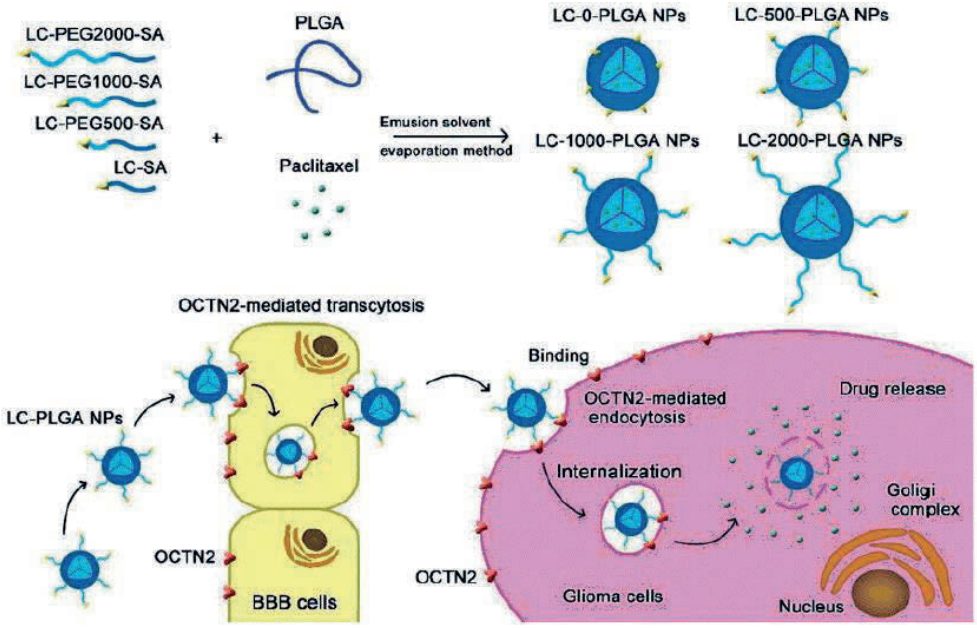

Figure 6. Scheme of the composition of L-Carnitine-conjugated nanoparticles with varied lengths of PEG spacers, and OCTN2-mediated BBB transcytosis and glioma targeting. Extracted from Kou*et al*.(49)

In terms of depression treatment, plain venlafaxine-PLGA nanoparticles and venlafaxine-PLGA nanoparticles modified with transferrin or a specific peptide against transferrin receptor were prepared by Cayero-Otero and collaborators. (50) *In vitro* studies carried out with these particles in hCMEC/D3 cells showed that the highest permeability through the BBB was obtained with particles modified with a specific peptide against transferrin receptor. Nevertheless, *in vivo* tests demonstrated that, after nasal administration, the particles that reach the brain in a highest amount were the plain ones, fact that, according to the authors, would propose that, effectively, functionalized nanoparticles arrive at the brain by receptor-mediated endocytosis (taking longer) while plain NPs can quickly reach the brain by facilitated transport. (50)

Polymeric micelles

A last example of polymer-based nanocarriers is polymeric micelles. They are amphiphilic particles, usually composed by a hydrophobic polymer core and a hydrophilic shell, for instance, a core of PLGA and a shell of PEG.(11)

Several polymeric micelles have been studied for the treatment of cancer. (51) A study with several micelles loaded with paclitaxel shows that they were able to reduce the tumor volume more effectively than the equivalent dose of the free drug. (52)

Metal-based nanocarriers

Magnetic nanoparticles

Magnetic nanoparticles are alternative nanocarriers for penetrating the blood-brain barrier. The most common magnetic nanoparticles are those prepare with iron oxides, such as: magnetite (Fe_3O_4), hematite (α-Fe_2O_3), and maghemite (γ-Fe_2O_3 and β-Fe_2O_3).(53)

When a drug is carried in magnetic nanoparticles an external magnetic field, generated by a magnet, is used to generate a driving force enabling the passage of such particles from the blood to the brain. (54) Furthermore, in the case of brain tumours, as glioblastoma, once the particles have reached the tumour area, an external alternating magnetic field can be used for warming up the carriers and killing the malignant cells, without damaging too much the healthy cells placed around it. (53)

Several *in vitro* and *in vivo* tests, with small animal models, have proved the promising potential of this type of carriers, although it is important to remember that big difficulties must be overcame to be able to move these therapies to the clinical environment. One of the most important problems is to find a magnetic force strong enough for moving the particles inside the human body, as the field strength quickly decreases with target depth in the body. Moreover, there is a poor retention of the particles in the target area once the external force is removed, so new strategies for speeding up the internalization of the particles must to be found. (54)

Non-magnetic nanoparticles

Metallic non-magnetic nanoparticles, as gold nanoparticles or silver nanoparticles, have been proposed as diagnostic tools due to their extraordinary optical properties. For instance, gold nanoparticles can absorb and emit different colours depending on size, shape and aggregate status, this property is known as Localized Surface Plasmon Resonance (LSPR). (14)

Nonetheless, besides their diagnostic utility, the drug carrying and therapeutical application of non-magnetic metal-based nanoparticles have been also studied. In fact, the cell-mediated transport mechanism (“Trojan horse”), using macrophages and monocytes loaded with gold nanoparticles, has been studied for the treatment of brain tumours. After reaching the brain, when an infrared irradiation is applied, particles are warmed and they can destroy cancer cells. (55)

5. Conclusions

The pathologies of the CNS are increasingly frequent due to the aging of the population and, during their treatment, health professionals usually find difficulties to cross the BBB. In fact, some molecules with adequate therapeutic activity have to be dismissed because they are not able to arrive at their therapeutic target in the CNS.

For that reason, nanotechnology opens up new possibilities for the treatment of these pathologies. Specifically, lipid nanocarriers such as liposomes have proven useful for the treatment of Alzheimer's and Parkinson's diseases and different types of solid lipid particles have been successfully demonstrated for the treatment of brain tumours and depression. Functionalized polymer-based particles (dendrimers, nanocapsules or micelles) allow reaching cancer cells and increasing the effectiveness of antitumor treatments. Likewise, polymeric dendrimers have proven to be promising molecules in the prevention of memory loss caused by Alzheimer's disease and polymeric particles have been studied to increase the drug permeability in depression illness. On the other hand, metal-based nanocarriers have improved the quality of the diagnosis of CNS diseases as well as the efficacy of the treatment of brain tumours by reducing the impact of the side effects caused by the chemotherapy.

In that sense, nanomedicine has brought great benefits to the treatment of CNS pathologies and, since many research groups are working in this field, it is expected that the benefits of nanomedicine will soon be even greater.

References

1. Tortora GJ, Derrickson B. Chapter 12: Nervous Tissue. In: Principles of anatomy and physiology. 11th ed. John Wiley and Sons, Inc.; 2011. p. 407–42.
2. Mulroney SE, Myers AK. 4. Organization and General Functions of the Nervous System. In: Netter's Essential Physiology. 1 st. Elsevier Inc.; 2011. p. 49–58.
3. Tortora GJ, Derrickson B. Chapter 14: The Brain and Cranial Nerves. In: Principles of Anatomy and Physiology. John Wiley and Sons, Inc.; 2011. p. 477–527.
4. Parodi A, Rudzińska M, Deviatkin A, Soond S, Baldin A, Zamyatnin A. Established and Emerging Strategies for Drug Delivery Across the Blood-Brain Barrier in Brain Cancer. Pharmaceutics. 2019 May 24;11(5):245.
5. Chen Y, Liu L. Modern methods for delivery of drugs across the blood-brain barrier. Adv Drug Deliv Rev. 2012 May 15;64(7):640–65.
6. He Q, Liu J, Liang J, Liu X, Li W, Liu Z, et al. Towards Improvements for Penetrating the Blood–Brain Barrier—Recent Progress from a Material and Pharmaceutical Perspective. Cells. 2018 Mar 23;7(4):24.
7. Abbot NJ, Patabendige AAK, Dolman DEM, Yusof SR, Begley DJ. Structure and function of the blood-brain barrier. Neurobiol Dis. 2010;37(1):13–25.
8. Vendel E, Rottschäfer V, de Lange ECM. The need for mathematical modelling of spatial drug distribution within the brain. Fluids Barriers CNS. 2019 May 16;16(1):12.
9. Xie J, Shen Z, Anraku Y, Kataoka K, Chen X. Nanomaterial-based blood-brain-barrier (BBB) crossing strategies. Biomaterials. 2019 Dec;224:119491.
10. Teleanu DM, Negut I, Grumezescu V, Grumezescu AM, Teleanu RI. Nanomaterials for drug delivery to the central nervous system. Nanomaterials. 2019 Mar 1;9(3).
11. Lu CT, Zhao YZ, Wong HL, Cai J, Peng L, Tian XQ. Current approaches to enhance CNS delivery of drugs across the brain barriers. Int J Nanomedicine. 2014 May 10;9(1):2241–57.
12. Gabathuler R. Approaches to transport therapeutic drugs across the blood-brain barrier to treat brain diseases. Neurobiol Dis. 2010 Jan;37(1):48–57.
13. WHO. Ageing and health [Internet]. 2018 [cited 2019 Nov 30]. Available from: https://www.who.int/news-room/fact-sheets/detail/ageing-and-health#:~:targetText=Common conditions in older age,conditions at the same time.
14. Kang YJ, Cutler EG, Cho H. Therapeutic nanoplatforms and delivery strategies for neurological disorders. Nano Converg. 2018 Dec 1;5(1).
15. Central nervous system gliomas – 2016 | Startoncology [Internet]. [cited 2019 Nov 30]. Available from: http://www.startoncology.net/professional-area/cns-gliomas/?lang=en
16. Glioblastoma Multiforme – Symptoms, Diagnosis and Treatment Options [Internet]. [cited 2019 Nov 30]. Available from: https://www.aans.org/Patients/Neurosurgical-Conditions-and-Treatments/Glioblastoma-Multiforme#:~:targetText=Prevalence and

Incidence&targetText=GBM has an incidence of,ages of 45 and 70.

17. Orphanet: Search a disease [Internet]. [cited 2019 Nov 30]. Available from: https://www.orpha.net/consor/cgi-bin/Disease_Search.php?lng=EN&data_id=3752
18. Association A. 2019 Alzheimer's Diseases Facts and Figures. 2019.
19. Today PN. Parkinson's Disease Statistics [Internet]. [cited 2019 Nov 30]. Available from: https://parkinsonsnewstoday.com/parkinsons-disease-statistics/#:~:targetText=An estimated seven to 10,who are 80 and older.
20. WHO. Depression and Other Common Mental Disorders Global Health Estimates. 2017.
21. National Institute of Mental Health. NIMH » Major Depression [Internet]. [cited 2019 Nov 30]. Available from: https://www.nimh.nih.gov/health/statistics/major-depression.shtml
22. Abdul Razzak R, Florence GJ, Gunn-Moore FJ. Approaches to CNS Drug Delivery with a Focus on Transporter-Mediated Transcytosis. Int J Mol Sci. 2019 Jun 2;20(12).
23. Peluffo H, Unzueta U, Negro-Demontel ML, Xu Z, Váquez E, Ferrer-Miralles N, et al. BBB-targeting, protein-based nanomedicines for drug and nucleic acid delivery to the CNS. Biotechnol Adv. 2015 Mar 1;33(2):277–87.
24. Leyva-Gómez G, Cortés H, Magaña JJ, Leyva-García N, Quintanar-Guerrero D, Florán B. Nanoparticle technology for treatment of Parkinson's disease: the role of surface phenomena in reaching the brain. Drug Discov Today. 2015 Jul 9;20(7):824–37.
25. Chemicalize - Instant Cheminformatics Solutions [Internet]. [cited 2019 Nov 18]. Available from: https://chemicalize.com/welcome
26. Meairs S. Facilitation of drug transport across the blood–brain barrier with ultrasound and microbubbles. Pharmaceutics. 2015 Aug 31;7(3):275–93.
27. Aparicio-Blanco J, Martín-Sabroso C, Torres-Suárez AI. In vitro screening of nanomedicines through the blood brain barrier: A critical review. Biomaterials. 2016 Oct 1;103:229–55.
28. Saraiva C, Praça C, Ferreira R, Santos T, Ferreira L, Bernardino L. Nanoparticle-mediated brain drug delivery: Overcoming blood-brain barrier to treat neurodegenerative diseases. J Control Release. 2016 Aug 10;235:34–47.
29. Mallapragada SK, Brenza TM, McMillan JEM, Narasimhan B, Sakaguchi DS, Sharma AD, et al. Enabling nanomaterial, nanofabrication and cellular technologies for nanoneuromedicines. Nanomedicine Nanotechnology, Biol Med. 2015;11(3):715–29.
30. Alexander A, Agrawal M, Uddin A, Siddique S, Shehata AM, Shaker MA, et al. Recent expansions of novel strategies towards the drug targeting into the brain . Int J Nanomedicine. 2019 Jul;Volume 14:5895–909.
31. Agrawal M, Ajazuddin, Tripathi DK, Saraf S, Saraf S, Antimisiaris SG, et al. Recent advancements in liposomes targeting strategies to cross blood-brain barrier (BBB) for the treatment of Alzheimer's disease. J Control Release. 2017 Aug 28;260:61–77.
32. Immordino ML, Dosio F, Cattel L. Stealth liposomes: Review of the basic science,

rationale, and clinical applications, existing and potential. Int J Nanomedicine. 2006;1(3):297–315.

33. Tanifum EA, Dasgupta I, Srivastava M, Bhavane RC, Sun L, Berridge J, et al. Intravenous Delivery of Targeted Liposomes to Amyloid-β Pathology in APP/PSEN1 Transgenic Mice. Herholz K, editor. PLoS One [Internet]. 2012 Oct 31 [cited 2019 Nov 20];7(10):e48515. Available from: http://dx.plos.org/10.1371/journal.pone.0048515
34. Qu M, Lin Q, He S, Wang L, Fu Y, Zhang Z, et al. A brain targeting functionalized liposomes of the dopamine derivative N-3,4-bis(pivaloyloxy)-dopamine for treatment of Parkinson's disease. J Control Release. 2018 May 10;277:173–82.
35. Kammari R, Das NG, Das SK. Nanoparticulate Systems for Therapeutic and Diagnostic Applications. In: Emerging Nanotechnologies for Diagnostics, Drug Delivery and Medical Devices. Elsevier Inc.; 2017. p. 105–44.
36. Martins S, Tho I, Reimold I, Fricker G, Souto E, Ferreira D, et al. Brain delivery of camptothecin by means of solid lipid nanoparticles: Formulation design, in vitro and in vivo studies. Int J Pharm. 2012 Dec 15;439(1–2):49–62.
37. Martins SM, Sarmento B, Nunes C, Lúcio M, Reis S, Ferreira DC. Brain targeting effect of camptothecin-loaded solid lipid nanoparticles in rat after intravenous administration. Eur J Pharm Biopharm. 2013;85(3 PART A):488–502.
38. Kuo YC, Hong TY. Delivering etoposide to the brain using catanionic solid lipid nanoparticles with surface 5-HT-moduline. Int J Pharm. 2014 Apr 25;465(1–2):132–42.
39. Kuo YC, Lee CH. Inhibition against growth of glioblastoma multiforme in vitro using etoposide-loaded solid lipid nanoparticles with p-aminophenyl-α-D-manno-pyranoside and folic acid. J Pharm Sci. 2015;104(5):1804–14.
40. Venishetty VK, Komuravelli R, Kuncha M, Sistla R, Diwan P V. Increased brain uptake of docetaxel and ketoconazole loaded folate-grafted solid lipid nanoparticles. Nanomedicine Nanotechnology, Biol Med. 2013 Jan;9(1):111–21.
41. Venishetty VK, Samala R, Komuravelli R, Kuncha M, Sistla R, Diwan P V. β-Hydroxybutyric acid grafted solid lipid nanoparticles: A novel strategy to improve drug delivery to brain. Nanomedicine Nanotechnology, Biol Med. 2013 Apr;9(3):388–97.
42. Zhou Y, Zhang G, Rao Z, Yang Y, Zhou Q, Qin H, et al. Increased brain uptake of venlafaxine loaded solid lipid nanoparticles by overcoming the efflux function and expression of P-gp. Arch Pharm Res. 2015 Jul 25;38(7):1325–35.
43. Gupta M, Sharma V, Chauhan NS. Nanotechnology for oral delivery of anticancer drugs: An insight potential. In: Nanostructures for Oral Medicine. Elsevier Inc.; 2017. p. 467–510.
44. Aparicio Blanco J, Torres Suárez AI. Development of lipid nanocapsules as a strategy to overcome the passage across the blood-brain barrier of drug substances acting on the central nervous system. 2019.
45. Liu C, Zhao Z, Gao H, Rostami I, You Q, Jia X, et al. Enhanced blood-brain-barrier

penetrability and tumor-targeting efficiency by peptide-functionalized poly(Amidoamine) dendrimer for the therapy of gliomas. Nanotheranostics. 2019;3(4):311–30.

46. Aso E, Martinsson I, Appelhans D, Effenberg C, Benseny-Cases N, Cladera J, et al. Poly(propylene imine) dendrimers with histidine-maltose shell as novel type of nanoparticles for synapse and memory protection. Nanomedicine Nanotechnology, Biol Med. 2019 Apr 1;17:198–209.
47. Fink MA, Paland H, Herzog S, Grube M, Vogelgesang S, Weitmann K, et al. L-carnitine–mediated tumor cell protection and poor patient survival associated with OCTN2 overexpression in glioblastoma multiforme. Clin Cancer Res. 2019;25(9):2874–86.
48. Miecz D, Januszewicz E, Czeredys M, Hinton BT, Berezowski V, Cecchelli R, et al. Localization of organic cation/carnitine transporter (OCTN2) in cells forming the blood–brain barrier. J Neurochem. 2008 Nov 8;104(1):113–23.
49. Kou L, Hou Y, Yao Q, Guo W, Wang G, Wang M, et al. L-Carnitine-conjugated nanoparticles to promote permeation across blood–brain barrier and to target glioma cells for drug delivery via the novel organic cation/carnitine transporter OCTN2. Artif Cells, Nanomedicine, Biotechnol. 2017 Oct 3;1–12.
50. Cayero-Otero MD, Gomes MJ, Martins C, Álvarez-Fuentes J, Fernández-Arévalo M, Sarmento B, et al. In vivo biodistribution of venlafaxine-PLGA nanoparticles for brain delivery: plain vs functionalized nanoparticles. Expert Opin Drug Deliv [Internet]. 2019 Nov 7 [cited 2019 Nov 30]; Available from: https://www.tandfonline.com/doi/full/10.1080/17425247.2019.1690452
51. Zhang Y, Huang Y, Li S. Polymeric micelles: Nanocarriers for cancer-targeted drug delivery. AAPS PharmSciTech. 2014;15(4):862–71.
52. Lu J, Huang Y, Zhao W, Chen Y, Li J, Gao X, et al. Design and characterization of PEG-derivatized vitamin e as a nanomicellar formulation for delivery of paclitaxel. Mol Pharm. 2013 Aug 5;10(8):2880–90.
53. Verma J, Lal S, Van Noorden CJF. Nanoparticles for hyperthermic therapy: Synthesis strategies and applications in glioblastoma. Int J Nanomedicine. 2014 Jun 10;9(1):2863–77.
54. D'Agata F, Ruffinatti FA, Boschi S, Stura I, Rainero I, Abollino O, et al. Magnetic nanoparticles in the central nervous system: Targeting principles, applications and safety issues. Molecules. 2018;23(1).
55. Hirschberg H, Madsen SJ. Cell Mediated Photothermal Therapy of Brain Tumors. J Neuroimmune Pharmacol. 2017 Mar 1;12(1):99–106.

2. Marine based biopolymers for central nervous system drug delivery

Type of publication	Chapter of book
Title	Marine based biopolymers for central nervous system drug delivery
Authors	Bárbara Sánchez-Dengra, Isabel González-Álvarez, Marival Bermejo and Marta González-Álvarez
Book	Marine Biomaterials
Publisher	SpringerNature
Year of publication	2022 *(Accepted for publication)*
Web	https://link.springer.com/book/9789811647864

Abstract:

Marine polymers are a great group of macromolecules of interest for biomedical applications due to their biocompatibility, non toxicity and physical, chemical, structural and pharmacological features. The possibilities to apply them for central nervous system (CNS) diseases are double: a) as active substances: some marine polymers has biological activity *per se* and can be explored due to their pharmacological properties for diseases treatments and b) as materials: other marine polymers are excellent candidates as nano or micro vehicles to encapsulate drugs in order to overcome blood brain barrier (BBB) access limitations or even target an specific area in the CNS. In this chapter, a brief anatomical/physiological review of the central nervous system and the blood brain barrier, as well as, the main drug access routes and limitations to target injured areas will be carried out. The most common pathologies will be addressed with an emphasis on the therapeutic target of each of them and the current applications described of marine polymers for central nervous system pathologies will be reviewed. The study revealed that marine polymers have a great potential for their application in CNS formulations and that a lot of research in this field is required to explore all the potential of these aquatic substances.

Keywords:

Central nervous system (CNS), Blood brain barrier (BBB), marine polymers, nanotechnology, pharmaceutical activity, encapsulation, marine materials

1. Central nervous system (CNS) physiology and anatomy

The nervous system is one of the most complex systems in living beings and, together with the endocrine system, it is responsible of maintaining homeostasis. (Tortora and Derrickson 2011a) The nervous system can be divided in two parts: central nervous system (CNS) and peripheral nervous system (PNS), the first of them is composed by the brain and the spinal cord and, the second one, is constituted by nerves, ganglia and sensitive receptors outside the CNS. (Mulroney and Myers 2011)

1.1. Brain

The brain can be divided in four parts, each of them with different and crucial functions: cerebrum, diencephalon, cerebellum and brain stem.

The cerebrum is the biggest part of the brain and it is responsible of its most complex functions. In its most external part, the cerebral cortex, it has sensitive areas which participate in the perception of touch, vision, hearing, smell or taste, it also has motor zones which control the muscles and it has association areas associated to memory, personality or consciousness. (OpenStax College; Tortora and Derrickson 2011b) The basal ganglia and the limbic system can be found under the cerebral cortex, both structures are part of the cerebrum: the basal ganglia connect different parts of the cerebral cortex, the diencephalon and the brain stem, and they are considered to be responsible of fine motions and automatic movements; the limbic system (amygdala and hippocampus), meanwhile, acts in emotions and long-term memory. (Mayfield Brain & Spine 2018)

The diencephalon is located at the core of the brain and its two most important structures are the thalamus and hypothalamus, parts of the limbic system. The thalamus is responsible of transmitting sensitive information to the cortex and processing the motor information that brain cortex sends. (Mulroney and Myers 2011) The hypothalamus has different nuclei and it controls digestion, thermoregulation, sexual activity and reproduction, emotional behaviour, response to stress and circadian regulation. (Crumbie and Johnson 2020)

The cerebellum coordinates the function of skeletal muscles, balance and posture. It is known as the little brain, because of its size, but it has as many neuronal cells as all the rest of the brain together. (OpenStax College; Raz and Perouansky 2018; Mayfield Brain & Spine 2018)

The brain stem is the lowest part of the brain and it connects it to the spinal cord. The brain stem is composed by the midbrain, the pons and the medulla. The midbrain

participates in the control of eyes movements and in the transmission of the visual and auditory information. The pons and the medulla by their part control autonomous functions as respiration, heart beating, swallowing, vomiting, and coughing. (Mulroney and Myers 2011)

1.2. Spinal cord

The spinal cord is the second component of the CNS, it originates from the brain stem and it can be found inside the vertebral column until the lumbar section. Its main functions are transmitting information from and to the brain and integrating that information. The spinal cord is also responsible of spinal reflexes. When a person suffers a spinal cord injury, he/she can experiment paralysis, loss of sensation below the injury or even dying. (Tortora and Derrickson 2011c)

1.3. Protective structures

Due to all the important functions of which the CNS is responsible it is surrounded by several protective structures: the skull and the vertebral column, the meninges, the cerebrospinal fluid (CSF) and a special circulatory system.

The skull and the vertebral column are bones and they constitute the most external protection of the CNS. Under these bones, the meninges can be found; they are membranes of connective tissue divided in three layers: the dura mater (the most external one), the arachnoid mater (in the middle) and the pia mater (the closest to the brain and the spinal cord). (Tortora and Derrickson 2011b; Aghoghovwia and Mytilinaios 2020)

The CSF is a transparent liquid produced from arterial blood and free of proteins which surrounds the CNS and helps to maintain the brain and spinal cord homeostasis by three ways:

a) Giving a mechanical protection, as it cushions the blows of the CNS with the skull and the vertebral column. (Tortora and Derrickson 2011b; Huff and Varacallo 2019)

b) Giving a chemical protection, maintaining the optimal environment for the transmission of information between the neuronal cells. (Tortora and Derrickson 2011b)

c) Allowing the exchange of nutrients and waste substances between the blood and the CNS. (Tortora and Derrickson 2011b; Huff and Varacallo 2019)

Finally, the circulatory system present in the CNS acts as a protective structure in a molecular level, because its endothelial cells are more tighten than the rest of endothelial cells present in the body. The circulatory system in the CNS can be divided in three structures (Figure 1): the blood-brain barrier (BBB), the blood-cerebrospinal fluid barrier (BCSFB) and the blood-arachnoid barrier.

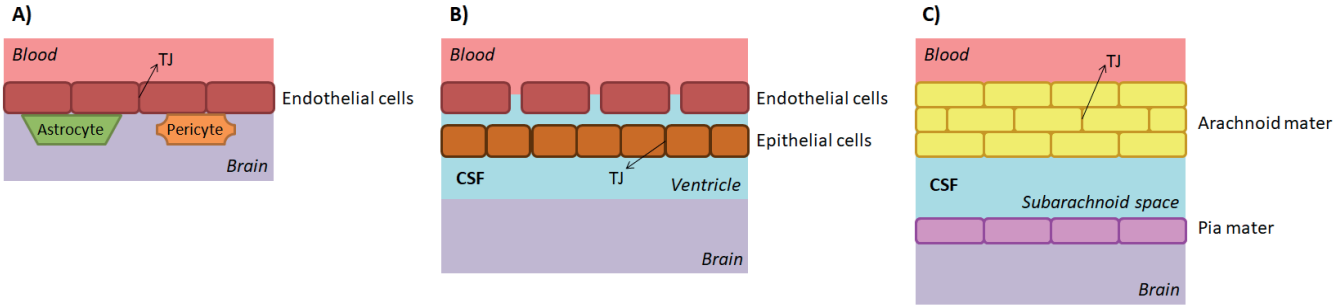

Figure 1. Scheme of the three brain barriers. A) Blood-brain barrier, B) blood-cerebrospinal fluid barrier and C) blood-arachnoid barrier. TJ: Tight junctions. Adapted from (Vendel et al. 2019).

The main brain barrier is the BBB which has a surface area for the exchange of substances of 150-250 cm^2/g brain. (Wong et al. 2013) Despite its anatomical differences (figure 1) all the barriers protect the brain by means of tight junctions and specific transporters. (Sweeney et al. 2019) The tight junctions seal the space between cells and are responsible of controlling the paracellular transport of polar molecules and ions to and out the brain. (Abbot et al. 2010) On the other hand, brain barriers have influx transporters as the organic anion transporters and the organic cation transporters which allow nutrients to reach the brain and which can be a target for the delivery of substances to the CNS (Sanchez-Covarrubias et al. 2014). Furthermore, brain barriers have efflux transporters, like the ATP-binding cassette (ABC) transporter P-glycoprotein (P-gp), the multidrug resistance protein (MRP) family or the breast cancer resistance protein (BCRP), which help to eliminate waste substances from the brain and protect it from neurotoxic substances. (Löscher and Potschka 2005) Nevertheless, the presence of tight junctions and efflux transporters makes difficult the delivery of substances to the CNS when a neurological disorder exists and a molecule needs to reach the brain.

2. CNS diseases

The CNS diseases also known as CNS disorders are defined as a group of pathologies which alter the function of the brain and/or the spinal cord. Some examples of these diseases are shown below.

2.1. Autism Spectrum Disorder (ASD)

The ASD is a neurodevelopmental disorder which appears soon in the childhood and is characterized by persistent deficits in communication and social interaction and repetitive and restricted patterns of behaviour, activities and interests. (American Psychiatric Association 2013) It affects to 1 out of 160 children worldwide, most of them boys, and its prevalence seems to increase over the years. (World Health Organization 2019a)

Nowadays, there is not a treatment able to cure the ASD, but some drugs are employed for reducing symptoms, like anxiety, panic disorders, irritability or aggressive behaviours. (National Institute of Child Health and Human Development 2019) Because of that, it is important to have therapeutic strategies able to reach the CNS. Besides the symptomatic treatment, psychological interventions can help to improve the communication abilities and social interactions of the patients with ASD.

2.2. Depression

Depression is a mental disorder that affects more than 264 million of people worldwide, the majority of them women. (World Health Organization 2020) It provokes emotional problems and it is characterized by depressed mood and/or absence of interest or pleasure in almost all the activities of the day. (American Psychiatric Association 2013) If it is not properly treated, depression can lead to suicide, the second leading cause of death among people who are 15-29 years old. (World Health Organization 2020)

2.3. Epilepsy

Epilepsy is a neurological disorder characterized by the presence of uncontrolled seizures that last around 2 minutes and are followed by fatigue and confusion. (Encyclopædia Britannica 2019) It was firstly described in 4000 B.C and, nowadays, it affects around 50 million people worldwide, being responsible for 0.5% of the global disease burden. (World Health Organization 2019b) In 2017, it was estimated that the incidence rate of epilepsy was 61.4 per 100,000 person-years, but this incidence was higher in low/middle-income countries, as their population are more frequently exposed to risks factors for developing this disorder (CNS infections, road traffic injuries; birth-related injuries and worse sanitary system). (Beghi 2020) Generally, epilepsy can be treated with different drugs that reduce neuronal hyperexcitability, but, the brain damaged that appears after a seizure cannot be reversed. (Encyclopædia Britannica 2019)

2.4. Migraine

Migraine is an extremely common headache disorder with an important genetic component whose prevalence varies from 2.6% to 21.7% between countries. (Yeh et al. 2018) It affects three times more women than men and its most common symptoms are: unilateral throbbing headache, sick feeling and sensitivity to light or sound. (NHS 2019a) Because of the high levels of pain that patients with migraine suffer, it is consider one of the most common causes of disability worldwide and it has high financial costs for the society (for instance, only in the UK, 25 million working- or school-days are lost every year because of migraine). (World Health Organization 2016; Renjith et al. 2016)

2.5. Neurodegenerative diseases

Neurodegenerative diseases are defined as a group of pathologies in which the structures of the CNS get progressively atrophied and lose their functions. (Virtual Health Library 2017) Some examples of neurodegenerative diseases are: Alzheimer's disease, Huntington's disease, Parkinson's disease or Amyotrophic Lateral Sclerosis (ALS).

2.5.1. Alzheimer's disease

Alzheimer's disease is the most common type of dementia. It was firstly described in 1906 when Dr. Alois Alzheimer observed abnormalities in the brain of a woman that had died after suffering memory loss, problems for speaking and unpredictable behaviours. (National Institute on Aging 2019) Alzheimer's disease symptoms start with sporadic memory lapses, which become worse with time until patients need full-time care. (NHS 2018)

Nowadays, around 50 million people have dementia all over the world, of which 60-70% suffer Alzheimer's disease. (World Health Organization 2019c) This high prevalence is translated in a high economical cost for the society which was estimated in 818.000 million dollars in 2015. (Garre-Olmo 2018)

2.5.2. Huntington's disease

Huntington's disease is a genetic disorder in which neurons degenerate and provoke cognitive, emotional and motor problems. Although, the patients who suffer Huntington's disease are born with a defective gene, it is not until they are 30-50 years old when they develop the symptoms, moment from which the average survival is of around 10-20 years. (Huntington's Disease Society of America 2020)

2.5.3. Parkinson's disease

Parkinson's disease is the second most common neurodegenerative disorder after Alzheimer's disease. (Sweeney et al. 2019) Nowadays, more than 10 million people have Parkinson's disease worldwide and, although, it is more prevalent in old people, approximately a 4% of the patients are diagnosed before being 50 years old. (Parkinson's Foundation 2020)

Neurons affected by Parkinson's disease are those responsible of the production of dopamine and while the disease progresses the level of dopamine in the CNS decreases. The most common symptomatology of this disease is tremor, stiffness, slowness of movement, imbalance and lack of coordination and it gets worse with time. Currently, there is not cure for Parkinson's disease, but levodopa, a prodrug of dopamine, is the most common treatment used to relieve the symptoms. (National Institute on Aging 2017)

2.5.4. Amyotrophic Lateral Sclerosis (ALS)

Amyotrophic Lateral Sclerosis is a rare motor neuron disease which affects the neurones that control the muscles responsible of voluntary movements, provoking progressive weakness and muscle atrophy. In a 5-10% of the cases the origin of the ALS is genetic, but in the other 90%, the origin of the pathology is not known. (National Institute of Neurological Disorders and Stroke 2013)

2.6. Spinal cord injury

The damage of the spinal cord caused by a trauma, disease or degeneration is known as spinal cord injury. The main causes of spinal cord injuries are trauma and most of them are preventable as those caused by road traffic crashes, falls or violence. (Shepherd Center) When a person suffers a spinal cord injury, the nerves get striped and he or she may lose part or all of his/her sensory and motor capabilities, fact that can be translated in laboral inability and high social and economical costs. (World Health Organization 2013) Unfortunately, nowadays, there is not an approved treatment able to reverse the damage of the spinal cord, so the only thing that it can be done is preventing further damage. (National Institute of Child Health and Human Development 2016)

2.7. Stroke

Stroke or cerebrovascular accidents are the second most common cause of death and the third leading cause of disability worldwide. (Johnson et al. 2016) They happen

when the blood supply to brain cells is interrupted. Depending on the cause of the interruption, strokes can be divided in: ischemic stroke, the most common one, in which the interruption is due to an obstruction of a blood vessel, or hemorrhagic stroke, in which the rupture of a blood vessel is the cause of the interruption. (NHS 2019b) Additionally, when the obstruction of a brain blood vessel is temporary, the stroke is known as transient ischemic attack (TIA) and, although, it does not cause permanent damage to the patient, it signal that a bigger stroke may happen.(American Stroke Association 2018) After a stroke the most common treatment is the use of anticoagulant, antihypertensive and/or lipid lowering drugs, besides rehabilitation and, in some cases, surgery. (NHS 2019b)

2.8. Tumors

Glioblastoma is the most common type of malignant intracranial tumor, accounting around 50% of all primary intracranial tumors. (Osama et al. 2020) Furthermore, once diagnosed, people with glioblastoma have an extremely low life expectancy (they tend to die in the first 15 months after diagnosis). (American Association of Neurological Surgeons) Because of that, new treatments alternative to the ones nowadays available (surgery for removing the tumor, followed by radiation and chemotherapy) are needed.

3. Access routes to the CNS

There are 6 different transport routes that allow substances enter to the CNS: paracellular diffusion, transcellular diffusion, carrier-mediated transport, receptor-mediated transport, adsorptive-mediated transport and cell-mediated transport. Furthermore, there are efflux transporters that prevent potentially toxic products to reach the brain (figure 2). (Sánchez-Dengra et al. 2020)

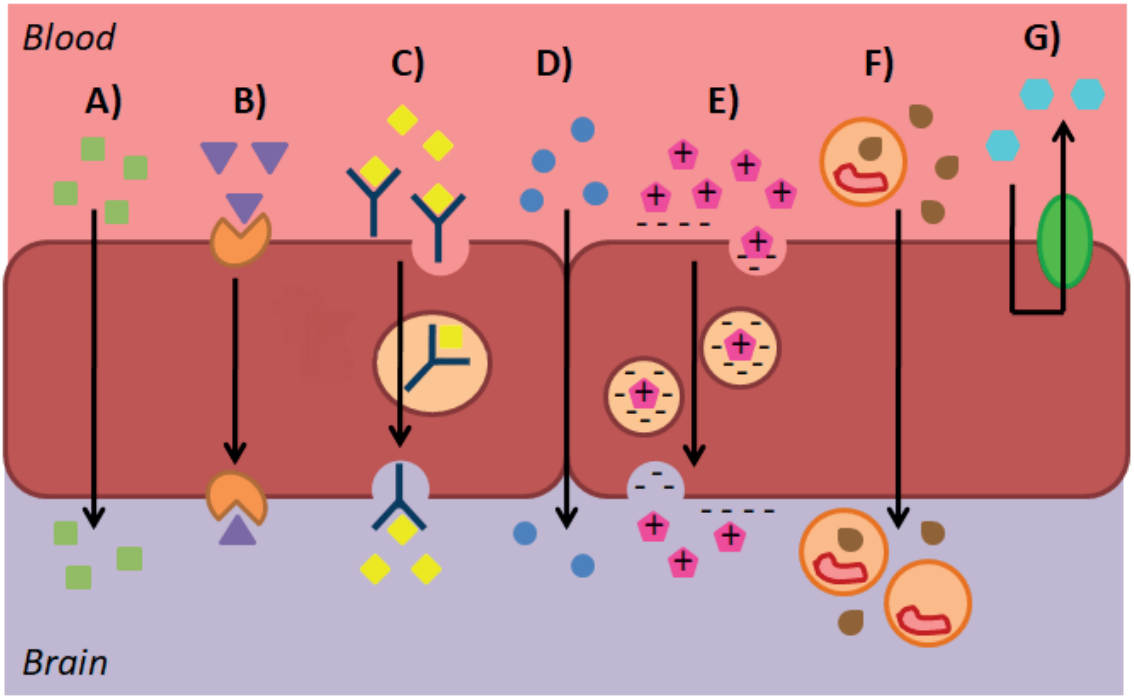

Figure 2. Scheme of the transport routes through the BBB. A) Transcellular diffusion, B) Carrier-mediated transport, C) Receptor-mediated transport, D) Paracellular diffusion, E) Adsorptive-mediated transport, F) Cell-mediated transport and G) Efflux transport.

Paracellular and transcellular diffusions are two methods of passive transport in which molecules pass from the most to the least concentrated side of the BBB. The paracellular diffusion route is used by extremely small hydrophilic molecules that are able to traverse the tight junctions; this is the case of erythropoietin and antibodies. On the other hand, transcellular diffusion allows small lipophilic molecules (MW = 400-500 Da, neutral charge, logP ≈ 2, H-bond <10) to access to the CNS, i.e. steroids. (Teleanu et al. 2019; Sánchez-Dengra et al. 2020) Nevertheless, once they enter in endothelial cells, lipophilic molecules can be returned to the blood circulation by efflux transporters, such as: P-glycoprotein (Pgp), multidrug resistance protein (MRP) and breast cancer resistance protein (BCRP) efflux transporters. (Löscher and Potschka 2005)

Bigger hydrophilic molecules need some help to cross the BBB and, at this point, carrier-mediated, receptor-mediated and adsorptive-mediated routes become important. (Gabathuler 2010)

The first route which implies the carrier-mediated transport is the most important one and it helps essential nutrients to reach the brain. The transporters from this route belong to the group of solute-like carrier (SLC) transporters and they can move from 270 to 3000 molecules/s from one side of the BBB to the other. SLC transporters can be

divided in 6 groups depending on their substrate: hexose transporters, like the one used by glucose to cross the BBB, amino acid transporters, peptide transporters, monocarboxylic acids transporters, amine transporters, like the one used by choline, and other transporters (i.e. for carnitine, nucleosides of medium-chain fatty acids). (Khan et al. 2019)

The receptor-mediated route, also known as receptor-mediated transcytosis, allows different macromolecules, such as insulin, transferrin or lipoproteins, to penetrate across the BBB. With this aim, when the macromolecule binds its receptor a vesicle is formed and it travels to the other side of the cell, where the molecule is released. (Lu et al. 2014) The most common vesicles that take part in this process are known as clathrin-coated pits and they are associated to more than 20 different receptors in the BBB cells. (Pulgar 2019)

The formation of vesicles that transport molecules from one side of the BBB to the other is also a key piece in the adsorptive-mediated route. Nevertheless, in this case, there is not a receptor binding that initializes the transcytosis. This route is used by molecules with positive charge, i.e. albumin, which interact directly with the negative charged surface of the endothelial cells. After this interaction happens, caveolae that can cross the BBB are formed. (Hervé et al. 2008; Pulgar 2019)

Finally, there is an alternative route, the cell-mediated transport, in which some substances can access to the brain using the immune cells, like in a “Trojan horse”. (Sánchez-Dengra et al. 2020)

At the end of the last century, researchers started to develop several strategies to increase the permeability of drugs through the BBB. Some of these strategies use the transport routes mentioned above and others try to administer drugs going beyond the BBB. Table 1 summarizes the strategies that have been developed for the delivery of drugs to the CNS.

Table 1. Summary of the strategies used for the delivery of drugs to the CNS.

Strategies to deliver drugs going BEYOND the BBB	
Invasive strategies	**Non-invasive strategies**
• Intracerebral injections • Intracerebral implants	• Intranasal administration

Strategies to deliver drugs THROUGH the BBB		
Chemical strategies	**Physical strategies**	**Nanotechnological strategies**
• Prodrugs • Chemical drug delivery systems (CDDS) • Co-administration of opening substances	• Ultrasounds • Microbubble-assisted focused-ultrasounds.	• Lipid-based nanocarriers • Polymer-based nanocarriers • Metal-based nanocarriers

4. Marine polymers employed in the treatment of CNS pathologies

Due to its huge surface, 70% of the Earth, the marine ecosystem is a great source of different substances, most of them not sufficiently exploited. In the treatment of CNS pathologies, marine biopolymers have been studied as raw material for the development of new drug delivery systems, but also, as direct active substances because of their neuroprotective properties. Table 2 shows a classification of the different marine polymers depending on their origin.

Table 2. Summary of marine polymers classified depending on their origin.

Origin	Polymer	Structure
Green algae	Ulvans	Repeating disaccharide units of rhamnose, xylose, glucuronic acid and iduronic acid. [a]
Brown algae	Alginate	Blocks of D-mannuronic acid and L-guluronic acid. [b]
	Fucoidans	Alternating (1-3) and (1-4) L-fucose units. [c]
	Laminarin	Repeating β-D-glucan finishing in mannitol or glucose residues. [d]
Red algae	Carrageenan	Repeating dissacharides of α-D-galactopyranose. [e]
	Galactans	Repeating units of galactose. [f]
	Porphyran	Agarose substituted with O-sulfation in the L-galactose units and O-methylation in the D-galactose units. [g]
	Agarose	Repeating dissacharides of D-galactose and L-galactopyranose. [h]
Crustaceans and other marine waste	Chitin	Repeating units of N-acetyl glucosamine. [i]
	Chitosan	Deacetylated derivative of chitin. [j]
	Chitooligosaccharides	Oligomers of chitosan. [k]
	Hyaluronans	Repeating units of alternating N-acetyl glucosamine and D-glucuronic acid. [l]
	Chondroitin sulfate	Repeating disaccharide units of glucuronic acid and sulfated galactosamine. [m]
Microalgae and microbes	Exopolysaccharides	Variable structure.[n]

[a] (Kidgell et al. 2019), [b](Abhilash and Thomas 2017), [c](Azeem et al. 2017), [d](Mišurcová et al. 2012), [e](CyberColloids), [f](Delattre et al. 2011), [g](Morrice et al. 1984), [h](ChEBI), [i](Moussian 2019), [j](Islam et al. 2017), [k](Aam et al. 2010), [l](TRB Chemedica UK), [m](PubChem), [n](Laurienzo 2010).

4.1. Green algae

4.1.1. Ulvans

Ulvans are the most common and the most known polysaccharides from green algae (*Ulva* spp. and *E. prolifera*). Chemically, they are formed by repeating disaccharide

units of rhamnose, xylose, glucuronic acid and/or iduronic acid. (de Jesus Raposo et al. 2015; Kidgell et al. 2019) Ulvans are considered dietary fibre which favours a healthy gastrointestinal tract in its consumers, which is associated with a lower incidence of chronic diseases. Ulvans are soluble in aqueous solutions and can form gels depending on the pH of the environment, in low and neutral pHs, ulvans form low viscous solutions, while, at basic pHs, they tend to form more viscous solutions and the properties of the gels are improved. (Kidgell et al. 2019)

Regarding their biological activities, several studies have demonstrated that ulvans can act as anti-viral, anti-oxidant, anti-coagulant, anti-hyperlipidemic, immunostimulating and anti-proliferative molecules. (Alves et al. 2013) On the other hand, besides having several biological activities which make ulvans interesting for pharmaceutical applications, they also have potential in the biomedical field as drug carriers, wound dressings or tissue engineering devices. In this field, ulvans nano-fibres, membranes, particles, hydrogels and 3D porous structures have been tested. (Alves et al. 2013)

4.2. Brown algae

4.2.1. Alginate

Alginate is a natural biopolymer composed by blocks of D-mannuronic acid and L-guluronic acid, that can be extracted from brown algae (*Phaeophyceae*). (Abhilash and Thomas 2017) It has the capacity of giving rise to two types of gels: an acid one and an ionotropic one depending on the pH of the solution. On the one hand, when alginate is in solution and its pH is below 6, it can form gels by combination with calcium, barium and zinc ions. On the other hand, at lower pH, alginate increases its viscosity and is able to form another type of gel known as “acid gel”. (Laurienzo 2010) Because of this exceptional capacity, alginate has proven to be of interest for various biomedical applications, like drug carriers, encapsulation, scaffolds for ligaments and tissue engineering, regeneration of tissues, moulding in dentistry and/or wound healing and dressings. (de Jesus Raposo et al. 2015)

4.2.2. Fucoidans

Fucoidans are marine sulfated polysaccharides which were discovered in 1913 and are extracted from brown algae. They are composed by L-fucose units joint between them by alternating α-(1-3) and α-(1-4) bonds. (Azeem et al. 2017; Barbosa et al. 2019)

They have proved to have several applications in the fields of: therapeutics, diagnosis, cosmetics and pharmaceutical technology. In therapeutics, some applications of fucoidans, that have already been proved, are: anti-viral, anti-metabolic syndrome, anti-leishmaniasis, inmunostimulant, anti-metastasis, anti-malaria, gastrointestinal tract, cardio, renal and hepatic protective, pro-angiogenic and alleviation of diabetic complications. By its part, fucoidans have proved to be useful for the diagnosis by imaging of cardiovascular diseases. In cosmetics, they can be apply as anti-photoaging, for increasing the skin bright, reducing the age spot and increasing the skin immunity, as soothing and protection and for reconstruction of the skin. Finally, there are several formulations that use fucoidans as vehicles for drug delivery. (Zayed and Ulber 2020)

4.2.3. Laminarin

Laminarin is an underexploited polysaccharide extracted from brow algae (*Laminaria* spp., *Saccharina* spp. or *Eisenia* spp), whose backbone structure has been defined as repeating β-glucans which finish in mannitol (M-type) or glucose (G-type) residues. The bioactivity of laminarin varies according to its final structure and more studies about the structure-activity relationship are needed, but, at the moment, they have shown to be interesting for several biomedical applications, such as: anti-cancer, tissue engineering, anti-inflammatory, anti-oxidant, anti-coagulant or intestinal modulator. (Mišurcová et al. 2012; Zargarzadeh et al. 2020)

4.3. Red algae

4.3.1. Carrageenan

Carrageenans are marine polysaccharides which are obtained from red algae. They are composed by repeating dissacharides of α-D-galactopyranose and they owe their name to a small village from the coast of Ireland where the seaweed *Chondrus crispus*, that gives rise to carrageenans, grows. (CyberColloids; Pangestuti and Kim 2014) Carrageennans are currently used in foods, cosmetics, medicines, and pharmacy products, because of that they are industrially produced, in 2003, 33,000 tons of carrageenans were produced worldwide and, in 2007/2008, the production exceeded 55,000 tons. (Laurienzo 2010; Pangestuti and Kim 2014) In terms of bioactivity, these polymers have demonstrated to be interesting as antiviral agents, anticoagulants, antithrombotic, immunomodulator, antioxidant and antitumor molecules. Besides that,

they can be used for the construction of drug delivery carriers, due to their thickening, gelling, and stabilizing properties. (Pangestuti and Kim 2014)

4.3.2. Galactans

Galactans are other type of polysaccharide produced by red algae, whose backbone structure is formed by repeating units of galactose. (Delattre et al. 2011) They have shown to have anticoagulant activity such as carrageenans, but galactans are also: anti-inflammatory, antinociceptive and antiherpetic molecules. (de Jesus Raposo et al. 2015)

4.3.3. Porphyran

Chemically, porphyran is a polysaccharide equal to agarose, but substituted with O-sulfation in the L-galactose units and O-methylation in the D-galactose units. (Morrice et al. 1984) It can be obtained from red algae of the genus *Porphyra*, which grows all over the world. It has several biological activities, like being antioxidant, immunomodulator, anticancer, anticoagulant, cardio-protector, anticerebrovascular diseases and appropriate for drug delivery. (Venkatraman and Mehta 2019; Geng et al. 2019) Besides that, other molecules extracted from *Porphyra* have shown to have antihypertensive and anti-inflammatory activities. (Venkatraman and Mehta 2019)

4.3.4. Agarose

The last polysaccharide from red algae is agarose, which is composed by repeating dissacharides of D-galactose and L-galactopyranose. (ChEBI) It has been widely studied for the development of new drug delivery systems, because it has excellent chemical and physical properties, for instance, it can be dissolved at different pHs, it has neutral surface charge, it has a reversible thermogelling behaviour and it can be easily functionalized. (Yazdi et al. 2020) It has been tested for the delivery of chemotherapeutics, the delivery of DNA and genes, the delivery of proteins and peptides, the delivery of cells and transplantation. Nevertheless, some challenges have limited the applications of agarose in drug delivery, such as, its low capacity to load hydrophobic drugs or its low degradation rate. (Yazdi et al. 2020)

4.4. Crustaceans and other marine waste

4.4.1. Chitin

Chitin is a marine polysaccharide that was first isolated in 1884, it is the second most abundant natural polymer after cellulose, it is composed by repeating units of N-acetyl glucosamine and it can be extracted from crustaceans, mainly, shrimp and crabs. (Rinaudo 2006; Moussian 2019)

As other marine polymers, chitin is biodegradable and biocompatible what makes it an interesting polymer for the application in the health field. Nevertheless, it is insoluble in common solvents and because of that researchers have studied different modifications of chitin to be applied in biomedical devices, such as, sponges, beads, gels, membranes or scaffolds. Some examples of applications in which chitin has demonstrated to be appropriate are: cancer treatment, artificial skin implants, wound healing, ophthalmology and hemodialysis membranes. (Ahmad et al. 2020b)

4.4.2. Chitosan

Chitosan is the deacetylated derivative of chitin when it reaches a percentage of deacetylation around 50% and, thus, it becomes soluble in aqueous acidic media. (Rinaudo 2006; Islam et al. 2017) Like chitin, chitosan is biocompatible and biodegradable and depending on its degree of deacetylation and its molecular weight it can also be mucoadhesive, hemostatic, analgesic, antimicrobian, anticholesteloremic and antioxidant. (Islam et al. 2017)

Chitosan has been widely studied for the development of drug delivery systems and it has shown to be appropriate for the administration of drugs by almost all the possible routes: oral, in form of stable solid formulations, ophthalmic, with hydrogels, nanoparticles or colloidal systems, nasal and buccal, due to its mucoadhesive properties, vaginal, because of its robustness and parenteral, because it is non-toxic. (Barbosa et al. 2019)

4.4.3. Chitooligosaccharides

Chitooligosaccharides are oligomers of chitosan which can be obtained by acid or enzymatic hydrolisis. According to literature, they have a lot of biological activities like: anti-asthma, antibacterial, anticancer, anti-malaria, immunomodulator, anti-fungal, treatment for diabetes or osteoporosis, ingredient for wound-dressings and vector in gene-therapy. Nevertheless, the molecular mechanisms that involve those activities and

the chemical properties of the chitooligosaccharides are not always well-defined, so more studies with well-characterized chitooligosaccharides are needed to confirm their biological potential. (Aam et al. 2010)

4.4.4. Hyaluronans

Hyaluronans are polysaccharides composed by repeating units of alternating N-acetyl glucosamine and D-glucuronic acid. Because of its ability to bind water, hyaluronans have been used in ophthalmic formulations for the treatment of dry eyes. (TRB Chemedica UK) Besides that, it has demonstrated to have excellent properties for tissue engineering and biomedical applications. They have also shown to be appropriate for the treatment of osteoarthritis. (Almond 2007)

4.4.5. Chondroitin sulfate

Chondroitin sulfate is a sulfated polysaccharide composed by repeating disaccharide units of glucuronic acid and sulfated galactosamine. (PubChem) Due to its anti-inflammatory action, it has been used in the treatment of osteoarthritis, like hyaluronans. (Reginster and Veronese 2020; Abdallah et al. 2020) Furthermore, it has been used in tissue engineering and it has proved to promote wound healing. (Abdallah et al. 2020)

4.5. Microalgae and microbial exopolysaccharides (EPS)

The last type of polymers that can be obtained from marine environment are polysaccharides from microalgae and microbes (exopolysaccharides), whose interest lies in the human capacity to cultivate and obtain them in bioreactors. In nature, their structure is highly variable, but the aim of researchers is to obtain well-defined EPS with constant chemical and physical properties. Several of these EPS have proved be natural antioxidants, to have antimicrobial and anticancer activities, to be excellent bone-healing materials and to act as anticoagulant like a “heparin-mimetic” molecule. (Laurienzo 2010)

5. Applications of marine polymers in the treatment of CNS pathologies

In this section of the chapter, some applications of marine polymers in the treatment of CNS pathologies are going to be reviewed. Table 3 shows a summary of the marine polymers that have been used for treating CNS diseases.

Table 3. Summary of marine polymers applied in the treatment of CNS pathologies classified depending on their action.

Polymers	Bioactive polymer	Ref	Polymer as carrier	Type of carrier	Access route to the CNS	Ref
Ulvans	✓	1				
Fucoidans	✓	2-7				
Alginate				Ultra-viscous alginate	Cochlear implant coating	8-9
				NTCELL® capsules	Intra-striatal delivery	10-11
			✓	Nanocapsules	Adsorptive-mediated transport Nose-to-brain Brain implantation	12-14
				Hydrogel	Spinal cord implantation	15-17
Laminarin	✓	18-20				
Carrageenan	✓	21	✓	Nanomicelles	Adsorptive-mediated transport	22
				Aerogel microparticles	Nose-to-brain	23
				Nanohydrogels	Non-tested	24
Galactan	✓	25	✓	Chemical conjugate	Receptor-mediated transport	26
Porphyran	✓	27				

Agarose			✓	Hydrogel	Spinal cord implantation	28
Chitosan			✓	Nanogel particles	Transmigration across the tight junctions	29
					Nose-to-brain	30-32
				Nanoparticles	Enhanced permeability and retention effect due to glioma	
					Adsorptive-mediated transport	
				Nanostructured lipid carriers	Nose-to-brain	33
				Solid lipid nanoparticles	Nose-to-brain	34
				Scaffolds	Spinal cord implantation	35
				Hydrogels	Eye-to-nerve	36
Chitooligosaccharides		✓	37-39			

[1](Violle et al. 2018), [2-7](Zhang et al. 2018; Ahn et al. 2019; Liao et al. 2019; Park et al. 2019; Li et al. 2020; Dimitrova-Shumkovska et al. 2020), [8-9](Scheper et al. 2019; Schwieger et al. 2020), [10-11](Snow et al. 2019; Living Cell Technologies Limited 2020), [12-14](Mamo et al. 2018; Cardia et al. 2019; Gascon et al. 2020), [15-17](Blaško et al. 2017; Sitoci-Ficici et al. 2018; Nazemi et al. 2020), [18-20](Ye et al. 2020; Lee et al. 2020), [21](Liu et al. 2017), [22](Youssouf et al. 2019), [23](Gonçalves et al. 2016), [24](Bardajee et al. 2020), [25](Zhang et al. 2004), [26](Pinhassi et al. 2010), [27](Liu et al. 2018), [28](An et al. 2020), [29](Vashist et al. 2020), [30-32](Ahmad et al. 2020a; Caban-Toktas et al. 2020; Moghaddam et al. 2020), [33](Salem et al. 2020), [34](Cometa et al. 2020), [35](Ham et al. 2020), [36](Wang et al. 2020), [37-39](Lee et al. 2009; Xu et al. 2011; Eom et al. 2013)

5.1. Green algae

5.1.1. Ulvans

In 2018, Violle *et al*. published an article in which they tested the antidepressant and anxiolytic effects of an extract of the green algae *Ulva* sp. with a 45% of ulvans. They checked different doses of ulvans using the elevated plus-maze (EPM), as a model of anxiety, and the forced swimming test (FST), as a model of depression. (Violle et al. 2018)

The EPM is based in the aversion of rodents to open and elevated places. It consists in a cross with two opened-arms and two closed-arms placed perpendicularly, with a height of 70 cm from the floor. During the experiment, the time that the mouse spends in the different arms and the number of entries to those arms is measured and it is established that the longer the mouse is in the opened-arms, the lower is its anxiety. (Komada et al. 2008)

On the other hand, in the FST, the mouse is placed in a transparent beaker filled with water and its swimming movements trying to escape are evaluated. It is considered that, as the immobility of the animal is longer, more depressed it is. (Can et al. 2011a)

Violle and its collaborators concluded that ulvans have not a statistically significant effect in the treatment of anxiety, but they would be an appropriate candidate as antidepressants, as their effects at the maximum dose tested were equivalent to those provoked by the reference antidepressant used as control. (Violle et al. 2018) Nevertheless, it is the only article published until the moment where the effects of ulvans in the CNS are tested, so more research of the potential use of ulvans for the direct treatment or the delivery of substances to CNS is needed.

5.2. Brown algae

5.2.1. Alginate

Alginate has been widely studied for the delivery of drugs to CNS and for the treatment of its pathologies. (Blaško et al. 2017; Sitoci-Ficici et al. 2018; Mamo et al. 2018; Nguyen et al. 2018; Snow et al. 2019; Scheper et al. 2019; Cardia et al. 2019; Living Cell Technologies Limited 2020; Schwieger et al. 2020; Gascon et al. 2020; Nazemi et al. 2020)

In a particular study, published in 2018, alginate hollow fibers were used to construct a new *in vitro* BBB model. In this model, the fibers, which were permeable and biocompatible, simulated the brain vessels and they were co-cultured with human umbilical vein endothelial cells (HUVECs) and astrocytes, which allowed the researchers to reproduce the BBB properties. (Nguyen et al. 2018)

A german group, specialized in Otolaryngology, have studied the use of alginate to deliver drugs for the protection of auditory neurons. (Scheper et al. 2019; Schwieger et al. 2020) The success of a cochlear implant in a deaf person depends on the activity of its spiral ganglion neurons and this activity can be protected with the chronic administration of the brain-derived neurotrophic factor (BDNF). Because of that, this group proposes the encapsulation of genetically modified mesenchymal stem cells able to produce high levels

of BDNF in ultra-high viscous alginate. Using *in vitro* tests, in which the ultra-high viscous alginate filled with genetically modified mesenchymal stem cells were co-cultured with rat spiral ganglion neurons, researchers were able to prove that the mesenchymal stem cells were able to produce BDNF and it was able to diffuse out of the alginate increasing the growth of the spiral ganglion neurons. Besides that, as a cochlear implant works transforming the sounds in electric pulses, the ultra-high viscous alginate filled with genetically modified mesenchymal stem cells was stimulated with an electric current and it was stable. (Schwieger et al. 2020) When the same formulation was tested *in vivo*, it was proved that after 4 weeks, the best results were obtained when the electrode of the cochlear implant was coated with the ultra-high viscous alginate filled with genetically modified mesenchymal stem cells, while the injection of the alginate was not effective. (Scheper et al. 2019)

Alginate preparations have been also tested for the treatment of Parkinson's disease. NTCELL® is a technology that encapsulates neonatal porcine choroid plexus cells with alginate. Neonatal porcine choroid plexus cells are able to produce big amounts of CSF and neurotrophins which could contribute to the regeneration of damaged neural tissue. NTCELL® has demonstrated to be safe and to improve the motor functions of patients with Parkinson's disease in a Phase IIb clinical trial and, now, a phase III clinical trial is needed to get more information. (Snow et al. 2019; Living Cell Technologies Limited 2020)

Alginate nanocapsules filled with probucol has also proved to suppress neuroinflammation and neurodegeneration, so they could be an alternative treatment for neurodegenerative diseases, like Alzheimer's, Parkinson's, Huntington's or ALS diseases. In this case, nanocapsules were administered orally with diet for 24 weeks to mice and, after that time, it was seen that the plasma and brain levels of probucol were higher when it was administered encapsulated. Furthermore, it was observed that, when encapsulated, the drug was able to reverse the neurodegenerative effects of a high-fat diet in mice. (Mamo et al. 2018)

Besides the particles mentioned above, other particles in which two types of marine polymers were combined (alginate and chitosan), have also proved to be effective in the treatment of neurodegenerative disorders and glioblastoma. In the first case, particles were administered intranasally, going beyond the BBB, and the level of progesterone (the molecule inside the particles) that reached the brain was 5-fold the basal level before the administration. (Cardia et al. 2019) In the second case, a controlled

release device was prepared with the aim of being able to control the migration of cancerous cells. Using *in vitro* tests, it was proved that the nanoparticles were able to release the chemokine CXCL12 slowly and they were able to move the gliobastoma cells towards it. So, from this experiment, the researchers proposed that this type of particles could be administered to the brain after a tumor resection for attracting the remaining tumor cells to an specific zone before killing them, avoiding adverse effects. (Gascon et al. 2020)

Finally, alginate hydrogels have also been tested for treating spinal cord injuries, because they can act as a matrix were the damaged cells can regenerate. (Sitoci-Ficici et al. 2018) In a similar way to the strategies that have been explained previously, these hydrogels have been used to encapsulate both, mesenchymal stem cells or drugs and, in both cases, an increase in neuronal regeneration was observed. (Blaško et al. 2017; Nazemi et al. 2020) Particularly, when minocycline and paclitaxel were co-delivered from an alginate hydrogel, an improvement in the behaviour of the animals was observed in addition to the histological findings. (Nazemi et al. 2020)

5.2.2. Fucoidans

Besides spinal cord injuries, traumatic brain injuries can be also treated with marine biopolymers. In this sense, fucoidans have proved to have a neuroprotective activity that could be exploded for the treatment of this pathology. On the one hand, fucoidans prevent immune cells from entering to the brain, reducing the subsequent inflammation and, on the other hand, they promote the production of sirtuin-3, a soluble protein that reduces the production of reactive oxygen species by the mitochondria, when the brain is damaged. (Dimitrova-Shumkovska et al. 2020) An example of application of this neuroprotective capacity is the treatment of the damage caused by a cerebral ischemia. This application has already been tested in obese gerbils and the results suggest that fucoidans could be drug candidates in attenuating brain injury in obese patients with a high ischemic risk. (Ahn et al. 2019)

Due to its anti-inflammatory effect, fucoidans have been proposed as a possible treatment for major depression, pathology with a big inflammatory component. (Miller and Raison 2016; Li et al. 2020) After the oral administration of fucoidans, their antidepressant effects were measured with a tail suspension test (TST), a FST, a sucrose preference test (SPT), and a novelty-suppressed feeding test (NSFT). In the TST the mouse is suspended in the air from the tail and, like in the FST, the longer the mouse is immobile,

more depressed it is. (Can et al. 2011b) By its part, in the SPT, the animal is exposed to two different beverages, one with sucrose and another with just water, in a normal situation, mice prefer the sweet beverage, so when the intake of this beverage is reduced it is take as a sign of depression. (Serchov et al. 2016) Finally, the NSFT measures the time that the animal lasts to eat a familiar food in a new environment, when longer is this time, more depressed the animal is. (Blasco-Serra et al. 2017) Li *et al.* observed that the depression signs were reduced in all the tests when the fucoidans were administered to chronic restraint stress (CRS) model mice. Furthermore, they saw that in the hippocampus, fucoidans were able to restore the levels of BDNF to the normal ones, in absence of depression. (Li et al. 2020)

On the other hand, fucoidans have been tested for the treatment of glioblastoma. In 2019, Liao *et al*. administered a oligo-fucoidan extract from *Laminaria japonica* to two different glioblastoma cell lines (Grade III U87MG cells and Grade IV glioblastoma multiforme (GBM)8401 cells) and to healthy immortalized astrocyte SVGp12 cells. They observed that the extract was able to inhibit cell proliferation in both glioblastoma cells, but it does not affect the healthy astrocytes. Furthermore, the extract was able to promote the differentiation of the cells what became them to a less-oncogenic phenotype. (Liao et al. 2019)

The antioxidant activity of fucoidans that was interesting for the treatment of brain injuries (Dimitrova-Shumkovska et al. 2020) is also an excellent starting point for considering these polymers candidates in the treatment of neurodegenerative disorders. Because of that, they have been studied in animal models of Parkinson's disease and Alzheimer's disease and, in both cases, the antioxidant activity, due to the regulation of the mitochondrial function, has been confirmed. Besides that, in the animals with Alzheimer's disease, it was observed that after the administration of fucoidans, the cognitive function of the animals was improved, the acetylcholine levels were increased and amyloid-β production was down-regulated. (Park et al. 2019) In the animals with Parkinson's disease, fucoidans were able to reverse the loss of substantia nigra, to restore the levels of dopamine and to improve the movements of the animals. (Zhang et al. 2018)

5.2.3. Laminarin

In a similar way to fucoidans, laminarin also has neuroprotective properties which make it a candidate for the treatment and attenuation of brain injuries after a stroke. Ye *et al.* have proved which is the mechanism through which laminarin can prevent these

damage and it is inhibiting the pro-inflammatory Dectin-1/Syk pathway. (Ye et al. 2020) By its part, Korean researchers have recently demonstrated that a dose of 50 mg/kg of fucoidans is able to prevent the injuries derived from an ischemic stroke in adult gerbils when it is administered during 7 days previously to the ischemia (Lee et al. 2020) and this dose is also effective to prevent this type of damage in aged gerbils. (Park et al. 2020)

5.3. Red algae

5.3.1. Carrageenan

Carrageenan has been proposed as a carrier for drug delivery to the CNS in different forms: nanomicelles, aerogel microparticles and nanohydrogels. (Gonçalves et al. 2016; Youssouf et al. 2019; Bardajee et al. 2020)

In one experiment, nanomicelles were prepared after grafting polycaprolactone onto oligocarragenans to obtain an amphiphilic copolymer. Once formed, the micelles were loaded with different compounds of hydrophobic nature, such as: curcumin, rifampicin and Nile Red. Curcumin micelles were used, among others, to study the micelles uptake by endothelial cells (EA-hy926) and its toxicity in zebrafish. Besides that, Nile Red micelles were employed in biodistribution tests with mice to evaluate the organs in which the new formulation allowed to reach a higher concentration. Curcumin micelles demonstrated not being toxics in zebrafishes, animals accepted as model of toxicity in vertebrae, and they allowed a higher uptake of curcumin by the endothelial cells than when free curcumin was administered in solution. By its part, there was a statistically significant increment in the amount of Nile Red that reaches the brain with the micelles, so carrageenan micelles would be an excellent candidate for increasing the permeability of hydrophobic drugs through the BBB. (Youssouf et al. 2019)

In another occasion, aerogel microparticles were designed with the aim of delivering drugs to the CNS going beyond the BBB, via intranasal administration. The particles were prepared by the emulsion gelation method using a mixture of alginate and κ-carrageenan in a proportion 1:1 and they were loaded with ketoprofen. After that, their permeability was evaluated in human nasal epithelial cells (RPMI 2650) that were cultured during 22 days to allow them to resemble the human nasal mucosa, in terms of morphology and secretions. It was observed that the powder of aerogel microparticles was able to increase the permeability of ketoprofen through the nasal barrier in 2.3 fold, so this formulation could be used as a new strategy for the delivery of drugs to the CNS. (Gonçalves et al. 2016)

The other formulation in which carrageenans have been tested for the delivery of drugs to the CNS was a nanohydrogel. It was prepared with poly(N-isopropylacrylamide) and κ-carrageenan and loaded with levodopa and its *in vitro* studies revealed that at pH 7.4 it was able to release drug for 11 days. More *in vivo* studies are needed to prove the efficacy of this hydrogel, but the idea for its development was to protect levodopa from being decarboxylated outside the CNS and, in this manner, ensuring that the amount of drug that reaches the brain is higher. (Bardajee et al. 2020)

On the other hand, carrageenans have neuroprotective properties which make them potential candidates in the treatment of neurodegenerative diseases, like Alzheimer's disease. In fact, in a study of 2017, carrageenans demonstrated to increase the viability of SH-SY5Y cells when they were induced to apoptosis with β-amyloid. (Liu et al. 2017)

5.3.2. Galactans

Galactans polymers have also been studied for drug delivery. For instance, in 2010, a conjugate of arabinogalactan, folic acid and methotrexate, in which the galactan proceed from a tree, was able to increase the citotoxic activity of methotrexate in 6.3 fold in cells overexpressing folate receptors, like the malignant ones. This result suggests that marine galactans could be used for delivering drugs for the treatment of glioblastoma. (Pinhassi et al. 2010)

In addition to their function like carriers, it seems that galactans could be used in the treatment of neurodegenerative disorders associated to the aging process. It is because of their antioxidant activity, which was demonstrated by Zhang *et al*., after their administration to aged mice. Zhang and collaborators saw that an administration of 200 mg/kg of sulfated galactan fraction F1 from red algae was able to increase the activity of the superoxide dismutase and the glutathione peroxidase, to reduce the levels of malondialdehyde (marker of endogenous lipid peroxidation) and to increase the total antioxidant capacity of the brain of aged mice. (Zhang et al. 2004)

5.3.3. Porphyran

The polysaccharide porphyran has the same structure as sulfated galactan fraction F1 (Zhang et al. 2004), so the same antioxidant properties mentioned in the previous example can be assumed for this marine polymer, becoming it another candidate in the treatment of neurodegenerative diseases. One of these neurodegenerative

diseases is the Parkinson's disease, for which porphyran has demonstrated to ameliorate the neurobehavioral deficits. (Liu et al. 2018) In the study, oligo-porphyran was administered during 7 days after the induction of Parkinson's symptoms in C57BL/6 mice with MPTP and the behaviour of the animals was evaluated with three different tests: the open field test, the pole test and the traction test. In the first one, a mouse is placed in an open area and the number of movements that it does are evaluated, in the second one, the mouse is placed in the top of a pole and two times are registered (the time it lasts to turn downward and the total time taken to climb down the pole) and, in the third one, the mouse is suspended from an horizontal wire and the time it lasts in that position and the number of extremities it uses for grasping the wire are evaluated. In all cases, the results after the treatment with the porphyran were better than in the animals that suffered MPTP induction but were not treated, so this polymer is able to attenuate the behavioural deficits associated to Parkinson's disease.(Liu et al. 2018)

5.3.4. Agarose

Agarose, the last marine polymer obtained from red algae, has been formulated in form of hydrogels for the treatment of spinal cord injuries. In one case, agarose hydrogels were formulated in combination with poly(N-isopropylacrylamide) and were loaded with gold nanoparticles. The researchers of this work demonstrated that mesenchymal stem cells were able to grow between the holes of the hydrogel. Furthermore, after the *in vivo* implantation of the hydrogel, they could see that the spinal cord injury of the rats they used improved, as they have a better control of their bladder and a higher expression of neural markers in the surrounding of the damage. (An et al. 2020)

5.4. Crustaceans and other marine waste

5.4.1. Chitosan

Chitosan is one of the most studied marine biopolymers for the treatment of pathologies of the CNS and it is because chitosan is biocompatible, biodegradable and mucoadhesive. Besides that, it has been demonstrated that chitosan is non-toxic, non-allergenic, antifungal, antibacterial, antioxidant, anti-tumoral, anti-inflammatory, immunoadjuvant, anti-thrombogenic and anti-cholesterem. (Ojeda-Hernández et al. 2020) Due to all that properties, a huge number of articles in which applications of chitosan for the CNS are described can be found.

In the field of theranostics, which looks for the development of a unique dispositive able to treat and diagnose an illness, autofluorescent nanogel particles have been developed. The nanogel particles were prepared by water in oil emulsion technique combining chitosan, hydroxyethyl cellulose and linseed oil-based polyol to increase their lipophilicity and facilitate them to cross the BBB. When they were prepared, the characterization tests confirmed that the nanoparticles measured 60–70 nm, were autofluorescent at different wavelengths (605, 700 and 810 nm) and they were non-toxic and biocompatible with different cell lines. Besides that, it was proved that nanogels were uptaken by human peripheral blood mononuclear cells and microglial cell lines, and they were able to cross the BBB in an *in vitro* human BBB model. All the results, made the researchers conclude that these new nanoparticles have a great potential as drug delivery systems for the CNS, allowing an imaged-guide therapy. (Vashist et al. 2020)

When talking about nose-to-brain drug delivery, it can be observed that chitosan has been extensively studied for delivering drugs to the brain through this route. (Singh et al. 2020) This route has been tested for the treatment of epilepsy, migraine and Parkinson's disease, among others.(Ahmad et al. 2020a; Cometa et al. 2020; Salem et al. 2020)

In epilepsy, chitosan-coated-PLGA nanoparticles loaded with catechin hydrate (phytochemical with antioxidant and anti-inflammatory activities) have been developed to increase the bioavailability of the drug and, with it, to reduce the seizures provoked by the illness. The PLGA nanoparticles were prepared by a double emulsion methodology and the amount of PLGA, the amount of PVA, the sonication time and the temperature of the reaction were adjusted until getting a formulation with an appropriate particle size, polydispersity index (PDI) and zeta potential, which, finally, were 93.46 ± 3.94 nm, 0.106 ± 0.01and −12.63 ± 0.08 mV, respectively. After that, the particles were coated with chitosan to increase their adhesiveness to nasal mucosa, this fact increased the size of the particles, but, according to TEM measurements, they measured less than 110 nm. The *in vitro* release test and the *ex vivo* permeability test with goat nasal mucosa showed that, in 24 hours, the nanoparticles release around an 80% percent of its content and, also, around a 80% of drug cross the nasal mucosa. When tested *in vivo* in an animal model for epilepsy, the particles showed to be more effective in the control of myoclonic jerks and generalized seizures than the free drug. So, the authors developed an innovative mucoadhesive nanoformulation suitable for intranasal brain-targeted delivery. (Ahmad et al. 2020a)

In a similar way to that used in the previous example, Salem *et al*. prepared chitosan mucoadhesive formulations for the intranasal treatment of migraine, but, in this case, instead of using PLGA nanoparticles, they used nanostructured lipid carriers (NLCs) as the base of the formulation. Firstly, they prepared different formulations by hot homogenization and ultrasonication technique changing the ratio of solid lipid to liquid lipid, the type of solid lipid used, the type of surfactant and the presence or absence of chitosan until optimizing the particle size, PDI and zeta potential, which, finally, were 254.93 ± 1.85 nm, 0.27 ± 0.07and 34.11 ± 0.11 mV, respectively. The *ex vivo* permeation tests with sheep nasal mucosa showed that the formulation was able to enhance the penetration of almotriptan maleate (the anti-migraine drug loaded in the particles) reaching a 100% of diffusion after 1.5 h, while the drug solution only reached a 40% of diffusion. Finally, the *in vivo* absorption study, performed in rabbits, showed that the new intranasal formulation reached a maximum concentration (C_{max}) and an area under the curve (AUC) in the brain 6.6 and 4.6 times higher than those for the oral market product, an excellent result that makes this formulation a possible alternative to those currently marketed. (Salem et al. 2020)

Chitosan coated solid lipid nanoparticles have also been proposed for the treatment of Parkinson's disease, increasing the stability of dopamine and ensuring its prolonged release. (Cometa et al. 2020) Although *in vivo* studies are necessary to classify this possible nasal formulation as successful.

Other formulations that have been investigated using chitosan are scaffolds. In 2020, Ham *et al.* prepared a scaffold loaded with immobilized interferon-γ and rat neural stem cells for the treatment of spinal cord injury and it improved the motor activity in the rats in which it was tested. In their protocol, they first placed the scaffold subcutaneously and they waited 4 weeks to ensure its maturation, after that, the scaffold was relocated to a spinal cord gap that they provoked to the animal. They observed that the regenerated neurons were able to enter and grow through the scaffold gaps and, from week 6 after implantation, the mature scaffolds were able to improve the movements of the rats. (Ham et al. 2020)

Chitosan has been proposed as a candidate biomaterial for the delivery of drugs to brain tumors. For instance, chitosan-modified PLGA nanoparticles loaded with paclitaxel in combination with the same type of particles loaded with R-flurbiprofen have shown to be able to treat glioblastoma in rat when they are administered intraperitoneally. (Caban-Toktas et al. 2020) The combination of these two drugs has an

additive effect in the treatment of cancer because of the antitumoral activity of paclitaxel and the capacity of flurbiprofen to reduce the inflammatory environment that surrounds the glioblastoma. In another investigation, chitosan and PLGA were combined to create nanoparticles loaded with curcumin, molecule able to inhibit and eliminate brain cancer cells, which were functionalized with sialic acid, to use the receptor-mediated route to cross the BBB, and anti-aldehyde dehydrogenase, to target the glioblastoma cells, as cancer cells overexpress this enzyme. *In vivo* studies with this formulation are needed, but the *in vitro* tests performed by the researchers confirm its functionality. (Kuo et al. 2019)

When the pathologies that affect the CSN are named, the retina pathologies are frequently forgotten, but, in fact, the retina is part of the CNS and has a complex circuit of neurons that transforms the information received by the photoreceptors in electrical information that travels to the brain through the optic nerve. (Purves et al. 2001) Due to its mucoadhesiveness, chitosan hydrogels can be used for the treatment of eye's pathologies, specifically, a chitosan hydrogel loaded with FK506 (in micelle) and ciliary neurotrophic factor (CNTF) has been proposed for the treatment of traumatic optic nerve injuries. The FK506 is an immunosuppressant which helps to control the overactive immune system after a traumatic axon injury, slowing down the scar formation. By its part, according to the authors, the objective of adding the CNTF was to restore the neurotrophins levels after the injury to impede the apoptosis of the retinal ganglion cells and to promote the axon regeneration. The potential of this drug delivery system was demonstrated with *in vitro* and *in vivo* studies in which the drugs showed sustained release during 9 days and fulfilled their function in the animal model. (Wang et al. 2020)

Finally, silymarin-loaded chitosan nanoparticles have been tested as a protective pre-treatment for the damage provoked by global cerebral ischemia/reperfusion. Silymarin is a natural polyphenol with anti-oxidative and anti-inflammatory properties, so the new formulation would do its job by enhancing these properties. For demonstrating this, the researchers administered the particles to rats during 14 days prior provoking an artery occlusion, after that, they observed that the animals treated with the new formulation showed the lowest indicators of inflammation, a lower infarction volume and less depressive behaviours, which were analyzed with the forced swimming test and the tail suspension test, thus, the new formulation was successful in its aim of attenuate the negative effects of global cerebral ischemia/reperfusion. (Moghaddam et al. 2020)

5.4.2. Chitooligosaccharides

In the treatment of the consequences of a brain ischemia or neurodegenerative disorders, besides employing chitosan as a carrier of drugs, chitooligosaccharides, the degradation product of chitosan, have its own interest. That is because they have demonstrated to have anti-apoptotic effects when cells undergo glucose deprivation. (Xu et al. 2011) Furthermore, in Alzheimer's disease, chitooligosaccharides have demonstrated, on the one hand, to inhibit the β-site amyloid precursor protein (APP)-cleaving enzyme (BACE), the enzyme responsible of the limiting step in the production of amyloid plaques, (Eom et al. 2013) and, on the other hand, to inhibit the acetylcholinesterase, what can be used to curb the cognitive deficits caused by the disease. (Lee et al. 2009)

5.5. Microalgae and microbial exopolysaccharides (EPS)

There are not research works in which EPS are used to target central nervous system. So, further research is necessary to exploit the possibilities of these polymers as new biomaterials or to improve the treatment of CNS pathologies by their pharmacological action, which is reasonable as they have shown anticancer activity in extracranial tumors and they could be used for the treatment of glioblastoma. (Laurienzo 2010)

6. Conclusion

Along this chapter, a review of the most important applications of marine biopolymers in the treatment of pathologies of the CNS has been done. There are two reasons why these polymers are interesting for the treatment of these diseases: (1) their biological activity and (2) their physical and chemical properties, such as biocompatibility and biodegradability, which make them appropriate for drug delivery.

The CNS pathologies that can be treated with marine biopolymers due to their biological activity are the following ones:

- Ulvans, from green algae: anxiety and depression.
- Fucoidans, from brown algae: brain injuries, depression, glioblastoma and neurodegenerative diseases (Alzheimer's disease and Parkinson's disease).
- Laminarin, from brown algae: brain injuries after stroke.
- Carrageenans, from red algae: neurodegenerative diseases (Alzheimer's disease).
- Galactan, from red algae: neurodegenerative diseases.

- Porphyran, from red algae: neurodegenerative diseases (Parkinson's disease).
- Chitooligosaccharides, from crustaceans: brain injuries after ischemia and neurodegenerative diseases (Alzheimer's disease).

Furthermore, alginate, chitosan, galactan and agarose, have proved to be appropriate polymers for the development of drug delivery systems to the CNS going, both, through the BBB and beyond the BBB. These formulations have been used to treat the following diseases:

- Alginate, from brown algae: deafness, neurodegenerative diseases, glioblastoma and spinal cord injury.
- Carrageenans, from red algae: neurodegenerative diseases (Parkinson's disease).
- Galactan, from red algae: glioblastoma.
- Chitosan, from crustaceans: epilepsy, migraine, neurodegenerative diseases (Parkinson's disease), spinal cord injury, glioblastoma and optic nerve injury.

In conclusion, marine world is a surprising and enormous source of new active substances and new materials. Some of them are useful for biomedical applications in general, and, in particular, to treat central nervous system pathologies. However, research in this area is only starting and a lot of effort and much more research are required to determine the potential of these resources, both, because of their pharmacological ability to treat diseases and because of their potential to deliver other drugs to their therapeutic target.

References

Aam BB, Heggset EB, Norberg AL, et al (2010) Production of chitooligosaccharides and their potential applications in medicine. Mar Drugs 8:1482–1517.

Abbot NJ, Patabendige AAK, Dolman DEM, et al (2010) Structure and function of the blood-brain barrier. Neurobiol Dis 37:13–25.

Abdallah MM, Fernández N, Matias AA, Bronze M do R (2020) Hyaluronic acid and Chondroitin sulfate from marine and terrestrial sources: Extraction and purification methods. Carbohydr Polym 243:116441.

Abhilash M, Thomas D (2017) Biopolymers for Biocomposites and Chemical Sensor Applications. In: Biopolymer Composites in Electronics. Elsevier Inc., pp 405–435

Aghoghovwia B, Mytilinaios D (2020) Meninges of the brain and spinal cord: Anatomy, function | Kenhub. https://www.kenhub.com/en/library/anatomy/meninges-of-the-brain-and-spinal-cord. Accessed 25 Jun 2020

Ahmad N, Ahmad R, Alrasheed RA, et al (2020a) Quantification and evaluations of catechin hydrate polymeric nanoparticles used in brain targeting for the treatment of epilepsy. Pharmaceutics 12:. https://doi.org/10.3390/pharmaceutics12030203

Ahmad SI, Ahmad R, Khan MS, et al (2020b) Chitin and its derivatives: Structural properties and biomedical applications. Int J Biol Macromol 164:526–539.

Ahn JH, Shin MC, Kim DW, et al (2019) Antioxidant properties of fucoidan alleviate acceleration and exacerbation of hippocampal neuronal death following transient global cerebral ischemia in high-fat diet-induced obese gerbils. Int J Mol Sci 20:554.

Almond A (2007) Hyaluronan. Cell Mol Life Sci 64:1591–6.

Alves A, Sousa RA, Reis RL (2013) A practical perspective on ulvan extracted from green algae. J Appl Phycol 25:407–424.

American Association of Neurological Surgeons Glioblastoma Multiforme. https://www.aans.org/en/Patients/Neurosurgical-Conditions-and-Treatments/Glioblastoma-Multiforme. Accessed 5 Aug 2020

American Psychiatric Association (2013) Diagnostic and Statistical Manual of Mental Disorders (DSM-5), Fifth. Reviews

American Stroke Association (2018) What is a TIA. https://www.stroke.org/en/about-stroke/types-of-stroke/tia-transient-ischemic-attack/what-is-a-tia. Accessed 4 Aug 2020

An H, Li Q, Wen J (2020) Bone marrow mesenchymal stem cells encapsulated thermal-responsive hydrogel network bridges combined photo-plasmonic nanoparticulate system for the treatment of urinary bladder dysfunction after spinal cord injury. J Photochem Photobiol B Biol 203:. https://doi.org/10.1016/j.jphotobiol.2019.111741

Azeem M, Batool F, Iqbal N, Ikram-ul-Haq (2017) Algal-Based Biopolymers. In: Algae Based Polymers, Blends, and Composites: Chemistry, Biotechnology and Materials Science. Elsevier, pp 1–31

Barbosa AI, Coutinho AJ, Costa Lima SA, Reis S (2019) Marine Polysaccharides in Pharmaceutical Applications: Fucoidan and Chitosan as Key Players in the Drug Delivery Match Field. Mar Drugs 17:654.

Bardajee GR, Khamooshi N, Nasri S, Vancaeyzeele C (2020) Multi-stimuli responsive nanogel/hydrogel nanocomposites based on κ-carrageenan for prolonged release of levodopa as model drug. Int J Biol Macromol 153:180–189.

Beghi E (2020) The Epidemiology of Epilepsy. Neuroepidemiology 54:185–191.

Blasco-Serra A, González-Soler EM, Cervera-Ferri A, et al (2017) A standardization of the Novelty-Suppressed Feeding Test protocol in rats. Neurosci Lett 658:73–78.

Blaško J, Szekiova E, Slovinska L, et al (2017) Axonal outgrowth stimulation after alginate/mesenchymal stem cell therapy in injured rat spinal cord - PubMed. Acta Neurobiol Exp 77:337–350

Caban-Toktas S, Sahin A, Lule S, et al (2020) Combination of Paclitaxel and R-flurbiprofen loaded PLGA nanoparticles suppresses glioblastoma growth on systemic administration. Int J Pharm 578:119076.

Can A, Dao DT, Arad M, et al (2011a) The mouse forced swim test. J Vis Exp 3638. https://doi.org/10.3791/3638

Can A, Dao DT, Terrillion CE, et al (2011b) The tail suspension test. J Vis Exp 3769. https://doi.org/10.3791/3769

Cardia MC, Carta AR, Caboni P, et al (2019) Trimethyl chitosan hydrogel nanoparticles for progesteronedelivery inneurodegenerativedisorders. Pharmaceutics 11:. https://doi.org/10.3390/pharmaceutics11120657

ChEBI Agarose (CHEBI:2511). https://www.ebi.ac.uk/chebi/searchId.do?chebiId=2511. Accessed 14 Aug 2020

Cometa S, Bonifacio MA, Trapani G, et al (2020) In vitro investigations on dopamine loaded Solid Lipid Nanoparticles. J Pharm Biomed Anal 185:. https://doi.org/10.1016/j.jpba.2020.113257

Crumbie L, Johnson E (2020) Diencephalon: Anatomy and function | Kenhub. https://www.kenhub.com/en/library/anatomy/diencephalon. Accessed 20 Jun 2020

CyberColloids Introduction to Carrageenan - Structure . http://www.cybercolloids.net/information/technical-articles/introduction-carrageenan-structure. Accessed 14 Aug 2020

de Jesus Raposo M, de Morais A, de Morais R (2015) Marine Polysaccharides from Algae with Potential Biomedical Applications. Mar Drugs 13:2967–3028.

Delattre C, Fenoradosoa TA, Michaud P (2011) Galactans: An overview of their most important sourcing and applications as natural polysaccharides. Brazilian Arch Biol Technol 54:1075–1092.

Dimitrova-Shumkovska J, Krstanoski L, Veenman L (2020) Potential beneficial actions of fucoidan in brain and liver injury, disease, and intoxication-potential implication of sirtuins. Mar

Drugs 18:. https://doi.org/10.3390/md18050242

Encyclopædia Britannica (2019) Epilepsy. https://www.britannica.com/science/epilepsy. Accessed 29 Jul 2020

Eom TK, Ryu BM, Lee JK, et al (2013) β-secretase inhibitory activity of phenolic acid conjugated chitooligosaccharides. J Enzyme Inhib Med Chem 28:214–217.

Gabathuler R (2010) Approaches to transport therapeutic drugs across the blood-brain barrier to treat brain diseases. Neurobiol Dis 37:48–57.

Garre-Olmo J (2018) Epidemiology of alzheimer's disease and other dementias. Rev Neurol 66:377–386.

Gascon S, Solano AG, El Kheir W, et al (2020) Characterization and mathematical modeling of alginate/chitosan-based nanoparticles releasing the chemokine cxcl12 to attract glioblastoma cells. Pharmaceutics 12:356.

Geng L, Wang J, Zhang Z, et al (2019) Structure and Bioactivities of Porphyrans and Oligoporphyrans. Curr Pharm Des 25:1163–1171.

Gonçalves VSS, Matias AA, Poejo J, et al (2016) Application of RPMI 2650 as a cell model to evaluate solid formulations for intranasal delivery of drugs. Int J Pharm 515:1–10.

Ham TR, Pukale DD, Hamrangsekachaee M, Leipzig ND (2020) Subcutaneous priming of protein-functionalized chitosan scaffolds improves function following spinal cord injury. Mater Sci Eng C Mater Biol Appl 110:. https://doi.org/10.1016/j.msec.2020.110656

Hervé F, Ghinea N, Scherrmann JM (2008) CNS delivery via adsorptive transcytosis. AAPS J 10:455–472.

Huff T, Varacallo M (2019) Neuroanatomy, Cerebrospinal Fluid. StatPearls Publishing

Huntington's Disease Society of America (2020) Overview of Huntington's Disease . https://hdsa.org/what-is-hd/overview-of-huntingtons-disease/. Accessed 4 Aug 2020

Islam S, Bhuiyan MAR, Islam MN (2017) Chitin and Chitosan: Structure, Properties and Applications in Biomedical Engineering. J. Polym. Environ. 25:854–866

Johnson W, Onuma O, Owolabi M, Sachdev S (2016) Stroke: A global response is needed. World Health Organization

Khan NU, Miao T, Ju X, et al (2019) Carrier-mediated transportation through BBB. In: Brain Targeted Drug Delivery System. Elsevier, pp 129–158

Kidgell JT, Magnusson M, de Nys R, Glasson CRK (2019) Ulvan: A systematic review of extraction, composition and function. Algal Res. 39:101422

Komada M, Takao K, Miyakawa T (2008) Elevated plus maze for mice. J Vis Exp 1088. https://doi.org/10.3791/1088

Kuo YC, Wang LJ, Rajesh R (2019) Targeting human brain cancer stem cells by curcumin-loaded nanoparticles grafted with anti-aldehyde dehydrogenase and sialic acid: Colocalization of ALDH and CD44. Mater Sci Eng C 102:362–372.

Laurienzo P (2010) Marine Polysaccharides in Pharmaceutical Applications: An Overview. Mar

Drugs 8:2435–2465.

Lee SH, Park JS, Kim SK, et al (2009) Chitooligosaccharides suppress the level of protein expression and acetylcholinesterase activity induced by Aβ25-35 in PC12 cells. Bioorganic Med Chem Lett 19:860–862.

Lee TK, Ahn JH, Park CW, et al (2020) Pre-treatment with laminarin protects hippocampal CA1 pyramidal neurons and attenuates reactive gliosis following transient forebrain ischemia in gerbils. Mar Drugs 18:. https://doi.org/10.3390/md18010052

Li M, Sun X, Li Q, et al (2020) Fucoidan exerts antidepressant-like effects in mice via regulating the stability of surface AMPARs. Biochem Biophys Res Commun 521:318–325.

Liao CH, Lai IC, Kuo HC, et al (2019) Epigenetic modification and differentiation induction of malignant glioma cells by oligo-fucoidan. Mar Drugs 17:. https://doi.org/10.3390/md17090525

Liu Y, Geng L, Zhang J, et al (2018) Oligo-porphyran ameliorates neurobehavioral deficits in parkinsonian mice by regulating the PI3K/Akt/Bcl-2 pathway. Mar Drugs 16:. https://doi.org/10.3390/md16030082

Liu Y, Jiang L, Li X (2017) κ-carrageenan-derived pentasaccharide attenuates Aβ25-35-induced apoptosis in SH-SY5Y cells via suppression of the JNK signaling pathway. Mol Med Rep 15:285–290.

Living Cell Technologies Limited (2020) NTCELL. https://lctglobal.com/research/ntcell. Accessed 10 Aug 2020

Löscher W, Potschka H (2005) Blood-brain barrier active efflux transporters: ATP-binding cassette gene family. NeuroRx 2:86–98.

Lu CT, Zhao YZ, Wong HL, et al (2014) Current approaches to enhance CNS delivery of drugs across the brain barriers. Int J Nanomedicine 9:2241–2257.

Mamo JC, Lam V, Al-Salami H, et al (2018) Sodium alginate capsulation increased brain delivery of probucol and suppressed neuroinflammation and neurodegeneration. Ther Deliv 9:703–709.

Mayfield Brain & Spine (2018) Anatomy of the Human Brain. https://mayfieldclinic.com/pe-anatbrain.htm. Accessed 11 Jun 2020

Miller AH, Raison CL (2016) The role of inflammation in depression: From evolutionary imperative to modern treatment target. Nat Rev Immunol 16:22–34.

Mišurcová L, Škrovánková S, Samek D, et al (2012) Health Benefits of Algal Polysaccharides in Human Nutrition. In: Advances in Food and Nutrition Research. Academic Press Inc., pp 75–145

Moghaddam AH, Mokhtari Sangdehi SR, Ranjbar M, Hasantabar V (2020) Preventive effect of silymarin-loaded chitosan nanoparticles against global cerebral ischemia/reperfusion injury in rats. Eur J Pharmacol 877:. https://doi.org/10.1016/j.ejphar.2020.173066

Morrice LM, McLean MW, Long WF, Williamson FB (1984) Porphyran primary structure. In:

Eleventh International Seaweed Symposium. Springer Netherlands, pp 572–575

Moussian B (2019) Chitin: Structure, chemistry and biology. In: Advances in Experimental Medicine and Biology. Springer New York LLC, pp 5–18

Mulroney SE, Myers AK (2011) 4. Organization and General Functions of the Nervous System. In: Netter's Essential Physiology, 1 st. Elsevier Inc., pp 49–58

National Institute of Child Health and Human Development (2019) Medication Treatment for Autism . https://www.nichd.nih.gov/health/topics/autism/conditioninfo/treatments/medication-treatment. Accessed 27 Jul 2020

National Institute of Child Health and Human Development (2016) What are the treatments for spinal cord injury (SCI)? . https://www.nichd.nih.gov/health/topics/spinalinjury/conditioninfo/treatments. Accessed 4 Aug 2020

National Institute of Neurological Disorders and Stroke (2013) Amyotrophic Lateral Sclerosis (ALS) Fact Sheet. https://www.ninds.nih.gov/disorders/Patient-Caregiver-Education/Fact-Sheets/Amyotrophic-Lateral-Sclerosis-ALS-Fact-Sheet. Accessed 4 Aug 2020

National Institute on Aging (2019) Alzheimer's Disease Fact Sheet . https://www.nia.nih.gov/health/alzheimers-disease-fact-sheet. Accessed 2 Aug 2020

National Institute on Aging (2017) Parkinson's Disease . https://www.nia.nih.gov/health/parkinsons-disease. Accessed 4 Aug 2020

Nazemi Z, Nourbakhsh MS, Kiani S, et al (2020) Co-delivery of minocycline and paclitaxel from injectable hydrogel for treatment of spinal cord injury. J Control Release 321:145–158.

Nguyen TPT, Tran BM, Lee NY (2018) Microfluidic approach for the fabrication of cell-laden hollow fibers for endothelial barrier research. J Mater Chem B 6:6057–6066.

NHS (2019a) Migraine. https://www.nhs.uk/conditions/migraine/. Accessed 29 Jul 2020

NHS (2018) Alzheimer's disease. https://www.nhs.uk/conditions/alzheimers-disease/. Accessed 2 Aug 2020

NHS (2019b) Stroke. https://www.nhs.uk/conditions/stroke/. Accessed 4 Aug 2020

Ojeda-Hernández DD, Canales-Aguirre AA, Matias-Guiu J, et al (2020) Potential of Chitosan and Its Derivatives for Biomedical Applications in the Central Nervous System. Front Bioeng Biotechnol 8:. https://doi.org/10.3389/fbioe.2020.00389

OpenStax College The Central Nervous System | Anatomy and Physiology. https://courses.lumenlearning.com/nemcc-ap/chapter/the-central-nervous-system/. Accessed 11 Jun 2020

Osama M, Nasr Mostafa M, Ali Alvi M (2020) Astrocyte Elevated Gene-1 as a Novel Therapeutic Target in Malignant Gliomas and Its Interactions with Oncogenes and Tumor Suppressor Genes. Brain Res 147034. https://doi.org/10.1016/j.brainres.2020.147034

Pangestuti R, Kim SK (2014) Biological activities of Carrageenan. In: Advances in Food and

Nutrition Research. Academic Press Inc., pp 113–124

Park JH, Ahn JH, Lee TK, et al (2020) Laminarin pretreatment provides neuroprotection against forebrain ischemia/reperfusion injury by reducing oxidative stress and neuroinflammation in aged gerbils. Mar Drugs 18:. https://doi.org/10.3390/md18040213

Park SK, Kang JY, Kim JM, et al (2019) Fucoidan-Rich Substances from Ecklonia cava Improve Trimethyltin-Induced Cognitive Dysfunction via Down-Regulation of Amyloid β Production/Tau Hyperphosphorylation. Mar Drugs 17:. https://doi.org/10.3390/md17100591

Parkinson's Foundation (2020) Understanding Parkinson's: Statistics. https://www.parkinson.org/Understanding-Parkinsons/Statistics. Accessed 4 Aug 2020

Pinhassi RI, Assaraf YG, Farber S, et al (2010) Arabinogalactan-folic acid-drug conjugate for targeted delivery and target-activated release of anticancer drugs to folate receptor-overexpressing cells. Biomacromolecules 11:294–303.

PubChem Chondroitin sulfate | C13H21NO15S. https://pubchem.ncbi.nlm.nih.gov/compound/Chondroitin-sulfate. Accessed 14 Aug 2020

Pulgar VM (2019) Transcytosis to cross the blood brain barrier, new advancements and challenges. Front Neurosci 13:. https://doi.org/10.3389/fnins.2018.01019

Purves D, Augustine GJ, Fitzpatrick D, et al (2001) The Retina. In: Neuroscience, 2 nd. Sinauer Associates

Raz A, Perouansky M (2018) Central nervous system physiology: Neurophysiology. In: Pharmacology and Physiology for Anesthesia: Foundations and Clinical Application. Elsevier, pp 145–173

Reginster JY, Veronese N (2020) Highly purified chondroitin sulfate: a literature review on clinical efficacy and pharmacoeconomic aspects in osteoarthritis treatment. Aging Clin Exp Res 1–11. https://doi.org/10.1007/s40520-020-01643-8

Renjith V, Pai MS, Castelino F, et al (2016) Clinical profile and functional disability of patients with migraine. J Neurosci Rural Pract 7:250–256.

Rinaudo M (2006) Chitin and chitosan: Properties and applications. Prog Polym Sci 31:603–632.

Salem LH, El-Feky GS, Fahmy RH, et al (2020) Coated Lipidic Nanoparticles as a New Strategy for Enhancing Nose-to-Brain Delivery of a Hydrophilic Drug Molecule. J Pharm Sci 109:. https://doi.org/10.1016/j.xphs.2020.04.007

Sanchez-Covarrubias L, Slosky L, Thompson B, et al (2014) Transporters at CNS Barrier Sites: Obstacles or Opportunities for Drug Delivery? Curr Pharm Des 20:1422–1449.

Sánchez-Dengra B, González-Álvarez I, Bermejo M, González-Álvarez M (2020) Nanomedicine in the Treatment of Pathologies of the Central Nervous System Advances in Nanomedicine. In: Advances in Nanomedicine

Scheper V, Hoffmann A, Gepp MM, et al (2019) Stem cell based drug delivery for protection of auditory neurons in a guinea pig model of cochlear implantation. Front Cell Neurosci 13:.

https://doi.org/10.3389/fncel.2019.00177

Schwieger J, Hamm A, Gepp MM, et al (2020) Alginate-encapsulated brain-derived neurotrophic factor–overexpressing mesenchymal stem cells are a promising drug delivery system for protection of auditory neurons. J Tissue Eng 11:. https://doi.org/10.1177/2041731420911313

Serchov T, van Calker D, Biber K (2016) Sucrose Preference Test to Measure Anhedonic Behaviour in Mice. BIO-PROTOCOL 6:. https://doi.org/10.21769/bioprotoc.1958

Shepherd Center Spinal Cord Injury Information: Levels, Causes, Recovery. https://www.shepherd.org/patient-programs/spinal-cord-injury/about. Accessed 4 Aug 2020

Singh R, Brumlik C, Vaidya M, Choudhury A (2020) A Patent Review on Nanotechnology-Based Nose-to-Brain Drug Delivery. Recent Pat Nanotechnol 14:. https://doi.org/10.2174/1872210514666200508121050

Sitoci-Ficici KH, Matyash M, Uckermann O, et al (2018) Non-functionalized soft alginate hydrogel promotes locomotor recovery after spinal cord injury in a rat hemimyelonectomy model. Acta Neurochir (Wien) 160:449–457.

Snow B, Mulroy E, Bok A, et al (2019) A phase IIb, randomised, double-blind, placebo-controlled, dose-ranging investigation of the safety and efficacy of NTCELL® [immunoprotected (alginate-encapsulated) porcine choroid plexus cells for xenotransplantation] in patients with Parkinson's disease. Park Relat Disord 61:88–93.

Sweeney MD, Zhao Z, Montagne A, et al (2019) Blood-brain barrier: From physiology to disease and back. Physiol Rev 99:21–78.

Teleanu DM, Negut I, Grumezescu V, et al (2019) Nanomaterials for drug delivery to the central nervous system. Nanomaterials 9:. https://doi.org/10.3390/nano9030371

Tortora GJ, Derrickson B (2011a) Chapter 12: Nervous Tissue. In: Principles of anatomy and physiology, 11th edn. John Wiley and Sons, Inc., pp 407–442

Tortora GJ, Derrickson B (2011b) Chapter 14: The Brain and Cranial Nerves. In: Principles of Anatomy and Physiology, 11th edn. John Wiley and Sons, Inc., pp 477–527

Tortora GJ, Derrickson B (2011c) Chapter 13: The Spinal Cord and Spinal Nerves. In: Principles of anatomy and physiology, 11th edn. John Wiley and Sons, Inc., pp 443–476

TRB Chemedica UK Structure of Hyaluronan. https://vismed.trbchemedica.co.uk/business-professionals/role-and-purpose-of-hyaluronan/structure-of-hyaluronan. Accessed 14 Aug 2020

Vashist A, Atluri V, Raymond A, et al (2020) Development of Multifunctional Biopolymeric Auto-Fluorescent Micro- and Nanogels as a Platform for Biomedical Applications. Front Bioeng Biotechnol 8:. https://doi.org/10.3389/fbioe.2020.00315

Vendel E, Rottschäfer V, de Lange ECM (2019) The need for mathematical modelling of spatial drug distribution within the brain. Fluids Barriers CNS 16:12.

Venkatraman KL, Mehta A (2019) Health Benefits and Pharmacological Effects of Porphyra Species. Plant Foods Hum Nutr 74:10–17.

Violle N, Rozan P, Demais H, et al (2018) Evaluation of the antidepressant- and anxiolytic-like effects of a hydrophilic extract from the green seaweed Ulva sp. in rats. Nutr Neurosci 21:248–256.

Virtual Health Library (2017) Health Sciences Descriptors: DeCS. http://decs.bvsalud.org/I/homepagei.htm. Accessed 30 Jul 2020

Wang D, Luo M, Huang B, et al (2020) Localized co-delivery of CNTF and FK506 using a thermosensitive hydrogel for retina ganglion cells protection after traumatic optic nerve injury. Drug Deliv 27:556–564.

Wong AD, Ye M, Levy AF, et al (2013) The blood-brain barrier: An engineering perspective. Front Neuroeng 6:. https://doi.org/10.3389/fneng.2013.00007

World Health Organization (2019a) Autism spectrum disorders. https://www.who.int/news-room/fact-sheets/detail/autism-spectrum-disorders. Accessed 27 Jul 2020

World Health Organization (2020) Depression. https://www.who.int/news-room/fact-sheets/detail/depression. Accessed 28 Jul 2020

World Health Organization (2019b) Epilepsy. https://www.who.int/news-room/fact-sheets/detail/epilepsy. Accessed 19 Jun 2020

World Health Organization (2016) Headache disorders. https://www.who.int/news-room/fact-sheets/detail/headache-disorders. Accessed 29 Jul 2020

World Health Organization (2019c) Dementia. https://www.who.int/news-room/fact-sheets/detail/dementia. Accessed 19 Jun 2020

World Health Organization (2013) Spinal cord injury. https://www.who.int/news-room/fact-sheets/detail/spinal-cord-injury. Accessed 4 Aug 2020

Xu Y, Zhang Q, Yu S, et al (2011) The protective effects of chitooligosaccharides against glucose deprivation-induced cell apoptosis in cultured cortical neurons through activation of PI3K/Akt and MEK/ERK1/2 pathways. Brain Res 1375:49–58.

Yazdi MK, Taghizadeh A, Taghizadeh M, et al (2020) Agarose-based biomaterials for advanced drug delivery. J Control Release 326:523–543.

Ye XC, Hao Q, Ma WJ, et al (2020) Dectin-1/Syk signaling triggers neuroinflammation after ischemic stroke in mice. J Neuroinflammation 17:. https://doi.org/10.1186/s12974-019-1693-z

Yeh WZ, Blizzard L, Taylor B V. (2018) What is the actual prevalence of migraine? Brain Behav 8:. https://doi.org/10.1002/brb3.950

Youssouf L, Bhaw-Luximon A, Diotel N, et al (2019) Enhanced effects of curcumin encapsulated in polycaprolactone-grafted oligocarrageenan nanomicelles, a novel nanoparticle drug delivery system. Carbohydr Polym 217:35–45.

Zargarzadeh M, Amaral AJR, Custódio CA, Mano JF (2020) Biomedical applications of laminarin.

Carbohydr Polym 232:115774.

Zayed A, Ulber R (2020) Fucoidans: Downstream Processes and Recent Applications. Mar Drugs 18:170.

Zhang L, Hao J, Zheng Y, et al (2018) Fucoidan protects dopaminergic neurons by enhancing the mitochondrial function in a rotenone-induced rat model of parkinson's disease. Aging Dis 9:590–604.

Zhang Q, Li N, Liu X, et al (2004) The structure of a sulfated galactan from Porphyra haitanensis and its in vivo antioxidant activity. Carbohydr Res 339:105–111.

3. *In vitro* model for predicting the access and distribution of drugs in the brain using hCMEC/D3 cells

Type of publication	Article
Title	*In vitro* model for predicting the access and distribution of drugs in the brain using hCMEC/D3 cells
Authors	Bárbara Sánchez-Dengra, Isabel González-Álvarez, Flavia Sousa, Marival Bermejo, Marta González-Álvarez and Bruno Sarmento
Journal	European Journal of Pharmaceutics and Biopharmaceutics
Impact factor	5.571 (Q1 - Pharmacology and Pharmacy)
Year of publication	2021
DOI	doi.org/10.1016/j.ejpb.2021.04.002

Abstract:

The BBB is a protective entity that prevents external substances from reaching the CNS but it also hinders the delivery of drugs into the brain when they are needed. The main objective of this work was to improve a previously proposed *in vitro* cell-based model by using a more physiological cell line (hCMEC/D3) to predict the main pharmacokinetic parameters that describe the access and distribution of drugs in the CNS: $Kp_{uu,brain}$, $f_{u,plasma}$, $f_{u,brain}$ and $V_{u,brain}$. The hCMEC/D3 permeability of seven drugs was studied in transwell systems under different conditions (standard, modified with albumin and modified with brain homogenate). From the permeability coefficients of those experiments, the parameters mentioned above were calculated and four linear IVIVCs were established. The best ones were those that relate the *in vitro* and *in vivo* $V_{u,brain}$ and $f_{u,brain}$ (r^2= 0.961 and r^2 = 0.940) which represent the binding rate of a substance to the brain tissue, evidencing the importance of using brain homogenate to mimic brain tissue when an *in vitro* brain permeability assay is done. This methodology could be a high-throughput screening tool in drug development to select the CNS promising drugs in three different *in vitro* BBB models (hCMEC/D3, MDCK and MDCK-MDR1).

Keywords:

Blood−brain barrier (BBB); IVIVC; unbound fraction (f_u); distribution volume in brain ($V_{u,brain}$); plasma−brain partition coefficient ($Kp_{uu,brain}$).

Abbreviations

Apparent volume of distribution in brain ($V_{u,brain}$)

Blood-brain barrier (BBB)

Central nervous system (CNS)

Efflux clearance (Cl_{out})

Fetal bovine serum (FBS)

Hank's balanced salt solution (HBSS)

Influx clearance (Cl_{in})

In vitro-in vivo correlation (IVIVC)

Permeability coefficient (P_{eff})

Prediction error percentage (PE%)

Transepithelial electrical resistance (TEER)

Unbound fraction of drug in brain ($f_{u,brain}$)

Unbound fraction of drug in plasma ($f_{u,plasma}$)

Unbound plasma–brain partition coefficient ($Kp_{uu,brain}$)

INTRODUCTION

The blood-brain barrier (BBB) is a protective entity that acts preventing drugs or nutrients from reaching the central nervous system (CNS). This characteristic helps to maintain brain homeostasis and allows the brain to function properly. However, this protective mission of the BBB displays a huge drawback since it makes extremely difficult to deliver drugs into the CNS when they are needed. [1–3]

There are several pathways that molecules could use to cross the BBB: paracellular diffusion, transcellular diffusion, carrier-mediated transport, receptor-mediated transport, adsorptive-mediated transport and cell-mediated transport. [4–6] Nevertheless, the physicochemical properties of those molecules limit the use of one pathway or another. For instance, paracellular diffusion and transcellular diffusion are limited to very small hydrophilic or lipophilic molecules; carrier-mediated and receptor-meditated transports can be used by essential molecules, such as, glucose, amino acids, insulin or lipoproteins, that need to specifically bind their carrier or receptor; and molecules using the adsorptive-mediated route or the cell-mediated route need to have positive charge or be able to be internalized by an immune cell. [6] Furthermore, if a molecule reaches the brain, it can be returned to the circulatory system by means of several efflux transporters (ATP-binding cassette transporters). [7] Because of all that, permeability evaluation tools are needed for evaluating the ability of new drugs or new delivery systems to cross the BBB while they are developed.

Drug transport into brain can be measured by *in silico*, *in vitro*, *in situ* or *in vivo* methods.[8] *In vitro* methods can be considered the most interesting ones as **(a)** they normally give better predictions than the *in silico* methods (they can evaluate other properties besides permeability, as cell toxicity) and **(b)** they are faster, cheaper and easier to handle than the *in vivo* ones. [9] During the last years, different cell-based *in vitro* models have been tested to evaluate drug penetration across BBB, such as primary cell cultures or immortalized cell lines from different origins (RBE4 from rat, MBEC4 from mouse, MDCK from dog or hCMEC/D3 from human, among others).[10–13]

Physiologically, BBB is constituted by endothelial cells of brain capillaries which enter deeply into the brain structure and allow brain cells to exchange oxygen, nutrients and waste substances with the circulatory system.[14,15] An ideal cell-based BBB model should meet the following characteristics (a) expressing tight junctions to form a selective barrier and maintain a high electrical resistance, (b) exhibiting functional efflux and influx transporters and a polarized structure, (c) being able to classify substances in accordance

to their permeability, (d) being able to response to aggressions as *in vivo* BBB does and (e) simulating the differentiation pattern provoked by the shear stress from blood flow. [10,16]

A lot of *in vitro* methods have been tested to reproduce the characteristics mentioned above. [17,18] Except for the latter characteristic, which can only be reached when dynamic *in vitro* BBB models are used, the hCMEC/D3 cell line when properly culture, possesses all the other mentioned properties. This cell line is one of the best known and most applied as BBB model cell line until the moment.[19]

From a pharmacokinetic point of view, a good *in vitro* BBB model should be able to predict the rate and extent in which a substance will access to the brain. [20–22] Several factors can determine rate and extent of access to CNS, namely, the plasma levels of the substance, its binding to plasma protein (as only the free fraction will diffuse through the BBB), its effective permeability through the endothelial membrane, the contribution of influx and/or efflux transporters, the metabolic modifications occurred in the barrier itself and its binding to the brain tissue.[15,23]

In 2013, Mangas-Sanjuan et al. developed a new *in vitro* method, using MDCKII and MDCKII-MDR1 cell lines, able to predict the main pharmacokinetic parameters that describe the entrance and distribution of different drugs in the CNS ($Kp_{uu,brain}$, $f_{u,plasma}$, $f_{u,brain}$ and $V_{u,brain}$) from the apparent permeability values (P_{app}) of those drugs. [24] The $Kp_{uu,brain}$ is the ratio between the free drug concentration in plasma and the free drug concentration in brain once the steady state has been reached, the $f_{u,plasma}$ is the free fraction of drug in plasma, the $f_{u,brain}$ is the free fraction of drug in the brain and the $V_{u,brain}$ represents the apparent volume of distribution in this organ.

As the MDCKII and MDCKII-MDR1 cell lines, despite having extremely tighten junctions, which has made them a good model for assessing BBB permeability, they have any (MDCKII) or just one (MDCKII-MDR1) BBB transporter. [9] The purpose of this research was to improve the previously mentioned *in vitro* model by using a more physiological cell line, hCMEC/D3 cell line, which, coming from human temporal lobe microvessels, has much more BBB transporters in its surface and should be able to predict the BBB permeability for not just passives drugs, but also those substrates of transporters.[10,19] For assessing this objective, the permeability of seven drugs (some present in the other model and some new ones) was studied in hCMEC/D3 cells under different conditions and the pharmacokinetic parameters mentioned above were calculated. Finally, *in vitro-in vivo* correlations (IVIVCs) between the predicted parameters and experimental parameters

obtained in rat[25,26] were established.

MATERIALS AND METHODS

1. Drug and products

The drugs chosen because of their different properties, amitriptyline, atenolol, carbamazepine, fleroxacin, genistein, pefloxacin and zolpidem, were purchased from Sigma-Aldrich (Spain). Molecular properties and the *in vivo* $Kp_{uu,brain}$, $f_{u,plasma}$, $f_{u,brain}$ and $V_{u,brain}$ values of the studied drugs are shown in Table 1. [25–28]

Hydrocortisone, ascorbic acid, HEPES and bFGF (basic fibroblast growth factor) and HPLC grade chemicals as Methanol, water or Acetonitrile were purchased from Sigma-Aldrich. Fetal bovine serum (FBS), penicillin-streptomycin, chemically defined lipid concentrate, Hank's balanced salt solution (HBSS), collagen I rat protein and trypsin-EDTA were purchased from Gibco. EBM-2 medium was purchased from Lonza and Triton X-100 from Spi-Chem. Immortalized Human Cerebral Microvascular Endothelial Cell Line (hCMEC/D3 cell line) was purchased from Cedarlane (Canada).

Table 1. Physicochemical properties and *in vivo* data from rat for each drug tested.[25–28] $V_{u,brain}$ units are mL/g brain.

	MW (g/mol)	**logP**	**Strongest acidic pKa**	**Strongest basic pKa**	**BCS**	**P-gp**	**$Kp_{uu,brain}$**	**$f_{u,plasma}$**	**$f_{u,brain}$**	**$V_{u,brain}$**
Amitriptyline	277.411	4.81		9.76	I	Substrate	0.730	0.090	0.002	310.000
Atenolol	266.341	0.43	14.08	9.67	III	Substrate	0.030	1.000	0.261	2.500
Carbamazepine	236.274	2.77	15.96		II	Inductor	0.771	0.385	0.170	3.729
Fleroxacin	369.344	0.98	5.32	5.99	IV		0.250	0.793	0.555	1.281
Genistein	270.240	3.08	6.55		II	Inhibitor	0.181	0.010	0.053	11.499
Pefloxacin	333.363	0.75	5.5	6.44	I	Substrate	0.199	0.860	0.514	1.367
Zolpidem	307.397	3.02		5.39	I		0.447	0.267	0.265	2.464

2. Cell culture

hCMEC/D3 cells were maintained in EBM-2 culture medium adding 5% (v/v) FBS, 1 % (v/v) penicillin-streptomycin, hydrocortisone (0.5 µg/ml), ascorbic acid (5 µg/ml), 1 % (v/v) lipid concentrate, 1 % (v/v) HEPES and bFGF (1 ng/ml - added directly into the flasks when cells were cultured).

Cells were maintained in an incubator at 37ºC, 5% CO_2 and 90% humidity in 75 cm^2 flasks at a cell density of 2.5 x 10^4 cells/cm^2.

3. Permeability studies

The BBB *in vitro* model for carrying out the permeability tests was obtained after seeding hCMEC/D3 cells at a density of 2.5 x 10^4 cells/cm^2 in the apical chamber, previously coated with 50 µg/mL collagen I rat protein in 0.02 M acetic acid in a 6-transwell plates (effective area: 4.2 cm^2, pore size: 0.4 micron and pore density: 100 ± 10 x 10^6/cm^2) and incubating them until confluence (8 days) replacing the culture medium each two days.

The transepithelial electrical resistance (TEER) was measured all the days that the culture medium was changed and, additionally, at the beginning and at the end of the permeability studies to check that the cell monolayers maintained their integrity. The cell monolayers were considered properly formed when their TEER value, corrected by the value of an empty transwell, reached 30-50 Ω•cm^2.[29]

After 8 days of cell seeding, permeability tests were performed in non-sterile conditions in an orbital shaker at 37ºC and 100 rpm. The culture medium was replaced by HBSS, as isotonic buffer solution. Four types of experiments were carried out, in which the apical chamber (2 mL) of the transwell plates represents the plasma and the basolateral chamber (3 mL) of the transwell plates represents the brain.[24] Drug solutions were placed in one chamber and HBSS was placed in the other one. The volumes used in the apical chamber and the basolateral chamber correspond to those specified by the transwell manufacturer and allow liquids to reach the same height on both sides of it.

- Standard experiment (A-B) - This experiment was performed from apical-to-basolateral direction. Drug dissolved in HBSS (2 mL) was placed at time 0 in the apical chamber.
- Standard experiment (B-A) - In this case, the experiment was carried out from basolateral-to-apical direction. The drug dissolved in HBSS (3 mL) was placed at time 0 in the basolateral chamber.

- Albumin experiment (A-B) - In this case, the content of the apical compartment was modified adding albumin 4% (w/v), similar concentration that on human blood, with the aim of mimicking better the plasma compartment and implementing the protein binding of each drug. Transports experiments were done from apical-to-basolateral direction. Drug dissolved in 4% albumin HBSS (2 mL) was placed at time 0 in the apical chamber.
- Brain homogenate experiment (B-A) - For improving the simulation of the brain compartment, in this type of experiment, drug solution in the basolateral compartment (3 mL) was prepared in 1:3 pig brain homogenate:phosphate buffer (180 mM, pH 7.4) solution. Pig brain was selected as surrogate for human brain to mimic the lipid and protein composition of this organ. They were obtained from a local slaughterhouse and were kept frozen until their use. Previous to the experiment brain homogenate was prepared by using a hand blender and adding 3 parts of phosphate buffer to get a texture liquid enough to be able to take samples.

In all conditions, drug solutions were prepared 30 min before the beginning of the experiments and they were left in the orbital shaker at 37ºC during that time. As some of the drugs showed a very low water solubility, all the drugs studied were firstly dissolved in dimethyl sulfoxide (DMSO) and then diluted in HBSS, being the final concentration of DMSO 0.9% (v/v) for amitryptiline, 0.32% (v/v) for zolpidem and 0.09% (v/v) for the rest of the drugs. Final concentrations of drug solutions are shown in Table 2.

During permeability study, aliquots of 200 µL were taken after 15, 30, 60, 90, 120 and 180 min from acceptor compartment and the same volume was replaced with 200 µL of HBSS at 37ºC. Additionally, four extra samples, used for checking the mass balance of the permeability tests, were taken: a sample from the donor compartment at the final point, both samples from apical and basolateral chambers after washing the plates for measuring TEER values after the experiment and a sample from the cell monolayer disrupted by a Triton X-100 (1 %) solution at the end of the experiment.

4. HPLC analysis of the samples

Samples were evaluated using an ultraviolet (UV) HPLC set (Waters 2695 separation module and Waters 2487 UV detector) and a XBridge C18 column (3.5µM, 4.6 x 100 mm). Run temperature was established at 30ºC, injection volume was 90 µL and flow rate was 1 mL/min. Other chromatographic conditions are summarized in Table 2.

Table 2. Chromatographic methods used in HPLC. Acid water had 0.5 % (v/v) trifluoroacetic acid.

	C (µM)	Wavelength	Mobile phase	Retention time (min)
Amitriptyline	250	240 nm	40% Acid water 60% Acetonitrile	1.020
Atenolol	150	231 nm	20% Methanol 60% Acid water 20% Acetonitrile	1.330
Carbamazepine	18	280 nm	65% Acid water 35% Acetonitrile	1.926
Fleroxacin	1.39	285 nm	70% Acid water 30% Acetonitrile	1.348
Genistein	3.81	254 nm	60% Methanol 15% Acid water 25% Acetonitrile	1.334
Pefloxacin	8.91	285 nm	65% Acid water 35% Acetonitrile	0.721
Zolpidem	158	231 nm	60% Water 20% Methanol 20% Acetonitrile	4.624

All analytical methods were validated and demonstrated to be adequate regarding linearity, accuracy, precision, selectivity and specificity. Samples from albumin and brain homogenate experiments were diluted (50:50) with cold methanol to precipitate proteins. Then, all the samples, from all the experiments, were centrifuged at 10000 rpm for 10 min and supernatant was analyzed by HPLC. Acid water had 0.5 % (v/v) trifluoroacetic acid.

5. Data analysis

All the calculations and plots shown in this paper were obtained with Excel®.

Four different methodologies[30] were used for calculating the permeability coefficient (P_{eff}, cm/s) for each drug and each experimental condition:

- The Sink equation (eq.1), in which dQ/dt is the apparent arrival of drug in the acceptor compartment, S is the surface area of the monolayer and C_0 is the initial concentration of drug administered in the donor compartment. This equation assumes sink conditions during all the experiment which means that the acceptor

concentration is always lower than the 10% of the concentration administered in donor.

$$P_{eff} = \frac{\left(\frac{dQ}{dt}\right)}{S \cdot \boldsymbol{C_0}} \quad (1)$$

- The Sink Corrected equation (eq. 2) which, although assuming sink conditions, considers the change in donor concentration during the experiment. In this equation all the terms are the same as in the Sink one but C_D that is the concentration in the donor compartment at each sample time.

$$P_{eff} = \frac{\left(\frac{dQ}{dt}\right)}{S \cdot \boldsymbol{C_D}} \quad (2)$$

- The Non-Sink equation (eq. 3) which was developed with the aim of being able to calculate the permeability coefficient when sink conditions are, both, fulfilled or not fulfilled. $C_{receiver,t}$ is the concentration of the drug in receptor chamber at time t, Q_{total} is the total amount of compound in both chambers, $V_{receiver}$ and V_{donor} are the volumes of each compartment, $C_{receiver,t-1}$ is the drug concentration in receptor compartment at previous time, f is the sample replacement dilution factor, S is the area of the monolayer and Δt is the time interval.

$$C_{receiver,t} = \frac{Q_{total}}{V_{receiver} + V_{donor}} + \left(\left(C_{receiver,t-1} \cdot f \right) - \frac{Q_{total}}{V_{receiver} + V_{donor}} \right) \cdot e^{-\boldsymbol{P_{eff}} \cdot S \cdot \left(\frac{1}{V_{receiver}} + \frac{1}{V_{donor}} \right) \cdot \Delta t} \quad (3)$$

- The Modified Non-Sink Equation (eq. 4) which has the advantage of giving the opportunity of defining two different P_{eff} depending on time when the permeation rate is different at the beginning of the experiment. The terms of this equation are the same as in the Non-Sink one but the permeability coefficient can take two values $P_{eff,0}$ or $P_{eff,1}$. This methodology has demonstrated to be the best tool for obtaining the permeability values, in both sink and no sink conditions, when the initial permeation rate is altered in with regard to the rest of the transport profile.[30]

$$C_{receiver,t} = \frac{Q_{total}}{V_{receiver} + V_{donor}} + \left(\left(C_{receiver,t-1} \cdot f \right) - \frac{Q_{total}}{V_{receiver} + V_{donor}} \right) \cdot e^{-\boldsymbol{P_{eff0,1}} \cdot S \cdot \left(\frac{1}{V_{receiver}} + \frac{1}{V_{donor}} \right) \cdot \Delta t} \quad (4)$$

Finally, the permeability values obtained with the method that best suited each case were chosen for calculating the $Kp_{uu,brain}$, $f_{u,plasma}$, $f_{u,brain}$ and $V_{u,brain}$ parameters. The deduction of the equations used for obtaining the main pharmacokinetic parameters that describe the entrance and distribution of drugs in the CNS ($Kp_{uu,brain}$, $f_{u,plasma}$, $f_{u,brain}$ and $V_{u,brain}$) was previously explained in Mangas-Sanjuan *et al*. work. [24] Briefly:

- $Kp_{uu,brain}$ (eq. 5), defined as the ratio between the unbound concentration in plasma and the unbound concentration in brain once the steady state has been reached, is estimated from the combination of the permeability values obtained in both standard experiments, apical-to-basolateral ($P_{app\ A\rightarrow B}$) and basolateral-to-apical ($P_{app\ B\rightarrow A}$). It is because $Kp_{uu,brain}$ can be also expressed as the ratio between the influx clearance (Cl_{in}) and the efflux clearance (Cl_{out}) through the BBB and, assuming that a clearance can be expressed as the product of a permeability and a surface area, $Kp_{uu,brain}$ calculation can be simplified to a relation between permeabilities. [24]

$$Kp_{uu,brain} = \frac{Cl_{in}}{Cl_{out}} = \frac{P_{app\ A\rightarrow B} \cdot S}{P_{app\ B\rightarrow A} \cdot S} = \frac{P_{app\ A\rightarrow B}}{P_{app\ B\rightarrow A}} \quad (5)$$

- The ratio between the permeability coefficients obtained in both apical-to-basolateral experiments, the one modified with albumin ($P_{app\ ALB}$) and the standard one ($P_{app\ A\rightarrow B}$), gives the $f_{u,plasma}$ (eq.6). This parameter represents the unbound fraction of drug present in plasma and can be obtained from the experiments mentioned above because, in both cases, the transport from the donor to the receiver chamber depends on the free concentration in the donor one ($C_{u,D}$). In the standard experiment, all the concentration in donor is unbound as HBSS has not proteins to which the drug can bind, but in the modified with albumin one a concentration of albumin (the most abundant plasma protein [31]) equal to that present in human blood has been added and drugs can bind to it. As in the permeability equations (eq. 1-4), the total concentration in donor (C_D) is used (because the unbound fraction is not known), the permeability obtained in the modified experiment is an apparent one, that would be equal to the standard

one if the $f_{u,plasma}$ were known when starting the calculations. [24]

$$P_{app\ ALB} \cdot C_D = P_{app\ A\to B} \cdot f_{u,plasma} \cdot C_D \quad \rightarrow \quad f_{u,plasma} = \frac{P_{app\ ALB}}{P_{app\ A\to B}} \qquad (6)$$

- Following the same argumentation that in $f_{u,plasma}$, the unbound fraction of drug in brain, $f_{u,brain}$ (eq. 7), can be obtained combining the permeability values got from both basolateral-to-apical experiments, the modified with brain homogenate one ($P_{app\ HOM}$) and the standard one ($P_{app\ B\to A}$). Furthermore, the $f_{u,brain}$ parameter can be translated to the apparent distribution volume in brain, $V_{u,brain}$, one by means of the equation 8 where V_{ECF} is the volume of the brain extracellular fluid (0.2 mL/g brain) and V_{ICF} is the volume of the brain intracellular fluid (0.6 mL/g brain).

$$P_{app\ HOM} \cdot C_D = P_{app\ B\to A} \cdot f_{u,brain} \cdot C_D \quad \rightarrow \quad f_{u,brain} = \frac{P_{app\ HOM}}{P_{app\ B\to A}} \qquad (7)$$

$$V_{u,brain} = V_{ECF} + \left(\frac{1}{f_{u,brain}}\right) \cdot V_{ICF} \qquad (8)$$

In vitro-in vivo correlations were developed between the *in vivo* parameters obtained in rat by Friden *et al*.[25] and Kodaira *et al*.[26] (Table 1) and the *in vitro* parameters calculated with the equations above. Linear IVIVCs are shown in different graphs with their coefficient of determination (r^2) and their 95% confidence interval. The r^2 values were used for comparing the IVIVCs developed with this approach and the ones obtained by Mangas-Sanjuan *et al*. with the MDCKII and MDCKII-MDR1 cell lines. [24]

6. Statistical tests

Differences between groups were evaluated with a t-student test. $P < 0.05$ was established as a significance level. The statistical analysis was made with the software SPSS, V.20.00.

RESULTS AND DISCUSSION

One of the most important problems that industries find when a new drug is developed for CNS treatment is the lack of crossing the BBB and, therefore, to reach its target. This fact has boosted the study of new *in vitro* tools able to predict which drugs are most promising to reach the brain with the aim of avoiding the big losses of investment that the withdrawal of a drug in an advanced phase of its development causes.

In this work, an *in vitro* model for calculating the main pharmacokinetic parameters that describe the entrance and distribution of drugs in the CNS ($Kp_{uu,brain}$, $f_{u,plasma}$, $f_{u,brain}$ and $V_{u,brain}$) has been improved in the hCMEC/D3 cell line. This model would be especially relevant in the future establishment of new therapeutic strategies targeted to the treatment of CNS pathologies (epilepsies, brain tumours, meningitis, multiple sclerosis, encephalitis or dementias among others).

In 2013, Mangas Sanjuan *et al*. proposed this model using two epithelial cell lines, the Madin-Darby canine kidney II (MDCKII) cell line and the wild cell line transfected with P-glycoprotein (MDCKII-MDR1) as, due to their strong tight junctions, they are considered good models for mimicking the BBB.[24] Currently, the endothelial hCMEC/D3 cell line is the best characterized and most used BBB cell model[19] which, despite its relatively lack of tightness (its TEER values are around 30-50 $\Omega \bullet cm^2$)[29] is able to overcome some of the main disadvantages of both MDCKII and MDCKII-MDR1 cell lines, as their differences in morphology, growth, metabolism and transporters with human BBB.[9]

Although not measured, it is globally accepted that human brain microvessels have TEER values above 1000 $\Omega \bullet cm^2$ [29], which would be extremely far from the values detected in hCMEC/D3 monolayers. Nonetheless, previous studies have demonstrated that hCMEC/D3 cells monolayers express several proteins that are responsible of tight junctions' formation, such as: claudins, occludins or junction adhesion molecules, and they are able to restrict the permeability of lucifer yellow, a low molecular weight paracellular diffusion marker. [19,29]

1. Permeability values and *in vitro* BBB parameters

The permeability coefficients obtained for each drug and each experimental condition are summarized in Table 3. Additionally, Fig. 1 shows a comparison between these permeability values with their standard deviation obtained in each experimental setting for each drug.

Table 3. Permeability values obtained for each drug and each different experimental condition (standards, modified with albumin and modified with brain homogenate).

	$P_{app\ A\rightarrow B}$ ($x10^{-6}$ cm/s)	$P_{app\ B\rightarrow A}$ ($x10^{-6}$ cm/s)	$P_{app\ ALB}$ ($x10^{-6}$ cm/s)	$P_{app\ HOM}$ ($x10^{-6}$ cm/s)
Amitriptyline	124.24	66.21	3.00	16.72
Atenolol	19.01	26.89	18.33	10.19
Carbamazepine	70.14	51.93	8.62	20.04
Fleroxacin	29.96	25.73	24.40	19.12
Genistein	38.38	116.16	5.74	20.60
Pefloxacin	24.95	33.14	4.27	21.29
Zolpidem	106.16	80.76	26.83	32.93

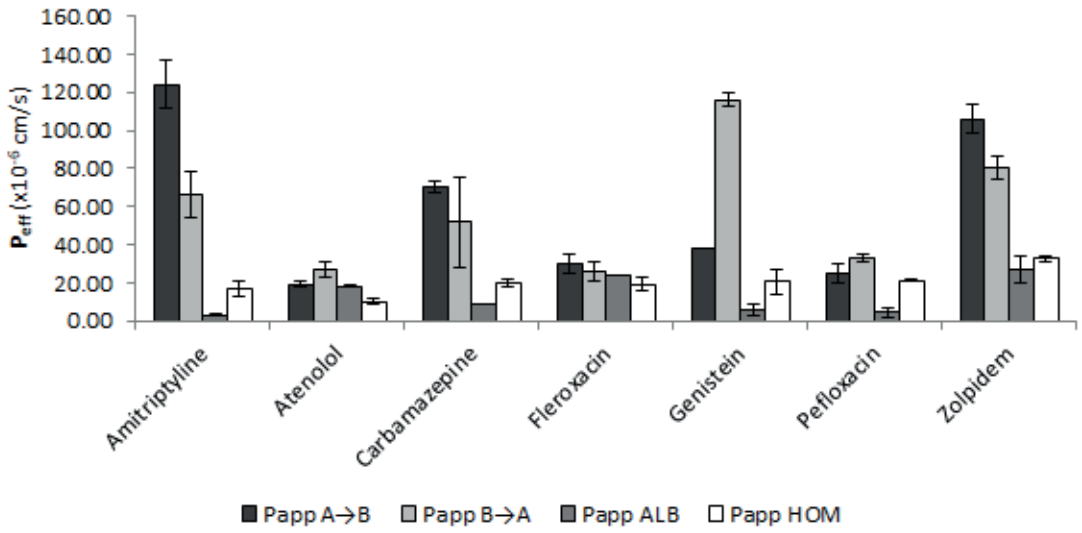

Figure 1. Comparison of the different permeability values with their standard deviation obtained in each experimental setting for each drug.

In Fig. 1, it is shown how the presence of albumin affects the permeability of those drugs that have some plasma protein binding, as amitriptyline, carbamazepine, genistein and zolpidem; in these drugs, the Peff values from apical-to-basolateral are considerably reduced when albumin is added to the experiment, but this fact does not happen in those drugs in which there is not *in vivo* protein binding, atenolol, fleroxacin and pefloxacin. On the other hand, the same figure shows the effect that brain homogenate provokes in the

basolateral-to-apical permeability when the drug has a high *in vivo* brain binding (amitriptyline, atenolol, carbamazepine, genistein and zolpidem), in which case the Peff values get reduced when the basolateral-to-apical experiment is modified with brain homogenate.

The pharmacokinetic parameters estimated from the *in vitro* permeability coefficients with the equations described previously are shown in Table 4.

Table 4. *In vitro* pharmacokinetic parameters calculated with the equations 5, 6, 7 and 8 from the permeability coefficients obtained in the different experimental settings and *in vivo* parameters published in Friden *et al* and Kodaira *et al*.[25,26]

	$Kp_{uu,brain}$		$f_{u,plasma}$		$f_{u,brain}$		$V_{u,brain}$ (mL/g brain)	
	In vitro	***In vivo***	***In vitro***	***In vivo***	***In vitro***	***In vivo***	***In vitro***	***In vivo***
Amitriptyline	1.876	0.730	0.024	0.090	0.252	0.002	2.577	310.00
Atenolol	0.707	0.030	0.964	1.000	0.379	0.261	1.784	2.500
Carbamazepine	1.351	0.771	0.123	0.385	0.386	0.170	1.755	3.729
Fleroxacin	1.164	0.250	0.814	0.793	0.743	0.555	1.007	1.281
Genistein	0.330	0.181	0.150	0.010	0.177	0.053	3.584	11.499
Pefloxacin	0.753	0.199	0.171	0.860	0.642	0.514	1.134	1.367
Zolpidem	1.314	0.447	0.253	0.267	0.408	0.265	1.671	2.464

2. *In vitro-in vivo* correlations

In this investigation, four different linear IVIVCs have been obtained (Fig. 2). Fig. 2 shows the linear IVIVCs obtained between the *in vitro* $Kp_{uu,brain}$, $f_{u,plasma}$, $f_{u,brain}$ and $V_{u,brain}$ values and the *in vivo* $Kp_{uu,brain}$, $f_{u,plasma}$, $f_{u,brain}$ and $V_{u,brain}$ values with their coefficients of determination (r^2) and their 95% confidence intervals.

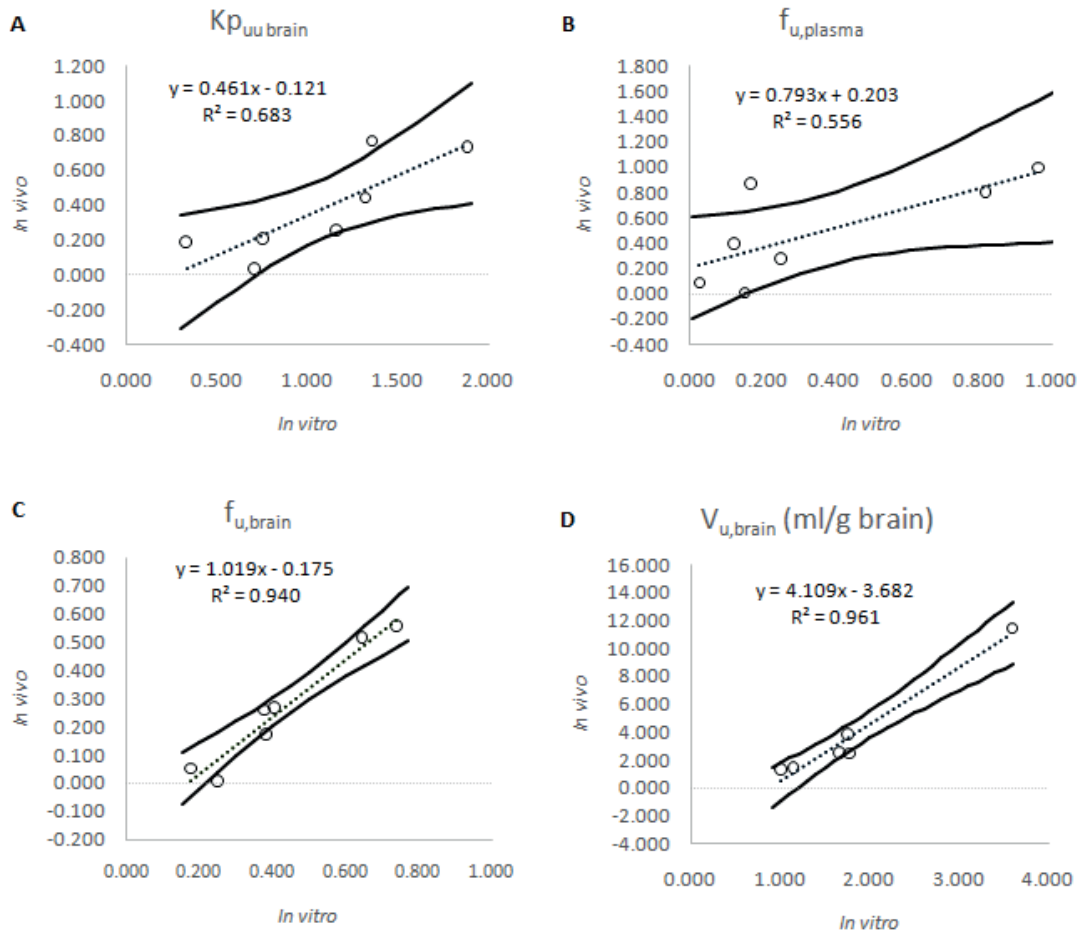

Figure 2. Linear in *vitro-in vivo* correlations (dotted line) with their coefficient of determination (r^2) and their 95% confidence interval (solid line). IVIVCs obtained between: A. the *in vitro* $Kp_{uu,brain}$ values and the *in vivo* $Kp_{uu,brain}$ values; B. the *in vitro* $f_{u,plasma}$ values and the *in vivo* $f_{u,plasma}$ values; C. the *in vitro* $f_{u,brain}$ values and the *in vivo* $f_{u,brain}$ values and D. the *in vitro* $V_{u,brain}$ values and the *in vivo* $V_{u,brain}$ values.

The best IVIVCs have been those that relate the *in vitro* $V_{u,brain}$ with the *in vivo* $V_{u,brain}$ and the *in vitro* $f_{u,brain}$ with the *in vivo* $f_{u,brain}$ with an r^2 of 0.961 and 0.940, respectively. These two parameters represent the binding rate of a substance to the brain tissue and, thus, they were obtained combining the permeability values from the studies performed in basolateral-to-apical direction, the standard one and the one modified with brain homogenate. The obtained results evidence the great utility of using brain homogenate to mimic brain tissue when an *in vitro* permeability test is developed. Nevertheless, the r^2 of 0.961 for the correlation between the *in vitro* $V_{u,brain}$ with the *in vivo* $V_{u,brain}$ was obtained after removing the amitriptyline data whose *in vivo* $V_{u,brain}$ value was 310.00 ml/g brain, a huge value in comparison with the rest of *in vivo* data (Table 4). It was

not necessary to remove this point when the correlation of $f_{u,brain}$ was obtained, fact that reveals that the use of this system and equation 8, that relates both parameters $f_{u,brain}$ and $V_{u,brain}$, it is not accurate when the binding of a drug to the tissue is extremely high. According to table 4 and the mentioned results, it can be said that, right now, the superior limit for the prediction of $V_{u,brain}$ with this methodology would be an *in vivo* $V_{u,brain}$ value of 11.5 ml/g brain (genistein *in vivo* $V_{u,brain}$).

For the other parameters, the unbound fraction of drug in plasma ($f_{u,plasma}$) and the unbound plasma−brain partition coefficient ($Kp_{uu,brain}$), the correlation is not as good as the other ones, although a clear tendency between *in vitro* data and *in vivo* data can be seen (Fig. 2). *In vitro* $Kp_{uu,brain}$ and *in vivo* $Kp_{uu,brain}$ correlation was developed with an r^2 of 0.683 and the correlation between the *in vitro* $f_{u,plasma}$ and the *in vivo* $f_{u,plasma}$ had an r^2 of 0.556.

In Table 5 the r^2 values for the IVIVCs obtained in this work and the ones obtained by Mangas-Sanjuan *et al*. with the MDCKII and MDCKII-MDR1 cell lines are summarized, for the comparison of the correlations from the different cell lines. The correlation between the *in vitro* $f_{u,brain}$ and the *in vivo* $f_{u,brain}$ for the MDCKII and the MDCKII-MDR1 was not published in Mangas-Sanjuan *et al*. and it was obtained after transforming the published $V_{u,brain}$ values into $f_{u,brain}$ values with equation 8.

Table 5. Coefficient of determination (r^2) values for the correlations obtained in hCMEC/D3 cell line in this work and in MDCKII and MDCKII-MDR1 cell lines by Mangas-Sanjuan *et al*.[24]

	MDCKII	**MDCKII-MDR1**	**hCMEC/D3**
$Kp_{uu,brain}$ IVIVC	0.063	0.401	0.683
$f_{u,plasma}$ IVIVC	0.846	0.452	0.556
$f_{u,brain}$ IVIVC	0.616	0.624	0.940
$V_{u,brain}$ IVIVC	0.985	0.839	0.961

In Table 5, it can be seen that for the $Kp_{uu,brain}$ and $f_{u,brain}$ IVIVCs, the highest r^2 values are reached with the hCMEC/D3 cell line. Additionally, the dissimilarity between the $f_{u,brain}$ and $V_{u,brain}$ r^2 values for both MDCKII ($f_{u,brain}$ r^2 = 0.616 and $V_{u,brain}$ r^2 = 0.985) and MDCKII-MDR1 ($f_{u,brain}$ r^2 = 0.624 and $V_{u,brain}$ r^2 = 0.839) cell lines confirms that the system and equation 8 are not completely accurate for relating both parameters. Otherwise,

according to the r^2 values, the best cell line for predicting the $f_{u,plasma}$ parameter would be the MDCKII cell line (r^2 = 0.846).[24]

As results differ from one parameter to other, it cannot be argued that hCMEC/D3 cell line is the best cell model for predicting all the pharmacokinetic parameters $Kp_{uu,brain}$, $f_{u,plasma}$, $f_{u,brain}$ and $V_{u,brain}$ and, thus, the three tested cells lines could be used for making predictions. Nonetheless, as hCMEC/D3 monolayers are a more physiological BBB model, their use will be more appropriate when the transport of new drugs or new delivery formulations want to be tested, especially, if these new therapeutic agents are substrates of several transporters.

Due to the lack of human *in vivo* data of the parameters employed in this work, a limitation of this study could be that in all the correlations the predicted parameters from the *in vitro* experiments were related with rat *in vivo* data[25,26], so parameters obtained with a BBB cell line of human origin are mixed with data that came from an animal. [32] Nevertheless, in 2011 Avdeef compared the permeabilities values obtained *in vitro* with several brain microcapillary endothelial cell models from different species (porcine, bovine, rodent and human) with the *in vivo* permeabilities obtained in rodents and he saw that there was not an evident difference in the correlations for the different species.[33] Therefore, this methodology is considered appropriate for the early stages of drug development, even before starting the preclinical *in vivo* studies, as it promotes the fulfilment of the 3Rs principles (reduction, refinement and replacement).[34]

CONCLUSION

A previous *in vitro* method developed by Mangas-Sanjuan *et al*. [30] has been tested in an alternative cell line (hCMEC/D3). This study confirms that the four proposed experimental settings (apical-to-basolateral standard experiment, basolateral-to-apical standard experiment, apical-to-basolateral with albumin experiment and basolateral-to-apical with brain homogenate experiment) can be used to predict the main pharmacokinetic parameters that describe the entrance and distribution of substances in the CNS ($Kp_{uu,brain}$, $f_{u,plasma}$, $f_{u,brain}$ and $V_{u,brain.}$). Therefore, this methodology can be further adapted to be a high-throughput screening tool to select the most promising drugs to reach the brain in early stages of drug development in, at least, three different *in vitro* BBB cell models (hCMEC/D3, MDCK and MDCK-MDR1 cell lines).

ACKNOWLEDGEMENTS

Funding: This work was supported, in part, by the project: “Modelos *in vitro* de evaluación biofarmacéutica” [SAF2016-78756 (AEI/FEDER, EU)] funded by Agencia Estatal Investigación and European Union, through FEDER (Fondo Europeo de Desarrollo Regional). This work was also financed by the project [NORTE-01-0145-FEDER-000012] by Norte Portugal Regional Operational Programme (NORTE 2020), and COMPETE 2020 - Operacional Programme for Competitiveness and Internationalisation (POCI), under the PORTUGAL 2020 Partnership Agreement, through the FEDER - Fundo Europeu de Desenvolvimento Regional, and by Portuguese funds through FCT - Fundação para a Ciência e a Tecnologia/ Ministério da Ciência, Tecnologia e Ensino Superior in the framework of the project "Institute for Research and Innovation in Health Sciences" [UID/BIM/04293/2019]. Bárbara Sánchez-Dengra received a grant from the Ministry of Science, Innovation and Universities of Spain [FPU17/00530] and an international mobility grant from Miguel Hernandez University [0762/19].

References

[1] Xie J, Shen Z, Anraku Y, Kataoka K, Chen X. Nanomaterial-based blood-brain-barrier (BBB) crossing strategies. Biomaterials 2019;224:119491. https://doi.org/10.1016/j.biomaterials.2019.119491.

[2] Alexander A, Agrawal M, Uddin A, Siddique S, Shehata AM, Shaker MA, et al. Recent expansions of novel strategies towards the drug targeting into the brain . Int J Nanomedicine 2019;Volume 14:5895–909. https://doi.org/10.2147/ijn.s210876.

[3] Langen UH, Ayloo S, Gu C. Development and Cell Biology of the Blood-Brain Barrier. Annu Rev Cell Dev Biol 2019;35:591–613. https://doi.org/10.1146/annurev-cellbio-100617-062608.

[4] Dong X. Current strategies for brain drug delivery. Theranostics 2018;8:1481–93. https://doi.org/10.7150/thno.21254.

[5] Kim J, Ahn SI, Kim YT. Nanotherapeutics engineered to cross the blood-brain barrier for advanced drug delivery to the central nervous system. J Ind Eng Chem 2019;73:8–18. https://doi.org/10.1016/j.jiec.2019.01.021.

[6] Sánchez-Dengra B, González-Álvarez I, Bermejo M, González-Álvarez M. Nanomedicine in the Treatment of Pathologies of the Central Nervous System Advances in Nanomedicine. Adv. Nanomedicine, 2020.

[7] Löscher W, Potschka H. Blood-brain barrier active efflux transporters: ATP-binding cassette gene family. NeuroRx 2005;2:86–98. https://doi.org/10.1602/neurorx.2.1.86.

[8] Mensch J, Oyarzabal J, Mackie C, Augustijns P. In vivo, in vitro and in silico methods for small molecule transfer across the BBB. J Pharm Sci 2009;98:4429–68. https://doi.org/10.1002/jps.21745.

[9] Mangas-Sanjuan V, González-Alvarez M, Gonzalez-Alvarez I, Bermejo M. Drug penetration across the blood-brain barrier: An overview. Ther Deliv 2010;1:535–62. https://doi.org/10.4155/tde.10.37.

[10] Gomes MJ, Mendes B, Martins S, Sarmento B. Cell-based in vitro models for studying blood-brain barrier (BBB) permeability. Concepts Model. Drug Permeability Stud. Cell Tissue based Vitr. Cult. Model., Elsevier Inc.; 2015, p. 169–88. https://doi.org/10.1016/B978-0-08-100094-6.00011-0.

[11] Mangas-Sanjuan V, Gonzalez-Alvarez M, Gonzalez-Alvarez I, Bermejo M. In vitro methods for assessing drug access to the brain. Adv. Non-Invasive Drug Deliv. to Brain, Marshall University, USA: Future Science Ltd; 2015, p. 44–61. https://doi.org/10.4155/9781909453937.FSEB2013.13.61.

[12] Neuhaus W, Lauer R, Oelzant S, Fringeli UP, Ecker GF, Noe CR. A novel flow based hollow-fiber blood-brain barrier in vitro model with immortalised cell line PBMEC/C1-2. J Biotechnol 2006;125:127–41. https://doi.org/10.1016/j.jbiotec.2006.02.019.

[13] Sano Y, Shimizu F, Abe M, Maeda T, Kashiwamura Y, Ohtsuki S, et al. Establishment of a new

conditionally immortalized human brain microvascular endothelial cell line retaining an in vivo blood-brain barrier function. J Cell Physiol 2010;225:519–28. https://doi.org/10.1002/jcp.22232.

[14] Engelhard HH, Arnone GD, Mehta AI, Nicholas MK. Biology of the Blood-Brain and Blood-Brain Tumor Barriers. Handb. Brain Tumor Chemother. Mol. Ther. Immunother. Second Ed., Elsevier Inc.; 2018, p. 113–25. https://doi.org/10.1016/B978-0-12-812100-9.00008-5.

[15] Vendel E, Rottschäfer V, de Lange ECM. The need for mathematical modelling of spatial drug distribution within the brain. Fluids Barriers CNS 2019;16:12. https://doi.org/10.1186/s12987-019-0133-x.

[16] Nicolazzo JA, Charman SA, Charman WN. Methods to assess drug permeability across the blood-brain barrier. J Pharm Pharmacol 2006;58:281–93. https://doi.org/10.1211/jpp.58.3.0001.

[17] Di L, Kerns EH, Carter GT. Strategies to assess blood-brain barrier penetration. Expert Opin Drug Discov 2008;3:677–87. https://doi.org/10.1517/17460441.3.6.677.

[18] Abbott N, Dolman D, Patabendige A. Assays to Predict Drug Permeation Across the Blood-Brain Barrier, and Distribution to Brain. Curr Drug Metab 2008;9:901–10. https://doi.org/10.2174/138920008786485182.

[19] Veszelka S, Tóth A, Walter FR, Tóth AE, Gróf I, Mészáros M, et al. Comparison of a rat primary cell-based blood-brain barrier model with epithelial and brain endothelial cell lines: Gene expression and drug transport. Front Mol Neurosci 2018;11. https://doi.org/10.3389/fnmol.2018.00166.

[20] de Lange EC. The mastermind approach to CNS drug therapy: translational prediction of human brain distribution, target site kinetics, and therapeutic effects. Fluids Barriers CNS 2013;10:12. https://doi.org/10.1186/2045-8118-10-12.

[21] Meihua Rose Feng BSP. Assessment of Blood-Brain Barrier Penetration: In Silico, In Vitro and In Vivo. Curr Drug Metab 2002;3:647–57. https://doi.org/10.2174/1389200023337063.

[22] Bagchi S, Chhibber T, Lahooti B, Verma A, Borse V, Jayant RD. In-vitro blood-brain barrier models for drug screening and permeation studies: An overview. Drug Des Devel Ther 2019;13:3591–605. https://doi.org/10.2147/DDDT.S218708.

[23] Hammarlund-Udenaes M, Fridén M, Syvänen S, Gupta A. On the rate and extent of drug delivery to the brain. Pharm Res 2008;25:1737–50. https://doi.org/10.1007/s11095-007-9502-2.

[24] Mangas-Sanjuan V, González-Álvarez I, González-Álvarez M, Casabó VG, Bermejo M. Innovative in vitro method to predict rate and extent of drug delivery to the brain across the blood-brain barrier. Mol Pharm 2013;10:3822–31. https://doi.org/10.1021/mp400294x.

[25] Fridén M, Gupta A, Antonsson M, Bredberg U, Hammarlund-Udenaes M. In vitro methods

for estimating unbound drug concentrations in the brain interstitial and intracellular fluids. Drug Metab Dispos 2007;35:1711–9. https://doi.org/10.1124/dmd.107.015222.

[26] Kodaira H, Kusuhara H, Fujita T, Ushiki J, Fuse E, Sugiyama Y. Quantitative evaluation of the impact of active efflux by P-glycoprotein and breast cancer resistance protein at the blood-brain barrier on the predictability of the unbound concentrations of drugs in the brain using cerebrospinal fluid concentration as a. J Pharmacol Exp Ther 2011;339:935–44. https://doi.org/10.1124/jpet.111.180398.

[27] Chemicalize. Chemicalize - Instant Cheminformatics Solutions n.d. https://chemicalize.com/welcome (accessed May 3, 2020).

[28] DrugBank. DrugBank n.d. https://www.drugbank.ca/ (accessed May 14, 2020).

[29] Weksler B, Romero IA, Couraud PO. The hCMEC/D3 cell line as a model of the human blood brain barrier. Fluids Barriers CNS 2013;10. https://doi.org/10.1186/2045-8118-10-16.

[30] Mangas-Sanjuan V, González-Álvarez I, González-Álvarez M, Casabó VG, Bermejo M. Modified nonsink equation for permeability estimation in cell monolayers: Comparison with standard methods. Mol Pharm 2014;11:1403–14. https://doi.org/10.1021/mp400555e.

[31] Biga LM, Dawson S, Harwell A, Hopkins R, Kaufmann J, LeMaster M, et al. The Cardiovascular System: Blood. In: Biga LM, Dawson S, Harwell A, Hopkins R, Kaufmann J, LeMaster M, et al., editors. Anat. Physiol., OpenStax/Oregon State University; n.d.

[32] Fridén M, Winiwarter S, Jerndal G, Bengtsson O, Wan H, Bredberg U, et al. Structure-brain exposure relationships in rat and human using a novel data set of unbound drug concentrations in brain interstitial and cerebrospinal fluids. J Med Chem 2009;52:6233–43. https://doi.org/10.1021/jm901036q.

[33] Avdeef A. How well can in vitro brain microcapillary endothelial cell models predict rodent in vivo blood-brain barrier permeability? Eur J Pharm Sci 2011;43:109–24. https://doi.org/10.1016/j.ejps.2011.04.001.

[34] The National Centre for the 3Rs. The 3Rs | NC3Rs n.d. https://www.nc3rs.org.uk/the-3rs (accessed June 29, 2020).

4. New *in vitro* methodology for kinetics distribution prediction in the brain. An additional step towards an animal-free approach.

Type of publication	Article
Title	New *in vitro* methodology for kinetics distribution prediction in the brain. An additional step towards an animal-free approach.
Authors	Bárbara Sánchez-Dengra, Isabel González-Álvarez, Marta González-Álvarez and Marival Bermejo
Journal	Animals
Impact factor	2.752 (Q1 - Veterinary Sciences)
Year of publication	2021
DOI	doi.org/10.3390/ani11123521

Abstract

The development of new drugs or formulations for central nervous system (CNS) diseases is a complex pharmacologic and pharmacokinetic process; it is important to evaluate their access to the CNS through the blood−brain barrier (BBB) and their distribution once they have acceded to the brain. The gold standard tool for obtaining this information is the animal microdialysis technique; however, according to 3Rs principles, it would be better to have an "animal-free" alternative technique. Because of that, the purpose of this work was to develop a new formulation to substitute the brain homogenate in the in vitro tests used for the prediction of a drug's distribution in the brain. Fresh eggs have been used to prepare an emulsion with the same proportion in proteins and lipids as a human brain; this emulsion has proved to be able to predict both the unbound fraction of drug in the brain ($f_{u,brain}$) and the apparent volume of distribution in the brain ($V_{u,brain}$) when tested in in vitro permeability tests. The new formulation could be used as a screening tool; only the drugs with a proper in vitro distribution would pass to microdialysis studies, contributing to the refinement, reduction and replacement of animals in research.

Keywords

blood−brain barrier (BBB); unbound fraction (f_u); distribution volume in brain ($V_{u,brain}$); 3Rs

Simple Summary

The prevalence of neurological disorders in humans is rising year after year. This fact necessitates the development of new drugs for treating these pathologies. Traditionally, drugs have been tested in animals prior to use in human experiments; however, the use of animals in experimentation must be controlled and as low as possible. Because of that, here we proposed a new in vitro approach with which the access and distribution of drugs into the brain can be evaluated without using/killing any animals.

1. Introduction

Neurological disorders are getting more and more frequent due to global aging. In fact, it is estimated that in 2050, 22% of people worldwide will be over 60 years old [1]. After that age, several physiological processes, such as, lower levels of acetylcholine, dopaminergic and cholinergic neurons, the accumulated DNA mutations and the presence of other comorbidities, like, obesity, diabetes, hypertension or hyperlipidaemia, can lead to an increase of neurodegenerative disorders (dementia, Alzheimer's disease or Parkinson's disease), brain tumors (glioblastoma), cerebral stroke, epilepsy or depression [2]. Table 1 shows the global levels of prevalence of neurological disorders in 2000 and 2019 for people of all ages and people from 60 to 89 years old (this data was obtained from the GBD online results tool [3]).

According to Table 1, in general, in the last decade, the prevalence of all neurological disorders has increased by at least 30%; however, this increment gets much more pronounced in the population over 60 years old, with a minimum increment of 65% [3]. One could think that the increments in prevalence may not be significant, because the total population in the world has also increased with time, moving from 6143.5 million people in 2000 to 7713.5 million people in 2019 for all ages, and from 602.7 to 996.7 million people for the group from 60 to 89 years. Nonetheless, as can be seen in the column Norm_Δ, where prevalence is normalized, there is a considerable increase in almost all neurological disorders.

Table 1. Global prevalence of neurological disorders for people of all ages and people over 60 years in 2000 and 2019 [3].

Disease	Prevalence (Millions of People)							
	All Ages				60 to 89 Years			
	2000	2019	Δ (%)	Norm _Δ (%)	2000	2019	Δ (%)	Norm _Δ (%)
Alzheimer's disease and other dementias	26.70	51.62	93%	54%	22.06	41.35	87%	13%
Parkinson's disease	4.82	8.51	76%	41%	3.91	6.87	76%	6%
Other neurological disorders	0.04	0.06	45%	16%	0.01	0.02	92%	16%
Motor neuron disease	0.19	0.27	45%	15%	0.05	0.09	81%	10%
Multiple sclerosis	1.24	1.76	41%	13%	0.29	0.49	66%	1%
Schizophrenia	17.31	23.60	36%	9%	1.82	3.12	72%	4%
Idiopathic epilepsy	18.53	25.11	35%	8%	2.48	4.68	89%	14%
Migraine	852.24	1128.1	32%	5%	64.62	111.20	72%	4%
Tension-type headache	1524.6	1995.2	31%	4%	176.3	291.7	65%	0%
Mental disorders	777.26	970.07	25%	−1%	84.54	140.19	66%	0%
Neurological disorders	2016.6	2659.0	32%	5%	228.1	385.5	69%	2%

Mental disorders: schizophrenia, depressive disorders (major depressive disorder or dysthymia), bipolar disorder, anxiety disorders, eating disorders (anorexia nervosa, bulimia nervosa), autism spectrum disorders, attention-deficit/hyperactivity disorder, conduct disorder, idiopathic developmental intellectual disability and other mental disorders. Δ expresses the increment in the prevalence of the disease from 2000 to 2019. Norm_Δ expresses the increment in the prevalence of the disease from 2000 to 2019 when the amount of people with that pathology in 2000 and 2019 is normalized by total amount of people in the world (from all ages and from 60 to 89 years old).

Treatment of brain diseases requires drugs that are able to reach brain targets; because of that, an extremely high number of molecules and formulations need to be studied to get a successful treatment for neurological disorders [4]. The common failures in the development of CNS drugs are lack of activity or, more commonly, lack of biopharmaceutical suitable properties. Furthermore, the current screening methods for

blood–brain barrier accessibility lack high-throughput capacity and rely on the intensive use of animal models or tissues.

When a new treatment that needs to reach the central nervous system (CNS) is developed, the gold standard for measuring the concentration it reaches in the different parts of the brain is microdialysis. Microdialysis allows researchers to measure the unbound concentration of drug at different times in a specific brain area and, although this measurement can be done in humans, it is more common to measure the levels in rats or mice and then translate the information into human brain levels using physiologically based pharmacokinetic (PBPK) modeling [5,6].

In brief, when the microdialysis technique is used for measuring drug levels in the CNS, a small cannula with an inner and an external conduct is introduced in the animal's brain. Then, a saline solution (perfusate) is supplied through the internal conduct and, when it gets in touch with the brain in the external conduct, which has a semipermeable membrane, it starts to mix with the components present in the extracellular fluid (ECF) of the CNS, because substances with a diameter smaller than the membrane pores, diffuse from the more concentrated solution to the less concentrated one. Finally, the "mixed" solution (dialysate) is recovered through the same cannula and, at different times, the amount of drug present in it is analyzed [7]. In Figure 1, a scheme of this system is shown.

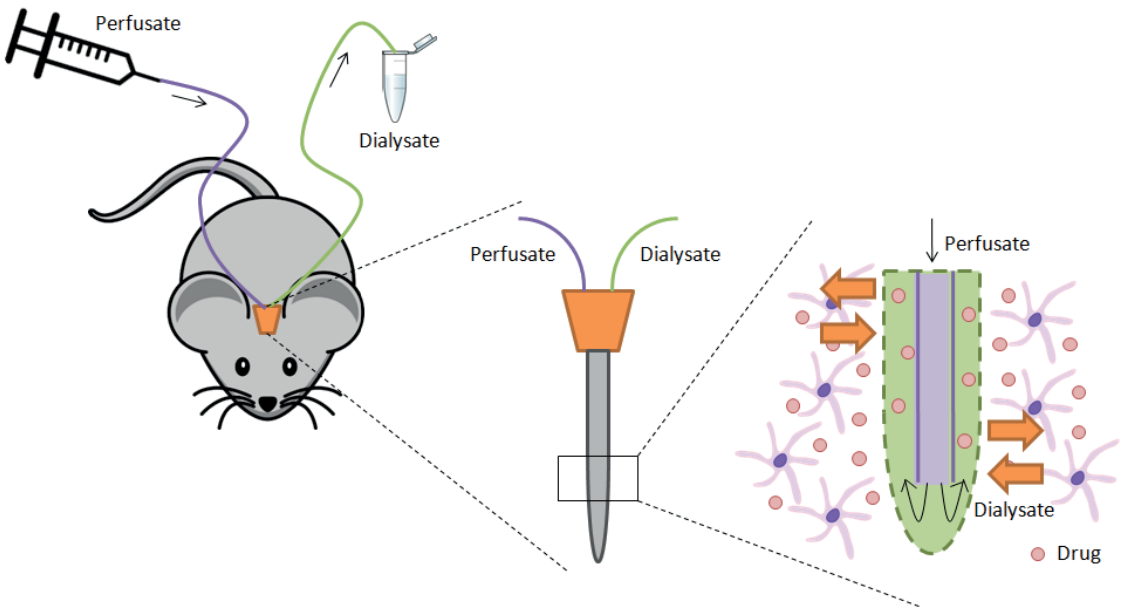

Figure 1. Scheme of brain microdialysis system.

The unbound concentration profiles obtained by microdialysis give, among others, information about the unbound fraction of drug in the brain ($f_{u,brain}$) and the apparent volume of distribution in the brain ($V_{u,brain}$). Both parameters are interrelated and are considered crucial when studying a new drug for the treatment of a neurological disorder. On the one hand, $f_{u,brain}$ is an important parameter, as only the free drug is able to cross membranes, so the free fraction of drug is the one that will contribute to the equilibrium between blood and brain through the blood−brain barrier (BBB) and, furthermore, it will be the only one able to enter into the cells or to bind its target [8]. On the other hand, $V_{u,brain}$ reflects the drug binding to the brain with independence of the BBB equilibrium; the value of this parameter can be compared with the physiological volumes of the CNS to study the drug affinity to the brain tissue [8]. If a drug is highly permeable through the BBB and, at the same time, has a high $V_{u,brain}$, it is more probable that it will perform properly.

Due to the high number of molecules and formulations to test, a great number of animals are required for these assays, along with the attendant ethical problems of experimenting on animals. Moreover, there are some issues with the translation of data from animals to humans; however, the use of human biology-based in vitro methods is vital for better understanding human diseases. Thus, the objective of the present work is to propose an innovative in vitro method amenable to high-throughput testing and which substitutes the use of brain animal/human homogenate in accordance to the 3 R's principles (replacement, reduction and refinement), which were established in the 20th century by Russell and Burch and which, nowadays, are strictly followed by scientists all over the world [9]. In fact, nowadays, several legislative documents that regulate animal experimentation can be found in the majority of animal testing countries.

Having in mind the 3Rs principles, several in vitro and in silico methods have been proposed to study the access and distribution of drugs into the brain. In vitro methods can be classified according to its base in: non-cell based in vitro methods, such as, PAMPA-BLM (black lipid membrane) or PAMPA-BBB models [10,11], and cell based in vitro methods, like, MDCK, MDCK-MDR1, Caco-2 or hCMEC/D3 cell lines [12,13]. All these in vitro methods have demonstrated that they are capable of predicting the permeability clearance into the brain (Cl_{in}) of most of the molecules (the passive ones). For instance, in 2010, the PAMPA-BBB model was able to classify 13 compounds out of 14 in BBB+ or BBB- according to their in vivo LogBB (logarithm of the ratio of the steady-state total concentration of a compound in the brain to that in the plasma), and the misclassified

compound was corrected using Caco-2 monolayers [14], as the Cl_{in} also depends on the transporters present on the BBB (not present in PAMPA models).

Nonetheless, knowing the Cl_{in} of a drug on its own is not enough, as only the unbound fraction of drug in the brain will be able to reach its target and give an effect. Taking two opioid drugs, morphine and loperamide, as an example, and consulting the bibliography for its ability to access CNS, it can be seen that morphine (10.4 ± 3 µL/min × g brain) has a lower Cl_{in} than loperamide (98.6 ± 17.3 µL/min × g brain), so morphine has a lower permeability through the BBB [15,16]. Despite that, morphine is a much more potent drug, so Cl_{in} alone is not a good metric for potency.

Cases such as the one mentioned above show that in order to correctly determine whether a drug will carry out its function in the CNS, it is necessary, in addition to its access, to know its distribution once it has crossed the BBB. This distribution is defined by the previously mentioned parameters ($f_{u,brain}$ and $V_{u,brain}$). Thus, in 2013, Mangas-Sanjuan et al. [17] designed a new in vitro system with which the $f_{u,brain}$ the $V_{u,brain}$, and also the unbound plasma-brain partition coefficient ($Kp_{uu,brain}$) and the unbound fraction of drug in plasma ($f_{u,plasma}$), could be obtained. A scheme of this system which, some years later, was tested and validated using another cell line [18], is shown in Figure 2.

In this in vitro approach, the $f_{u,brain}$ and $V_{u,brain}$ parameters are obtained by means of the combination of the permeability values from two basolateral-to-apical experiments, a standard one and one modified with brain homogenate (Figure 2) [17,18]. The system meets the reduction principle of the 3Rs, as the brain homogenate of the same animal can be divided and used in several wells, a fact that can be considered a great advance in the techniques used in the development of drugs for the CNS, as an extremely high number of molecules and formulations need to be studied to get a successful treatment for neurological disorders [4].

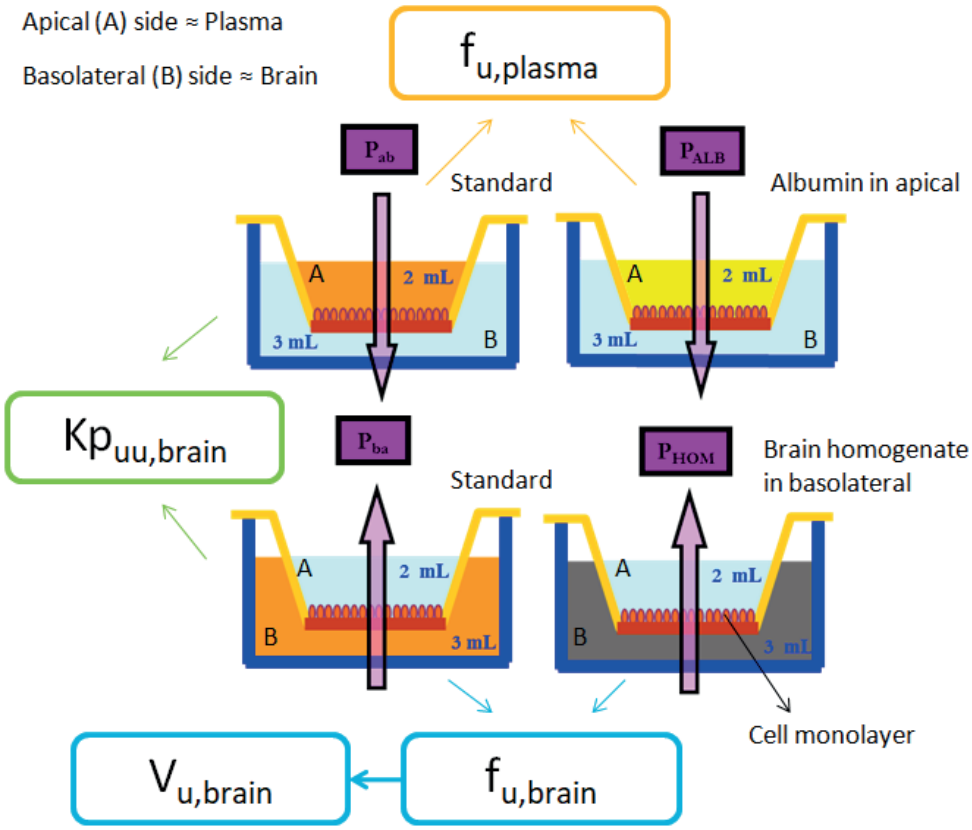

Figure 2. Scheme of the in vitro system with which the main parameters that describes the access and distribution of drugs in the CNS can be obtained. P_{ab}: Apparent permeability from apical to basolateral in the standard experiment. P_{ALB}: Apparent permeability from apical to basolateral in the experiment modified with albumin in apical. P_{ba}: Apparent permeability from basolateral to apical in the standard experiment. P_{HOM}: Apparent permeability from basolateral to apical in the experiment modified with brain homogenate.

However, although the model proposed in 2013 by Mangas-Sanjuan et al. [17] could be used as a screening tool that would reduce the number of animals used in neurological research, it still uses brain homogenate from pigs. Thereby, with the aim of improving the model and meeting the replacement principle of the 3Rs, the purpose of this work was to develop a new formulation, based on unfertilized chicken eggs, to substitute the brain homogenate of the system and create an "animal-free" in vitro screening tool, able to predict both the $f_{u,brain}$ and $V_{u,brain}$ parameters.

2. Materials and Methods

2.1. Drugs and Products

The nine drugs tested (amitryptiline, atenolol, carbamazepine, fleroxacin, loperamide, norfloxacin, pefloxacin, propranolol and zolpidem) and HPLC grade solvents

(acetonitrile, methanol and water) were purchased from Sigma-Aldrich (Barcelona, Spain). MDCK cell line was purchased from ATCC (USA) and MDCK-MDR1 cells were provided by Dr. Gottessman, MM (Nathional Institutes of Health, Bethesda). Pig brain homogenate was kindly supplied by a local slaughterhouse and fresh unfertilized chicken eggs were bought in a local supermarket. Table 2 shows the molecular properties of the nine drugs mentioned above.

Table 2. Molecular properties of the nine drugs tested [19,20].

Drug	MW (g/mol)	Solubility logS (pH 7)	logP	Strongest Acidic pKa	Strongest Basic pKa	Charge (pH 7.4)	Transporters (Substrates)
Amitriptyline	277.411	−1.63	4.81		9.76	+	ABCB1 (Pgp)
Atenolol	266.341	0.43	0.43	14.08	9.67	+	ABCB11
Carbamazepine	236.274	−3.79	2.77	15.96		0	ABCC2 RALBP1
Fleroxacin	369.344	−1.33	0.98	5.32	5.99	-	
Loperamide	477.050	−2.23	4.77	13.96	9.41	+	ABCB1 (Pgp)
Norfloxacin	319.336	−2.06	−0.97	5.58	8.77	0	ABCB1 (Pgp)
Pefloxacin	333.363	−1.21	0.75	5.5	6.44	-	ABCB1 (Pgp)
Propranolol	259.349	−1.03	2.58	14.09	9.67	+	ABCB1 (Pgp)
Zolpidem	307.397	−4.27	3.02		5.39	0	

MW = molecular weight.

Dulbecco's modified Eagle's medium (DMEM) with high content of glucose, L-glutamine, HEPES, MEM non-essential aminoacid, penicillin−streptomycin, trypsin-EDTA, Hank's balanced salt solution (HBSS) and fetal bovine serum (FBS) for the cell culture of MDCK and MDCK-MDR1 cell lines were purchased from Sigma-Aldrich.

2.2. Preparation of the Brain Homogenate and the New Formulation for Substituting It

The brain homogenate was obtained after triturating the pig brains that were kindly supplied by a local slaughterhouse and mixing them with phosphate buffer (180 mM, pH 7.4) solution in a ratio 1:3 (brain:buffer).

For preparing 100 g of the new formulation for substituting the brain homogenate, 2 medium size eggs, whose weight without the shell is around 100 g [21], were crushed; the whites and the yolks were separated. Then, 15.35 g of whites were mixed with 67.73 mL of water. In another beaker, 16.92 g of yolk were weighed separately. The yolk was poured into the white-water mixture and stirred vigorously until obtaining an emulsion.

2.3. Cell Culture and Permeability Studies

The permeability studies were carried out in two different cell lines: MDCK and MDCK-MDR1. MDCK and MDCK-MDR1 cells come from the kidney of dogs; however, when they are properly cultured, they form monolayers with quite strong and tight junctions [22,23]. It is for that reason that they are accepted as appropriate tools to simulate the BBB, although they do not have BBB transporters. In the MDCK-MDR1 cell line, the issue of the lack of transporters is partially solved with the transfection with P-glycoprotein (Pgp), the most common efflux transporter in the BBB; thus, this line would be ideal for studying drugs with a passive access to the CNS, as well as drugs which are substrates of Pgp, while MDCK would be better for studying passive drugs.

Both types of cells were cultured and seeded following the protocol explained in [17]. When the monolayers were confluent, three types of experiments, from the basolateral to the apical chamber, were carried out:

- Standard BA: In this experiment, drugs previously dissolved in HBSS at the concentration shown in Table 3, were placed at the basolateral chamber. After taking the samples and making the necessary calculations, the apparent efflux permeability ($P_{app\ B\rightarrow A}$) was obtained from this experiment.
- Brain homogenate BA: In this case, the free drug apparent efflux permeability ($P_{app\ HOM}$) was obtained after adding the drug dissolved in a 1:3 pig brain homogenate:phosphate buffer (180 mM, pH 7.4) solution to the basolateral chamber.
- Emulsion BA: Finally, in this third condition, as it is the equivalent to the brain homogenate BA experiment, but using the new formulation as a substitute of brain homogenate, the parameter obtained was also the free drug apparent efflux permeability, but in this case labeled as $P_{app\ EMUL}$.

In all cases, cells were seeded in 6-transwell plates (effective area: 4.2 cm^2, pore size: 0.4 micron and pore density: (100 ± 10) × $10^6/cm^2$) and its transepithelial electrical

resistance (TEER) was measured before and after the experiments, considering that cells were confluent when the TEER values reach around 130–150 kΩ·cm^2 for MDCK cells and around 120–140 kΩ·cm^2 for MDCK-MDR1 cells [22]. The apical side of the system was filled in with HBSS and samples were taken at 15, 30, 60 and 90 min. Additionally, for evaluating the mass balance, two samples were taken from basolateral at time 0 and 90 min and one sample was taken after disrupting the membrane with methanol. During the experiments, cells were maintained in an orbital shaker at 37 °C and 100 rpm, so the agitation prevents the drug from precipitating and reduces the formation of a non-stirred layer over the cells, which would decrease the apparent permeability. Once the experiments were finished, samples were frozen at −20 °C, until their analysis.

Table 3. Chromatographic conditions.

Drug	C (μM)	Wavelength	Mobile Phase	Retention Time (Min)
Amitriptyline	250	240 nm	40% Acid water 60% Acetonitrile	1.020
Atenolol	150	231 nm	20% Methanol 60% Acid water 20% Acetonitrile	1.330
Carbamazepine	150	280 nm	65% Acid water 35% Acetonitrile	1.926
Fleroxacin	150	285 nm	70% Acid water 30% Acetonitrile	1.348
Loperamide	241	260 nm	60% Methanol 40% Acid water	3.199
Norfloxacin	150	285 nm	70% Acid water 30% Acetonitrile	1.730
Pefloxacin	8.91	285 nm	65% Acid water 35% Acetonitrile	0.721
Propranolol	150	291 nm	30% Methanol 40% Acid water 30% Acetonitrile	1.950
Zolpidem	158	231 nm	60% Water 20% Methanol 20% Acetonitrile	4.624

Acid water had 0.05% (*v*/*v*) trifluoroacetic acid.

2.4. HPLC Analysis of the Samples

Samples were analyzed by UV-HPLC, using a Waters 2695 separation module, a Waters 2487 UV detector and a column XBridge C18 (3.5µM, 4.6 × 100 mm); before this, they were centrifuged at 10,000 rpm for 10 min. Additionally, before centrifugation, samples from brain homogenate and emulsion experiments were diluted (50:50) with cold methanol to precipitate proteins. A flow rate of 1 mL/min, a run temperature of 30 °C and an injection volume of 90 µL were defined. The rest of chromatographic conditions that were used are summarized in Table 3. All analytical methods were validated and demonstrated to be adequate regarding linearity, accuracy, precision, selectivity and specificity (see Table S1 in the Supplementary Materials for the validation parameters).

2.5. Parameters Calculation: P_{app}, $f_{u,brain}$ and $V_{u,brain}$.

The apparent efflux permeabilities ($P_{app\ B\rightarrow A}$, $P_{app\ HOM}$ and $P_{app\ EMUL}$) were calculated using the modified non-sink equation [24] (Equation (1)), in which $C_{r,t}$ and $C_{r,t-1}$ are the concentrations in the receiver compartment (in this case, apical) at time t and time t-1, V_r and V_d are the volumes of the receiver (apical) and donor (basolateral) compartments, Q_t is the total amount of drug in both chambers at time t, f is the sample replacement dilution factor, S is the surface area of the monolayer and Δt is the time interval. $P_{eff,0}$ and $P_{eff,1}$ are the apparent permeability values, which can differ if the permeation rate is different at the beginning of the experiment with regard to the rest of the transport profile.

$$C_{r,t} = \frac{Q_t}{V_r + V_d} + \left(\left(C_{r,t-1} \cdot f \right) - \frac{Q_t}{V_r + V_d} \right) \cdot e^{-\boldsymbol{P_{eff0,1}} \cdot S \cdot \left(\frac{1}{V_r} + \frac{1}{V_d} \right) \cdot \Delta t} \quad (1)$$

$P_{eff,1}$ was the parameter selected to define the apparent efflux permeabilities ($P_{app\ B\rightarrow A}$, $P_{app\ HOM}$ and $P_{app\ EMUL}$) and with the aid of the Equation (2), they were transformed to $f_{u,brain}$.

$$f_{u,brain} = \frac{P_{app\ HOM}}{P_{app\ B\rightarrow A}} \quad or \quad \frac{P_{app\ EMUL}}{P_{app\ B\rightarrow A}} \quad (2)$$

Finally, the $f_{u,brain}$ were translated to $V_{u,brain}$ with Equation (3), where V_{ECF} is the volume of extracellular fluid and V_{ICF} is the volume of intracellular fluid. The comparison of the $V_{u,brain}$ with the physiological volumes of the CNS gives an idea of the drug affinity to the brain tissue (the greater the affinity for the tissue, the greater the $V_{u,brain}$) [8].

$$V_{u,brain} = V_{ECF} + \frac{1}{f_{u,brain}} \cdot V_{ICF} = 0.2 + \frac{1}{f_{u,brain}} \cdot 0.6 \quad (mL/g\ brain) \qquad (3)$$

2.6. In Vitro-In Vivo Correlations (IVIVCs): Linear Regression

Both in vitro parameters, $f_{u,brain}$ and $V_{u,brain}$ were related with their correspondent value in vivo to obtain different in vitro–in vivo correlations (IVIVCs). The in vivo data were obtained from the literature, specifically, from the following articles: [25,26]. The IVIVCs were adjusted to a linear model with the following structure: y = a + bx.

3. Results

Table 4 shows the apparent permeability values for all the drugs obtained in the different experimental conditions, Table 5 shows the in vitro $f_{u,brain}$ obtained from the different experiments as well as the in vivo values [25,26] for the same parameter. Table 6 is equivalent to Table 5, but for the $V_{u,brain}$ parameter. Results in tables 5 and 6 are more visually summarized in Figures 3 and 4.

Table 4. Apparent permeability obtained from the in vitro tests under different conditions (standard, brain homogenate or emulsion).

		MDCK Cell Line ($\times 10^{-6}$ cm/s)			MDCK-MDR1 Cell Line ($\times 10^{-6}$ cm/s)		
Drug	**C (µM)**	**$P_{app\ B\rightarrow A}$**	**$P_{app\ HOM}$**	**$P_{app\ EMUL}$**	**$P_{app\ B\rightarrow A}$**	**$P_{app\ HOM}$**	**$P_{app\ EMUL}$**
Amitriptyline	250	13.51	2.35	2.75	15.97	1.63	1.98
Atenolol	150	168.67	66.78	36.86	271.49	78.20	37.62
Carbamazepine	150	476.65	72.40	31.15	408.31	90.63	29.34
Fleroxacin	150	49.92 *	43.91 *	42.88	47.07 *	44.94 *	37.80
Loperamide	241	29.30	1.27	5.03	29.29	4.08	4.89
Norfloxacin	150	42.38	34.68	40.22	49.28	44.11	41.08
Pefloxacin	8.91	37.49 *	34.10 *	35.30	35.39 *	32.93 *	24.53
Propranolol	150	97.00	33.01	10.11	106.66	38.33	16.36
Zolpidem	158	36.48	35.42	13.03	33.43	29.46	16.52

* Data already published in [16].

Table 5. $f_{u,brain}$ predicted with the different experiments and in vivo $f_{u,brain}$ values obtained in rat by Kodaira et al. and Friden et al. [25,26].

		Rat	MDCK		MDCK-MDR1	
Drug	**C (µM)**	**$f_{u,brain}$**	**$f_{u,brain\ HOM}$**	**$f_{u,brain\ EMUL}$**	**$f_{u,brain\ HOM}$**	**$f_{u,brain\ EMUL}$**
Amitriptyline	250	0.002	0.174	0.204	0.102	0.124
Atenolol	150	0.261	0.396	0.219	0.288	0.139
Carbamazepine	150	0.170	0.152	0.065	0.222	0.072
Fleroxacin	150	0.555	0.880 *	0.859	0.955 *	0.803
Loperamide	241	0.002	0.043	0.172	0.139	0.167
Norfloxacin	150	0.222	0.818	0.949	0.895	0.834
Pefloxacin	8.91	0.514	0.910 *	0.942	0.931 *	0.693
Propranolol	150	0.005	0.340	0.104	0.359	0.153
Zolpidem	158	0.265	0.971	0.357	0.881	0.494

* Data already published in [16].

Table 6. $V_{u,brain}$ predicted with the different experiments and in vivo $V_{u,brain}$ values obtained in rat by Kodaira et al. and Friden et al. [25,26].

		Rat	MDCK		MDCK-MDR1	
Drug	**C (µM)**	**$V_{u,brain}$**	**$V_{u,brain\ HOM}$**	**$V_{u,brain\ EMUL}$**	**$V_{u,brain\ HOM}$**	**$V_{u,brain\ EMUL}$**
Atenolol	150	2.500	1.715	2.946	2.283	4.530
Carbamazepine	150	3.729	4.150	9.380	2.903	8.550
Fleroxacin	150	1.281	0.882	0.898	0.828	0.947
Norfloxacin	150	2.900	0.933	0.832	0.870	0.920
Pefloxacin	8.91	1.367	0.860	0.837	0.845	1.065
Zolpidem	158	2.464	0.818	1.880	0.881	1.414

Figure 3 shows the relationships obtained for the parameter $f_{u,brain}$ when the predicted values obtained with the brain homogenate are compared with the in vivo values for each drug.

Figure 3A,C show the $f_{u,brain}$ predictions for the MDCK cell line when the basolateral chamber is filled in with the brain homogenate or with the new emulsion, respectively, while in Figure 3B,D, the $f_{u,brain}$ predictions with the brain homogenate or with the new emulsion are also shown, but for the MDCK-MDR1 cell line. In the four cases, it can be seen that the smallest values in vitro correspond with the smallest values in vivo and that the biggest values in vitro correspond with the biggest values in vivo.

In Figure 3E,F, in which the predictions from the new emulsion are represented versus the predictions of the brain homogenate, it can be seen that they are more similar when using the MDCK-MDR1 cell line (r^2 = 0.886).

Figure 4 shows the same relationships as Figure 3, but for the parameter $V_{u,brain}$. In this case, it can be seen that for both cell lines MDCK (4A, 4C and 4E) and MDCK-MDR1 (4B, 4D and 4F), the predictions are quite similar. Moreover, when the new emulsion predictions and the brain homogenate predictions are represented together, the coefficient of determination is higher than 0.900 for both types of cells (r^2 = 0.978 for MDCK cells and r^2 = 0.954 for MDCK-MDR1 cells).

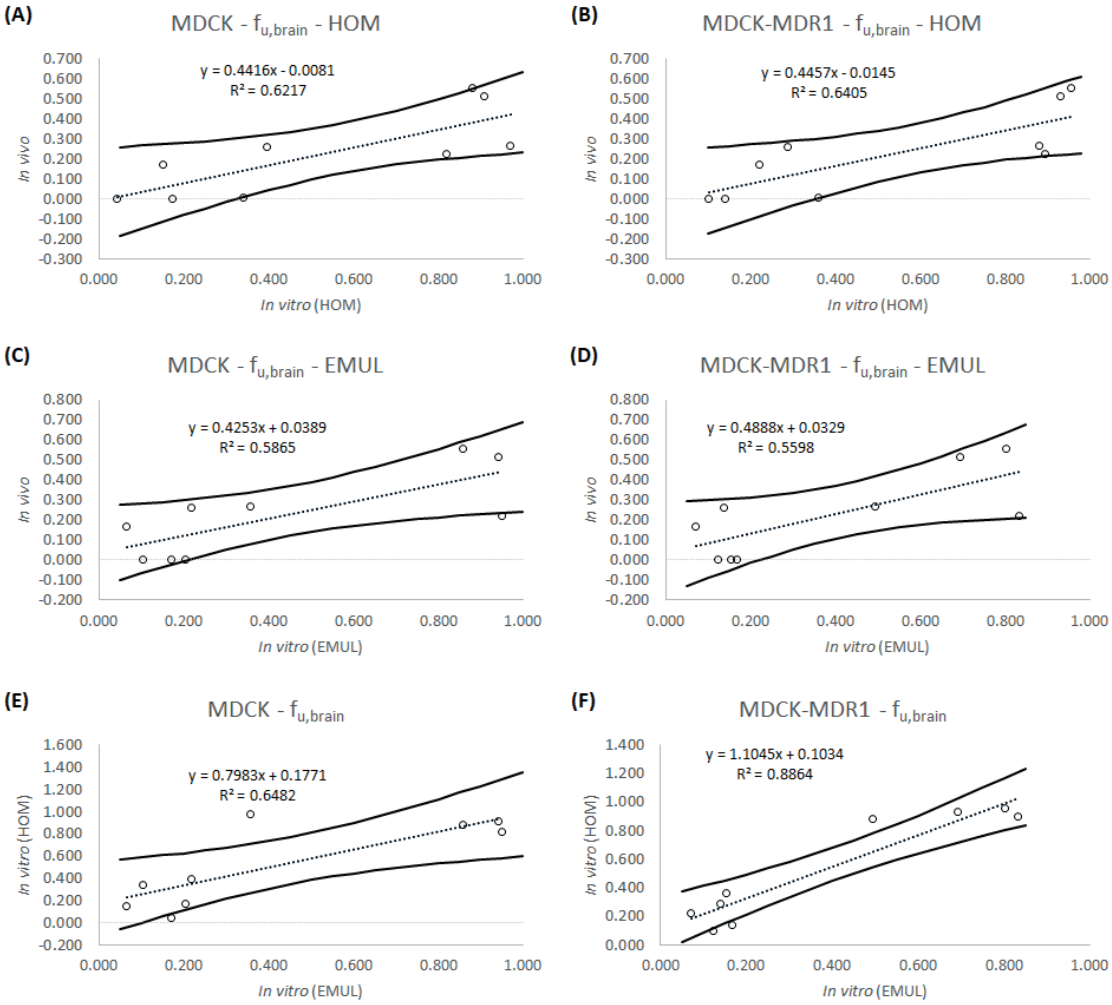

Figure 3. Correlations obtained for the $f_{u,brain}$ parameter. (**A**) IVIVC between the in vitro parameter obtained using the brain homogenate and the MDCK cell line and the in vivo parameter. (**B**) IVIVC between the in vitro parameter obtained using the brain homogenate and the MDCK-MDR1 cell line and the in vivo parameter. (**C**) IVIVC between the in vitro parameter obtained using the new emulsion and the MDCK cell line and the in vivo parameter. (**D**) IVIVC between the in vitro parameter obtained using the new emulsion and the MDCK-MDR1 cell line and the in vivo parameter. (**E**) Relationship between the parameters predicted using the new emulsion and the parameters predicted using the brain homogenate in the MDCK cell line. (**F**) Relationship between the parameters predicted using the new emulsion and the parameters predicted using the brain homogenate in the MDCK-MDR1 cell line. Solid lines represent the 95% confidence interval.

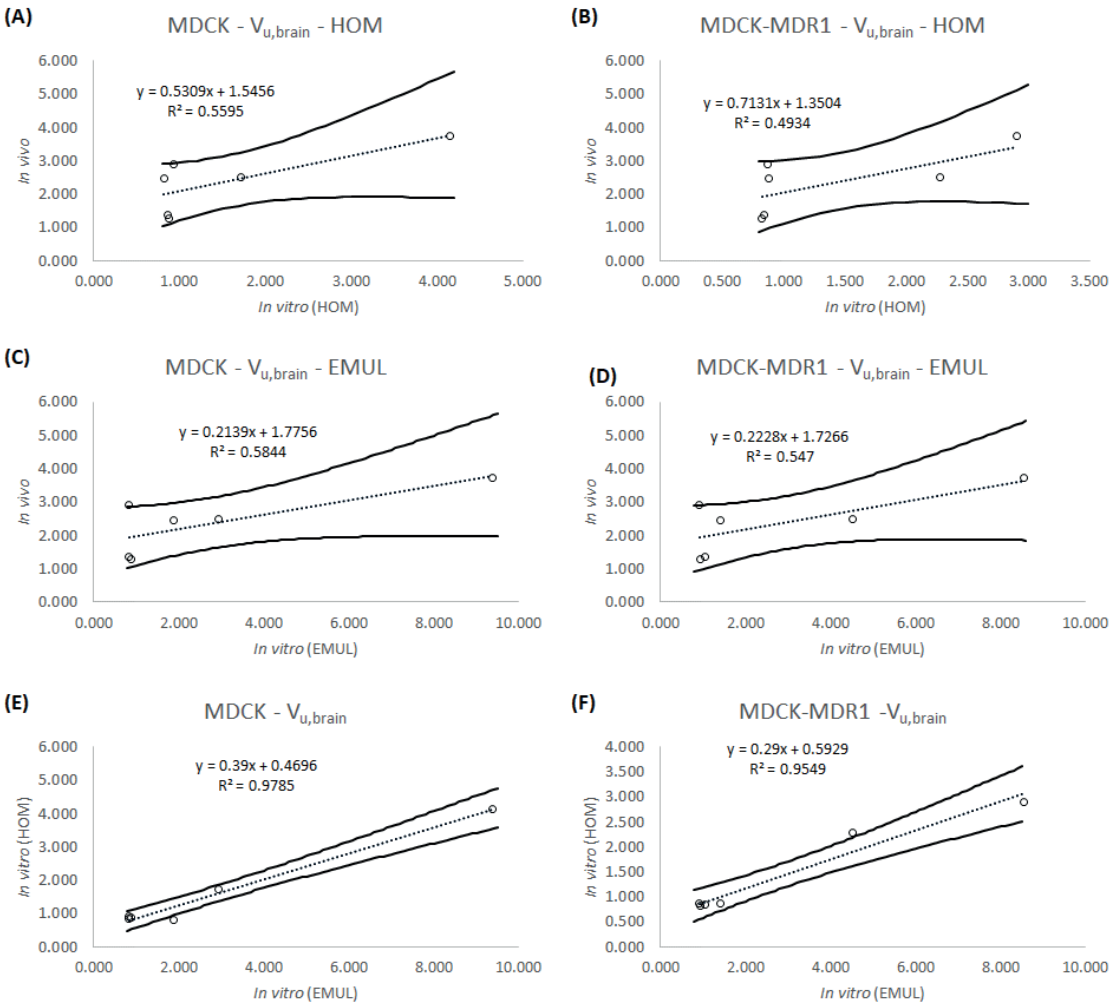

Figure 4. Correlations obtained for the $V_{u,brain}$ parameter. (**A**) IVIVC between the in vitro parameter obtained using the brain homogenate and the MDCK cell line and the in vivo parameter. (**B**) IVIVC between the in vitro parameter obtained using the brain homogenate and the MDCK-MDR1 cell line and the in vivo parameter. (**C**) IVIVC between the in vitro parameter obtained using the new emulsion and the MDCK cell line and the in vivo parameter. (**D**) IVIVC between the in vitro parameter obtained using the new emulsion and the MDCK-MDR1 cell line and the in vivo parameter. (**E**) Relationship between the parameters predicted using the new emulsion and the parameters predicted using the brain homogenate in the MDCK cell line. (**F**) Relationship between the parameters predicted using the new emulsion and the parameters predicted using the brain homogenate in the MDCK-MDR1 cell line. Solid lines represent the 95% confidence interval.

4. Discussion

Some decades ago, the use of animals in experimentation became controversial; from that moment to nowadays, the search for alternatives to these animals has become necessary [27]. In this work, a new formulation alternative to brain homogenate has been

developed as a substitute of this component in the study of the distribution of drugs in the central nervous system.

In an adult human, the CNS weight is around 3% of the total human body weight [28] and, in terms of biochemical composition, the whole human brain is approximately 77–78% water, 10–12% lipids, 8% proteins, 1% carbohydrates, 2% soluble organic substances and 1% inorganic salts [29]. On the other hand, fresh eggs are 12.5% proteins (38% of them in the yolk and 62% in the whites) and 11.1% lipids (all of them in the yolk) [21,30]. Taking into account these concentrations, a new formulation has been prepared in order to obtain an emulsion with the same composition as a human brain; the final concentration of protein has been 8% (5.1% from the yolk + 2.9% from the whites) and the concentration of lipids 12% (from the yolk).

The new formulation has been tested in a previously developed in vitro model [17] with the cell lines MDCK and MDCK-MDR1 (equal to the MDCK cell line, but transfected with P-glycoprotein). Despite their dog kidney origin and their lack of BBB transporters, both cell lines are accepted as appropriate tools to simulate the BBB because, when they are properly cultured, they form monolayers with quite strong and tight junctions [22,23].

Table 2 shows the molecular properties of the drugs used in this study. The selection of the different molecules was done considering their ability to bind P-glycoprotein, their charge at physiological pH, their solubility and their lipophilicity (logP), with the aim of having drugs with different properties. It is because P-glycoprotein is the most relevant transporter in MDCK-MDR1 cells [23] and because the other properties have been previously used in several in silico models (quantitative structure activity relationships–QSAR) when trying to predict the behaviour of drugs in the CNS [31–33]. In terms of the concentrations used in the study (Table 3), they were selected according to the ones previously used by Mangas-Sanjuan et al. [17], and the plasma values detected in vivo by Kodaira et al. [26] (when necessary, plasma concentrations were increased until making them detectable by HPLC.)

Figure 3 shows how the new emulsion is able to predict the $f_{u,brain}$ parameter, as well as the brain homogenate, because the coefficients of determination from Figure 3A,B are quite similar to those from Figure 3C,D. A clear tendency can be observed in all the correlations, and the values of r^2 are consistent to those obtained by Mangas Sanjuan et al. in 2013 (MDCK r^2 = 0.616 and MDCK-MDR1 r^2 = 0.624) [17], which although, not published, can be obtained from the $V_{u,brain}$ correlations with Equation (3). The inability to

obtain better IVIVCs can be explained by the homogenization process that may denaturalize some proteins of the brain tissue and damage the lipidic structures, altering their binding properties [12]. In a similar way, in the case of the new emulsion, the proportion of lipid and proteins present in brain are respected, but there is not an organized structure in it.

On the other hand, the $f_{u,brain}$ correlations are better for the MDCK-MDR1 cell line, which has an r^2 of 0.886 when the predictions from brain homogenate and from the new emulsion are represented together (Figure 3F). Probably, this better prediction can be attributed to the presence of the P-glycoprotein in the monolayers of the MDCK-MDR1 cells, as the fraction of drug that binds the efflux transporter does not contribute to the $f_{u,brain}$.

In terms of the $V_{u,brain}$ parameter, predictions from both cell lines are also quite similar as seen in Figure 4. Furthermore, in this case, there is a huge similarity between the predictions of both cell lines (MDCK and MDCK-MDR1), as can be deduced from the higher than 0.900 coefficients of determination from Figure 4E,F. The absence of differences between cell lines can be explained when the definition of the $V_{u,brain}$ parameter is taken into account, since it represents the drug in the brain with independence of the BBB equilibrium [8], thus without being affected by the transporters. As happened with the $f_{u,brain}$ correlations, the low r^2 in Figure 4A–D, may be explained by the lack of an organized structure in both the brain homogenate and the new emulsion [12].

Despite his success in the prediction of drug brain distribution, this type of in vitro model will not substitute the brain microdialysis technique, at least at the moment, because it cannot reflect all the physiological properties of an alive CNS. Maybe a future approach may be exploring the possibility of developing an organized animal-free slice with an organized structure which could be able to predict $f_{u,brain}$ the $V_{u,brain}$ in a better way. To do this, first, the model should be tested substituting the brain homogenate by brain slices and evaluate its ability to predict brain distribution and then, if it is able to do it properly, the brain slices could be compared with the new animal-free slices. Nevertheless, as it is now, it is a useful tool that can be used in a complementary way when a new drug or an innovative delivery strategy is being developed. Thus, this model can be used as a rapid screening tool and its information, on its own, or combined with other information obtained from in silico [31–33] or PBPK [16,34,35] models, could be used to move only a few selected candidates to in vivo studies.

Other in vitro BBB models could also be adapted to use this new "animal-free" (based on unfertilized chicken eggs) emulsion and obtain more information. On the one hand, the cell monolayer could be substituted by a more complex cell line, such as hCMEC/D3, as was previously done by the authors with the Mangas-Sanjuan et al. model [18], for studying new drugs or delivery systems substrate of other transporters different to P-glycoprotein. On the flip side, moving to a simpler way, the new emulsion in combination with PAMPA-BBB or PAMPA-BLM models, which have demonstrated to be able to correctly classify drugs into BBB+ and BBB- groups according to their total concentration [10,11,14], could be used to evaluate not just the access of substances through the BBB, but also their distribution once in the CNS.

It cannot be forgotten that the final aim of this type of study is to try to guess what would happen if the drug is administered to human beings. In this respect, the differences on the specific composition (not in proportion) in lipids and proteins between chickens and humans may hinder the translation of data. Nonetheless, the development of PBPK models has proved to be a helpful tool in this process [16]. Therefore, the data of this paper may be applied into already stablished models [16,34,35], or in a new one to obtain the final information.

In the field of ethics, replacing the brain homogenate with the "animal free" (based on unfertilized chicken eggs) emulsion proposed in this work would speed up the procedures regarding the in vitro model proposed in 2013 by Mangas-Sanjuan et al. [17]. This acceleration is mainly due to the fact that, although using brain homogenate in the permeability tests reduces the number of animals used in research, an ethics committee approval is still needed, while, for using the egg emulsion, this approval is not necessary; i.e., for obtaining pig brain homogenate, it is necessary to sacrifice pigs, while for using eggs, no animal has to die.

Furthermore, in the economic and industrial field, the fulfillment of the 3Rs principles can also be beneficial because, generally, the time and the costs needed for applying the new alternative methods are much smaller than when using animals [36]. For instance, for applying the technique proposed in this paper, the industry needs the cells and the facilities for cell culture, which can be obtained after an initial investment, whereas, for applying the microdialysis, the maintenance of a stable and staff that take care of the animals is continuously necessary.

5. Conclusions

A new formulation (based on unfertilized chicken eggs) with the same proportion in proteins and lipids as a human brain has been developed in order to improve the ethics and reduce the costs of in vitro permeability tests. This formulation has proved to be a good alternative to brain homogenate in the preliminary study of drug distribution in the CNS, allowing researchers to obtain two different parameters ($f_{u,brain}$ and $V_{u,brain}$) in a quick and cheap way, as it is much more simple to gain access to eggs than to dead pig brains. Besides that, this methodology contributes to the protection of animals, as it replaces them successfully when, in an initial phase, the binding of a drug to the brain is studied. In this sense, the new formulation proposed here could be used in in vitro tests as a high throughput tool to select the most promising molecules and formulations in the early development of drugs for the treatment of CNS diseases; it is thus a great advance in the respectful use of animal lives.

Supplementary Materials: The following are available online at www.mdpi.com/article/10.3390/ani11123521/s1, Table S1: Chromatographic conditions validation.

Author Contributions: Conceptualization, M.B. and M.G.-Á.; methodology, B.S.-D. and I.G.-Á.; software, B.S.-D.; validation, B.S.-D., M.B., M.G.-Á. and I.G.-Á.; formal analysis, B.S.-D.; investigation, B.S.-D. and I.G.-Á.; resources, M.B.; data curation, I.G.-Á.; writing—original draft preparation, B.S.-D.; writing—review and editing, M.B., M.G.-Á. and I.G.-Á.; visualization, B.S.-D.; supervision, M.B., M.G.-Á. and I.G.-Á.; project administration, I.G.-Á.; funding acquisition, M.B. All authors have read and agreed to the published version of the manuscript.

Funding: This research was funded by Agencia Estatal Investigación and European Union, through FEDER (Fondo Europeo de Desarrollo Regional) with the project: "Modelos in vitro de evaluación biofarmacéutica" [SAF2016-78756 (AEI/FEDER, EU)]. B.S.-D. received a grant from the Ministry of Science, Innovation and Universities of Spain [FPU17/00530].

Institutional Review Board Statement: Not applicable.

Informed Consent Statement: Not applicable.

Data Availability Statement: The authors confirm that the data supporting the findings of this study are available within the article and its Supplementary Materials.

Conflicts of Interest: The authors declare no conflict of interest. The funders had no role in the design of the study; in the collection, analyses, or interpretation of data; in the writing of the manuscript, or in the decision to publish the results.

References

1. World Health Organization Facts About Ageing. Available online: http://www.who.int/ageing/about/facts/en/ (accessed on 20 October 2020).
2. Kowalska, M.; Owecki, M.; Prendecki, M.; Wize, K.; Nowakowska, J.; Kozubski, W.; Lianeri, M.; Dorszewska, J. Aging and Neurological Diseases. In *Senescence—Physiology or Pathology*; Dorszewska, J., Kozubski, W., Eds.; InTech: London, UK, 2017.
3. Global Burden of Disease Collaborative Network Global Burden of Disease Study 2019. Results. 2019. Available online: http://ghdx.healthdata.org/gbd-results-tool (accessed on 9 September 2021).
4. Gribkoff, V.K.; Kaczmarek, L.K. The need for new approaches in CNS drug discovery: Why drugs have failed, and what can be done to improve outcomes. *Neuropharmacology* **2017**, *120*, 11–19, doi:10.1016/j.neuropharm.2016.03.021.
5. Yamamoto, Y.; Danhof, M.; de Lange, E.C.M. Microdialysis: The key to physiologically based model prediction of human CNS target site concentrations. *AAPS J.* **2017**, *19*, 891–909, doi:10.1208/s12248-017-0050-3.
6. Hammarlund-Udenaes, M. Microdialysis as an Important Technique in Systems Pharmacology—A Historical and Methodological Review. *AAPS J.* **2017**, *19*, 1294–1303, doi:10.1208/s12248-017-0108-2.
7. Penicaud, L.; Benani, A.; Datiche, F.; Fioramonti, X.; Leloup, C.; Lienard, F. Animal Models and Methods to Study the Relationships Between Brain and Tissues in Metabolic Regulation. In *Animal Models for the Study of Human Disease*; Elsevier: Amsterdam, The Netherlands, 2013; pp. 569–593. ISBN 9780124158948.
8. Hammarlund-Udenaes, M.; Fridén, M.; Syvänen, S.; Gupta, A. On the rate and extent of drug delivery to the brain. *Pharm. Res.* **2008**, *25*, 1737–1750, doi:10.1007/s11095-007-9502-2.
9. The National Centre for the 3Rs. The 3Rs NC3Rs. Available online: https://www.nc3rs.org.uk/the-3rs (accessed on 29 June 2020).
10. Müller, J.; Esso, K.; Dargó, G.; Könczöl, Á.; Balogh, G.T. Tuning the predictive capacity of the PAMPA-BBB model. *Eur. J. Pharm. Sci.* **2015**, *79*, 53–60, doi:10.1016/J.EJPS.2015.08.019.
11. Mensch, J.; Melis, A.; Mackie, C.; Verreck, G.; Brewster, M.E.; Augustijns, P. Evaluation of various PAMPA models to identify the most discriminating method for the prediction of BBB permeability. *Eur. J. Pharm. Biopharm.* **2010**, *74*, 495–502, doi:10.1016/J.EJPB.2010.01.003.
12. Summerfield, S.G.; Dong, K.C. In vitro, in vivo and in silico models of drug distribution into the brain. *J. Pharmacokinet. Pharmacodyn.* **2013**, *40*, 301–314, doi:10.1007/S10928-013-9303-7.
13. Di, L.; Kerns, E.H.; Bezar, I.F.; Petusky, S.L.; Huang, Y. Comparison of blood–brain barrier permeability assays: In situ brain perfusion, MDR1-MDCKII and PAMPA-BBB. *J. Pharm. Sci.* **2009**, *98*, 1980–1991, doi:10.1002/JPS.21580.

14. Mensch, J.; Oyarzabal, J.; Mackie, C.; Augustijns, P. In vivo, in vitro and in silico methods for small molecule transfer across the BBB. *J. Pharm. Sci.* **2009**, *98*, 4429–68, doi:10.1002/jps.21745.
15. Dagenais, C.; Graff, C.L.; Pollack, G.M. Variable modulation of opioid brain uptake by P-glycoprotein in mice. *Biochem. Pharmacol.* **2004**, *67*, 269–76, doi:10.1016/j.bcp.2003.08.027.
16. Sánchez-Dengra, B.; Gonzalez-Alvarez, I.; Bermejo, M.; Gonzalez-Alvarez, M. Physiologically Based Pharmacokinetic (PBPK) Modeling for Predicting Brain Levels of Drug in Rat. *Pharmaceutics* **2021**, *13*, 1402, doi:10.3390/pharmaceutics13091402.
17. Mangas-Sanjuan, V.; González-Álvarez, I.; González-Álvarez, M.; Casabó, V.G.; Bermejo, M. Innovative in vitro method to predict rate and extent of drug delivery to the brain across the blood-brain barrier. *Mol. Pharm.* **2013**, *10*, 3822–3831, doi:10.1021/mp400294x.
18. Sánchez-Dengra, B.; González-Álvarez, I.; Sousa, F.; Bermejo, M.; González-Álvarez, M.; Sarmento, B. In vitro model for predicting the access and distribution of drugs in the brain using hCMEC/D3 cells. *Eur. J. Pharm. Biopharm.* **2021**, *163*, 120–126, doi:10.1016/j.ejpb.2021.04.002.
19. Chemicalize Chemicalize-Instant Cheminformatics Solutions. Available online: https://chemicalize.com/welcome (accessed on 3 May 2020).
20. DrugBank. Available online: https://www.drugbank.ca/ (accessed on 14 May 2020).
21. Instituto de Estudios del Huevo Composición. Nutricional del Huevo. Available online: https://www.institutohuevo.com/composicion-nutricional-del-huevo/#1501003984074-a5111b1a-4b63 (accessed on 3 July 2020).
22. Mangas-Sanjuan, V.; Gonzalez-Alvarez, M.; Gonzalez-Alvarez, I.; Bermejo, M. In vitro methods for assessing drug access to the brain. In *Advances in Non-Invasive Drug Delivery to the Brain*; Future Science Ltd: London, UK; Marshall University: Huntington, WV, USA, 2015; pp. 44–61. ISBN 9781909453937.
23. Veszelka, S.; Tóth, A.; Walter, F.R.; Tóth, A.E.; Gróf, I.; Mészáros, M.; Bocsik, A.; Hellinger, É.; Vastag, M.; Rákhely, G.; et al. Comparison of a rat primary cell-based blood-brain barrier model with epithelial and brain endothelial cell lines: Gene expression and drug transport. *Front. Mol. Neurosci.* **2018**, *11*, 166, doi:10.3389/fnmol.2018.00166.
24. Mangas-Sanjuan, V.; González-Álvarez, I.; González-Álvarez, M.; Casabó, V.G.; Bermejo, M. Modified nonsink equation for permeability estimation in cell monolayers: Comparison with standard methods. *Mol. Pharm.* **2014**, *11*, 1403–1414, doi:10.1021/mp400555e.
25. Fridén, M.; Gupta, A.; Antonsson, M.; Bredberg, U.; Hammarlund-Udenaes, M. In vitro methods for estimating unbound drug concentrations in the brain interstitial and intracellular fluids. *Drug Metab. Dispos.* **2007**, *35*, 1711–1719, doi:10.1124/dmd.107.015222.
26. Kodaira, H.; Kusuhara, H.; Fujita, T.; Ushiki, J.; Fuse, E.; Sugiyama, Y. Quantitative evaluation of the impact of active efflux by P-glycoprotein and breast cancer resistance protein at the blood-brain barrier on the predictability of the unbound concentrations of drugs in the brain

using cerebrospinal fluid concentration as a. *J. Pharmacol. Exp. Ther.* **2011**, *339*, 935–944, doi:10.1124/jpet.111.180398.

27. The European Commission's Science and Knowledge Service EU. Reference Laboratory for Alternatives to Animal Testing EU Science Hub. Available online: https://ec.europa.eu/jrc/en/eurl/ecvam (accessed on 19 July 2020).
28. Sánchez-Dengra, B.; González-Álvarez, I.; Bermejo, M.; González-Álvarez, M. Nanomedicine in the Treatment of Pathologies of the Central Nervous System Advances in Nanomedicine. Advances in Nanomedicine. 2020. Available online: https://www.openaccessebooks.com/advances-in-nanomedicine/nanomedicine-in-the-ttreatment-of-pathologies-of-the-central-nervous-system.pdf (accessed on 19 July 2020).
29. McIlwain, H.; Bachelard, H. *Biochemistry and the Central Nervous System*; 5th ed.; Churchill Livingstone: Edingburg, UK, 1985; ISBN 0-443-01961-4.
30. Wikipedia Huevo (Alimento). Available online: https://es.wikipedia.org/wiki/Huevo_(alimento) (accessed on 19 July 2020).
31. Garg, P.; Jitender, V. In Silico Prediction of Blood Brain Barrier Permeability: An Artificial Neural Network Model. *J. Chem. Inf. Model.* **2005**, *46*, 289–297, doi:10.1021/CI050303I.
32. Pajouhesh, H.; Lenz, G.R. Medicinal Chemical Properties of Successful Central Nervous System Drugs. *NeuroRx* **2005**, *2*, 541, doi:10.1602/NEURORX.2.4.541.
33. Carpenter, T.S.; Kirshner, D.A.; Lau, E.Y.; Wong, S.E.; Nilmeier, J.P.; Lightstone, F.C. A Method to Predict Blood-Brain Barrier Permeability of Drug-Like Compounds Using Molecular Dynamics Simulations. *Biophys. J.* **2014**, *107*, 630, doi:10.1016/J.BPJ.2014.06.024.
34. Loryan, I.; Sinha, V.; Mackie, C.; Van Peer, A.; Drinkenburg, W.; Vermeulen, A.; Morrison, D.; Monshouwer, M.; Heald, D.; Hammarlund-Udenaes, M. Mechanistic understanding of brain drug disposition to optimize the selection of potential neurotherapeutics in drug discovery. *Pharm. Res.* **2014**, *31*, 2203–2219, doi:10.1007/s11095-014-1319-1.
35. Ball, K.; Bouzom, F.; Scherrmann, J.M.; Walther, B.; Declèves, X. A physiologically based modeling strategy during preclinical CNS drug development. *Mol. Pharm.* **2014**, *11*, 836–848, doi:10.1021/mp400533q.
36. Schiffelers, M.J.W.A.; Blaauboer, B.J.; Hendriksen, C.F.M.; Bakker, W.E. Regulatory acceptance and use of 3R models: A multilevel perspective. *ALTEX* **2012**, *29*, 287–300, doi:10.14573/altex.2012.3.287.

Supplementary material

Table S1. Chromatographic conditions validation.

	r^2	LLQ (µM)	Accuracy	Precision	REF
Amitriptyline	0.996	8.20	6.1	3.2	[1]
Atenolol	0.996	1.49	6.3	5.1	
Carbamazepine	0.994	0.76	3.9	3.6	[1]
Fleroxacin	0.997	0.05	6.0	5.2	[1]
Loperamide	0.995	2.65	4.0	4.5	
Norfloxacin	0.991	2.42	3.9	4.9	
Pefloxacin	0.998	0.61	3.9	3.7	[1]
Propranolol	0.999	5.74	3.9	3.4	
Zolpidem	0.997	4.30	6.3	4.8	[1]

1. Sánchez-Dengra, B.; Gonzalez-Alvarez, I.; Bermejo, M.; Gonzalez-Alvarez, M. Physiologically Based Pharmacokinetic (PBPK) Modeling for Predicting Brain Levels of Drug in Rat. *Pharmaceutics* **2021**, *13*, 1402, doi:10.3390/pharmaceutics13091402.

5. Physiologically Based Pharmacokinetic (PBPK) Modeling for Predicting Brain Levels of Drug in Rat

Type of publication	Article
Title	Physiologically Based Pharmacokinetic (PBPK) Modeling for Predicting Brain Levels of Drug in Rat
Authors	Bárbara Sánchez-Dengra, Isabel González-Álvarez, Marival Bermejo and Marta González-Álvarez
Journal	Pharmaceutics
Impact factor	6.321 (Q1 - Pharmacology and Pharmacy)
Year of publication	2021
DOI	doi.org/10.3390/pharmaceutics13091402

Abstract

One of the main obstacles in neurological disease treatment is the presence of the blood–brain barrier. New predictive high-throughput screening tools are essential to avoid costly failures in the advanced phases of development and to contribute to the 3 Rs policy. The objective of this work was to jointly develop a new in vitro system coupled with a physiological-based pharmacokinetic (PBPK) model able to predict brain concentration levels of different drugs in rats. Data from in vitro tests with three different cells lines (MDCK, MDCK-MDR1 and hCMEC/D3) were used together with PK parameters and three scaling factors for adjusting the model predictions to the brain and plasma profiles of six model drugs. Later, preliminary quantitative structure–property relationships (QSPRs) were constructed between the scaling factors and the lipophilicity of drugs. The predictability of the model was evaluated by internal validation. It was concluded that the PBPK model, incorporating the barrier resistance to transport, the disposition within the brain and the drug–brain binding combined with MDCK data, provided the best predictions for passive diffusion and carrier-mediated transported drugs, while in the other cell lines, active transport influence can bias predictions.

Keywords

blood−brain barrier (BBB); physiologically based pharmacokinetics (PBPK); quantitative structure–property relationships (QSPRs); distribution volume in brain ($V_{u,brain}$); plasma−brain partition coefficient ($Kp_{uu,brain}$)

1. Introduction

The brain is the most important organ in living beings as it controls their vital functions: nutrition, interaction and reproduction. The importance of the brain means all the capillaries that supply it with oxygen and nutrients are composed of extremely tight endothelial cells surrounded by a thick layer of astrocytes and pericytes, all of this to prevent dangerous substances from reaching it. This group of protective and regulating cells is known as the blood–brain barrier (BBB).

Besides the physicochemical protection of the BBB, the brain is also protected by the cerebrospinal fluid (CSF), a constantly secreted liquid that helps to maintain the brain's homeostasis for normal neurological function, acts as a cushion between the brain and the skull, and makes the central nervous system (CNS) apparently "lighter", as it is floating in this liquid [1]. There are two different barriers that separate the CSF from the rest of the body—the blood–cerebrospinal fluid barrier (BCSFB), which is around the capillaries within brain ventricles, and the blood–arachnoid barrier, around the subarachnoid space [2,3].

The extra protection of the CNS hinders the development of new drugs for the treatment of neurological pathologies (glioblastoma, Alzheimer's disease, depression, Parkinson's disease or epilepsy, among others), as molecules experience difficulties in reaching their target. Because of this, the pharmaceutical industry has developed several strategies to bypass the BBB: chemical strategies, such as the development of prodrugs or chemical drug delivery systems (CDDS), physical strategies, such as the use of ultrasounds to temporarily open the tight junctions of the endothelial cells, or nanotechnological strategies, which include developing lipid-based, polymer-based or metal-based nanocarriers [4].

On the other hand, the use of reliable methods to evaluate whether a new candidate will reach the brain is as important as the development of new strategies to bypass the BBB. This type of method can include in silico, in vitro, in situ or in vivo tests; however, except for the in vivo tests that directly measure the brain concentration of a drug over time, the results obtained with the other methodologies have been considered controversial, as they do not sufficiently accurately reflect whether the drug will reach the brain and perform its action [5,6].

Frequently, researchers use the permeability clearance into the brain (Cl_{in}), or the influx permeability surface area product (PS_{in}), which is the same, to define whether or not a drug will permeate the BBB, or at least to say if a new delivery system will improve

on the action of a previous one [6]. Nevertheless, this parameter is not the only one that should be used to define the potential success of a drug in the treatment of a neurological pathology, because it gives a measurement of the rate of transport through the BBB; however, fast permeation does not mean fast action or a better performance, as concentrations in the brain are also influenced by (A) the binding of the drug to the tissue once it crosses the BBB, (B) the binding of the drug to the proteins in blood, and (C) the presence of efflux transporters that remove the drug from the brain [5]. According to Dagenais et al., the PS_{in} of loperamide obtained by the in situ brain perfusion method was 98.6 ± 17.3 µL/min × g brain, while, the value of the same parameter, obtained by the same method, for morphine was 10.4 ± 3 µL/min × g brain; thus, loperamide is more permeable than morphine through the BBB, although morphine is much more active in the CNS. This gives a clear example of the lack of reliability of the influx clearance parameter when it is taken on its own [5,7].

When the efflux clearance (Cl_{out}) is taken into account as well as the unbound fractions of drug, then the other two neuropharmacokinetic (neuroPK) parameters can be defined too: the unbound plasma–brain partition coefficient ($Kp_{uu,brain}$) and the apparent volume of distribution in the brain ($V_{u,brain}$) [5,8].

The $Kp_{uu,brain}$ is defined as the relationship between the concentration of free drug in plasma ($C_{u,p}$) and the concentration of free drug in the brain ($C_{u,b}$) at a steady state. It can be obtained according to Equation 1, in which the AUC_u is the area under the unbound concentration versus time curve. This parameter includes the passive and active transport of the unbound drug through the BBB in both directions (influx and efflux); because of this, and considering that only the free fraction of the drug can cross the BBB, the $Kp_{uu,brain}$ is judged as a more informative parameter than the Kp_{brain} (also known as logBB), a previously described parameter that used total concentrations to evaluate the permeability through the BBB [5,9,10].

$$Kp_{uu,brain} = \frac{AUC_{u,brain}}{AUC_{u,plasma}} = \frac{Cl_{in}}{Cl_{out}} = \frac{PS_{in}}{PS_{out}} \quad (1)$$

The $V_{u,brain}$, meanwhile, reflects the distribution of the drug once it has crossed the BBB, and can be defined as a relationship between the total amount of drug present in the brain and the concentration of free drug in the brain ($C_{u,b}$). If the drug has a high affinity for brain tissue, its unbound fraction of drug in the brain ($f_{u,brain}$) will decrease, and therefore, the $V_{u,brain}$ will be greater, as shown in Equation 2, where V_{ECF} is the volume of extracellular fluid and V_{ICF} is the volume of intracellular fluid [11]. A higher $V_{u,brain}$ can be

translated into a longer half-life of the drug in the brain, independently of its transport through the BBB or its plasma concentration [5]. So, it is particularly helpful to know this parameter or the $f_{u,brain}$ when a new candidate for the treatment of a neurological disease is evaluated.

$$V_{u,brain} = V_{ECF} + \frac{1}{f_{u,brain}} \cdot V_{ICF} = 0.2 + \frac{1}{f_{u,brain}} \cdot 0.6 \quad (mL/g\ brain) \qquad (2)$$

Besides the different tests for obtaining the parameters mentioned above, over the last few years, researchers have also worked on the development of mathematical models, such as physiologically based pharmacokinetic (PBPK) models, for describing and predicting the behaviour of CNS drugs after being administered. In 2019, Vendel et al. published a review wherein they summarized different types of mathematical models for describing drug distribution within the brain, and all the processes and properties that should be taken into account to develop the "perfect" model [2]:

- Brain-specific properties, such as the properties of the brain vascular network and the different brain barriers, the characteristics of the brain tissue and the CSF, the fluid movements within the brain or the presence of metabolic enzymes in the CNS;
- Drug-specific properties, such as molecular (molecular weight, polar surface area, shape or number of hydrogen bond donors and acceptors), physicochemical (pKa, solubility or lipophilicity) and pharmacokinetic properties;
- Processes affecting drug distribution within the brain, e.g., the drug transport through the brain vascular system, the brain barriers or within the brain fluids, the drug extra-/intracellular exchange, the drug binding or the drug metabolism.

It is shown that, despite the high number of models available, some are too complex, others are not completely predictable, and none are able to cover all the processes mentioned above. At the end of the review, it is concluded that there are three important points that a neuro-PBPK model should include in order to give accurate predictions of the in vivo behaviour: A) the barrier transport, B) the transport of the drug once in the brain, and C) drug–brain binding [2].

Normally, neuroPK parameters (PS_{in}, $Kp_{uu,brain}$ and $V_{u,brain}$) are obtained using different experimental models. In this work, a previously proposed and validated single in vitro system [11,12] was used to derive those parameters. Later, these in vitro data were combined with in silico and in vivo pharmacokinetic information from outside the brain to develop a new neuro-semi-physiological mathematical model, including the three

factors mentioned above (the barrier transport, the transport within the brain and the drug–brain binding). Thus, the main objective of this work was to jointly develop a new in vitro system coupled with a physiological-based pharmacokinetic (PBPK) model able to predict brain concentration levels for different drugs in a rat. Furthermore, the predictability of the new PBPK model was compared across different cell lines chosen for obtaining the in vitro neuroPK parameters.

2. Materials and Methods

2.1. Drugs and Products

The six drugs used for constructing the mathematical model (amitriptyline, caffeine, carbamazepine, fleroxacin, pefloxacin and zolpidem) and HPLC-grade solvents (acetonitrile, methanol and water) were purchased from Sigma-Aldrich (Barcelona, Spain). The MDCK cell line was purchased from ATCC (USA), MDCK-MDR1 cells were provided by Dr. Gottessman, and the MM (National Institutes of Health, Bethesda, MD, USA) and hCMEC/D3 cell lines were purchased from Cedarlane (Burlington, ON, Canada). Pig brain homogenate was kindly supplied by a local slaughterhouse.

Dulbecco's modified eagle's medium (DMEM) with a high content of glucose, L-glutamine, HEPES, MEM non-Essential aminoacid, penicillin−streptomycin, trypsin-EDTA, Hank's balanced salt solution (HBSS) and fetal bovine serum (FBS) for the cell culture of MDCK and MDCK-MDR1 cell lines were purchased from Sigma-Aldrich (Barcelona, Spain).

The products needed for the culture of hCMEC/D3 cells were purchased from Sigma-Aldrich (Barcelona, Spain) (hydrocortisone, ascorbic acid, HEPES, Triton X-100 and bFGF), Gibco (Barcelona, Spain) (FBS, penicillin–streptomycin, chemically defined lipid concentrate, HBSS, collagen I rat protein and trypsin-EDTA), Lona (Barcelona, Spain) (EBM-2 medium).

2.2. Cell Culture and Permeability Studies

MDCK and MDCK-MDR1 cells were cultured and seeded according to the protocol explained in [11], while the culture and seeding of hCMEC/D3 cell line was done as explained in [12].

On the day of the experiment, the cells were seeded in 6-transwell plates (effective area: 4.2 cm^2, pore size: 0.4 micron and pore density: $100 \pm 10 \times 10^6/cm^2$), which were supposed to be confluent, washed twice with HBSS, and transepithelial electrical resistance (TEER) was measured. If the TEER values were around 30–40 $k\Omega \cdot cm^2$ [13] for

hCMEC/D3 cells, around 130–150 kΩ·cm^2 [13] for MDCK cells and around 120–140 kΩ·cm^2 [13] for MDCK-MDR1 cells, then the integrity of the monolayers was considered appropriate, and three types of experiments were carried out according to [11,12]:

1. Standard AB. This experiment was designed for obtaining the apparent influx permeability ($P_{app\ A\to B}$). The drug was dissolved in HBSS; this solution was put into the apical chamber of the transwell and the basolateral chamber was filled with cleaned HBSS. Four samples were taken from the basolateral chamber at pre-established times (15, 30, 60 and 90 min) [11,12]. Three replicates were carried out for each drug;
2. Standard BA. In this case, the montage was the opposite to the first condition and the basolateral chamber was filled with a drug solution in HBSS, while the apical chamber was filled with cleaned HBSS. Four samples were taken from the apical chamber at pre-established times (15, 30, 60 and 90 min) [11,12]. With this test, the apparent efflux permeability ($P_{app\ B\to A}$) was obtained. Three replicates were carried out for each drug;
3. Brain homogenate BA. This last condition gives the free drug apparent efflux permeability ($P_{app\ HOM}$), as the drug is added to the basolateral chamber after being dissolved in a 1:3 pig brain homogenate:phosphate buffer (180 mM, pH 7.4) solution, and only the free fraction of drug will be able to cross to the apical chamber, where 4 samples were taken at pre-established times (15, 30, 60 and 90 min) [11,12]. Three replicates were carried out for each drug.

The neuroPK parameters ($Kp_{uu,brain}$, $f_{u,brain}$ and $V_{u,brain}$) were obtained by means of the combination of the apparent permeabilities mentioned above with Equations 1, 3 and 2, respectively.

$$f_{u,brain} = \frac{P_{app\ B\to A}}{P_{app\ HOM}} \quad (3)$$

2.3. HPLC Analysis of the Samples

Samples from brain homogenate experiments were diluted (50:50) with cold methanol to precipitate proteins, and all the samples were centrifuged at 10,000 rpm for 10 min. Then, the supernatants were analyzed by HPLC. An UV-HPLC equipment (Barcelona, Spain) (Waters 2695 separation module and Waters 2487 UV detector) with a column XBridge C18 (3.5µM, 4.6 x 100 mm) (Barcelona, Spain), a flow rate of 1 mL/min, a run temperature of 30 °C and an injection volume of 90 µL was used for the analysis.

Table S1 summarizes the rest of the chromatographic conditions. All analytical methods were validated and demonstrated to be adequate regarding linearity, accuracy, precision, selectivity and specificity.

2.4. Model Construction

Figure 1 shows the scheme of the semi-physiological model. An extra absorption site was added when needed (if the available in vivo data were not from intravenous administration).

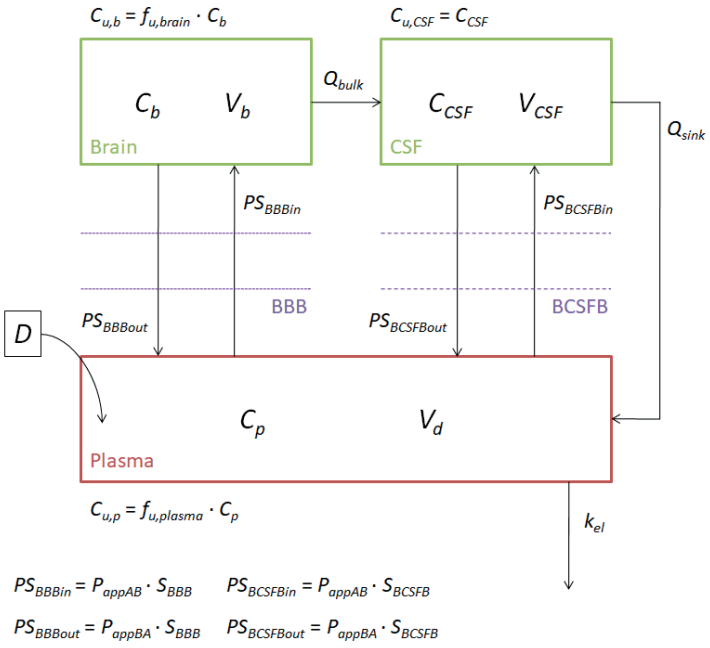

Figure 1. PBPK model scheme.

We defined one compartment for plasma and two compartments for the CNS (one representing the brain tissue itself and the other representing the CSF). According to the scheme, drugs can go in or out of the CNS through the BBB or through the BCSFB, depending on the area that they reach or leave (the tissue or the CSF). Additionally, it was considered that drugs can pass from brain tissue to the CSF following the bulk flow (Q_{bulk}) of the ECF to the CSF, and they can also return to plasma with the drainage of the CSF (Q_{sink}). As CSF is considered a clear liquid, all the drug concentration inside it was considered the unbound drug concentration, while in the plasma and brain tissue, the unbound concentrations were considered equal to the unbound fraction of the drug in that compartment multiplied by the total concentration (the $f_{u,brain}$ that was used in this calculation was obtained from the permeability studies). Influx and efflux clearances through the different brain barriers were obtained by multiplying the apparent

permeabilities of the in vitro studies by the surface areas of those barriers. Differential Equations 4, 5 and 6 describe the processes mentioned above for the administration of an intravenous single dose. The values of the physiological parameters, brain volume (V_b), CSF volume (V_{CSF}), Q_{bulk}, Q_{sink}, BBB surface area (S_{BBB}) and BCSFB surface area (S_{BCSFB}) were fixed and equal for all drugs, according to Ball et al. (V_b = 1.28 cm^3, V_{CSF} = 0.25 cm^3, Q_{bulk} = 0.012 cm^3/s, Q_{sink} = 0.132 cm^3/s, S_{BBB} = 187.5 cm^2) and Engelhard et al. (S_{BCSFB} = 0.0375 cm^2) [14,15].

$$V_d \cdot \frac{dC_p}{dt} = -PS_{BBBin} \cdot C_{u,p} + PS_{BBBout} \cdot C_{u,b} - PS_{BCSFBin} \cdot C_{u,p} + PS_{BCSFBout} \cdot C_{CSF} + Q_{sink} \cdot C_{CSF} - k_{el} \cdot C_p \cdot V_d \quad (4)$$

$$V_b \cdot \frac{dC_b}{dt} = PS_{BBBin} \cdot C_{u,p} - PS_{BBBout} \cdot C_{u,b} - Q_{bulk} \cdot C_{u,b} \quad (5)$$

$$V_{CSF} \cdot \frac{dC_{CSF}}{dt} = PS_{BCSFBin} \cdot C_{u,p} - PS_{BCSFBout} \cdot C_{CSF} - Q_{sink} \cdot C_{CSF} + Q_{bulk} \cdot C_{u,b} \quad (6)$$

Plasma and brain concentration profiles were obtained from the literature [16–20] for the six drugs studied. Depending on the publication, the brain concentration profiles derived were for free drug in the brain, total drug in the brain or drug in the ECF (which was considered equivalent to free drug in the brain). The type of data found does not affect the objective of this study, as both free and total drug concentrations are defined in the model.

When the drug administration was performed extravascularly, Equation 7 was added to the model, and Equation 4 was substituted by Equation 8, in which k_a is the absorption rate constant. On the other hand, if an intravenous infusion was the method of administration, Equation 4 was substituted by Equation 9, where k_0 is the infusion rate constant.

$$\frac{dA}{dt} = -k_a \cdot A \quad (7)$$

$$V_d \cdot \frac{dC_p}{dt} = k_a \cdot A - PS_{BBBin} \cdot C_{u,p} + PS_{BBBout} \cdot C_{u,b} - PS_{BCSFBin} \cdot C_{u,p} + PS_{BCSFBout} \cdot C_{CSF} + Q_{sink} \cdot C_{CSF} - k_{el} \cdot C_p \cdot V_d \quad (8)$$

$$V_d \cdot \frac{dC_p}{dt} = k_0 - PS_{BBBin} \cdot C_{u,p} + PS_{BBBout} \cdot C_{u,b} - PS_{BCSFBin} \cdot C_{u,p} + PS_{BCSFBout} \cdot C_{CSF} + Q_{sink} \cdot C_{CSF} - k_{el} \cdot C_p \cdot V_d \quad (9)$$

Then, the plasma and brain profiles were adjusted to the model with the Berkeley-Madonna® software (Berkeley, USA), assuming that three scaling factors were needed for

transforming the in vitro data obtained from cell cultures into in vivo information (Equation 10–14).

$$PS_{BBBin} = SC_1 \cdot P_{app\ A\to B} \cdot S_{BBB} \quad (10)$$

$$PS_{BCSFBin} = SC_1 \cdot P_{app\ A\to B} \cdot S_{BCSFB} \quad (11)$$

$$PS_{BBBout} = SC_2 \cdot P_{app\ B\to A} \cdot S_{BBB} \quad (12)$$

$$PS_{BCSFBout} = SC_2 \cdot P_{app\ B\to A} \cdot S_{BCSFB} \quad (13)$$

$$C_{u,b} = SC_3 \cdot f_{u,brain} \cdot C_b \quad (14)$$

Most mathematical predictive models use scaling factors to transform the in vitro data/parameters into in vivo data due to the different characteristics between the in vitro cells/tissues used and the whole organism; for example, physiological characteristics, such as the surface area available for transport. Therefore, every in vitro parameter used in the model needs to have a scaling factor [21,22]. The first and second scaling factors (SC1 and SC2) were used to adjust the in vitro apparent permeabilities to the physiological permeability, as in [14], because of the differences in terms of surface area and transporters between the in vitro tests and rat physiology. Moreover, the third scaling factor (SC3) was used to correct the possible deviation present in the in vitro $f_{u,brain}$ values, due to the different composition and behavior of the pig brain homogenate and a healthy rat brain. The use of scaling factors allows researchers to obtain an empiric approximation of how a drug accesses the brain. Later on, a refined mechanistic model may be obtained by including both passive and active transport parameters in the differential equations and the expression level differences between the in vitro and in vivo situation.

Table 1 shows the values of the rest of the PK parameters, which were used in the model and were different for each drug. Due to the difficulties of obtaining research articles with all the PK information for rats, in some cases, parameters had to be calculated from human data. The V_d of drugs marked with a + symbol (Table 1) was calculated using the human value (L/kg), and then multiplying it by the weight of the rats used in the studies (from which the plasma and brain profiles were obtained). The rats' weights varied between 250 and 300 g.

Table 1. PK parameters which were different for each drug.

Drug	$f_{u,plasma}$	V_d (cm³)*	k_{el} (s⁻¹)*	k_a (s⁻¹)*	D (ng)	k_0 (ng/s)	Rat weight (g)
Amitriptyline	0.090 [a]	4000 [c,+]	$7.70\cdot10^{-5}$ [h]	$1.54\cdot10^{-4}$ [#]	5,000,000 [h]		250 [h]
Caffeine	0.917 [b]	180 [c,+]	$3.55\cdot10^{-5}$ [i,$]			833.333 [i]	300 [i]
Carbamazepine	0.385 [b]	1490.5 [d]	$4.50\cdot10^{-5}$ [j]	$8.99\cdot10^{-5}$ [#]	3,600,000 [j]		300 [j]
Fleroxacin	0.793 [b]	427.5 [e,+]	$7.13\cdot10^{-5}$ [k]		1,114,350 [l]	83.125 [l]	285 [l]
Pefloxacin	0.860 [b]	361.1 [f,+]	$5.83\cdot10^{-5}$ [k]		3,676,500 [l]	214.542 [l]	285 [l]
Zolpidem	0.267 [b]	304 [g]	$1.56\cdot10^{-4}$ [g]		499,700 [g]		190 [g]

* indicates that the parameter was later adjusted; + indicates that the V_d from the reference was from human data, so it was recalculated for rat; $ this initial estimate corresponds to the α constant rate from the reference; # k_a initial estimates were calculated as double the k_{el} initial estimates; [a][23], [b][24], [c][25], [d][26], [e][27], [f][28], [g][20], [h][16], [i][17], [j][18], [k][29], [l][19].

2.5. Quantitative Structure–Property Relationships (QSPRs)

Once all the profiles were adjusted and the three scaling factors were defined for each drug, they were related with their lipophilicity in order to obtain three different QSPRs for each cell line. We are aware that the scaling factors could be influenced by several physicochemical properties, such as lipophilicity, molecular weight, polar surface area, *pKa*, etc.; nevertheless, the reduced number of compounds precluded the evaluation of complex models. As lipophilicity seems to be the main factor affecting membrane permeation, we selected this parameter to explore its influence. Table S2 shows the molecular and physicochemical properties of the six drugs studied, as well as the transporters for which they are substrates.

Finally, an internal validation of the model was performed to evaluate its predictability in the different cell lines. So, the adjusted scaling factors were substituted in the model by the ones predicted from the QSPRs, and the prediction error percentages (PE%) for brain C_{max} and brain AUC were calculated according to Equation 15.

$$PE\% = \left|\frac{Experimental\ value - Predicted\ value}{Experimental\ value}\right| \cdot 100 \quad (15)$$

3. Results

Apparent permeability values and the $f_{u,brain}$ obtained from the in vitro tests with MDCK, MDCK-MDR1 and hCMEC cell lines are summarized in Table 2. These values were used later as fixed parameters in the model for obtaining the simulated plasma and brain profiles (Figure 2).

Table 2. Apparent permeability values and the $f_{u,brain}$ obtained from the in vitro tests with MDCK, MDCK-MDR1 and hCMEC cell lines.

Drug	MDCK cell line			MDCK-MDR1 cell line			hCMEC cell line		
	$P_{app\ A\to B}$ ($\times10^{-6}$ cm/s)	$P_{app\ B\to A}$ ($\times10^{-6}$ cm/s)	$f_{u,brain}$	$P_{app\ A\to B}$ ($\times10^{-6}$ cm/s)	$P_{app\ B\to A}$ ($\times10^{-6}$ cm/s)	$f_{u,brain}$	$P_{app\ A\to B}$ ($\times10^{-6}$ cm/s)	$P_{app\ B\to A}$ ($\times10^{-6}$ cm/s)	$f_{u,brain}$
Amitriptyline	74.77 [a]	178.48 [a]	0.037 [a]	17.95 [a]	16.91 [a]	0.104 [a]	124.24 [b]	66.21 [b]	0.252 [b]
Caffeine	26.10	35.31	0.857	33.57	30.59	0.613	63.93	194.70	0.095
Carbamazepine	114.64	78.66	0.673	142.96	75.64	0.238	70.14 [b]	51.93 [b]	0.386 [b]
Fleroxacin	88.48	63.44	0.471	67.40	42.57	0.813	29.96 [b]	25.73 [b]	0.743 [b]
Pefloxacin	41.21	37.49	0.910	30.82	35.39	0.931	24.95 [b]	33.14 [b]	0.642 [b]
Zolpidem	21.32	36.48	0.971	8.92	33.43	0.881	106.16 [b]	80.76 [b]	0.408 [b]

[a] Data already published in [11]. [b] Data already published in [12].

As seen in Figure 2, the model is able to describe the behavior of the six model drugs, in terms of both plasma and brain concentration profiles, after adjusting the initial V_d, k_a, k_{el} and the scaling factors (SC1, SC2 and SC3), which were defined initially as one. Table 3 shows the values of the parameters mentioned above after being fitted for the different drugs and cell lines.

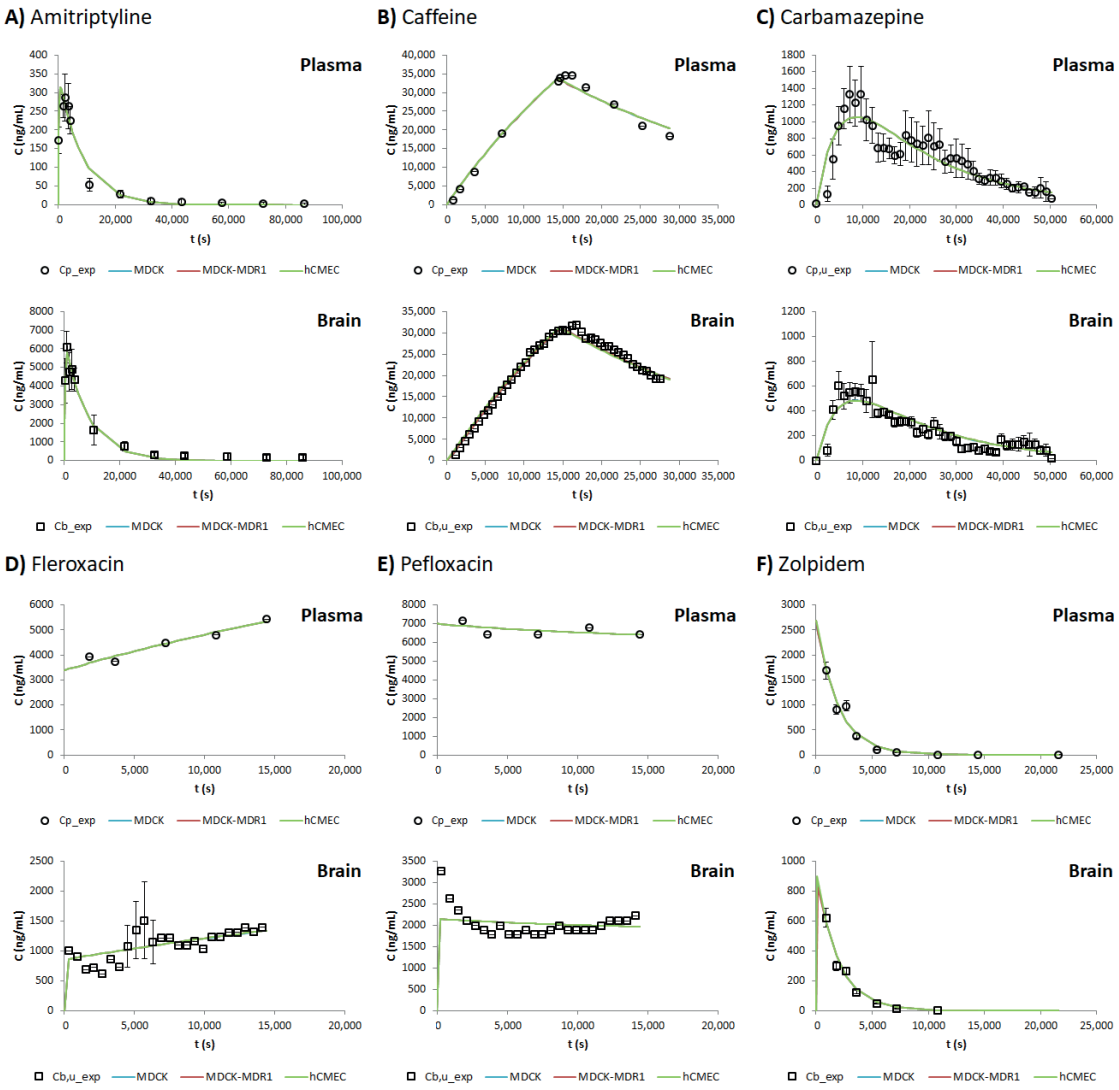

Figure 2. Experimental and fitted plasma and brain profiles for each drug and cell line studied: **2A.** Amitriptyline, **2B.** Caffeine, **2C.** Carbamazepine, **2D.** Fleroxacin, **2E.** Pefloxacin and **2F.** Zolpidem. *Cp_exp* = Experimental total plasma concentration; *Cp,u_exp* = Experimental unbound plasma concentration; *Cb_exp* = Experimental total brain concentration; *Cb,u_exp* = Experimental unbound brain concentration.

Table 3. PK parameters (V_d, k_a, k_{el}) and scaling factors (SC1, SC2 and SC3) for each drug and cell line after being adjusted.

Drug	V_d (cm^3)	k_{el} (s^{-1})	k_a (s^{-1})	MDCK Cell Line			MDCK-MDR1 Cell Line			hCMEC Cell Line		
				SC1	**SC2**	**SC3**	**SC1**	**SC2**	**SC3**	**SC1**	**SC2**	**SC3**
Amitriptyline	14,632.6	$1.17 \cdot 10^{-4}$	$5.86 \cdot 10^{-3}$	220.59	224.82	0.05	920.39	2377.06	0.02	132.89	606.69	0.01
Caffeine	273.6	$3.55 \cdot 10^{-5}$		3.85	1.00	0.22	2.85	1.00	0.31	4.09	1.00	2.15
Carbamazepine	827.0	$5.39 \cdot 10^{-5}$	$2.15 \cdot 10^{-4}$	25.71	81.01	1.16	95.00	391.22	0.71	193.66	569.98	0.44
Fleroxacin	327.3	$2.69 \cdot 10^{-5}$		3.18	12.96	1.07	1.59	6.43	0.68	3.58	10.65	0.74
Pefloxacin	524.3	$6.75 \cdot 10^{-5}$		4.88	13.32	0.55	6.15	13.19	0.56	7.59	14.09	0.81
Zolpidem	185.9	$5.12 \cdot 10^{-4}$		16.53	26.79	0.27	20.59	14.51	0.30	10.26	38.70	0.65

With the aim of seeing how accurate the adjustment was, the initial PE% values were calculated. The first row of Table 4 shows the mean PE% for brain C_{max} and brain the AUC for each cell line; due to the similarity of all the values, it can be seen that the model adjusts properly to all the cell lines.

Figure 3 shows the three QSPRs developed for each cell line after combining the logP of each drug with the natural logarithm of each scaling factor (LnSC).

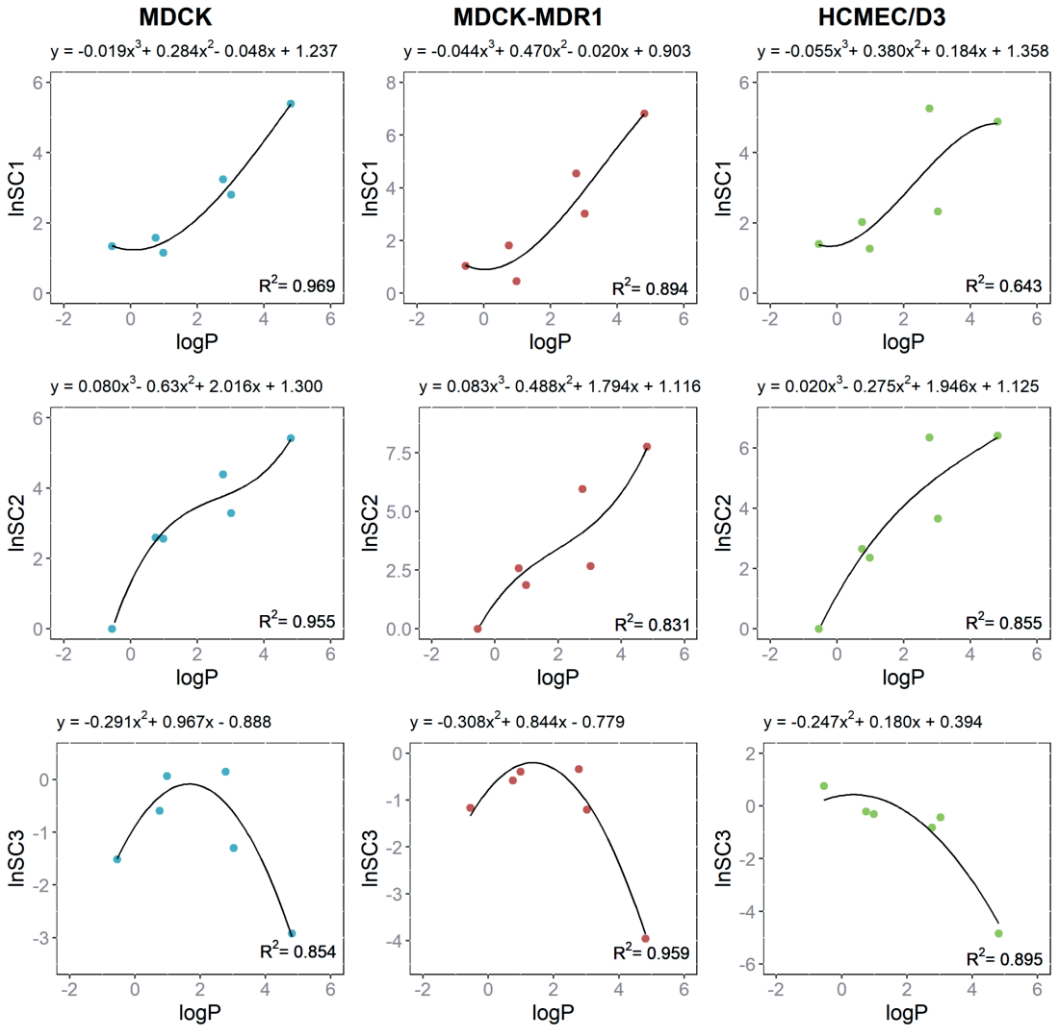

Figure 3. QSPRs developed for each cell line after combining the logP of each drug with the natural logarithm of each scaling factor (LnSC1, LnSC2, LnSC3): **3A.** MDCK cell line, **3B.** MDCK-MDR1 cell line and **3C.** hCMEC/D3 cell line.

When the internal validation of the model was complete, the equations of each QSPR were used to calculate the predicted LnSC, which were transformed into SC and substituted into the model to obtain the simulated profiles. Figure 4 shows the simulated brain profiles and visual predictive checks for each drug after using the QSPR equations, and in the second row of Table 4, the PE% values for the C_{max} and the AUC for these brain predictions are summarized.

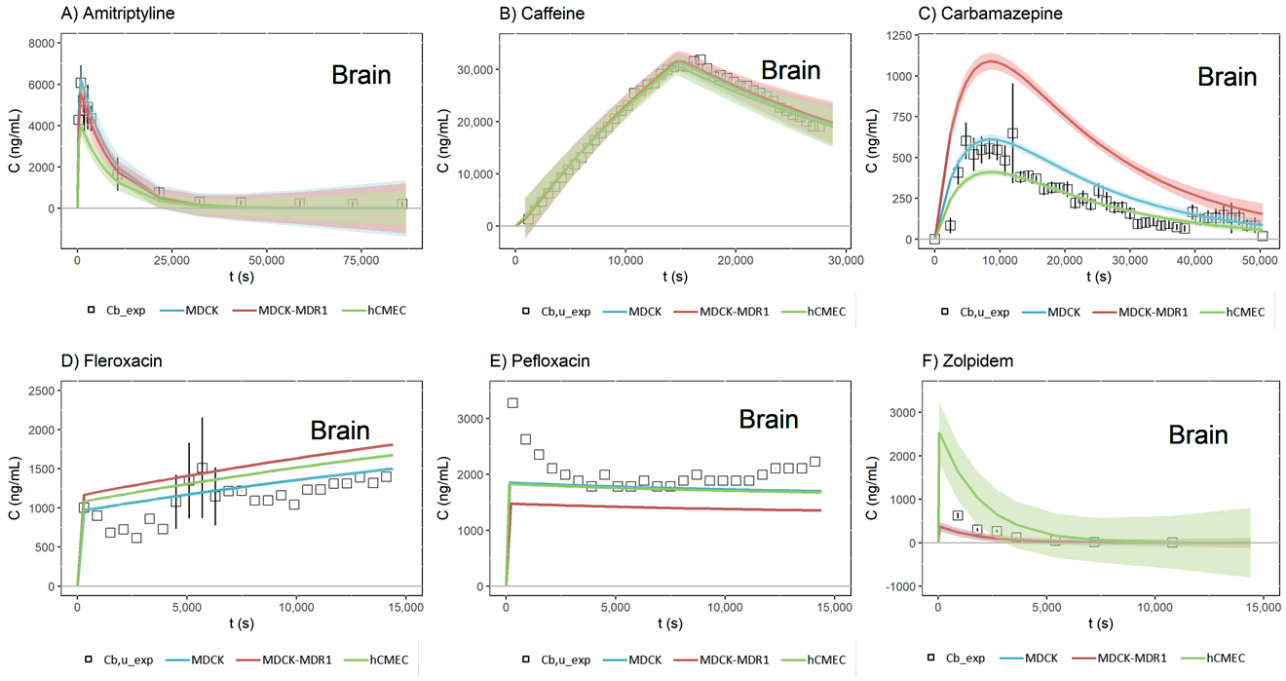

Figure 4. Simulated brain profiles and visual predictive check (VPC, shaded areas above and below fitted lines) for each drug and cell line, after using the QSPR equations: **4A.** Amitriptyline, **4B.** Caffeine, **4C.** Carbamazepine, **4D.** Fleroxacin, **4E.** Pefloxacin and **4F.** Zolpidem. *Cb_exp* = Experimental total brain concentration; *Cb,u_exp* = Experimental unbound brain concentration.

Table 4. The mean brain C_{max} and AUC PE% for each cell line after fitting the model and after obtaining the simulated profiles using the QSPR equation.

Profile	MDCK Cell Line		MDCK-MDR1 Cell Line		hCMEC Cell Line	
	%PE C_{max}	%PE AUC	%PE C_{max}	%PE AUC	%PE C_{max}	%PE AUC
Fitted	14.34	5.28	15.05	5.45	13.56	5.16
Simulated	19.23	22.34	35.71	48.21	49.77	46.69

%PE = prediction error percentages, C_{max} = maximum concentration, AUC = area under the curve.

Although all the PE% values were increased from the fitted profiles to the simulated ones, all of them remained below 50%, which can be considered appropriate due to the complexity of the model, which mixes in silico, in vitro and in vivo data for obtaining brain profiles. Furthermore, a clear tendency can be seen when both the PE% values of each cell line are added: as the complexity of the cell line increases, the error increases, which could be explained by the influence that transporters have on the SC of the drugs that are substrates of them, and not on the passive drugs.

4. Discussion

The development of new in vitro and mathematical tools able to predict concentration levels of drugs in humans is extremely interesting for pharmaceutical industries, as they can help avoid failures after huge investments of money, and they can also bypass ethical problems. With this aim, over many years, several researchers have worked on the development of new in vitro dissolution tools or in vitro–in vivo correlations in the field of oral absorption, and biowaivers have been highly legislated [30–33]. In terms of CNS medicine, although it is less regulated, the development of new PBPK models has become even more important, due to the difficulties in obtaining new treatments able to cross the BBB. The major problem, however, in obtaining this type of neuroPK tool is the lack of human in vivo data to compare with, as obtaining brain profiles is not as simple as obtaining plasma ones. So, in this work, a new PBPK model was developed as an initial tool to predict the brain levels of drugs in rats.

Table 2 shows the values of the apparent permeabilities ($P_{app\ A\rightarrow B}$ and $P_{app\ B\rightarrow A}$) and the $f_{u,brain}$ obtained with the MDCK, the MDCK-MDR1 and the hCMEC/D3 cell lines. $P_{app\ A\rightarrow B}$ corresponds to the Cl_{in} of the drug through the BBB. With the combination of $P_{app\ A\rightarrow B}$ and $P_{app\ B\rightarrow A}$, the $Kp_{uu,brain}$ can be obtained, and using Equation 2, the in vitro $f_{u,brain}$ parameter can be translated to $V_{u,brain}$. As such, the three most important neuroPK parameters (Cl_{in}, $Kp_{uu,brain}$ and $V_{u,brain}$) used to describe the rate and extent of drug delivery to the brain can be obtained with the same methodology, a fact that has already been highlighted in [11] and [12], investigations in which it was proven that the in vivo neuroPK parameters could be predicted from the in vitro ones. In 2013, the methodology was established in MDCK and MDCK-MDR1, cell lines and in 2021 the predictions were compared with the ones obtained in hCMEC/D3 using the same methodology; in all cases, an adequate r^2 was obtained [11,12]. The $P_{app\ A\rightarrow B}$, $P_{app\ B\rightarrow A}$ and $f_{u,brain}$ values in Table 2 are variable from one cell line to the other, which could be due to the morphological and physiological differences between them, in terms of both tight junctions and transporters [34–36].

For obtaining an ideal in vitro BBB model, an environment reflecting the extracellular matrix and the cells surrounding the endothelial cells that constitute the BBB vessels should be simulated. Nonetheless, this environment has not yet been obtained, and cell monolayers lack of pericytes, astrocytes, neurons or different constituents of the neuroglia vascular unit (NGVU). Because of this, in vitro models can express some of the different transporters present in the BBB, but not all. Furthermore, depending on the cell type, in vitro models can express more or less tight junctions, avoiding the passage of

drugs through the BBB [37]. The main advantage of cell monolayers is their utility for high-throughput screening [38].

The variability in the in vitro parameters is also reflected when the profiles are fitted with Berkeley-Madonna® and the three scaling factors are obtained for each cell line, as seen in Table 3. The use of scaling factors when establishing a PBPK model of the CNS was previously seen in other studies, as in [14]. Ball et al. defined two scaling factors for transforming in vitro Caco-2 permeability values into the influx and efflux BBB rate constants [14]. In this work, three different scaling factors were defined:

- SC1 and SC2 were equivalent to those defined by Ball et al., as they transform the apparent permeabilities of the MDCK, MDCK-MDR1 and hCMEC/D3 cell lines into influx and efflux clearances through the BBB. The main justification for introducing these scaling factors is the difference between the rat BBB and the in vitro monolayers. For instance, in terms of tight junctions, it has been proven that primary rat brain endothelial cell cultures have high levels of occludin, endothelial cell-specific adhesion molecule (ESAM) and claudin-5, while in MDCK and MDCK-MDR1 cells, the most abundant proteins are claudin-1 and claudin-2, and in hCMEC/D3, claudin-11 [34]. Furthermore, there are differences in the morphology of the different cell lines and in transporter expressions [34];
- The reasons for adding SC3, which re-scale the in vitro $f_{u,brain}$, were, on the one hand, to bypass the inter-species differences, as the brain homogenate used in the in vitro studies came from pigs and the model was to be used to predict rat brain profiles, and, on the other hand, to correct the possible error present in the parameter due to the homogenization process, as brain structures are broken and membrane and internal proteins get mixed.

These scaling factors have been shown to allow the model to fit to the profiles regardless of the origin of the in vitro data, as seen in Figure 2, where the MDCK, MDCK-MDR1 and hCMEC/D3 cell lines are all overlapping in both plasma and brain profiles. Nevertheless, these scaling factors are not useful if they cannot be known in advance when a new drug is developed, because the brain profiles could not be predicted with the current model. Because of this, three different QSPRs were developed for each cell line (Figure 3), relating the lipophilicity of the drugs to the natural logarithm of the scaling factors; thus, in the future, the scaling factors for a new drug could be predicted from its logP.

In Figure 3, two clear non-linear tendencies can be seen: for SC1 and SC2, as the lipophilicity of drugs increases, the value of the scaling factors increases too; for SC3, the relationship follows a parabolic function, and, firstly, the value of the scaling factor increases with logP, but then it arrives to a top zone, and then it decreases.

Sigmoidal and parabolic relationships with lipophilicity have been described for parameters such as intestinal and gastric membrane permeability [39–41]. In the case of the intestinal barrier, its lipidic nature favors the permeation of lipidic compounds up to the limit, due to unstirred water layer diffusion. We have not observed any asymptote in our correlations, but this could be due to the moderate lipophilicity of the assayed drugs. In the case of the gastric barrier, the combined alternate presence of hydrophilic and lipophilic layers determines a parabolic correlation between lipophilicity and gastric permeation. As SC3 is related to the differences in composition of the used brain homogenates, which contain different balances of hydrophilic/lipophilic components, a parabolic relationship is a reasonable approach.

In all cases, the tendency is clear and, except for one of the QSPRs (the one for the SC1 in the hCMEC/D3 cell line), the r^2 of all of them is greater than 0.80. logP was chosen as the property to relate to the scaling factors because it is one of the major descriptors used by researchers for both calculating BBB permeability [10,42] and obtaining a theoretical unbound fraction of the drug in plasma or brain [42,43].

However, to conclude on whether a given mathematical model is good enough to fulfil its design, it is not enough to look at the r^2 parameter of its correlations, but it is necessary to evaluate its predictability by internal validation, comparing the predictions that the model gives with the experimental data that were used for obtaining it. Figure 4 shows, therefore, the simulated brain profiles for the drug studied. In this Figure, it can be seen that there are differences in the predictions between the different cell lines; in fact, when the fitted profiles were presented (Figure 2), all the MDCK, MDCK-MDR1 and hCMEC/D3 profiles were shown to be overlapping, but now, in some cases, they are quite different. Regarding the MDCK cell line, it can be seen that the simulated profiles are, in all drugs, near to the experimental line; meanwhile, the worst prediction for the MDCK-MDR1 cells is found to be that for carbamazepine, a drug substrate of the ABCC2 and RALBP1 transporters [25], and in the case of hCMEC/D3, the zolpidem (passively transported [25]) profile is clearly overpredicted. These clear prediction errors in Figure 4, whose quantitative values (from Equation 15) are shown in Table 4, confirm that the

simulated profiles are worse than the fitted ones, and the best profiles are the ones obtained with the MDCK cell line.

The MDCK cell line is a fairly simple model of BBB, defined as a surrogate for in vivo permeability studies because of its tight junctions, but it does not have significant levels of any BBB transporter [6]. Because of this, some transfected cell lines of MDCK have been created, such as the MDCK-MDR1, which has the benefits of MDCK's tight junctions, but incorporates the P-glycoprotein (ABCB1) efflux transporter, or the MDCK-MRP2 cell line, which incorporates the multidrug resistance-associated protein 2 transporter (ABCC2) [44]. On the other hand, hCMEC/D3 cells are much more complex, and, despite being less tight in vitro, they contain many more transporters [34,45]. As such, it is thought that they are the most reliable for obtaining brain profile predictions. However, in this study, it was seen that, as the complexity of the cell line was increased, the predictions deteriorated (Table 4). A potential explanation for this fact is that the proposed PBPK model does not include any active transporter in its differential equations, so all the active components of BBB penetration are summarized in the in vitro parameters employed ($P_{app\ A\rightarrow B}$, $P_{app\ B\rightarrow A}$ and $f_{u,brain}$), and thus in the three scaling factors. The model would be more physiological if the active components were included in the equations, but the passive pathway with a scaling factor was assumed as a simplification, because only one concentration of each drug was tested, and for modeling the active transport, at least three concentrations of each drug must be studied [21]. Thus, with the scaling factor, an over-parameterization of the model was avoided. Different types of drugs were used in this study (Table S2); some of them with theoretical passive access to the BBB and others of different transporters. In consequence, when the MDCK cell line is used, as it has no transporters, all the scaling factors contain only a passive component. On the other hand, in the other two cell models, the scaling factors vary depending on their transport; the passive drugs will only have these components in their SCs, while the drugs that interact with a transporter will have both the passive and active components in their SCs. Furthermore, the active component of the SC will be different depending on the transporter, so in the hCMEC/D3 cell line, in which there are more transporters, the variability will be greater than in MDCK-MDR1, where the only significant transporter is the P-gp.

In summary, in this study, a new PBPK model, which is able to predict the brain profiles of different types of drugs (both passive and substrate of transporters), has been developed for the cell line MDCK. For obtaining a predictive model for the other two cell

lines, two future approaches could be followed: A) introducing the active component of BBB transport into the model or B) studying more drugs and dividing them into groups depending on the transporter that they bind to, so a different QSPR could be obtained for each transporter acting in the BBB, and its active component would be summarized in each SC.

5. Conclusions

A new semi-physiological mathematical model, which includes the three most important factors in brain delivery (barrier transport, the disposition within the brain and drug–brain binding) and is able to predict brain concentration levels in rats for different drugs, has been developed. The best predictions obtained are those that used in vitro data from the MDCK cell line, so these cells together with the new mathematical model could be used as a screening tool by the pharmaceutical industry when a new treatment for a neurological disorder is developed. The model could also be used with data from other more complex cell lines, such as MDCK-MDR1 or hCMEC/D3, although it has been proven that the influence of transporters can bias their predictions. Additional studies are needed, with drug batteries of different transporter substrates, in order to refine these results.

Supplementary Materials: The following are available online at www.mdpi.com/1999-4923/13/9/1402/s1, Table S1: Chromatographic conditions. Table S2: Molecular and physicochemical properties and transporter information for the studied drugs.

Author Contributions: Conceptualization, M.B. and M.G.-A.; methodology, B.S.-D. and I.G.-A.; software, B.S.-D.; validation, B.S.-D., M.B., M.G.-A. and I.G.-A.; formal analysis, B.S.-D.; investigation, B.S.-D. and I.G.-A.; resources, M.B.; data curation, I.G.-A.; writing—original draft preparation, B.S.-D.; writing—review and editing, M.B., M.G.-A. and I.G.-A.; visualization, B.S.-D.; supervision, M.B., M.G.-A. and I.G.-A.; project administration, I.G.-A.; funding acquisition, M.B. All authors have read and agreed to the published version of the manuscript.

Funding: This research was funded by Agencia Estatal Investigación and European Union, through FEDER (Fondo Europeo de Desarrollo Regional), under the project: “Modelos in vitro de evaluación biofarmacéutica” [SAF2016-78756 (AEI/FEDER, EU)]. B.S.-D. received a grant from the Ministry of Science, Innovation and Universities of Spain [FPU17/00530] and an international mobility grant from Miguel Hernandez University [0762/19].

Institutional Review Board Statement: Not applicable.

Informed Consent Statement: Not applicable.

Data Availability Statement: The authors confirm that the data supporting the findings of this study are available within the article and its supplementary material.

Conflicts of Interest: The authors declare no conflict of interest. The funders had no role in the design of the study; in the collection, analyses, or interpretation of data; in the writing of the manuscript, or in the decision to publish the results.

References

1. Telano, L.N.; Baker, S. *Physiology, Cerebral Spinal Fluid (CSF)*; StatPearls Publishing,: Treasure Island, FL, United States of America, 2018.
2. Vendel, E.; Rottschäfer, V.; de Lange, E.C.M. The need for mathematical modelling of spatial drug distribution within the brain. *Fluids Barriers CNS* **2019**, *16*, 12, doi:10.1186/s12987-019-0133-x.
3. Abbot, N.J.; Patabendige, A.A.K.; Dolman, D.E.M.; Yusof, S.R.; Begley, D.J. Structure and function of the blood-brain barrier. *Neurobiol. Dis.* **2010**, *37*, 13–25, doi:10.1016/j.nbd.2009.07.030.
4. Sánchez-Dengra, B.; González-Álvarez, I.; Bermejo, M.; González-Álvarez, M. Nanomedicine in the Treatment of Pathologies of the Central Nervous System Advances in Nanomedicine. In *Advances in Nanomedicine*; Open Access Ebooks: Las Vegas, USA, 2020.
5. Hammarlund-Udenaes, M.; Fridén, M.; Syvänen, S.; Gupta, A. On the rate and extent of drug delivery to the brain. *Pharm. Res.* **2008**, *25*, 1737–1750, doi:10.1007/s11095-007-9502-2.
6. Mangas-Sanjuan, V.; González-Alvarez, M.; Gonzalez-Alvarez, I.; Bermejo, M. Drug penetration across the blood-brain barrier: An overview. *Ther. Deliv.* **2010**, *1*, 535–562, doi:10.4155/tde.10.37.
7. Dagenais, C.; Graff, C.L.; Pollack, G.M. Variable modulation of opioid brain uptake by P-glycoprotein in mice. *Biochem. Pharmacol.* **2004**, *67*, 269–276, doi:10.1016/j.bcp.2003.08.027.
8. Loryan, I.; Sinha, V.; Mackie, C.; Van Peer, A.; Drinkenburg, W.; Vermeulen, A.; Morrison, D.; Monshouwer, M.; Heald, D.; Hammarlund-Udenaes, M. Mechanistic understanding of brain drug disposition to optimize the selection of potential neurotherapeutics in drug discovery. *Pharm. Res.* **2014**, *31*, 2203–2219, doi:10.1007/s11095-014-1319-1.
9. Carpenter, T.S.; Kirshner, D.A.; Lau, E.Y.; Wong, S.E.; Nilmeier, J.P.; Lightstone, F.C. A Method to Predict Blood-Brain Barrier Permeability of Drug-Like Compounds Using Molecular Dynamics Simulations. *Biophys. J.* **2014**, *107*, 630–641, doi:10.1016/j.bpj.2014.06.024.
10. Geldenhuys, W.J.; Mohammad, A.S.; Adkins, C.E.; Lockman, P.R. Molecular determinants of blood-brain barrier permeation. *Ther. Deliv.* **2015**, *6*, 961–971, doi:10.4155/tde.15.32.
11. Mangas-Sanjuan, V.; González-Álvarez, I.; González-Álvarez, M.; Casabó, V.G.; Bermejo, M. Innovative in vitro method to predict rate and extent of drug delivery to the brain across the blood-brain barrier. *Mol. Pharm.* **2013**, *10*, 3822–3831, doi:10.1021/mp400294x.
12. Sánchez-Dengra, B.; González-Álvarez, I.; Sousa, F.; Bermejo, M.; González-Álvarez, M.; Sarmento, B. In vitro model for predicting the access and distribution of drugs in the brain using hCMEC/D3 cells. *Eur. J. Pharm. Biopharm.* **2021**, *163*, 120–126, doi:10.1016/j.ejpb.2021.04.002.

13. Mangas-Sanjuan, V.; Gonzalez-Alvarez, M.; Gonzalez-Alvarez, I.; Bermejo, M. In vitro methods for assessing drug access to the brain. In *Advances in Non-Invasive Drug Delivery to the Brain*; Future Science Ltd.: Marshall University, USA, 2015; pp. 44–61; ISBN 9781909453937.
14. Ball, K.; Bouzom, F.; Scherrmann, J.M.; Walther, B.; Declèves, X. A physiologically based modeling strategy during preclinical CNS drug development. *Mol. Pharm.* **2014**, *11*, 836–848, doi:10.1021/mp400533q.
15. Engelhard, H.H.; Arnone, G.D.; Mehta, A.I.; Nicholas, M.K. Biology of the Blood-Brain and Blood-Brain Tumor Barriers. In *Handbook of Brain Tumor Chemotherapy, Molecular Therapeutics, and Immunotherapy: Second Edition*; Elsevier Inc.: Amsterdam, The Netherlands, 2018; pp. 113–125 ISBN 9780128121009.
16. Coudore, F.; Besson, A.; Eschalier, A.; Lavarenne, J.; Fialip, J. Plasma and brain pharmacokinetics of amitriptyline and its demethylated and hydroxylated metabolites after one and six half-life repeated administrations to rats. *Gen. Pharmacol.* **1996**, *27*, 215–219, doi:10.1016/0306-3623(95)02008-x.
17. Hansen, D.K.; Scott, D.O.; Otis, K.W.; Lunte, S.M. Comparison of in vitro BBMEC permeability and in vivo CNS uptake by microdialysis sampling. *J. Pharm. Biomed. Anal.* **2002**, *27*, 945–958, doi:10.1016/s0731-7085(01)00542-8.
18. Graumlich, J.F.; McLaughlin, R.G.; Birkhahn, D.; Shah, N.; Burk, A.; Jobe, P.C.; Dailey, J.W. Subcutaneous microdialysis in rats correlates with carbamazepine concentrations in plasma and brain. *Epilepsy Res.* **2000**, *40*, 25–32, doi:10.1016/s0920-1211(00)00110-8.
19. Ooie, T.; Terasaki, T.; Suzuki, H.; Sugiyama, Y. Quantitative brain microdialysis study on the mechanism of quinolones distribution in the central nervous system. *Drug Metab. Dispos.* **1997**, *25*, 784–789.
20. Garrigou-Gadenne, D.; Burke, J.T.; Durand, A.; Depoortere, H.; Thénot, J.P.; Morselli, P.L. Pharmacokinetics, brain distribution and pharmaco-electrocorticographic profile of zolpidem, a new hypnotic, in the rat. *J. Pharmacol. Exp. Ther.* **1989**, *248*, 1283–1288.
21. González-Alvarez, I.; Fernández-Teruel, C.; Casabó-Alós, V.G.; Garrigues, T.M.; Polli, J.E.; Ruiz-García, A.; Bermejo, M. In situ kinetic modelling of intestinal efflux in rats: Functional characterization of segmental differences and correlatlon with in vitro results. *Biopharm. Drug Dispos.* **2007**, *28*, 229–239, doi:10.1002/bdd.548.
22. Fernandez-Teruel, C.; Gonzalez-Alvarez, I.; Casabó, V.; Ruiz-Garcia, A.; Bermejo, B. Kinetic modelling of the intestinal transport of sarafloxacin. Studies in situ in rat and in vitro in Caco-2 cells. *J. Drug Target.* **2005**, *13*, 199–212, doi:10.1080/10611860500087835.
23. Fridén, M.; Gupta, A.; Antonsson, M.; Bredberg, U.; Hammarlund-Udenaes, M. In vitro methods for estimating unbound drug concentrations in the brain interstitial and intracellular fluids. *Drug Metab. Dispos.* **2007**, *35*, 1711–1719, doi:10.1124/dmd.107.015222.
24. Kodaira, H.; Kusuhara, H.; Fujita, T.; Ushiki, J.; Fuse, E.; Sugiyama, Y. Quantitative evaluation of the impact of active efflux by P-glycoprotein and breast cancer resistance protein at the

blood-brain barrier on the predictability of the unbound concentrations of drugs in the brain using cerebrospinal fluid concentration as a. *J. Pharmacol. Exp. Ther.* **2011**, *339*, 935–944, doi:10.1124/jpet.111.180398.

25. DrugBank DrugBank. Available online: https://www.drugbank.ca/ (accessed on 14 May 2020).
26. Remmel, R.P.; Sinz, M.W.; Cloyd, J.C. Dose-Dependent Pharmacokinetics of Carbamazepine in Rats: Determination of the Formation Clearance of Carbamazepine-10,11-epoxide. *Pharm. Res. An Off. J. Am. Assoc. Pharm. Sci.* **1990**, *7*, 513–517, doi:10.1023/A:1015872901523.
27. Weidekamm, E.; Portmann, R.; Suter, K.; Partos, C.; Dell, D.; Lucker, P.W. Single- and multiple-dose pharmacokinetics of fleroxacin, a trifluorinated quinolone, in humans. *Antimicrob. Agents Chemother.* **1987**, *31*, 1909–1914, doi:10.1128/AAC.31.12.1909.
28. Bulitta, J.B.; Jiao, Y.; Landersdorfer, C.B.; Sutaria, D.S.; Tao, X.; Shin, E.; Höhl, R.; Holzgrabe, U.; Stephan, U.; Sörgel, F. Comparable bioavailability and disposition of pefloxacin in patients with cystic fibrosis and healthy volunteers assessed via population pharmacokinetics. *Pharmaceutics* **2019**, *11*, doi:10.3390/pharmaceutics11070323.
29. Chartrand, S.A. Quinolones in Animal Models of Infection. In *The New Generation of Quinolones*; Siporin, C., Heifetz, C., Domagala, J., Eds.; Marcel Dekker: New York, NY, USA, 1990; ISBN 0-8247-8224-0.
30. Bransford, P.; Cook, J.; Gupta, M.; Haertter, S.; He, H.; Ju, R.; Kanodia, J.; Lennernäs, H.; Lindley, D.; Polli, J.E.; et al. ICH M9 Guideline in Development on Biopharmaceutics Classification System-Based Biowaivers: An Industrial Perspective from the IQ Consortium. *Mol. Pharm.* **2020**, *17*, 361–372, doi:10.1021/acs.molpharmaceut.9b01062.
31. EMA-Committee for Medicinal Products for Human Use (CHMP). *Guideline on the Pharmacokinetic and Clinical Evaluation of Modified Release Dosage Forms (EMA/CPMP/EWP/280/96 Corr1)*; European Medicines Agency: London, United Kingdom, 2014.
32. Ruiz Picazo, A.; Martinez-Martinez, M.T.; Colón-Useche, S.; Iriarte, R.; Sánchez-Dengra, B.; González-Álvarez, M.; García-Arieta, A.; González-Álvarez, I.; Bermejo, M. In Vitro Dissolution as a Tool for Formulation Selection: Telmisartan Two-Step IVIVC. *Mol. Pharm.* **2018**, *15*, 2307–2315, doi:10.1021/acs.molpharmaceut.8b00153.
33. Figueroa-Campos, A.; Sánchez-Dengra, B.; Merino, V.; Dahan, A.; González-Álvarez, I.; García-Arieta, A.; González-Álvarez, M.; Bermejo, M. Candesartan Cilexetil In Vitro-In Vivo Correlation: Predictive Dissolution as a Development Tool. *Pharmaceutics* **2020**, *12*, 633, doi:10.3390/pharmaceutics12070633.
34. Veszelka, S.; Tóth, A.; Walter, F.R.; Tóth, A.E.; Gróf, I.; Mészáros, M.; Bocsik, A.; Hellinger, É.; Vastag, M.; Rákhely, G.; et al. Comparison of a rat primary cell-based blood-brain barrier model with epithelial and brain endothelial cell lines: Gene expression and drug transport. *Front. Mol. Neurosci.* **2018**, *11*, doi:10.3389/fnmol.2018.00166.

35. Weksler, B.; Romero, I.A.; Couraud, P.O. The hCMEC/D3 cell line as a model of the human blood brain barrier. *Fluids Barriers CNS* **2013**, *10*, doi:10.1186/2045-8118-10-16.
36. Garberg, P.; Ball, M.; Borg, N.; Cecchelli, R.; Fenart, L.; Hurst, R.D.; Lindmark, T.; Mabondzo, A.; Nilsson, J.E.; Raub, T.J.; et al. In vitro models for the blood-brain barrier. *Toxicol. Vitr.* **2005**, *19*, 299–334, doi:10.1016/j.tiv.2004.06.011.
37. Molino, Y.; Jabès, F.; Lacassagne, E.; Gaudin, N.; Khrestchatisky, M. Setting-up an In Vitro Model of Rat Blood-brain Barrier (BBB): A Focus on BBB Impermeability and Receptor-mediated Transport. *J. Vis. Exp.* **2014**, *88*, 51278, doi:10.3791/51278.
38. Bagchi, S.; Chhibber, T.; Lahooti, B.; Verma, A.; Borse, V.; Jayant, R.D. In-vitro blood-brain barrier models for drug screening and permeation studies: An overview. *Drug Des. Devel. Ther.* **2019**, *13*, 3591–3605, doi:10.2147/DDDT.S218708.
39. Bermejo, M.; Avdeef, A.; Ruiz, A.; Nalda, R.; Ruell, J.A.; Tsinman, O.; González, I.; Fernández, C.; Sánchez, G.; Garrigues, T.M.; et al. PAMPA-A drug absorption in vitro model: 7. Comparing rat in situ, Caco-2, and PAMPA permeability of fluoroquinolones. *Eur. J. Pharm. Sci.* **2004**, *21*, 429–441, doi:10.1016/j.ejps.2003.10.009.
40. Garrigues, T.M.; Pérez-Varona, A.T.; Climent, E.; Bermejo, M. V.; Martín-Villodre, A.; Plá-Delfina, J.M. Gastric absorption of acidic xenobiotics in the rat: Biophysical interpretation of an apparently atypical behaviour. *Int. J. Pharm.* **1990**, *64*, 127–138, doi:10.1016/0378-5173(90)90261-2.
41. Sánchez-Castaño, G.; Ruíz-García, A.; Bañón, N.; Bermejo, M.; Merino, V.; Freixas, J.; Garriguesx, T.M.; Plá-Delfina, J.M. Intrinsic absolute bioavailability prediction in rats based on in situ absorption rate constants and/or in vitro partition coefficients: 6-Fluoroquinolones. *J. Pharm. Sci.* **2000**, *89*, 1395–1403, doi:10.1002/1520-6017(200011)89:11<1395::AID-JPS3>3.0.CO;2-U.
42. Lanevskij, K.; Dapkunas, J.; Juska, L.; Japertas, P.; Didziapetris, R. QSAR analysis of blood-brain distribution: The influence of plasma and brain tissue binding. *J. Pharm. Sci.* **2011**, *100*, 2147–2160, doi:10.1002/jps.22442.
43. Watanabe, R.; Esaki, T.; Kawashima, H.; Natsume-Kitatani, Y.; Nagao, C.; Ohashi, R.; Mizuguchi, K. Predicting Fraction Unbound in Human Plasma from Chemical Structure: Improved Accuracy in the Low Value Ranges. *Mol. Pharm.* **2018**, *15*, 5302–5311, doi:10.1021/acs.molpharmaceut.8b00785.
44. Tang, F.; Horie, K.; Borchardt, R.T. Are MDCK cells transfected with the human MRP2 gene a good model of the human intestinal mucosa? *Pharm. Res.* **2002**, *19*, 773–779, doi:10.1023/A:1016192413308.
45. Gomes, M.J.; Mendes, B.; Martins, S.; Sarmento, B. Cell-based in vitro models for studying blood-brain barrier (BBB) permeability. In *Concepts and Models for Drug Permeability Studies: Cell and Tissue Based In Vitro Culture Models*; Elsevier Inc.: Amsterdam, The Netherlands, 2015; pp. 169–188; ISBN 9780081001141.

Supplementary material

Table S1. Chromatographic conditions.

	C (µM)	λ	Mobile phase	Retention time (min)	r^2	LLQ (µM)	Accuracy	Precision	REF
Amitriptyline	250	240 nm	40% Acid water 60% Acetonitrile	1.020	0.996	8.20	6.1	3.2	[1,2]
Caffeine	2.14	273 nm	35% Methanol 65% Acid water	1.200	0.999	0.05	3.1	4.3	[3]
Carbamazepine	18	280 nm	65% Acid water 35% Acetonitrile	1.926	0.994	0.76	3.9	3.6	[2]
Fleroxacin	1.39	285 nm	70% Acid water 30% Acetonitrile	1.348	0.997	0.05	6.0	5.2	[2]
Pefloxacin	8.91	285 nm	65% Acid water 35% Acetonitrile	0.721	0.998	0.61	3.9	3.7	[2]
Zolpidem	158	231 nm	60% Water 20% Methanol 20% Acetonitrile	4.624	0.997	4.30	6.3	4.8	[2]

Acid water had 0.05 % (v/v) trifluoroacetic acid.

1. Mangas-Sanjuan, V.; González-Álvarez, I.; González-Álvarez, M.; Casabó, V.G.; Bermejo, M. Innovative in vitro method to predict rate and extent of drug delivery to the brain across the blood-brain barrier. *Mol. Pharm.* **2013**, *10*, 3822–3831, doi:10.1021/mp400294x.
2. Sánchez-Dengra, B.; González-Álvarez, I.; Sousa, F.; Bermejo, M.; González-Álvarez, M.; Sarmento, B. In vitro model for predicting the access and distribution of drugs in the brain using hCMEC/D3 cells. *Eur. J. Pharm. Biopharm.* **2021**, *163*, 120–126, doi:10.1016/j.ejpb.2021.04.002.
3. del Moral-Sanchez, J.; Ruiz-Picazo, A.; Gonzalez-Alvarez, M.; Navarro, A.; Gonzalez-Alvarez, I.; Bermejo, M. Impact on intestinal permeability of pediatric hyperosmolar formulations after dilution: Studies with rat perfusion method. *Int. J. Pharm.* **2019**, *557*, 154–161, doi:10.1016/J.IJPHARM.2018.12.047.

Table S2. Molecular and physicochemical properties and transporters information for the studied drugs.[4,5]

	MW (g/mol)	**Solubility logS** (pH 7)	**logP**	**Strongest acidic pKa**	**Strongest basic pKa**	**Charge** (pH 7.4)	**Transporters** (substrates)
Amitriptyline	277.411	-1.63	4.81		9.76	+	ABCB1 (Pgp)
Caffeine	194.194	-0.44	-0.55		-1.16	0	
Carbamazepine	236.274	-3.79	2.77	15.96		0	ABCC2 RALBP1
Fleroxacin	369.344	-1.33	0.98	5.32	5.99	-	
Pefloxacin	333.363	-1.21	0.75	5.5	6.44	-	ABCB1 (Pgp)
Zolpidem	307.397	-4.27	3.02		5.39	0	

MW = molecular weight

4. Chemicalize Chemicalize - Instant Cheminformatics Solutions Available online: https://chemicalize.com/welcome (accessed on May 3, 2020).
5. DrugBank DrugBank Available online: https://www.drugbank.ca/ (accessed on May 14, 2020).

6. Access to the CNS: Strategies to overcome the BBB.

Type of publication	Review article
Title	Access to the CNS: Strategies to overcome the BBB
Authors	Bárbara Sánchez-Dengra, Isabel González-Álvarez, Marival Bermejo and Marta González-Álvarez
Journal	Expert Opinion on Drug Delivery
Impact factor	6.648 (Q1 - Pharmacology and Pharmacy)
Year of publication	
DOI	Under preparation

Abstract

Introduction: The blood-brain barrier (BBB) limits the access of substances to the central nervous system (CNS) which hinders the treatment of pathologies affecting the brain and the spinal cord. So new strategies to overcome the BBB and treat the pathologies affecting the CNS are needed.

Areas covered: In this review, the different strategies that allow and increase the access of substances to the CNS are analysed and extended commented. These strategies can be divided in: invasive strategies and non-invasive strategies. The invasive techniques include the direct injection into the brain parenchyma or the CSF and the therapeutic opening of the BBB, while the non-invasive techniques include the use of alternative routes of administration (nose-to-brain route), the inhibition of efflux transporters, the chemical modification of the molecules (prodrugs and chemical drug delivery systems (CDDS)) and the use of nanocarriers.

Expert Opinion: In the future, knowledge about nanocarriers to treat CNS diseases will continue to increase, but the use of other strategies such as drug repurposing or drug reprofiling, which are cheaper and less time consuming, may limit its transfer to society. The combination of different strategies may be the most interesting approach to increase the access of substances to the CNS.

Keywords

blood-brain barrier, central nervous system, drug delivery, nanocarriers

Article highlights

- The blood-brain barrier (BBB) limits the access of substances to the central nervous system (CNS) which hinders the treatment of pathologies affecting the brain and the spinal cord. There are 6 different access routes through the BBB: paracellular diffusion, transcellular diffusion, carrier-mediated transport, receptor-mediated transport, adsorptive-mediated transport and cell-mediated transport.

- When trying to overcome the BBB, several strategies can be attempted which can be divided in: invasive strategies and non-invasive strategies.

- The direct injection of drugs or the implantation of controlled release systems into the brain parenchyma and the therapeutic opening of the tight junctions in the BBB are two invasive techniques which allow the access of substances to CNS, but tend to be avoided because of the inconveniences and discomfort that they cause to the patient.

- The use of nanocarriers, small particles ranging from 1 to 100 nm, has proved to facilitate the delivery of drugs to the CNS, in a non-invasive way, because they are able to protect the drug from enzymatic degradation and they can improve plasma stability and solubility. Furthermore, they can be designed to be directed towards a specific targeting, thus, minimizing non-desired side effects.

- There are a lot of different types of nanocarriers which have been tested to increase the delivery of drugs to the CNS: liposomes, solid lipid nanoparticles, lipid nanocapsules, polymeric nanoparticles, inorganic nanoparticles, dendrimers, cyclodextrins, quantum dots, nanogels, nanoemulsions and viral vectors.

- The use of the nose-to-brain route, prodrugs and chemical drug delivery systems (CDDS) or the inhibition of efflux transporters are other non-invasive strategies that have proved to increase the amount of drug that reaches the CNS.

1. Introduction

The central nervous system (CNS), the brain and the spinal cord, is responsible for the integration of all the sensations that peripheral nerves detect and for the coordination of responses to those sensations [1]. These responsibilities make the brain and the spinal cord the most important organs of human beings and, for this reason, they are protected by several structures: bones, meninges, cerebrospinal fluid (CSF) and blood-brain barrier (BBB) [2–4].

The BBB limits the access of substances to the CNS, due to the presence of tight junctions, efflux transporters, pericytes and astrocytes. Nonetheless, 6 different access routes through the BBB can be defined, as seen in figure 1:

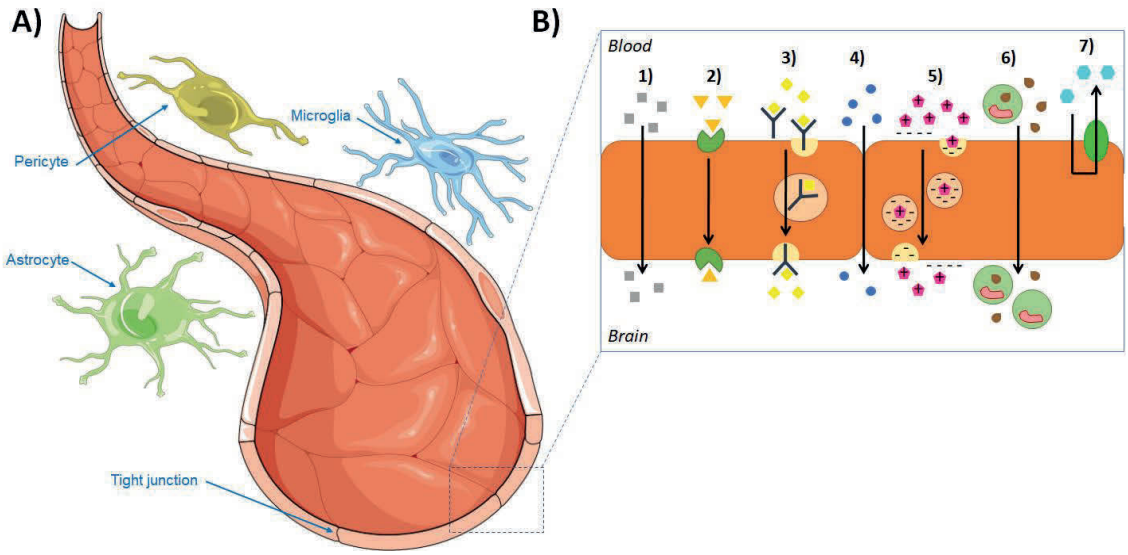

Figure 1. Scheme of the BBB structure **(A)** and the different mechanisms of transport that can be found on it **(B)**: **1)** Transcellular diffusion, **2)** Carrier-mediated transport, **3)** Receptor-mediated transport, **4)** Paracellular diffusion, **5)** Adsorptive-mediated transport, **6)** Cell-mediated transport and **7)** Efflux transport. Vectors downloaded from Servier Medical Art [5].

1) Paracellular diffusion: This term refers to the passive transport that happens between cells moving molecules from the side in which they are more concentrated to the side in which the concentration is lower. It is strictly regulated by the presence of tight junctions between the endothelial cells [6]. So, only extremely small hydrophilic molecules can use this route, such as erythropoietin and antibodies [7].

2) Transcellular diffusion: Also refers to a passive transport which moves molecules from the side of the BBB with the greater concentration to the side with the lower one, but, in this case, the transport takes place across the cells and not between them. Because of that, it is only possible for small lipophilic drugs (i.e. steroids), which meet the following characteristics: low molecular weight ≤500 Da, neutral charge, not too high or too low lipophilicity (logP ≈ 2) and a limited number of potential H-bonds (<10) [8].

3) Carrier-mediated transport: This pathway is responsible for the transport of essential molecules such as glucose and amino acids to the brain, but, any molecule similar to the glucose or to those amino acids could benefit from this route [7]. System L (LAT1 + 4F2hc) is a sodium-independent neutral amino acid transporter and it is one of the most important transporters involved in this route together with GLUT1. GLUT1 is a sodium-independent glucose transporter which contribute to the homeostasis of glucose and L-ascorbic acid in the CNS. Other influx transporters are responsible for the transport of monocarboxlic acids, such as lactate and pyruvate (MCT1), basic amino acids, like L-lysine and L-arginine (CAT1), nucleosides (CNT1) and organic anions and opioids (Oatp2) [9].

4) Receptor-mediated transport: It is also known as receptor-mediated transcytosis and moves molecules from one side of the BBB to the other using vesicles that are formed after they join a specific receptor. This is the case for big macromolecules such as insulin, transferrin or lipoproteins [7,10].

5) Adsorptive-mediated transport: This pathway conforms a non-specific way of transcytosis which can be used by polycationic substances, such as albumin or other peptides, which, after interacting with the negative surface of endothelial cells, are embedded into vesicles [7].

6) Cell-mediated transport: Finally, in this route, cells, normally from the immune system, move directly across the BBB by means of transcytosis. In some cases, as in virus infections, these cells are used as “trojan horses” to introduce molecules into the brain [7].

In addition to those 6 routes, which would allow molecules to reach the brain or the spinal cord, the BBB has several efflux transporters whose mission is to expel from the CNS those toxic or potentially dangerous substances that manage to reach it. Some examples of efflux transporters present in the BBB are the ATP-binding cassette (ABC) transporters: P-glycoprotein (Pgp - MDR1), the multidrug resistance protein (MRP) family and the breast cancer resistance protein (BCRP) [11]. Pgp was first detected in endothelial cells of human BBB in 1989 and since then several studies to evaluate its function and location have been carried out. In fact, it is the most studied efflux transporter of the BBB. It has been seen that, in mammals, Pgp can be found in the apical side of endothelial cells, so those molecules that enter these cells are directly pushed back to the blood. Furthermore, Pgp has also been detected in parenchymal and perivascular astrocytes and in neurons, especially when the animal models suffer seizures [11–13].

All the pathologies that affect the CNS, with the exception of meningitis, have increased their global prevalence in the last two decades. Specifically, from 2000 to 2019, the prevalence of brain and CNS cancers has increased by 46%, the prevalence of stroke by 36%, neurological disorders by 24%, mental disorders by 20%, substance disorders by 17% and encephalitis by 2% [14]. This fact makes necessary the development of new treatments to combat them. Nonetheless, about 85% of CNS trials fail [15] and, in some cases, it is because the new molecule cannot cross the BBB, problem that can be can be tackled with different strategies.

2. Strategies to increase and allow the access of substances to the CNS

When trying to overcome the BBB, several strategies can be attempted which can be divided in: invasive strategies and non-invasive strategies. The invasive techniques include the direct injection into the brain parenchyma or the CSF and the therapeutic opening of the BBB, while the non-invasive techniques include the use of alternative routes of administration (nose-to-brain route), the inhibition of efflux transporters, the chemical modification of the molecules (prodrugs and chemical drug delivery systems (CDDS)) and the use of nanocarriers [7,16].

2.1. Invasive strategies

Invasive strategies tend to be the least used ones because of the inconveniences and discomfort that they cause to the patient. Nonetheless, in some pathologies they are the only feasible option.

2.1.1. Direct injection

The direct injection of drugs or the implantation of controlled release systems into the brain parenchyma have been studied for the treatment of different pathologies: cancers, stroke, neurological disorders or mental disorders [17]. The implantation of controlled release systems requires the opening of the skull, but allows long-term treatments, as drugs can be released during even several months [18]. In the following bullet point list, some examples of brain implants studied in different diseases are summarized:

- Glioblastoma: In 1996, the FDA approved a carmustine implant (Gliadel® wafer) for the treatment of glioblastoma. Currently, it is indicated for the treatment of recurrent glioblastoma and newly-diagnosed high-grade glioma as an adjunct to surgery and radiation. It has the advantage that it can be implanted during the same surgery in which the tumor is resected and it helps to eliminate the tumor cells that are not removed during the surgery, avoiding the adverse effects of a systemic administration of carmustine [19]. Studies have proved that carmustine is released by diffusion during several days and significant levels of drug can be measured within 5 cm of the implant for 30 days after implantation. Besides that, these implants are able to increase the survival rate of glioblastoma patients by 2–3 months [17] and, according to a post-marketing study carried out in Japan, the risk of toxicity with the wafers is tolerable as, only 35.7% of the patients studied suffered adverse effects (22.2% cerebral edema, 9.9% convulsions, 4.8% impaired healing and 3.4% infection) [20].
- Epilepsy: The direct injection of antiepileptic drugs to the seizure focus has proved to be well tolerated and effective in terms of anticonvulsant activity in several animal studies [17,21]. For instance, the direct injection of phenytoin into the cortical focus of an epilepsy animal model was able to control the seizures better than a systemic administration of a higher dose of the same drug [21]. More sophisticated devices which are able to measure the electrical activity of the brain and release drug according to this activity have also been proposed for the

management of epilepsy [17]. The device proposed in 2012 by Salam *et al*. was able to release drug just 16 seconds after the beginning of the electographical detection of a seizure onset [22].

- Schizophrenia: A long-term (5 months) delivery system has been also tested for the treatment of schizophrenia in animal models [17,23]. The reason for studying this kind of systems is that they would improve patient autonomy as they solve the problem of lack of adherence to the treatment normally associated to mental disorders [24].
- Stroke: Solid implants to prevent neurological damage after stroke have been studied during years [17]. For instance, since 1999, nicardipine prolonged-release implants have been tested with success for the prevention of vasospasm in patients with subarachnoid hemorrhage (SAH) [25]. In fact, nowadays, we can find a phase 2 clinical trial, that is currently recruiting participants, in which rod-shaped implants loaded with 4 mg of nicardipine (NicaPlant®) will be administered to patients with SAH to test if they are able to reduce neurological complications associated to this pathology [26].

On the other hand, the direct injection into the CSF is more accessible, but it is not really efficient because of the lack of diffusion between CSF and ECF [16]. Furthermore, it must be considered that only if the drug is injected into the ventricles, it will be distributed in the whole CSF. Nonetheless, this type of injection is indicated in some infectious diseases, such as meningitis [27].

2.1.2. Therapeutic opening of the BBB

The other invasive technique that can be used to increase the access of substances to the CNS is the therapeutic opening of the tight junctions in the BBB, which can be obtained by either administering hyperosmolar solutions or using ultrasounds [7].

The administration of hyperosmolar solutions typically prepared with mannitol or other aromatic substances makes endothelial cells to release water and reduce their size, resulting in an increase in the space between them [16]. This type of treatment is only used for treating life-threatening diseases, as the shrinkage of endothelial cells derives in a non-selective opening of the BBB and both, drugs and toxic substances, could reach the CNS provoking neurological complications (aphasia and hemiparesis) [28]. In addition to that, the administration of mannitol with several penetration markers has shown that the

mannitol derived BBB disruption is not homogenously distributed and different permeability rates can be detected depending on the region of the brain analysed [29].
A more selective opening of the BBB can be obtained by means of combining the use of ultrasounds with the administration of microbubbles (small particles of 1-10 μm which contain heavy gases). When using this technique, microbubbles are directed towards a specific area of the brain, moving them with ultrasounds, and once in the correct place they interact with the endothelial cells and disrupt the tight junctions, leaving a free way for drugs to access the BBB [7]. Besides that, microbubbles can also be loaded or externally modified to carry some drugs on them. This technique has the advantage of safely opening just a desired area of the BBB without requiring a high ultrasound energy [18].

2.2. Non-invasive strategies

As said before, the non-invasive strategies to increase the access of substances to the CNS include the nose-to-brain route of administration, the inhibition of efflux transporters, the development of prodrugs and CDDS and the use of nanocarriers [7,16].

2.2.1. Nose-to-brain route

The olfactory area of the nasal cavity can be used as an alternative route for the delivery of molecules to the CNS. It is not clearly defined how drugs can reach the brain by means of this route, but what is clear is that olfactory nerves connect directly the nasal cavity with the CNS without having any BBB around them. It is thought that drugs administered into the nasal cavity can use two different pathways to travel until the brain: a) the olfactory nerves transportation or b) the trigeminal nerves transportation. The second one can only happen after the drug has been absorbed from nasal mucosa [30]. The main advantages and limitations of this route of administration are summarized in table 1.

Table 1. Summary of the main advantages and limitations of the nasal route of administration for the treatment of pathologies affecting the CNS [30,31].

	Advantages
1	Avoidance of plasma exposure, peripheral metabolism and peripheral side-effects, as the amount of drug that can reach general circulation through the nasal vasculature is depreciable (bioavailability = 0.01% - 0.1%).
2	Reduced risk of infection due to the lack of invasiveness of the administration technique.
3	Ease of administration for the patient, because drugs can be formulated in nasal sprays.
	Limitations
1	Only a small volume (100-250 µL) and a small amount of powder (20-50 mg) can be directly administered to the nasal cavity. So, this route is only feasible for very potent drugs which do not need high doses.
2	Enzymes present in nasal mucosa may metabolize the drugs administered into nasal cavity.
3	Drugs and formulations designed to be administered by this route should not irritate the nasal cavity.
4	The presence of an upper respiratory infection may alter the nasal environment and hinder the drug delivery to the brain.

For example, the intranasal administration of insulin has been considered a promising option for the treatment of Alzheimer's disease. In fact, several studies have proved that after administering insulin via intranasal, it can be detected in CSF and not in plasma and it can improve the cognitive response of Alzheimer's disease patients [30,32]. Nonetheless, a recent clinical trial with 289 patients concludes that no cognitive or functional benefits of intranasal insulin administration could be observed after 12 months and it proposes that more efforts need to be done in the development of intranasal delivery devices [33].

Migraine is another pathology in which intranasal administration has been deeply studied [34–38]. The last device approved by FDA for the treatment of this pathology, Trudhesa®, was allowed to be commercialized in the USA in September 2021. This product contains dihydroergotamine mesylate, a well-known anti-migraine drug, that is directly delivered to the upper part of the nasal cavity. A phase 3, open-label safety study has

shown that pain can start disappearing just 15 minutes after administration and relief can last 2 days after just one dose [39,40].

2.2.2. Inhibition of efflux transporters

As already said, efflux transporters such as Pgp, MRP family and BCRP, are responsible for expelling potentially toxic substances from the CNS. Because of that, when the drug of choice is a substrate of this type of transporter, they hinder the treatment of pathologies affecting the brain or the spinal cord. The coadministration of the drug in question with an inhibitor of the efflux transporter for which it is substrate is another strategy for overcoming the BBB, but it must be used with care as the inhibition of efflux transporters can lead to the massive entrance of xenobiotics to the CNS and, subsequent, unwanted side effects [16,18].

Industries have worked in the development of efflux transporters during several years, specially, in the development of inhibitors for Pgp, for which three generations of molecules can be distinguished [11]:

- 1st generation: This generation of Pgp inhibitors includes several molecules, i.e. verapamil, quinidine or cyclosporin A, which, having been developed for the treatment of different pathologies, showed to have some cytotoxicity as they competed for the efflux transporter with other molecules. Nonetheless, these molecules, which were not specifically designed for inhibiting Pgp and have low affinity for it, can interact with other transporters and enzymes provoking unexpected adverse effects and need a too higher dose to induce a proper inhibition of the efflux transporter [41].
- 2nd generation: Trying to reduce the pharmacological effect and increase the inhibition power of the molecules from first generation, several chemical modifications were performed to the original drugs. Following this basis, dexverapamil, the R-enantiomer of verapamil, or valspodar, derivative of cyclosporin A, were discovered. However, the inhibitors from this second generation are not selective of Pgp and interact with metabolic enzymes, causing undesirable adverse effects. This is the case of valspodar which competes with other molecules for cytochrome P450 leading to an increase in the concentration of other xenobiotics [41].

- 3rd generation: Finally, in this last generation, new molecules, such as zosuquidar, tariquidar or laniquidar, have been directly designed making use of computational tools and QSARs. So, they are able to specifically inhibit Pgp without interacting with other transporters or metabolic enzymes. Nevertheless, not everything is ideal, as some unexpected adverse effects have been observed when testing these molecules in clinical trials [41].

HIV can reach the brain using the infected immune cells as "trojan horses" to cross the BBB. Once there, the virus can multiply and use the CNS as a reservoir, as the drugs designed for their elimination fail to cross this barrier [42]. In this regard, the use of Pgp inhibitors have proved to be effective in the treatment of HIV CNS infections [16]. In 2017, Namanja-Magliano *et al.* developed a homodimer of azidothymidine, an antiretroviral drug also known as zidovudine, which was able to inhibit both, the Pgp and the ABCG2 efflux transporter. Researchers concluded that this type of homodimer has potential to enhance the delivery of antiretrovirals across the BBB, as they block two transporters at the same time allowing the free drug to stay in the brain [43].

2.2.3. Chemical strategies: prodrugs and chemical drug delivery systems (CDDS)

The chemical modification of molecules is a strategy that has been used not only for obtaining more powerful inhibitors of the efflux transporters present in the BBB, but also for obtaining new drug candidates with more chances to cross this barrier.

On the one hand, the development of prodrugs consists in the chemical modification of an active molecule with the aim of increasing its lipophilicity. Once it has crossed the BBB, the prodrug loses its "extra" portion and becomes an active molecule ready to perform its mission. When talking about prodrugs for the treatment of pathologies affecting the CNS, the typical example is L-Dopa, an inactive prodrug of dopamine used in the treatment of Parkinson's disease [7,16].

On the other hand, when a chemical modification is used for appending a bioremovable targeting structure to a drug, then, a chemical drug delivery system (CDDS) is obtained [7]. The route for obtaining the active drug from a CDDS is more complex than when using prodrugs, which allows researchers to obtain intermediary molecules that once cross the BBB are trapped in brain parenchyma where they are not active yet but where they can be accumulated, this is known as the "lock-in" strategy [28,44]. For instance, linking dihydrotrigonelline to a drug forms a CDDS which works in three phases [45], as shown in figure 2:

1) Dihydrotrigonelline increases the lipophilicty of the drug enabling it to cross the BBB.
2) When the CDDS crosses the BBB it is oxidized and a positively charge molecule is obtained. The positive charge prevents the intermediary molecule from crossing the BBB back to plasma.
3) Finally, esterases hydrolyse the intermediate molecule and slowly release the active drug.

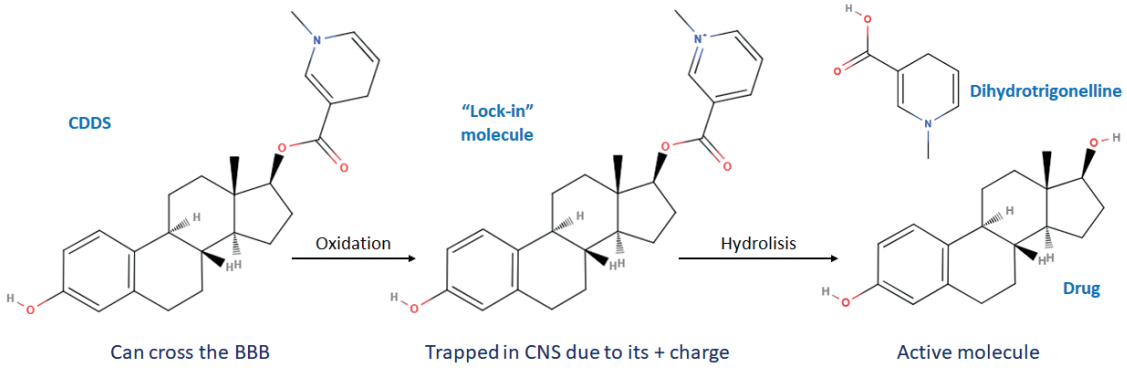

Figure 2. Mechanism of action of a dihydrotrigonelline CDDS.

2.2.4. Nanocarriers

The use of nanocarriers, small particles ranging from 1 to 100 nm, has proved to facilitate the delivery of drugs to the CNS. It is because they are able to protect the drug from enzymatic degradation and they can improve plasma stability and solubility. Furthermore, they can be designed to be directed towards a specific targeting, thus, minimizing non-desired side effects [46]. Nonetheless, it is important to remark that for all this to happen the nanocarrier must not release its content prematurely, so, the ideal nanocarriers for CNS delivery have: A) two different ligands, a first one which contributes to BBB passage and a second one, whose aim is to target the carrier to a specific area of the brain and B) a responsive (pH or enzymatic triggered) system which quickly releases the drug once it has reached its target but prevents it from leaving the carrier while it is on its way to it [47].

Liposomes

Liposomes a are small vesicles, first discovered in the 1960s, formed by a phospholipid bilayer which entraps a small volume of aqueous phase inside them. Because of that, they can incorporate both lipophilic drugs, among the lipids of the

bilayer, and hydrophilic drugs, on the inside core [16,48]. Depending on their complexity, liposomes can be classified in three different generations:

- 1st generation: These are the simplest model of liposomes. They are constituted just by the lipid bilayer and, because of that, they tend to aggregate and be eliminated by the reticuloendothelial system [16].
- 2nd generation: In this second group, the phospholipid bilayer is surrounded by polyethylene glycol, which makes liposomes less recognisable as foreign bodies and increases their stability. Liposomes from this group are also known as stealth liposomes [16].
- 3rd generation: The most complex liposomes are included in this group. They are PEGylated like in the 2nd generation, but they also have other moieties linked around them which help in targeting [16].

Liposomes from third generation have been widely studied for the treatment of different pathologies affecting to the CNS [48]. For instance, multifunctionalized liposomes, with apolipoprotein-E (ApoE) and phosphatidic acid (PA), have been tested for the treatment of Alzheimer's disease. ApoE acts as a first ligand helping the particle to cross the BBB and PA targets the liposome towards β-amyloid plaques and is able to break them [49–51]. *In vitro* tests with hCMEC/D3 monolayers show an increase in BBB permeability after the functionalization of PA-liposomes with ApoE. This increase in permeability was confirmed later on with a biodistribuiton assay in healthy mice in which researchers observed that after 24 horas the brain/blood ratio was 5-fold higher with dual liposomes than with PA ones [50].

On the other hand, in 2019, Xiao *et al*. designed ascorbic acid-thiamine disulfide system liposomes loaded with docetaxel which may be an interesting tool for the treatment of glioblastoma. These liposomes followed a "lock-in" behaviour similar to that presented above when talking about CDDS: once the liposomes cross the BBB, the thiamine disulphide system is reduced gaining a positive charge which entrap them in the brain. The pharmacokinectic parameters obtained after the administration of the liposomes and free docetaxel to adult mice show a 3.24-fold and a 5.61-fold increase in the area under the curve (AUC) and the maximum concentration (Cmax) in the brain [52].

Solid lipid nanoparticles

Solid lipid nanoparticles (SLNs) are constituted by a matrix of lipids, because of that they are useful for the delivery of hydrophobic drugs [7]. In 2019, He *et al*. studied

SLNs, composed of glyceryl monostearate and glycerol tristearate and loaded with β-elemene, for the treatment of glioblastoma. β-elemene is a natural essential oil with anti-tumor activity. The SLNs loaded with this drug proved to reach a greater concentration in plasma and in the brain, both in mice and rats, which would propose this formulation to improve BBB permeability of β-elemene [53].

The previous study together with others in which plain SLNs are administered *in vivo* prove that this type of nanocarrier can inherently increase the penetration of drugs across the BBB [54]. Nonetheless, in other studies the SLNs have been functionalized and they have obtained very promising results too, for instance:

- SLNs loaded with quinine dihydrochloride and conjugated with transferrin, which were designed for the management of cerebral malaria, showed an enhanced uptake in the brain than the free drug in solution [55]. This can be explained by the fact that transferrin promotes the receptor mediated transport of the SLNs.
- The use of cationic bovine serum albumin (CBSA) as a ligand for the functionalization of SLNs have also proved to be a promising strategy for bypassing the BBB [56]. Nonetheless, in this case, the mechanism for this enhancement in the penetration is not due to the use of receptor mediated mechanisms, but adsorptive transcytosis, as the positive charge of the albumin can interact with the negative charge of the surface of the endothelial cells.

Lipid nanocapsules

Finally, lipid nanocapsules can be found as the last type of lipid-based nanocarriers. They have the advantages of being more stable than liposomes and being able to encapsulate greater amounts of lipophilic drug. It is because they have a lipoprotein-like structure, with an oily core surrounded by a rigid membrane of polymer or tensioactive [57].

In 2020, Elhesaisy and Swidan proved that they were able to reduce the immobility time of mice when they forced them to swim in a beaker, a stressful situation in which animals tend to desperate, resign and stop moving, after the administration of lipid core nanoparticles loaded with trazodone hydrochloride. In fact, the immobility time for the group without treatment was 158 ± 15 seconds, for the group which received a solution of free trazodone was 128 ± 12 seconds, but in the group treated with the nanocapsules the immobility time dropped until 88 ± 8 seconds (1.8-fold lower than the

control group). So, researchers conclude that these carriers were a promising alternative for controlling depression [58].

From May 2018 to April 2020, the project BIONICS founded by Horizon 2020 worked in the development of lipid nanoparticles with anti-oxidant effects for the treatment and prevention of post-stroke side effects [59]. The reason for this is that the current treatment for ischeamic stroke, the administration of tissue plasminogen activator or the physical removal of the thrombo, can restore the blood flow in the affected area, but it cannot avoid the damage of brain tissue due to the release of reactive oxygen and reactive nitrogen species. Preliminary results show that the new carrier was able to target both BBB and neuronal cells and, now, the group is working to prove its antioxidant and neuroprotective effect [59].

Polymeric nanoparticles

Polymeric nanoparticles can be divided in two groups depending on their structure: nanospheres (a solid polymeric matrix) or nanocapsules (an inner core surrounded by polymer). Several biodegradable and biocompatible polymers have been studied for the development of CNS nanocarriers, i.e. polylactic acid (PLA), polylactic-co-glycolic acid (PLGA), chitosan and polycaprolactone (PCL), among others [7,47]. The next bullet points show examples of polymeric nanocarriers developed with the polymers mentioned above:

- Polylactic acid (PLA): PEGylated PLA nanoparticles modified with an anti-transferrin receptor antibody and loaded with amphotericin B were developed in 2015 for the treatment of fungal meningitis. The PEG modification increases the stability of the particles in the blood and the anti-transferrin receptor antibody promotes the receptor-mediated transport through the BBB. The studies carried out with this formulation showed that the particles were able to significantly reduce the necrosis of brain tissue after 15 days of infection and increase the survival rate of mice whose lethality rate dropped from 100% in day 16 post-infection in the untreated group to 50% after 24 days [60].
- Polylactic-co-glycolic acid (PLGA): In the prospect of treating Alzheimer's disease, PLGA nanoparticles loaded with curcumin were prepared by Barbara and co-workers in 2017. Curcumin has proved to be able to inhibit the formation of Aβ plaques and disaggregate those already formed, but, as many other drugs, it has a low ability to cross the BBB. The new particles, which were modified with a

peptide ligand (g7) for BBB crossing, showed to be able to reduce the number of Aβ aggregates in an *in vitro* model with hippocampal cells. Besides that, they seemed to reduce the inflammatory process associated to Alzheimer's disease. Nonetheless, further studies in in vivo models are needed to obtain further conclusions [61].

- Chitosan: Chitosan is a natural polysaccharide, which can be obtained after the deacetylation of chitin extracted from crustacean shells and has been studied for the treatment of many conditions, mainly Alzheimer's disease and Parkinson's disease [62]. Nanoparticles of chitosan loaded with rotigotine have proved that, after being administered intranasally, are able to reduce catalepsy, akinesia and improve the swimming ability in a Parkinson-induced animal model. Furthermore, pharmacokinetics studies showed a greater accumulation of rotigotine in the brain in comparison with the intranasal administration of the free drug or the administration of the particles by other ways [63].
- Polycaprolactone (PCL): *In vitro* studies carried out in three different cell lines with PCL nanoparticles loaded with clozapine, an antipsychotic drug used in the treatment of schizophrenia, show that this type of formulation may be a valuable alternative for the management of this pathology. The PEGylated particles were not toxic nor immunogenic and increased the permeability of clozapine in hCMEC/D3 monolayers [64].

Inorganic nanoparticles

Inorganic nanoparticles prepared with metals, metal oxides or silica are useful for, both, diagnosis and treatment of pathologies affecting the CNS, this is, they can act as theragnostic devices. Nonetheless, they have the big drawback that, in contrast to those nanoparticles mentioned previously, they are not biodegradable and they can be toxic [47].

Due to their surface plasmon property, gold nanoparticles can absorb and emit light at different wavelengths according to their size, shape and aggregate status [7]. Besides that, the surface plasmon property also makes this kind of particle ideal for photothermal therapy as the light they absorb can be converted into heat [65]. The photothermal therapy with gold nanoparticles has been tested in several *in vitro* and *in vivo* models of glioblastoma, but, for translating the findings obtained in those models to the treatment of human beings several challenges must be faced, such as: the several

barriers that the irradiating light needs to cross until it reachs the particles in the tumor without damaging any other cerebral structures [66].

Magnetic nanoparticles prepared from iron oxides have also been studied as a thermal therapy for the treatment of glioblastoma or as contrast agents for imaging techniques [54]. In addition, these nanoparticles can be used as a driving force for promoting the passage of other types of nanocarriers through the BBB [7]. For instance, magneto-liposomes entrap a magnetic core in its inner part, which facilitates the delivery of drugs across the BBB, as proved by Saiyed *et al*. and Ding *et al*. in 2010 and 2014, respectively [67–69].

Mesoporous silica nanoparticles (MSNs) have a high surface area, can load big amounts of cargo, are biocompatible and are easy to functionalize. Because of that, a lot of researchers try to use this system for the development of new nanocarriers [47]. In 2016, an *in vitro* study carried out in two different monolayers, which are able to simulate the BBB (MDCK and RBE4 cells), showed that bare MSNs had low permeability and external functionalization was necessary to improve BBB penetration [70]. After that, several studies with functionalized MSNs have been carried out. For instance, lactoferrin-MSNs proved to reach the brain due to the use of the receptor-mediated pathway in a triculture *in vitro* model [71]. Also, Ri7 antibody-MSNs increased the drug delivery to the brain by means of binding to the transferrin receptor [70].

Dendrimers

Dendrimers are three-dimensional and regular polymeric macromolecules with three different areas: A) a central core, B) branches and C) surface groups. The number of ramifications in a dendrimer defines its generation and the spaces that there are in between the branches can be used to transport other molecules [7,18].

The most studied dendrimer is poly-amidoamine (PAMAM) [18]. In 2016, Xu and collaborators loaded PAMAM with doxorubicin and did several *in vitro* and *in vivo* studies to prove its efficacy against glioblastoma. As surface groups, they selected two molecules: borneol, whose mission is to open the tight junctions in between the endothelial cells of the BBB, and, folic acid, to target the dendrimers to cancer cells, as they overexpressed the folic acid receptor. The *in vitro* studies showed that the nanocarriers prepared by Xu and collaborators were not toxic for BBB cells, but they were able to kill the glioblastoma cells. Besides that, a sustained released of doxorubicin was observed when the dendrimers were placed in pH 5.5 buffer and the permeability of the drug in HBMEC

monolayers was enhanced. Once in the *in vivo* studies, dendrimers showed a greater accumulation in brain and tumor than the free drug, a significant reduction of tumor volume and an increase in the survival of the animals tested [72].

Cyclodextrins

Cyclodextrins are cyclic polysaccharides used for delivering lipophilic drugs in an aqueous environment, as they are highly hydrophilic in their surface, but more hydrophobic in their inner part. Furthermore, cyclodextrins are able to interact with lipid membranes, so, they can be used to increase BBB permeability by means of altering its membrane fluidity [18,73].

Recently, a new complex of crocetin and γ-cyclodextrin was proposed for the treatment of Alzheimer's disease. The *in vitro* evaluation of the new complex showed that it was nontoxic and it was able to reduce the levels of Aβ in 7PA2 cell line. The pharmacokinetic evaluation in rats showed that, after an intraperitoneal injection, the maximum concentration in plasma of crocetin was 43.5 times higher when it was administered in the cyclodextrin complex than when it was administered on its own and the AUC was also 13.1 times higher. In terms of biodistribution, it was seen that the crocetin-γ-cyclodextrin complex was able to penetrate the BBB and reach the brain after its administration [74].

Quantum dots

Quantum dots (QDs) are small nanosystems ranging from 2 to 10 nm with semiconductor properties. In a similar way that gold nanoparticles, QDs can emit light in different wavelengths depending on their size, shape, and composition, because of that they have been proposed as theragnostic tools [75].

In the treatment of CNS pathologies, QDs have been explored to target and identify brain tumors, to detected areas affected by ischemia after a stroke or to treat HIV-associated encephalopathy [47,76]. In the last case, quantum dots conjugated with transferrin, as a targeting ligand to BBB, and saquinavir, as an antiretroviral drug, have proved to efficiently cross the BBB and inhibit HIV replication in infected PBMC cells, using a triculture *in vitro* model [76].

Nanogels

Nanogels can be defined as nanoparticles composed of a cross-linked hydrophilic polymer network [77]. Its capacity to retain water promotes nanogels biocompatibility and facilitates drug release. Nonetheless, this type of nanocarrier have been less studied for the treatment of pathologies affecting the CNS [47]. In June 2021, Ribovski *et al*. published an article in which they discuss the influence of nanogel' stiffness in BBB permeability. Briefly, they prepared 4 types of nanogels with different percentages of polymer and different polymerization times. Once obtained, they analysed the permeability of the different particles in a hCMEC/D3 BBB *in vitro* model. They saw that the low stiffness promotes intracellular trafficking and exocytosis through the cell monolayers [77]. So, soft nanogels would be the most promising ones for developing drugs directed towards the CNS.

Nanoemulsions

Nanoemulsions (NEs) are composed of kinetically stable dispersions of two immiscible liquids [78]. They can transport both hydrophilic and hydrophobic drugs and the smaller are the droplets of the emulsion, the greater is its stability. The mechanisms by which this type of nanocarrier can promote BBB permeability are:

- Lipid exchange, because of the interactions between the lipid phase of the NEs and the lipids of the endothelial cell's membranes [78].
- Carrier-mediated or receptor-mediated transport, which can occur if the external phase of the NE is decorated with a specific ligand [78].
- Adsorptive-mediated transcytosis, if the hydrophilic head of the lipids forming the droplets of the NE are positively charged [78].
- Efflux transport inhibition, as the droplets of the NEs can mask the drug from its efflux transporter and some surfactants present in the NE, i.e. polysobate 80, are well-known Pgp inhibitors [78].

NEs have been studied for the treatment of: brain tumors, neurodegenerative disorders, HIV-associated CNS disorders, ischemic stroke and schizophrenia [78]. Several examples of NEs intended for the treatment of those pathologies is shown in table 2.

Table 2. Examples of nanoemulsions intended for the treatment of CNS diseases [78].

Disease	Nanocarrier	Outcomes
Brain tumors	Kaempferol mucodhesive NE	Increased brain levels after intranasal administration.
		Reduced glioma (C6 cell line) viability.
	Chloroaluminun phtalocyanine NE	Reduced glioma (U87 cell line) viability.
	Paclitaxel ClinOleic®	Reduced glioma (U87 cell line) viability.
		Selectivity towards cancerous cells.
	Honokiol NE	Inhibition of tumor growth *in vivo*.
Neurodegenerative disorders	Oridonin NE	Less Aβ plaques and Aβ deposition.
		Restored construction behaviour.
	Rivastigmine NE	Increased brain levels after intranasal administration.
	Thymoquinone-rich fraction NE	Less Aβ generation and more Aβ degradation.
		Increased antioxidant levels.
	Selegiline NE	Increased antioxidant enzymes.
		Higher dopamine levels in Parkinson's disease rats.
	Riluzole NE	Increased brain levels after intranasal administration.
HIV-associated CNS disorders	Saquinavir mesylate NE	Increased brain levels after intranasal administration.
	Indinavir NE	Increased brain levels after intravenous administration.
	Atovaquone NE	Increased bioavailability after oral administration.
		Reduced parasitemia and less brain cysts in a toxoplasmosis.
Ischemic stroke	Thymoquinone mucoadhesive NE	Increased brain levels after intranasal administration.
		Better motor skills.
	Olmesartan NE	Increased brain levels after oral administration.
	Quercetin mucoadhesive NE	Better motor skills.
		Lower infarction volume and less hematoma.
		Increased antioxidant capacity.
Schizophrenia	Quetiapine NE	Increased brain levels after intranasal administration.
	Risperidone NE	Increased bioavailability and brain levels after intraperitoneal administration.
		Early onset of antipsychotic action.
		Less locomotor side symptoms.

Viral vectors

Finally, in terms of gene therapy, viral vectors have become extremely popular for the treatment of neurological disorders due to its high transfection efficiency and its long-term expression [46]. The adeno-associated virus serotype 9 (AAV9) is the most promising vector for CNS gene therapy as it has proved to be able to cross the endothelial cells by active transport without disrupting the BBB [18,79].

AVV9 has been tested for the treatment of spinal muscular atrophy (SMA) in several clinical trials [80]. SMA is a genetic disease affecting the alpha motor neurons of the spinal cord and brainstem. The degeneration of these neurons causes several difficulties in speaking, walking, breathing, and swallowing; it can lead to paralysis and death too, being the leading cause of mortality in infants [81]. Early-diagnosed patients treated with AAV9 showed a better motor behaviour and an increase in its rate of survival. Nonetheless, more efforts are needed before obtaining the final vector for treating this disease, as there were patients who developed antibodies against the vector and this may cause severe side effects [81].

3. Conclusion

Along this document, an extended revision of different strategies to allow or increase the access of substances to the CNS has been done. It can be seen that there are several options which can be used and are able to increase the levels of drug in the brain. So, when trying to treat a pathology of the CNS, both the development of new molecules and its combination with a proper method to overcome the BBB must be done.

Expert Opinion:

As said in the review, in the last two decades, there has been a considerable increase in the prevalence of most diseases that affect CNS which highlights the need for new treatments to combat them. Nonetheless, about 85% of CNS trials fail, which is the second highest failure rate just after the oncology trials [15]. Among the reasons for these failures, we can find: problems with the target, lack of biomarkers, problems with the design of the study, issues with the transition from animals to human because animal models tend not to be as complex as human beings and drugs not crossing the BBB [82–84]. In our opinion, the development of strategies to allow or increase the access of substances to the CNS would solve most of the failures. Nonetheless, trying to overcome

these failures, industries tend to opt for a repositioning strategy, a more cost-effective and time-saving alternative also known as drug repurposing or drug reprofiling [85].

Although having been used as interchangeable terms, there is a subtle difference between repurposing and repositioning. In repurposing, a drug already approved and without suffering any molecular modification is reapproved for a different indication, while in repositioning, the drug suffers some change in its structure before being approved for another indication [85]. Historically, reposition has happened unintentionally, but, recently, researchers and industries have realized its benefits and used it with those drugs which have proved to be safe, but not effective, in their clinical trials. This is the reason why, year after year, the number of articles including on their keywords “drug repositioning” increases [85]. In the field of CNS treatments, approximately 30% of the drugs have been repurposed two or more times [85], mainly because once the drug crosses the BBB it is easier to find a new target for it. Thus, this trend, although having clear advantages in the treatment of pathologies of the CNS, would reduce the investment of big industries for the development of new devices to increase the access of substances to the CNS.

When talking about nanocarriers, the most sophisticated and non-invasive strategy to improve the treatment of pathologies affecting the CNS, the articles published in this field have increased by more than 80% in the last 10 years (results after searching: "nanocarrier" and "brain" in Pubmed). This tendency makes us think that, there is a clear interest in knowing about these formulations. So, probably in the next five or ten years the knowledge about them will continue increasing. However, if the knowledge is obtained from public institutions, such as universities or research centres, the key for a global benefit will lay in the results transfer from the public to the private ambit. It is useless to accumulate tons of knowledge, if society cannot benefit from it. From some institutions, great work is being done and, increasingly, university researchers patent their ideas before publishing them. This fact can greatly help industries to notice them, buy them and work on the development of new nanocarriers with certain guarantees of success.

In our opinion, the ideal approach to increase the access of substances to the CNS should combine the use of nanocarriers with other strategies to increase drug penetration such as, the physical opening of the BBB with ultrasounds and microbubbles or the nasal administration to get a non-invasive direct administration to the CNS.

Funding

This work was supported by the project "Modelos *in vitro* de evaluación biofarmacéutica" SAF2016-78756(AEI/FEDER, EU) funded by Agencia Estatal Investigación and European Union, through FEDER (Fondo Europeo de Desarrollo Regional). Bárbara Sánchez-Dengra received a grant from the Ministry of Science, Innovation and Universities of Spain [grant number FPU17/00530].

References

[1] Biga LM, Dawson S, Harwell A, et al. The Nervous System and Nervous Tissue. Anat. Physiol. OpenStax/Oregon State University;

[2] Tortora GJ, Derrickson B. Chapter 12: Nervous Tissue. Princ. Anat. Physiol. 11th ed. John Wiley and Sons, Inc.; 2011. p. 407–442.

[3] Tortora GJ, Derrickson B. Chapter 13: The Spinal Cord and Spinal Nerves. Princ. Anat. Physiol. 11th ed. John Wiley and Sons, Inc.; 2011. p. 443–476.

[4] Tortora GJ, Derrickson B. Chapter 14: The Brain and Cranial Nerves. Princ. Anat. Physiol. 11th ed. John Wiley and Sons, Inc.; 2011. p. 477–527.

[5] SMART - Servier Medical ART [Internet]. [cited 2021 Sep 8]. Available from: https://smart.servier.com/.

[6] Wong AD, Ye M, Levy AF, et al. The blood-brain barrier: An engineering perspective. Front. Neuroeng. [Internet]. 2013 [cited 2020 Jul 24];6. Available from: /pmc/articles/PMC3757302/?report=abstract.

[7] Sánchez-Dengra B, González-Álvarez I, Bermejo M, et al. Nanomedicine in the Treatment of Pathologies of the Central Nervous System Advances in Nanomedicine. Adv. Nanomedicine [Internet]. 2020 [cited 2020 Mar 3]. Available from: www.openaccessebooks.com.

*** it describes the different access routes to the CNS**

[8] Teleanu DM, Negut I, Grumezescu V, et al. Nanomaterials for drug delivery to the central nervous system. Nanomaterials. 2019;9.

[9] Ohtsuki S, Terasaki T. Contribution of Carrier-Mediated Transport Systems to the Blood–Brain Barrier as a Supporting and Protecting Interface for the Brain; Importance for CNS Drug Discovery and Development. Pharm. Res. [Internet]. 2007 [cited 2021 Oct 13];24:1745–1758. Available from: https://link.springer.com/article/10.1007/s11095-007-9374-5.

[10] Pulgar VM. Transcytosis to cross the blood brain barrier, new advancements and challenges. Front. Neurosci. [Internet]. 2019 [cited 2020 Aug 6];13. Available from: /pmc/articles/PMC6337067/?report=abstract.

[11] Löscher W, Potschka H. Blood-brain barrier active efflux transporters: ATP-binding cassette gene family. NeuroRx [Internet]. 2005 [cited 2020 Jul 27];2:86–98. Available from: /pmc/articles/PMC539326/?report=abstract.

[12] Volk H., Burkhardt K, Potschka H, et al. Neuronal expression of the drug efflux transporter P-glycoprotein in the rat hippocampus after limbic seizures. Neuroscience [Internet]. 2004 [cited 2021 Oct 13];123:751–759. Available from: https://pubmed.ncbi.nlm.nih.gov/14706787/.

[13] Volk H, Potschka H, Löscher W. Immunohistochemical Localization of P-glycoprotein in Rat Brain and Detection of Its Increased Expression by Seizures Are Sensitive to Fixation and Staining Variables. J. Histochem. Cytochem. [Internet]. 2005 [cited 2021 Oct 13];53:517–531. Available from: https://pubmed.ncbi.nlm.nih.gov/15805426/.

[14] Global Burden of Disease Collaborative Network. Global Burden of Disease Study 2019

(GBD 2019) Results. [Internet]. Seattle, United States: Institute for Health Metrics and Evaluation (IHME); 2020 [cited 2021 Sep 9]. Available from: http://ghdx.healthdata.org/gbd-results-tool.

*** excellent tool to evaluate disease prevalences**

[15] WCG Institute. CNS Trial Failures Problematic But Fixable, Experts Agree [Internet]. [cited 2021 Sep 9]. Available from: https://www.wcgclinical.com/insights/institute/cns-trial-failures-problematic-but-fixable-experts-agree.

[16] Passeleu-Le Bourdonnec C, Carrupt P-A, Scherrmann JM, et al. Methodologies to Assess Drug Permeation Through the Blood–Brain Barrier for Pharmaceutical Research. Pharm. Res. [Internet]. 2013 [cited 2021 Oct 24];30:2729–2756. Available from: https://link.springer.com/article/10.1007/s11095-013-1119-z.

[17] Kaurav H, Kapoor DN. Implantable systems for drug delivery to the brain. Ther. Deliv. [Internet]. 2017 [cited 2021 Nov 3];8:1097–1107. Available from: https://pubmed.ncbi.nlm.nih.gov/29125063/.

[18] Bors L, Erdő F. Overcoming the Blood–Brain Barrier. Challenges and Tricks for CNS Drug Delivery. Sci. Pharm. [Internet]. 2019 [cited 2021 Nov 3];87:6. Available from: https://www.mdpi.com/2218-0532/87/1/6/htm.

[19] Arbor Pharmaceuticals LLC. Gliadel [Internet]. 2021 [cited 2021 Nov 3]. Available from: https://www.gliadel.com/hcp/index.php.

[20] Nishikawa R, Iwata H, Sakata Y, et al. Safety of Gliadel Implant for Malignant Glioma: Report of Postmarketing Surveillance in Japan. Neurol. Med. Chir. (Tokyo). [Internet]. 2021 [cited 2021 Nov 3];61:oa.2021-0024. Available from: https://pubmed.ncbi.nlm.nih.gov/34092748/.

[21] Gernert M, Feja M. Bypassing the Blood–Brain Barrier: Direct Intracranial Drug Delivery in Epilepsies. Pharmaceutics [Internet]. 2020 [cited 2021 Nov 3];12:1134. Available from: https://pubmed.ncbi.nlm.nih.gov/33255396/.

[22] Salam MT, Mirzaei M, Ly MS, et al. An Implantable Closedloop Asynchronous Drug Delivery System for the Treatment of Refractory Epilepsy. IEEE Trans. Neural Syst. Rehabil. Eng. [Internet]. 2012 [cited 2021 Nov 3];20:432–442. Available from: https://pubmed.ncbi.nlm.nih.gov/22491131/.

[23] Siegel S, Winey K, Gur R, et al. Surgically Implantable Long-term Antipsychotic Delivery Systems for the Treatment of Schizophrenia. Neuropsychopharmacology [Internet]. 2002 [cited 2021 Nov 4];26:817–823. Available from: https://www.nature.com/articles/1395869.

[24] Siegel SJ. Increased patient autonomy through long-term antipsychotic delivery systems for the treatment of schizophrenia. Expert Rev. Neurother. [Internet]. 2002 [cited 2021 Nov 4];2:771–773. Available from: https://www.tandfonline.com/doi/abs/10.1586/14737175.2.6.771.

[25] Krischek B, Kasuya H, Onda H, et al. Nicardipine prolonged-release implants for preventing cerebral vasospasm after subarachnoid hemorrhage: effect and outcome in the first 100 patients. Neurol. Med. Chir. (Tokyo). [Internet]. 2007 [cited 2021 Nov 4];47:389–394; discussion 394-6. Available from: https://pubmed.ncbi.nlm.nih.gov/17895611/.

[26] US National Library of Medicines. A Safety and Efficacy Study of NicaPlant® in Aneurysmal Subarachnoid Haemorrhage Patients Undergoing Aneurysm Clipping - Full Text View - ClinicalTrials.gov [Internet]. 2021 [cited 2021 Nov 4]. Available from: https://clinicaltrials.gov/ct2/show/NCT04269408.

[27] Nau R, Sörgel F, Eiffert H. Penetration of Drugs through the Blood-Cerebrospinal Fluid/Blood-Brain Barrier for Treatment of Central Nervous System Infections. Clin. Microbiol. Rev. [Internet]. 2010 [cited 2021 Nov 3];23:858–883. Available from: /pmc/articles/PMC2952976/.

[28] He Q, Liu J, Liang J, et al. Towards Improvements for Penetrating the Blood–Brain Barrier—Recent Progress from a Material and Pharmaceutical Perspective. Cells. 2018;7:24.

**** review about different methods to improve BBB penetration**

[29] Brown RC, Egleton RD, Davis TP. Mannitol opening of the blood–brain barrier: regional variation in the permeability of sucrose, but not 86Rb+ or albumin. Brain Res. [Internet]. 2004 [cited 2021 Nov 4];1014:221–227. Available from: https://pubmed.ncbi.nlm.nih.gov/15213006/.

[30] Wang Z, Xiong G, Tsang WC, et al. Nose-to-Brain Delivery. J. Pharmacol. Exp. Ther. [Internet]. 2019 [cited 2021 Nov 5];370:593–601. Available from: https://jpet.aspetjournals.org/content/370/3/593.

[31] Veronesi MC, Alhamami M, Miedema SB, et al. Imaging of intranasal drug delivery to the brain. Am. J. Nucl. Med. Mol. Imaging [Internet]. 2020 [cited 2021 Nov 5];10:1–31. Available from: /pmc/articles/PMC7076302/.

[32] Freiherr J, Hallschmid M, Frey WH, et al. Intranasal Insulin as a Treatment for Alzheimer's Disease: A Review of Basic Research and Clinical Evidence. CNS Drugs [Internet]. 2013 [cited 2021 Nov 5];27:505–514. Available from: /pmc/articles/PMC3709085/.

[33] Craft S, Raman R, Chow TW, et al. Safety, Efficacy, and Feasibility of Intranasal Insulin for the Treatment of Mild Cognitive Impairment and Alzheimer Disease Dementia. JAMA Neurol. [Internet]. 2020 [cited 2021 Nov 5];77:1099. Available from: https://jamanetwork.com/journals/jamaneurology/fullarticle/2767376.

[34] Logemann CD, Rankin LM. Newer Intranasal Migraine Medications. Am. Fam. Physician. 2000;61:180–186.

[35] Chi P-W, Hsieh K-Y, Chen K-Y, et al. Intranasal lidocaine for acute migraine: A meta-analysis of randomized controlled trials. Cheungpasitporn W, editor. PLoS One [Internet]. 2019 [cited 2021 Nov 5];14:e0224285. Available from: /pmc/articles/PMC6808552/.

[36] Menshawy A, Ahmed H, Ismail A, et al. Intranasal sumatriptan for acute migraine attacks: a systematic review and meta-analysis. Neurol. Sci. [Internet]. 2018 [cited 2021 Nov 5];39:31–44. Available from: https://pubmed.ncbi.nlm.nih.gov/28942578/.

[37] Rapoport AM, Bigal ME, Tepper SJ, et al. Intranasal Medications for the Treatment of Migraine and Cluster Headache. CNS Drugs [Internet]. 2004 [cited 2021 Nov 5];18:671–685. Available from: https://pubmed.ncbi.nlm.nih.gov/15270595/.

[38] Dodick D, Brandes J, Elkind A, et al. Speed of Onset, Efficacy and Tolerability of

Zolmitriptan Nasal Spray in the Acute Treatment of Migraine. CNS Drugs [Internet]. 2005 [cited 2021 Nov 5];19:125–136. Available from: https://pubmed.ncbi.nlm.nih.gov/15697326/.

[39] NeuroPharma® I. Trudhesa™ (dihydroergotamine mesylate) nasal spray | Official Website [Internet]. 2021 [cited 2021 Nov 5]. Available from: https://www.trudhesa.com/.

[40] Drugs.com. Trudhesa (dihydroergotamine mesylate) FDA Approval History [Internet]. 2021 [cited 2021 Nov 5]. Available from: https://www.drugs.com/history/trudhesa.html.

[41] Palmeira A, Sousa E, H. Vasconcelos M, et al. Three Decades of P-gp Inhibitors: Skimming Through Several Generations and Scaffolds. Curr. Med. Chem. [Internet]. 2012 [cited 2021 Nov 6];19:1946–2025. Available from: http://www.eurekaselect.com/openurl/content.php?genre=article&issn=0929-8673&volume=19&issue=13&spage=1946.

[42] Osborne O, Peyravian N, Nair M, et al. The Paradox of HIV Blood–Brain Barrier Penetrance and Antiretroviral Drug Delivery Deficiencies. Trends Neurosci. [Internet]. 2020 [cited 2021 Nov 6];43:695–708. Available from: http://www.cell.com/article/S0166223620301491/fulltext.

[43] Namanja-Magliano HA, Bohn K, Agrawal N, et al. Dual inhibitors of the human blood-brain barrier drug efflux transporters P-glycoprotein and ABCG2 based on the antiviral azidothymidine. Bioorg. Med. Chem. [Internet]. 2017 [cited 2021 Nov 6];25:5128–5132. Available from: https://linkinghub.elsevier.com/retrieve/pii/S0968089617313536.

[44] Grabrucker AM, Chhabra R, Belletti D, et al. Nanoparticles as Blood–Brain Barrier Permeable CNS Targeted Drug Delivery Systems. Top. Med. Chem. [Internet]. Springer, Berlin, Heidelberg; 2013 [cited 2021 Nov 6]. p. 71–89. Available from: https://link.springer.com/chapter/10.1007/7355_2013_22.

[45] Rautio J, Laine K, Gynther M, et al. Prodrug Approaches for CNS Delivery. AAPS J. [Internet]. 2008 [cited 2021 Nov 6];10:92–102. Available from: /pmc/articles/PMC2751454/.

[46] Ahlawat J, Guillama Barroso G, Masoudi Asil S, et al. Nanocarriers as Potential Drug Delivery Candidates for Overcoming the Blood–Brain Barrier: Challenges and Possibilities. ACS Omega [Internet]. 2020 [cited 2021 Nov 8];5:12583–12595. Available from: https://pubs.acs.org/doi/full/10.1021/acsomega.0c01592.

**** interesting review about CNS nanocarriers**

[47] Alexander A, Agrawal M, Uddin A, et al. Recent expansions of novel strategies towards the drug targeting into the brain . Int. J. Nanomedicine. 2019;Volume 14:5895–5909.

[48] Vieira D, Gamarra L. Getting into the brain: liposome-based strategies for effective drug delivery across the blood–brain barrier. Int. J. Nanomedicine [Internet]. 2016 [cited 2021 Nov 8];Volume 11:5381–5414. Available from: /pmc/articles/PMC5077137/.

[49] Ross C, Taylor M, Fullwood N, et al. Liposome delivery systems for the treatment of Alzheimer's disease. Int. J. Nanomedicine [Internet]. 2018 [cited 2021 Nov 8];Volume 13:8507–8522. Available from: /pmc/articles/PMC6296687/.

[50] Bana L, Minniti S, Salvati E, et al. Liposomes bi-functionalized with phosphatidic acid and

an ApoE-derived peptide affect Aβ aggregation features and cross the blood–brain-barrier: Implications for therapy of Alzheimer disease. Nanomedicine Nanotechnology, Biol. Med. [Internet]. 2014 [cited 2021 Nov 8];10:1583–1590. Available from: https://linkinghub.elsevier.com/retrieve/pii/S1549963413006849.

[51] Agrawal M, Ajazuddin, Tripathi DK, et al. Recent advancements in liposomes targeting strategies to cross blood-brain barrier (BBB) for the treatment of Alzheimer's disease. J. Control. Release [Internet]. 2017 [cited 2021 Nov 8];260:61–77. Available from: https://linkinghub.elsevier.com/retrieve/pii/S0168365917305916.

[52] Xiao W, Fu Q, Zhao Y, et al. Ascorbic acid-modified brain-specific liposomes drug delivery system with "lock-in" function. Chem. Phys. Lipids [Internet]. 2019 [cited 2021 Nov 8];224:104727. Available from: https://linkinghub.elsevier.com/retrieve/pii/S0009308417303316.

[53] He H, Yao J, Zhang Y, et al. Solid lipid nanoparticles as a drug delivery system to across the blood-brain barrier. Biochem. Biophys. Res. Commun. [Internet]. 2019 [cited 2021 Nov 9];519:385–390. Available from: https://linkinghub.elsevier.com/retrieve/pii/S0006291X19317383.

[54] Lombardo SM, Schneider M, Türeli AE, et al. Key for crossing the BBB with nanoparticles: the rational design. Beilstein J. Nanotechnol. [Internet]. 2020 [cited 2021 Nov 9];11:866–883. Available from: https://www.beilstein-journals.org/bjnano/articles/11/72.

[55] Gupta Y, Jain A, Jain SK. Transferrin-conjugated solid lipid nanoparticles for enhanced delivery of quinine dihydrochloride to the brain. J. Pharm. Pharmacol. [Internet]. 2010 [cited 2021 Nov 9];59:935–940. Available from: https://academic.oup.com/jpp/article/59/7/935/6141633.

[56] Agarwal A, Majumder S, Agrawal H, et al. Cationized Albumin Conjugated Solid Lipid Nanoparticles as Vectors for Brain Delivery of an Anti-Cancer Drug. Curr. Nanosci. [Internet]. 2011 [cited 2021 Nov 9];7:71–80. Available from: http://www.eurekaselect.com/openurl/content.php?genre=article&issn=1573-4137&volume=7&issue=1&spage=71.

[57] Huynh NT, Passirani C, Saulnier P, et al. Lipid nanocapsules: A new platform for nanomedicine. Int. J. Pharm. [Internet]. 2009 [cited 2021 Nov 9];379:201–209. Available from: https://pubmed.ncbi.nlm.nih.gov/19409468/.

[58] Elhesaisy N, Swidan S. Trazodone Loaded Lipid Core Poly (ε-caprolactone) Nanocapsules: Development, Characterization and in Vivo Antidepressant Effect Evaluation. Sci. Rep. [Internet]. 2020 [cited 2021 Nov 10];10:1964. Available from: https://pubmed.ncbi.nlm.nih.gov/32029776/.

[59] EU Publications Office. A biomimetic and neuroprotective delivery nanocapsule for the targeted treatment of post-ischemic stroke effects | BIONICS Project | Fact Sheet | H2020 | CORDIS | European Commission [Internet]. 2020 [cited 2021 Nov 10]. Available from: https://cordis.europa.eu/project/id/793644.

[60] Tang X, Zhu Y, Dai J, et al. Anti-transferrin receptor-modified amphotericin B-loaded PLA-PEG nanoparticles cure Candidal meningitis and reduce drug toxicity. Int. J. Nanomedicine [Internet]. 2015 [cited 2021 Nov 10];10:6227. Available from: https://www.dovepress.com/anti-

transferrin-receptor-modified-amphotericin-b-loaded-plandashpeg-n-peer-reviewed-fulltext-article-IJN.

[61] Barbara R, Belletti D, Pederzoli F, et al. Novel Curcumin loaded nanoparticles engineered for Blood-Brain Barrier crossing and able to disrupt Abeta aggregates. Int. J. Pharm. [Internet]. 2017 [cited 2021 Nov 10];526:413–424. Available from: https://linkinghub.elsevier.com/retrieve/pii/S0378517317304258.

[62] Ojeda-Hernández DD, Canales-Aguirre AA, Matias-Guiu J, et al. Potential of Chitosan and Its Derivatives for Biomedical Applications in the Central Nervous System. Front. Bioeng. Biotechnol. [Internet]. 2020 [cited 2020 Aug 13];8. Available from: /pmc/articles/PMC7214799/?report=abstract.

[63] Bhattamisra SK, Shak AT, Xi LW, et al. Nose to brain delivery of rotigotine loaded chitosan nanoparticles in human SH-SY5Y neuroblastoma cells and animal model of Parkinson's disease. Int. J. Pharm. [Internet]. 2020 [cited 2021 Nov 10];579:119148. Available from: https://linkinghub.elsevier.com/retrieve/pii/S0378517320301320.

[64] Łukasiewicz S, Mikołajczyk A, Szczęch M, et al. Encapsulation of clozapine into polycaprolactone nanoparticles as a promising strategy of the novel nanoformulation of the active compound. J. Nanoparticle Res. [Internet]. 2019 [cited 2021 Nov 10];21:1–16. Available from: https://link.springer.com/article/10.1007/s11051-019-4587-1.

[65] Pissuwan D. Monitoring and tracking metallic nanobiomaterials in vivo. Monit. Eval. Biomater. their Perform. Vivo [Internet]. Elsevier; 2017 [cited 2021 Nov 10]. p. 135–149. Available from: https://linkinghub.elsevier.com/retrieve/pii/B9780081006030000079.

[66] Bastiancich C, Da Silva A, Estève M-A. Photothermal Therapy for the Treatment of Glioblastoma: Potential and Preclinical Challenges. Front. Oncol. [Internet]. 2021 [cited 2021 Nov 10];10. Available from: /pmc/articles/PMC7845694/.

[67] Thomsen LB, Thomsen MS, Moos T. Targeted drug delivery to the brain using magnetic nanoparticles. Ther. Deliv. [Internet]. 2015 [cited 2021 Nov 10];6:1145–1155. Available from: https://pubmed.ncbi.nlm.nih.gov/26446407/.

[68] Ding H, Sagar V, Agudelo M, et al. Enhanced blood–brain barrier transmigration using a novel transferrin embedded fluorescent magneto-liposome nanoformulation. Nanotechnology [Internet]. 2014 [cited 2021 Nov 10];25:055101. Available from: https://pubmed.ncbi.nlm.nih.gov/24406534/.

[69] Saiyed Z, Gandhi N, Nair M. Magnetic nanoformulation of azidothymidine 5’-triphosphate for targeted delivery across the blood–brain barrier. Int. J. Nanomedicine [Internet]. 2010 [cited 2021 Nov 10];5:157. Available from: https://pubmed.ncbi.nlm.nih.gov/20463931/.

[70] Mendiratta S, Hussein M, Nasser HA, et al. Multidisciplinary Role of Mesoporous Silica Nanoparticles in Brain Regeneration and Cancers: From Crossing the Blood–Brain Barrier to Treatment. Part. Part. Syst. Charact. [Internet]. 2019 [cited 2021 Nov 10];36:1900195. Available

from: https://onlinelibrary.wiley.com/doi/full/10.1002/ppsc.201900195.

[71] Song Y, Du D, Li L, et al. In Vitro Study of Receptor-Mediated Silica Nanoparticles Delivery across Blood–Brain Barrier. ACS Appl. Mater. Interfaces [Internet]. 2017 [cited 2021 Nov 10];9:20410–20416. Available from: /pmc/articles/PMC5533093/.

[72] Xu X, Li J, Han S, et al. A novel doxorubicin loaded folic acid conjugated PAMAM modified with borneol, a nature dual-functional product of reducing PAMAM toxicity and boosting BBB penetration. Eur. J. Pharm. Sci. [Internet]. 2016 [cited 2021 Nov 10];88:178–190. Available from: https://pubmed.ncbi.nlm.nih.gov/26965003/.

[73] Vecsernyés M, Fenyvesi F, Bácskay I, et al. Cyclodextrins, Blood–Brain Barrier, and Treatment of Neurological Diseases. Arch. Med. Res. [Internet]. 2014 [cited 2021 Nov 10];45:711–729. Available from: https://linkinghub.elsevier.com/retrieve/pii/S0188440914002690.

[74] Wong KH, Xie Y, Huang X, et al. Delivering Crocetin across the Blood-Brain Barrier by Using γ-Cyclodextrin to Treat Alzheimer's Disease. Sci. Rep. [Internet]. 2020 [cited 2021 Nov 10];10:3654. Available from: https://www.nature.com/articles/s41598-020-60293-y.

[75] Badıllı U, Mollarasouli F, Bakirhan NK, et al. Role of quantum dots in pharmaceutical and biomedical analysis, and its application in drug delivery. TrAC Trends Anal. Chem. 2020;131:116013.

[76] Xu G, Mahajan S, Roy I, et al. Theranostic quantum dots for crossing blood–brain barrier in vitro and providing therapy of HIV-associated encephalopathy. Front. Pharmacol. [Internet]. 2013 [cited 2021 Nov 10];4. Available from: /pmc/articles/PMC3828669/.

[77] Ribovski L, de Jong E, Mergel O, et al. Low nanogel stiffness favors nanogel transcytosis across an in vitro blood–brain barrier. Nanomedicine Nanotechnology, Biol. Med. [Internet]. 2021 [cited 2021 Nov 10];34:102377. Available from: https://linkinghub.elsevier.com/retrieve/pii/S1549963421000204.

[78] Karami Z, Saghatchi Zanjani MR, Hamidi M. Nanoemulsions in CNS drug delivery: recent developments, impacts and challenges. Drug Discov. Today [Internet]. 2019 [cited 2021 Nov 10];24:1104–1115. Available from: https://linkinghub.elsevier.com/retrieve/pii/S1359644618302678.

[79] Fu H, McCarty DM. Crossing the blood–brain-barrier with viral vectors. Curr. Opin. Virol. [Internet]. 2016 [cited 2021 Nov 12];21:87–92. Available from: https://linkinghub.elsevier.com/retrieve/pii/S187962571630102X.

[80] Chen W, Yao S, Wan J, et al. BBB-crossing adeno-associated virus vector: An excellent gene delivery tool for CNS disease treatment. J. Control. Release [Internet]. 2021 [cited 2021 Nov 12];333:129–138. Available from: https://linkinghub.elsevier.com/retrieve/pii/S0168365921001401.

[81] Pattali R, Mou Y, Li X-J. AAV9 Vector: a Novel modality in gene therapy for spinal muscular atrophy. Gene Ther. [Internet]. 2019 [cited 2021 Nov 12];26:287–295. Available from: https://www.nature.com/articles/s41434-019-0085-4.

[82] Cummings J. Lessons Learned from Alzheimer Disease: Clinical Trials with Negative Outcomes. Clin. Transl. Sci. [Internet]. 2018 [cited 2021 Sep 21];11:147–152. Available from: /pmc/articles/PMC5866992/.

*** interesting article to know about CNS trial failures**

[83] Savitz SI, Fisher M. Future of neuroprotection for acute stroke: In the aftermath of the SAINT trials. Ann. Neurol. [Internet]. 2007 [cited 2021 Sep 21];61:396–402. Available from: https://onlinelibrary.wiley.com/doi/full/10.1002/ana.21127.

[84] Wegener G, Rujescu D. The current development of CNS drug research. Int. J. Neuropsychopharmacol. [Internet]. 2013 [cited 2021 Sep 21];16:1687–1693. Available from: https://academic.oup.com/ijnp/article/16/7/1687/713860.

[85] Morofuji Y, Nakagawa S. Drug Development for Central Nervous System Diseases Using In vitro Blood-brain Barrier Models and Drug Repositioning. Curr. Pharm. Des. [Internet]. 2020 [cited 2021 Sep 21];26:1466–1485. Available from: /pmc/articles/PMC7499354/.

7. New nanotechnology strategy to increase ponatinib delivery to the brain.

Type of publication	Article
Title	New nanotechnology strategy to increase ponatinib delivery to the brain
Authors	Bárbara Sánchez-Dengra, María Alfonso, Isabel González-Álvarez, Marival Bermejo, Marta González-Álvarez and Ramón Martínez-Máñez
Journal	Journal of Controlled Release
Impact factor	9.776 (Q1 - Pharmacology and Pharmacy)
Year of publication	
DOI	Under preparation

INTRODUCTION

Unfortunately, from 2000 to 2019, the prevalence of brain and central nervous system (CNS) cancers has increased by 46% [1]. Among these cancers, the glioblastoma is the most common and lethal one, representing more than 50% of all the primary intracranial tumors [2]. The altered astrocytes and oligodendrocytes that form this type of tumor are able to invade the surrounding tissue very quickly and life expectancy is very low, around 15 months after diagnosis [3]. In fact, only 2.7% of the patients survive during 5 years [4–7].

The current treatment of glioblastoma combines surgery, radiation, and adjuvant chemotherapy with temozolomide and, in some cases, in combination with bevacizumab [8,9]. Nonetheless, it has been observed that glioblastoma tumors overexpressed the platelet-derived growth factor receptor-α (PDGFR-α) and the rearranged during transfection (RET), two tyrosine kinases, which may be responsible for the resistance of the glioblastoma tumors to the treatment with temozolomide [10,11]. So, other drugs, which inhibit tyrosine kinases, such as ponatinib, which is currently approved by the US Food and Drug Administration for the treatment of chronic myeloid leukemia and Philadelphia chromosome-positive acute lymphoblastic leukemia, have been proposed as an alternative for the treatment of several malignancies, among which glioblastoma can be found [12].

Despite the potential of ponatinib for treating glioblastoma, the presence of the blood-brain barrier (BBB) is always a limiting step when developing new treatments

directed towards the brain as it restricts the access and distribution of drugs in the CNS. In fact, ponatinib is a drug with a low BBB permeability because it is substrate of efflux transporters and it has a low unbound fraction of drug in plasma and only the fraction of drug that is not bound to proteins is able to cross the BBB [10,13].

The use of nanotechnology to encapsulate the drug and protect it from the efflux transporters and the plasma proteins may constitute a good option to overcome the limitations mentioned above.

In the last years, a lot of researchers have tried to use mesoporous silica nanoparticles (MSNs), which have a high surface area, can load big amounts of cargo, are biocompatible and are easy to functionalize for the development of new nanocarriers [14]. Although, in 2016, an *in vitro* study carried out in two different cell monolayers, which are able to simulate the BBB (MDCK and RBE4 cells), showed that bare MSNs had low permeability and external functionalization was necessary to improve BBB penetration [15]. Thus, just the encapsulation of the drug is not enough, but a functionalization is usually also necessary to increase BBB permeability.

Functionalization can be used to promote any of the accessing routes that the BBB already has: the paracellular diffusion, the transcellular diffusion, the carrier-mediated transport, the receptor-mediated transport, the adsorptive-mediated transport or the cell-mediated transport [16–20]. For instance, the use of amino acids promotes the carrier-mediated transport [20,21], other macromolecules, such as insulin or transferrin, promote the receptor-mediated transport [20,22] and polycationic substances, i.e. albumin and other peptides, promote the adsorptive-mediated transport [20]. The administration of substances that temporally open the BBB is another strategy to increase the access of substances to the CNS by means of promoting the paracellular diffusion. Mannitol, for example, creates a hyperosmolar environment which derives in a reduction in the size of the endothelial cells and a bigger space among them, borneol and other aromatic substances, also open the tight junctions and promote paracellular diffusion, but, in this case, because they provoke the translocation of the tight junctions proteins back to the cytoplasm of the endothelial cells [23].

Furthermore, when trying to treat cancer, functionalization can also be used to foster the active uptake of the nanocarriers by the tumor cells, thus reducing the side effects derived from the internalisation of the anticancer molecules by healthy cells [24]. With this objective, different molecules which are ligands of receptors that are overexpressed in tumor cells can be used: monoclonal antibodies, the antibody antigen-

binding fragments (Fabs), small peptides, natural proteins, aptamers, carbohydrates or small molecules [24]. Folic acid is one of those molecules that has been used to promote the active uptake of nanoparticles by cancer cells, as, due to nutritional requirements, this type of cells overexpress the folate receptor [24–26].

When talking about MSNs, the functionalization is also important to ensure that the drug is kept inside the nanoparticle until it reaches its target where a specific stimulus triggers the drug release. If molecules are used to obtain this type of functionalization, they are known as molecular gates, gate keepers or nanovalves [27,28].

Because of the extremely restrictive properties of the BBB, which only allows the passage of nanoparticles with a diameter below 100 nm [29], some researchers have started to combine the functionalization with the use of an external force to increase the accumulation of drug in the CNS. In this regard, the use of magnetic mesoporous silica nanoparticles (M-MSNs) with which an external magnetic field can be used to promote the BBB permeation are promising devices for treating pathologies affecting the CNS [30–32].

The objective of this work was to develop two new mesoporous nanostructures, a magnetic and a non-magnetic one, doubly functionalized, with borneol and folic acid, as molecular gate, to increase the access of ponatinib to the CNS and, thus, improve the treatment of glioblastoma.

MATERIALS AND METHODS

1. Drugs, cells and products

Ponatinib was purchased from Enamine (Riga, Latvia). Trypan blue, borneol, succinic anhydride and folic acid were purchased from Sigma-Aldrich (Barcelona, Spain). Cetyltrimethylammonium bromide (CTAB), diethanolamine (DEA), Tetraethylorthosilicate (TEOS), (3-aminopropyl)triethoxysilane (APTES), N-(3-dimethylaminopropyl)-N'-ethylcarbodiimide (EDC), N-hydroxysuccinimide (NHS), 4-dimethylaminopiridine (DMAP), $FeCl_3 \cdot 6H_2O$, $FeCl_2 \cdot 4H_2O$, oleic acid and anhydrous acetonitrile (ACN) were purchased from Sigma-Aldrich (Madrid, Spain). Chloroform, dimethylformamide (DMF), and anhydrous methylene chloride (DCM) were purchased from Acros Organics (Spain). Ammonia (32% v/v), ethanol, dimethyl sulfoxide (DMSO) and ethyl acetate were purchased from Scharlab (Barcelona, Spain).

Lysosomal extract was given by Dr. Martinez-Mañez (Valencia, Spain). The MDCK-MDR1 cell line was kindly provided by Dr. Gottesman, MM (National Institutes of Health,

Bethesda) and the U87 cell line was purchased from Sigma-Aldrich (Barcelona, Spain).

Dulbecco's modified Eagle's medium (DMEM) with high content of glucose, fetal bovine serum (FBS), MEM Non-Essential aminoacids, penicillin−streptomycin, L-glutamine, HEPES, phosphate buffer solution (PBS), trypsin-EDTA, Hank's balanced salt solution (HBSS), tween 80 and the cell proliferation kit I (MTT) were purchased from Sigma-Aldrich (Barcelona, Spain). DMEM with high content of glucose and high content of pyruvate used with the U87-MG cell line was obtained from Gibco (Barcelona, Spain).

2. Synthesis of mesoporous nanoparticles

2.1. Nonmagnetic mesoporous silica nanoparticles (MSNs)

Nonmagnetic mesoporous silica nanoparticles (MSNs) were prepared using as a basis the protocol described in [33]. Briefly, 1 g of CTAB and 20 mL of deionized water were placed in a two neck round bottom flask and stirred for 30 minutes at 500 rpm with a rugby shape magnet. Then, 160 µL of DEA were added and temperature was increased to 95 °C, temperature at which the mixture was stirred with reflux for 1 hour. After that time, 1.5 mL of TEOS were added dropwise and everything was again stirred for 1 hour, but at 950 rpm. Finally, the particles were recovered and washed with water at 13400 *g* (20 min) until reaching a neutral pH. The particles were then dried and calcined in the presence of air at 550 °C.

2.2. Ultrasmall superparamagnetic iron oxide nanoparticles (USPIONs)

Ultrasmall superparamagnetic iron oxide nanoparticles (USPIONs), which were used later on, as seeds for preparing magnetic mesoporous silica nanoparticles (M-MSNs), were prepared according to the protocol described in [34]. First, 50 mL of deionized water were placed under Argon atmosphere for 30 minutes. Then, 12 g of $FeCl_3 \cdot 6H_2O$, 4.9 g of $FeCl_2 \cdot 4H_2O$ and 19.53 mL of ammonia 32% (v/v) were added at 80 °C. After 30 minutes, 2.13 mL of oleic acid was added to the flask and the reaction was left stirring for 90 minutes at 80 °C. Finally, the particles were cooled at room temperature and recovered after washing 3 times with deionized water and 3 times with ethanol (12108 *g*, 10 min). The material was dried overnight under vacuum and the next day it was resuspended in chloroform to be kept it in the fridge until its use.

2.3. Magnetic mesoporous silica nanoparticles (M-MSNs)

M-MSNs were prepared following a slightly modified protocol already described

in [34]. 100 mg of CTAB and 10 mL of deionized water were placed in a vial and the mixture was stirred until the CTAB was dissolved. Then, 580 µL of a previously prepared suspension of USPIONs in chloroform (Fe concentration = 3.6 mg/mL) was added to the vial and it was sonicated with a probe sonicator (Branson 450 Sonifier) for 3 minutes. After sonication, chloroform was evaporated at 70 °C with manual agitation and 30 mL of deionized water, 0.547 mL of ammonia 32% (v/v) and the particles were placed in a two neck round bottom flask where the mixture was stirred at 400 rpm with reflux and a rugby shape magnet until the temperature reached 75 °C. Later on, 0.5 mL of TEOS and 3 ml of ethyl acetate were added to the flask (TEOS, dropwise) and the reaction was stirred for 2 minutes at 850 rpm and for 3 hours at 350 rpm. At the end of that time, the particles were cooled in an ice bath and they were washed 3 times with ethanol (13400 *g*, 10 min). Finally, the magnetic particles were separated from the non-magnetic ones with a magnet, they were dried and calcined in the presence of air at 550 °C.

3. Drug loading and functionalization of the nanoparticles

MSNs and M-MSNs were loaded following the immersion protocol, in which the particles are left stirring overnight in a solution of drug ((0.8 mmol of drug + 30 mL of solvent)/1 g nanoparticle)). Two different molecules were loaded in the particles: trypan blue and ponatinib, as trypan blue is soluble in water the solvent used for loading the particles was deionized water and as ponatinib is not soluble in water, but soluble in DMSO, this one was the solvent used for dissolving ponatinib. The day after loading, the particles were filtered and dried under vacuum.

Once loaded, both MSNs and M-MSNs were functionalized following the same protocol with the aim of obtaining double gated nanoparticles with: borneol and folic acid.

First, for allowing borneol to attach to the nanoparticles it was modified with succinic acid as done in [26]. Once this component was prepared, particles were reacted with APTES for 5.5 hours in anhydrous ACN ((6 mmol APTES + 30 mL of solvent)/1 g nanoparticles). Then, the particles were vacuum filtered and dried and they were made to react with gate components overnight. So, the following compounds were placed in a vial and left stirred overnight: modified borneol (0.3 mmol/100 mg nanoparticles), folic acid (0.3 mmol/100 mg nanoparticles), EDC (3 mmol/100 mg nanoparticles), NHS (3 mmol/100 mg nanoparticles), DMF (3 mL/100 mg nanoparticles) and DMSO (1 mL/100 mg nanoparticles). Finally, the particles were washed 4 times with DMF and 4 times with deionized water and dried at 37 °C.

4. Characterization of the nanoparticles

4.1. Dynamic light scattering (DLS)

Dynamic light scattering (DLS) experiments were conducted with a Zetasizer Nano ZS (Malvern Instruments). This technique was used for measuring the hydrodynamic size, the polydispersity index (PDI) and the Z potential of the particles. Suspensions of 1 mg/mL of nanoparticles were prepared in water and the characteristics mentioned above were measured thrice.

4.2. Transmission electron microscopy (TEM)

The proper size and shape of the MSNs and M-MSNs were checked in a 100 kV JEOL JEM-1010 transmission electronic microscope operated with AMT image capture engine software.

4.3. X-ray Powder Diffraction Analysis

The X-ray diffractograms of the USPIONS, the MSNs and the M-MSNs (as-made, calcined, calcined and functionalized with borneol and folic acid and loaded with trypan blue and functionalized with borneol and folic acid) were obtained with a Bruker D8 Advance diffractometer (Bruker, Coventry, UK).

4.4. Porosimetry

A Micromeritics TriStar II Plus automated analyser (Micromeritics Instrument Corporation, Norcross, GA, USA) was used for recording the N_2 adsorption–desorption isotherms of the MSNs and the M-MSNs. The samples were degassed at 120 °C in vacuum overnight. A BET model was used for calculating the specific surface areas from the adsorption data in the low-pressure range. On the other hand, the BJH method was used to determine the size and volume of the pores present in the particles.

4.5. Thermogravimetry

A TGA/SDTA 851e thermobalance from Mettler Toledo (Mettler Toledo Inc., Schwarzenbach, Switzerland) was used to obtain thermograms for different solid samples and evaluate the organic content in loaded and functionalized nanoparticles. So, the % of drug loaded in the MSNs and the M-MSNs could be obtained. Briefly, samples were heated in a dynamic step at 10 °C/min, from 25 °C to 100 °C. Then temperature was maintained at 100 °C for 60 mins and temperature was increased again until 1000 °C at 10 °C/min.

Samples were kept at 1000 °C for 30 minutes. Total organic content was evaluated in the range between 100 and 800 °C.

5. *In vitro* drug release

Release studies were carried out at 37 °C for both types of nanoparticles, MSNs and M-MSNs, loaded with trypan blue and ponatinib. First, a suspension of each type of particles, with a particle concentration of 10 µg/µL was prepared in PBS and it was divided into two eppendorfs. Then, PBS or lysosomal extract were added until reach a final concentration of particles of 1 µg/µL. Samples were taken at different times (2', 30', 1h, 2.5h, 4h and 5.5h). They were diluted with cold methanol, centrifuged (5 mins; 10000 rpm - Eppendorf Centrifuge 5424, Rotor FA-45-24-11) and kept in the freezer at -20 °C until their analysis.

6. Cytotoxicity assay *in vitro*

The cytotoxicity of the MSNs and the M-MSNs functionalized with borneol and folic acid and loaded with ponatinib and functionalized with borneol and folic acid was evaluated in two different cell types (U87-MG, glioblastoma cells and MDCK-MDR1, BBB cells) using an MTT kit.

MDCK-MDR1 cells were maintained in an incubator at 37 °C with an atmosphere of 5% CO2 and 90% humidity inside flasks of 75 cm^2 with DMEM with a high content of glucose completed with FBS (10% (v/v)), MEM Non-Essential aminoacids (1% (v/v)), penicillin−streptomycin (1% (v/v)), L-glutamine (1% (v/v)) and HEPES (1% (v/v)). U87-MG cells were kept using the same protocol as MDCK-MDR1, but with a cell culture medium with a higher concentration of pyruvate. When the cells reached 80% confluence, they were split and sub-cultured in new flasks. For detaching them and allowing the sub-culturing procedure a trypsin-EDTA:PBS (2:8) solution was used. The day after sub-culturing the medium of the flasks was replaced with new fresh medium to remove all the dead cells.

The protocol for carrying out the cytotoxicity assay is explained below:

1) 100 µL of cells were seeded in each well of a 96-well plate (2.5 x 10^4 cells/well).
2) After 24 hours at 37 °C, the medium was removed and replaced with 100 µL of a ponatinib solution or a particle suspension with ponatinib concentration ranging from 0.002 to 200 µM.
3) After 72 hours, the solutions/suspensions were aspirated and replaced with 100

µL of fresh culture medium. Then, 10 µL of the MTT labelling reagent were added to the wells and cells were kept in the incubator for 4 hours.

4) 100 µL of solubilization solution was added to the plates and incubated overnight.
5) Finally, the absorbance of the plate was measured at 570 and 630 nm using a microplate reader (Microplate Reader MB-850, Heales®).

7. BBB permeability

The penetrability of the formulations (MSN and M-MSN) was evaluated in MDCK-MDR1 monolayers. Cells were seeded in 6-transwell plates with a pore size of 0.4 micron, an effective area of 4.2 cm^2 and a pore density of (100 ± 10) x 10^6 pores/cm^2 and they were maintained, changing the culture medium every 2 days, during 8 days until confluence. Once, the cells were confluent (TEER = 120-140 kΩ/cm^2), the permeability study was carried out using an orbital shaker at 37 °C and 100 rpm.

Standard experiments from apical to basolateral were developed using an initial concentration of trypan blue of 10 and 30 µM and an initial concentration of ponatinib of 10 and 20 µM. In the experiments with the M-MSNs, circular neodymium magnets were placed under each well. Samples were taken from basolateral at 15, 30, 60, 90, 120, 180 and 240 minutes and the mass balance was checked by means of taking two samples from apical at time 0 and 240 minutes, a sample of the particles adhered to the cells and a sample after disrupting the cells with methanol. Samples were kept at -20 °C until their analysis.

8. Biodistribution *in vivo*

The biodistribution of the particles was evaluated in rats. The *in vivo* experiments were approved by the ethical committee of Miguel Hernández University (2021/VSC/PEA/0133 type 2).

After intraperitoneal anaesthesia, healthy wistar rats (≈ 300 g) were administered intravenously or intranasally with a solution of ponatinib or a suspension of MSNs or M-MSNs loaded with ponatinib with a concentration of drug of 3 mg/kg. The rats were previously cannulated at the jugular vein to allow intravenous administration and blood sampling. In addition, the skull of the rats which received the M-MSNs was shaved and a neodymium magnet was attached in between the ears and the eyes. In the intravenous pathway, 5 mL/kg of solvent (DMSO:Tween 80:PBS; 2:1:7) were used to administer the drug as done in [10]; and in the intranasal administration, 20 µL/nostril of the same solvent

mixture were used [35]. At different times, blood samples were taken by the cannula. In addition, when the animals were euthanized, its blood was removed with physiological serum and their brains and other organs were extracted to evaluate the amount of drug present on them. Proteins were precipitated using cold methanol and in the half of the samples, particles were forced to be opened with sodium hydroxide with DMSO (1 %, v/v) and the other half did not receive sodium hydroxide with DMSO (1 %, v/v). All the samples were kept at -20 °C until their analysis.

9. Analysis of the samples

Trypan blue was analysed by HPLC using a Waters 2695 separation module, a Waters 2487 UV detector and a XBridge C18 column (3.5 µM, 4.6 x 100 mm) (Spain). The method used was previously validated its characteristics are summarized in table 1. Ponatinib samples were sent to Valencia University to be analysed in a QTRAP 6500+ LC-MS/MS System.

Molecule	λ (nm)	Mobile phase	Retention time (min)	Flow rate (mL/min)	T (°C)	Injection volume (µL)	r^2
Trypan blue	300	20% H_2O 80% ACN	0.750	1	30	90	0.998

Table 1. HPLC method for detecting Trypan Blue.

RESULTS AND DISCUSSION

In this work, two different types of nanoparticles, to increase the access of drugs to the CNS, were prepared: MSNs and M-MSNs. Figure 1 shows TEM images of both types of particles. It can be observed that MSNs (figure 1A) have a grape form and a particle size which corresponds with the one obtained in the article from which the synthesis method was extracted [33]. In figure 1B, a core-shell structure can be observed in which the magnetic core is surrounded by mesoporous material which creates wormhole-like channels as reported in literature [34].

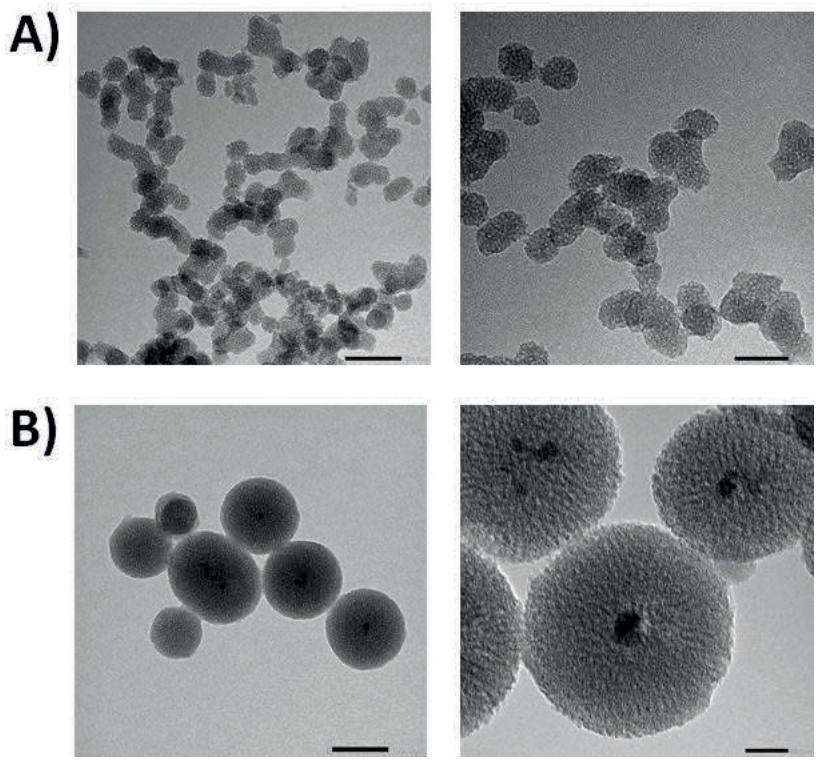

Figure 1. TEM images of **A)** MSNs and **B)** M-MSNs.

The hydrodynamic diameter, the surface charge and the polydispersity of the particles were analysed in a Zetasizer (Figure 2). Both types of particles have a negative charge on their surface once they are prepared and calcined, but once they are functionalized with borneol and folic acid, the charge becomes positive with independence of the loading. In terms of side, the MSNs are smaller than the M-MSNs, but they have a greater polydispersion index, so the batch is less homogeneous. In any case, the real particle size, measured by TEM, is below 100 nm, which allows the particles to cross the BBB [29].

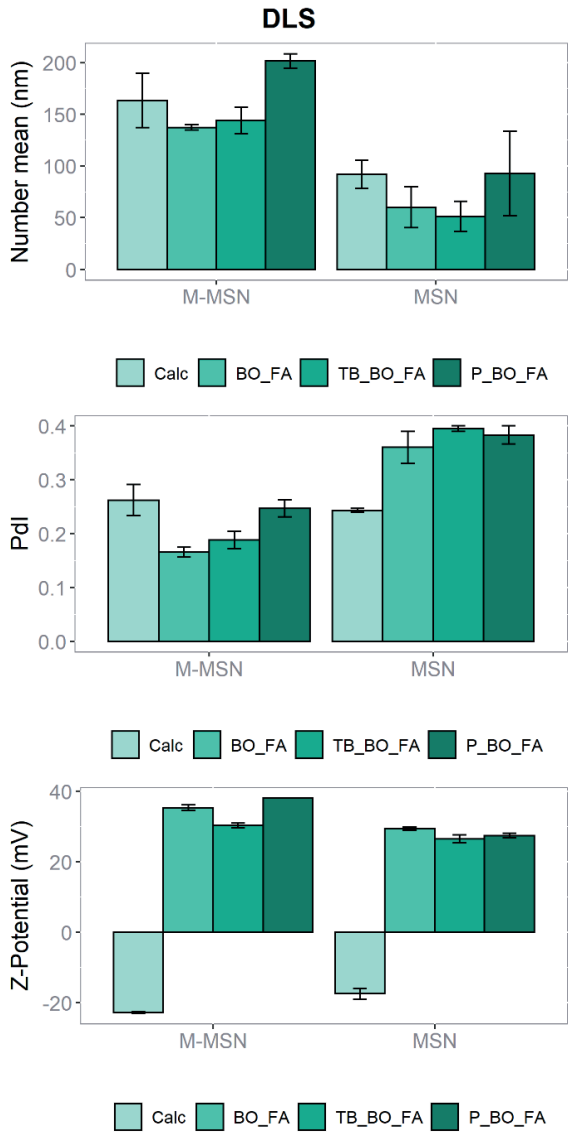

Figure 2. Dynamic light scattering (DLS) results of MSNs and M-MSNs. Calc = calcined, BO_FA = calcined and functionalized with borneol and folic, TB_BO_FA = calcined, loaded with trypan blue and functionalized with borneol and folic and P_BO_FA = calcined, loaded with ponatinib and functionalized with borneol and folic

Figure 3 shows the X-ray diffractograms (XRDs) for the USPIONS, the MSNs and the M-MSNs (as-made, calcined, calcined and functionalized with borneol and folic acid and loaded with trypan blue and functionalized with borneol and folic acid). The magnetic seeds have 6 different peaks whose position and intensity agree with the Bragg reflections of magnetite [34]. On the other hand, the MSNs and the M-MSNs show just one clear peak, which is due to the non-ordered structure of the MSNs and the radial growth of the shell in the M-MSNs [34].

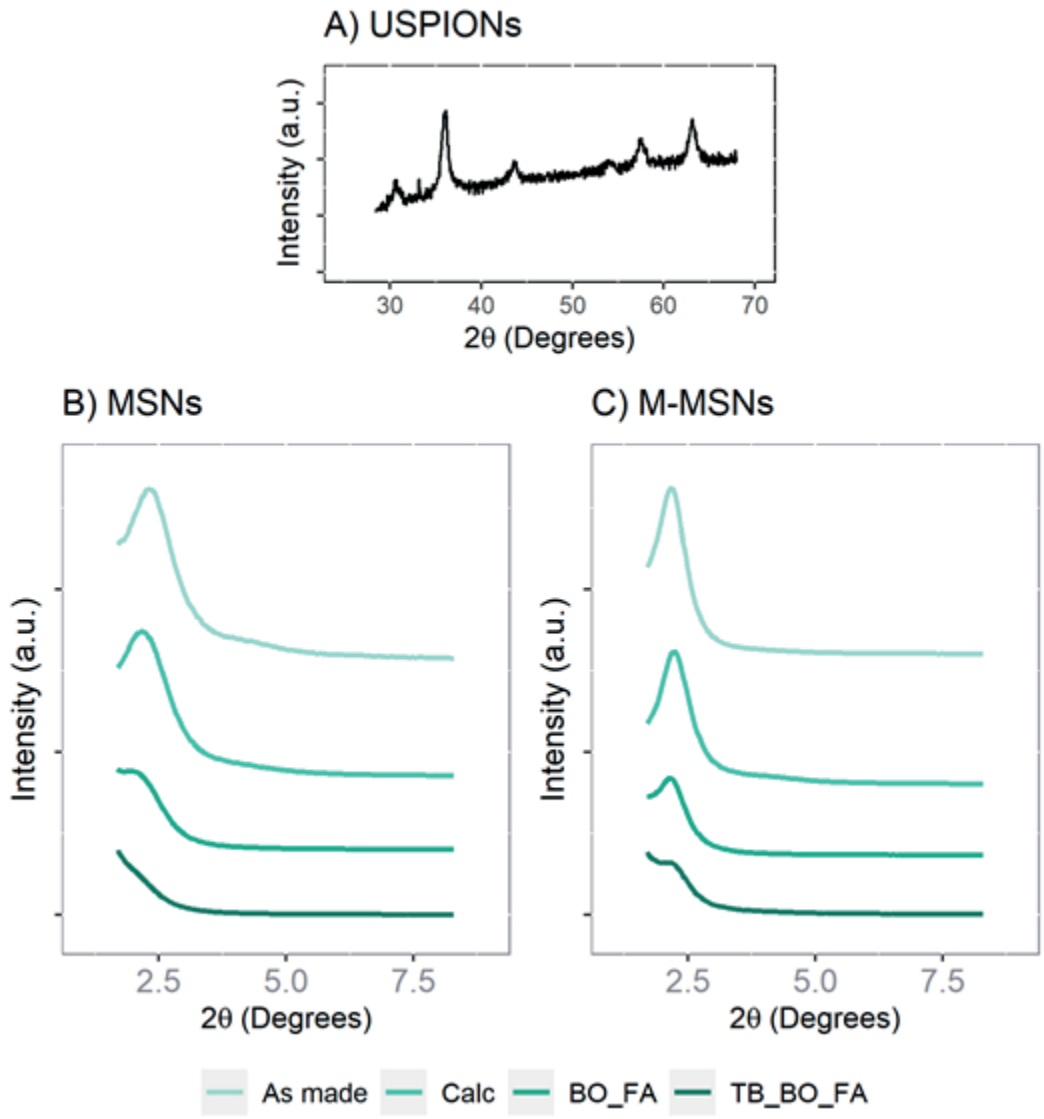

Figure 3. XRDs for **A)** USPIONs, **B)** MSNs and **C)** M-MSNs. Calc = calcined, BO_FA = calcined and functionalized with borneol and folic and TB_BO_FA = calcined, loaded with trypan blue and functionalized with borneol and folic.

The porosimetry analysis showed that, after being prepared and calcined, both types of particles (MSNs and M-MSNs) have similar surface area, pore volume, and pore size (table 2). In addition, as seen in figure 4, the adsorption and desorption isotherms are also very similar and are type IV, which corresponds to mesoporous material [36]. Furthermore, when doing the porosimetry of the nanoparticles with the borneol and folic acid gate, it can be seen that it covers the pores since the adsorption and desorption isotherms decrease and the peak of the pores disappears in the volume-size distribution (figure 4).

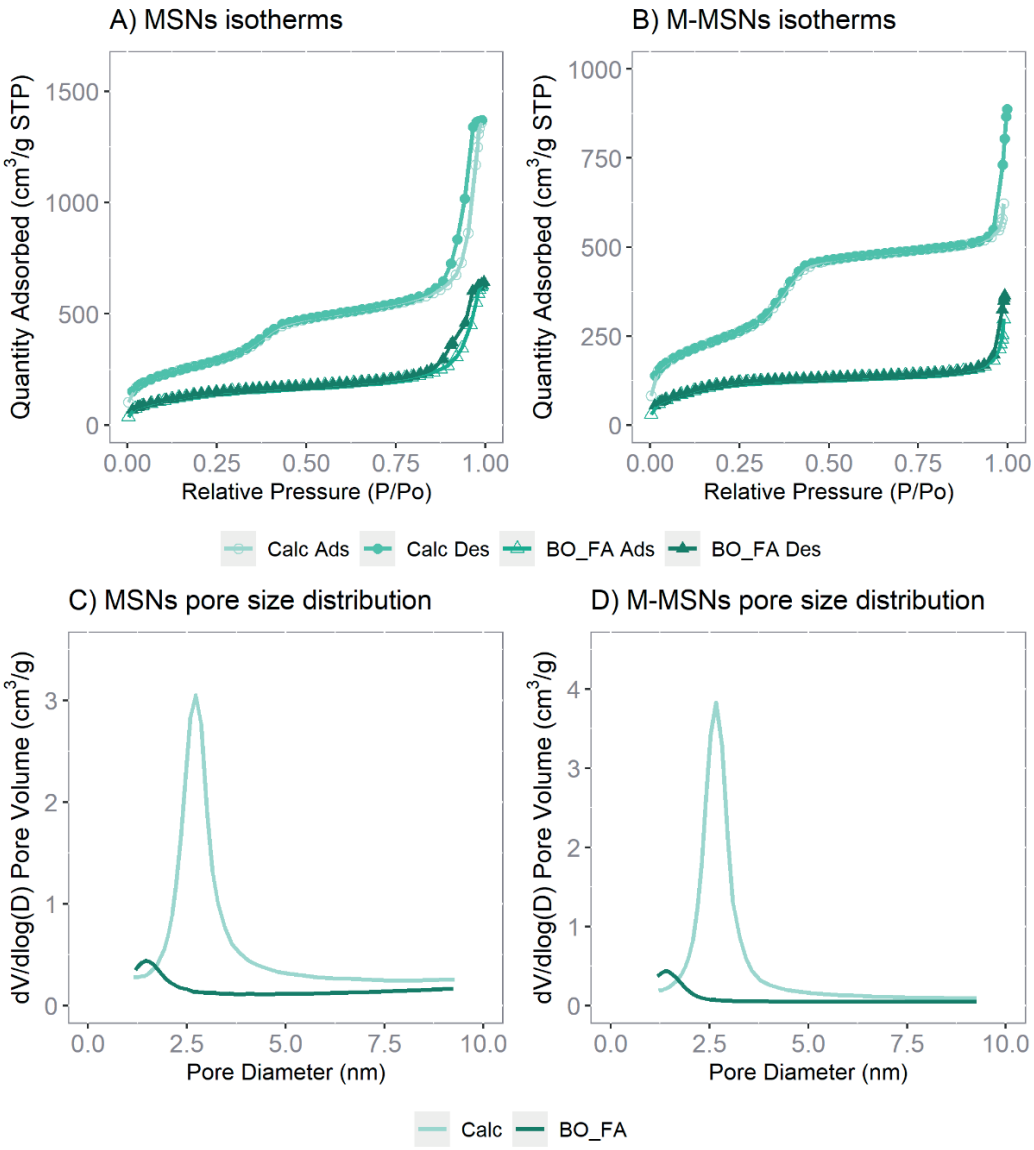

Figure 4. Porosimetry characterization for MSNs and M-MSNs. Calc = calcined, BO_FA = calcined and functionalized with borneol and folic, Ads = adsorption and Des = desorption.

Nanoparticle	BET surface area (m^2/g)	BJH Adsorption pore volume (cm^3/g)	BJH Adsorption pore size (nm)
Calcined MSNs	989.317	0.858	2.919
Calcined M-MSNs	896.343	0.802	2.871

Table 2. Mean %PE for the fitted and simulated brain profiles.

Finally, the last characterization was done by thermogravimetry and gave as a result the organic content of the particles, that is the content of drug loaded in each type of nanoparticle. This result is summarized in table 3.

	Trypan Blue (%)	Ponatinib (%)
Final MSNs	11.43	19.04
Final M-MSNs	13.86	14.84

Table 3. Content of trypan blue and ponatinib in each type of nanoparticle, once calcined and functionalized with borneol and folic acid.

Once the particles were prepared and characterized, the ability of the gate to keep the drug inside them and release it when they are in contact with the correct stimulus was evaluated with an *in vitro* release test. Figure 5 shows the release profiles for both the MSNs and the M-MSNs loaded with trypan blue (figure 5A) or with ponatinib (figure 5B). It can be seen that, when the particles are resuspended in PBS, there is not any released drug, but when they are in touch with an excess of lysozymes, from lysosomal extract, the content of the particles is rapidly released. Profiles were described with a Weibull kinetics model.

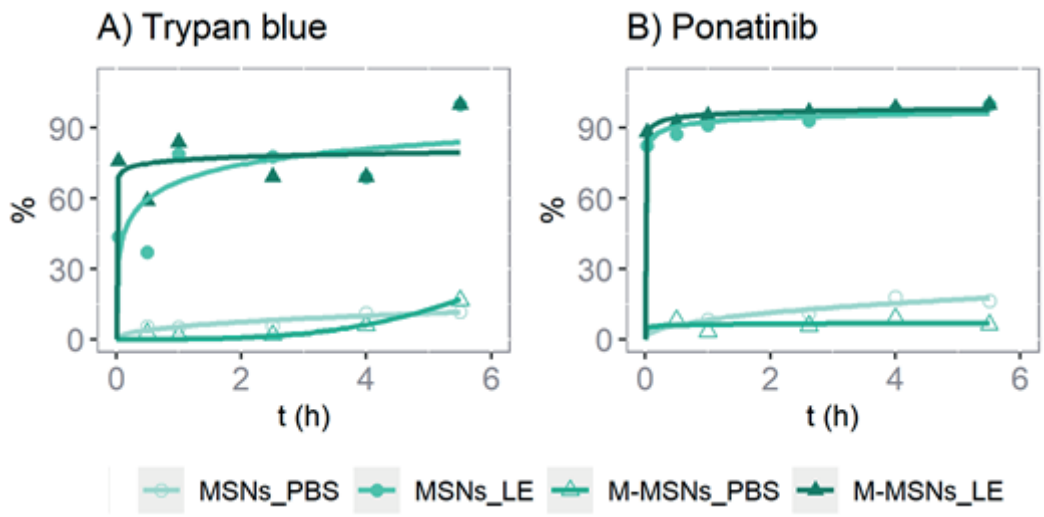

Figure 5. Release profiles for the different nanoparticles with and without stimulus to open the borneol and folic acid gate. LE = lysosomal extract.

In terms of cytotoxicity, two types of study were carried out. First, as it can be seen in figures 6A and 6B, the lack of toxicity of the empty nanoparticles functionalized with borneol and folic acid was evaluated in an *in vitro* BBB model (MDCK-MDR1) and in an *in vitro* glioblastoma model (U87-MG). In figures 6A and 6B, it can be observed that at the highest concentrations tested, 20 and 200 µM, the free Ponatinib is able to kill both types of cells, as it was previously observed by Zhang *et al*. in 2014 [37]. Nonetheless, neither

the empty nanoparticles nor the loaded ones, reduce the viability of the cells at any concentration after 72 hours. This fact confirms that both, the case and the gate of the particles, are not toxic. Besides that, the lack of toxicity of the particles loaded with ponatinib may be explained by the presence of low levels of lysosomes in the *in vitro* culture. So, an extra assay was carried out in the U87-MG cell line after resuspending the particles in lysosomal extract (figure 6C). In this second case, MSNs and M-MSNs with lysozymes are able to kill the glioblastoma cells at the highest concentration tested and, although, the levels of toxicity are not as high as the ones obtained with the free drug, this can be explained by the difficulties of the drug in getting out of the nanoparticle.

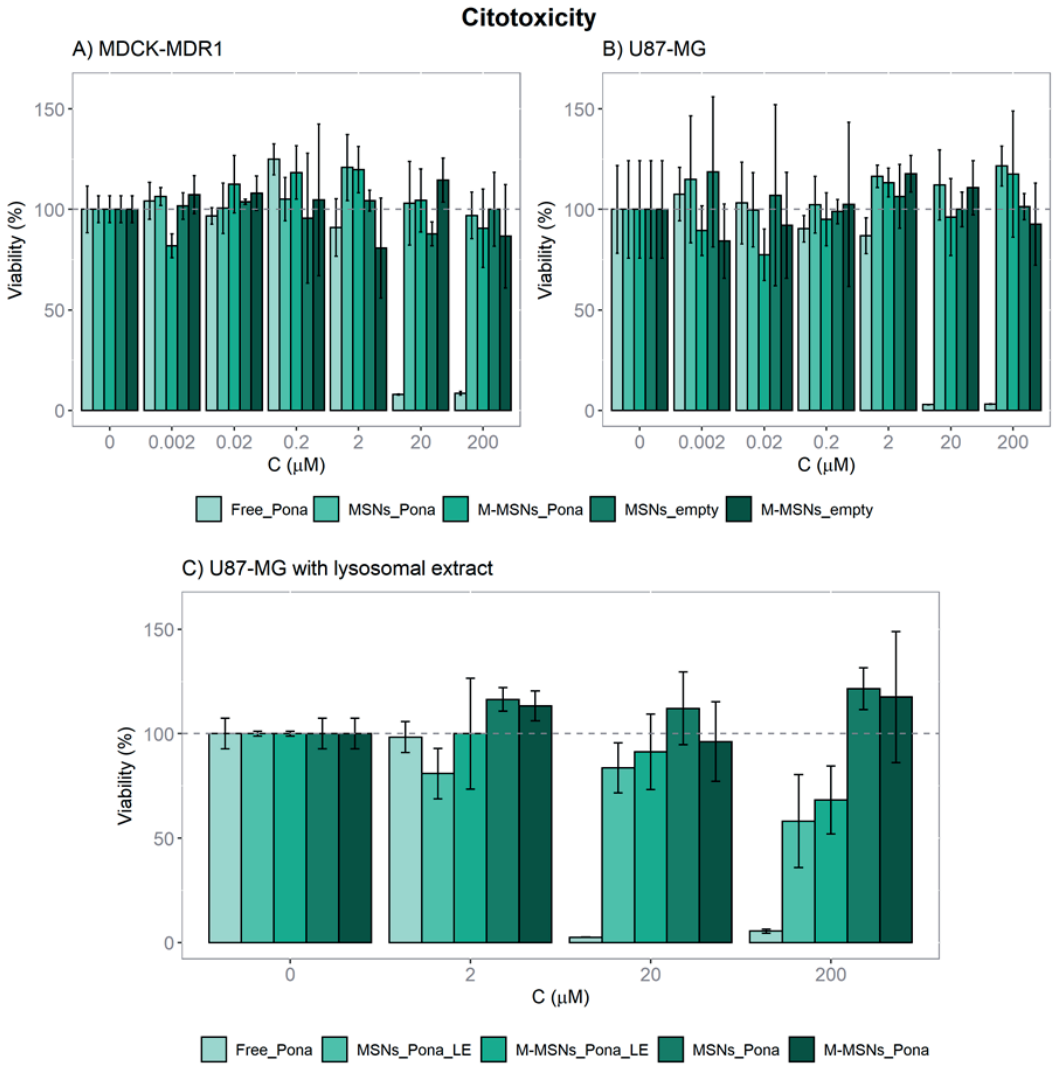

Figure 6. Cytotoxicity results obtained with an MTT assay in **A)** an *in vitro* BBB model and **B)** an *in vitro* glioblastoma model after administering different concentrations of free drug, empty nanoparticles and loaded nanoparticles. **C)** Efficacy results when adding lysosomal extract with the loaded nanoparticles. Pona = ponatinib, LE = lysosomal extract.

When evaluating the *in vitro* BBB permeability of the nanoparticles, it was observed that just in the case of the ones loaded with ponatinib there is a slight increment of the influx clearance (figure 7). Theoretically, both molecules, trypan blue and ponatinib have low access to the CNS. In fact, trypan blue was used in the 20th century when the BBB was discovered as it was observed that after an intravenous injection of this dye, the brain and the spinal cord were not stained [38]. Nonetheless, the toxicity of trypan blue in cell cultures has also been described [39–41], so it is considered that the high permeability rates obtained with both the free trypan blue and the trypan blue loaded in the nanoparticles are due to that toxicity which may alter the tight junctions in the monolayers. Ponatinib is substrate of efflux transporters and it has a low $f_{u,plasma}$ [10]. In this *in vitro* test, the particles increase the permeability rate of this drug, because they prevent the drug from binding to the efflux transporters and they open the tight junctions due to the presence of borneol [23].

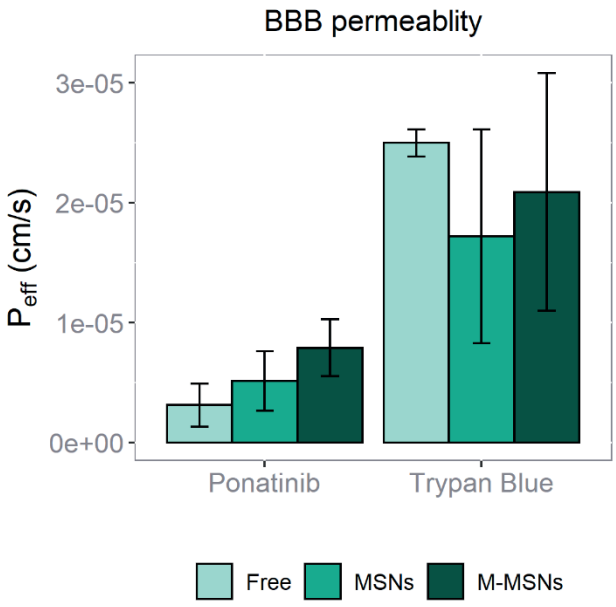

Figure 7. *In vitro* BBB permeability of ponatinib and trypan blue tested in MDCK-MDR1 monolayers as free drug or in MSNs and M-MSNs.

The MSNs and the M-MSNs loaded with ponatinib were selected to evaluate the *in vivo* biodistribution in rats. These studies revealed that the particles were not able to cross the BBB after being administered intravenously. Nonetheless, when the administration was done via intranasal a clear increase in the accumulation of drug in the brain was observed with both, the MSNs and the M-MSNs, in comparison to the free ponatinib (figure 8) and no drug was detected in the rest of the organs.

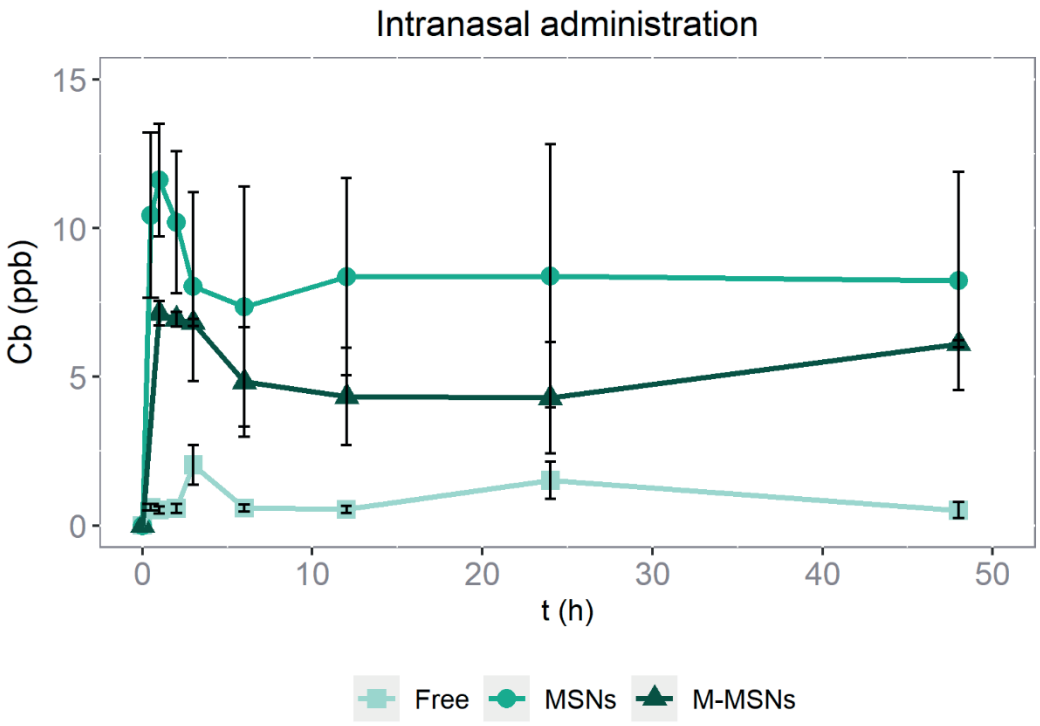

Figure 8. Brain profiles obtained after the intranasal administration of a free ponatinib solution or MSNs and M-MSNs loaded with ponatinib suspensions (Dose = 3 mg/kg).

In figure 8, it can be observed how the use of the nanoparticles increases both the penetration and the retention of ponatinib in the brain of the rats after a single intranasal administration. Probably, it is because the particles are better adhered to the nasal mucosa than the free drug, which may be expelled out of the nostrils or moved down to the respiratory system. Specifically, it can be observed that, after 48 hours, the concentration of ponatinib after the administration of MSNs is 8.9 times the concentration of free ponatinib and after the administration of M-MSNs it is 4.1 times the concentration of free ponatinib. One could expect a greater accumulation when the M-MSNs are used, due to the additional force of the magnet, but it is also true that this type of particle was bigger than the MSNs (figure 1 and 2). In fact, in 2020, a study carried out with a "nose-brain" *in vitro* cell model, showed that the cut-off point for silver nanoparticles to have good access to the brain through the nasal epithelium was 60 nm [42] and, according to the TEM images, the MSNs prepared in this thesis were below 60 nm, but the M-MSNs were above this limit. In addition, the presence of the USPIONs in the core of the M-MSNs can promote its aggregation, increasing even more the final size of the particles present in the administered suspension and hindering the passage to the CNS.

CONCLUSION

Considering all the results presented previously, it can be concluded that two new mesoporous nanostructures, a magnetic and a non-magnetic one, which increase the access of ponatinib to the CNS via intranasal have been developed, characterized and adequately evaluated *in vitro* and *in vivo*. Both of them constitute promising delivery systems in the treatment of glioblastoma, the most lethal brain tumor worldwide.

ACKNOWLEDGEMENTS

Funding: This work was supported, in part, by the project: "Modelos *in vitro* de evaluación biofarmacéutica" [SAF2016-78756 (AEI/FEDER, EU)] funded by Agencia Estatal Investigación and European Union, through FEDER (Fondo Europeo de Desarrollo Regional). Bárbara Sánchez-Dengra received a grant from the Ministry of Science, Innovation and Universities of Spain [FPU17/00530] and a complementary grant from the Ministry of Science, Innovation and Universities of Spain [EST19/00010].

References

[1] Global Burden of Disease Collaborative Network. Global Burden of Disease Study 2019 (GBD 2019) Results. 2020. http://ghdx.healthdata.org/gbd-results-tool (accessed September 9, 2021).

[2] Osama M, Nasr Mostafa M, Ali Alvi M. Astrocyte Elevated Gene-1 as a Novel Therapeutic Target in Malignant Gliomas and Its Interactions with Oncogenes and Tumor Suppressor Genes. Brain Res 2020:147034. https://doi.org/10.1016/j.brainres.2020.147034.

[3] American Association of Neurological Surgeons. Glioblastoma Multiforme n.d. https://www.aans.org/en/Patients/Neurosurgical-Conditions-and-Treatments/Glioblastoma-Multiforme (accessed August 5, 2020).

[4] Kang YJ, Cutler EG, Cho H. Therapeutic nanoplatforms and delivery strategies for neurological disorders. Nano Converg 2018;5. https://doi.org/10.1186/s40580-018-0168-8.

[5] Startoncology. Central nervous system gliomas 2016. http://www.startoncology.net/professional-area/cns-gliomas/?lang=en (accessed November 30, 2019).

[6] Thakkar J, Peruzzi P, Prabhu V. Glioblastoma Multiforme: Symptoms, Diagnosis and Treatment Options n.d. https://acortar.link/fdTpDR (accessed November 30, 2019).

[7] Grill J. Orphanet: Glioblastoma 2007. https://www.orpha.net/consor/cgi-bin/Disease_Search.php?lng=EN&data_id=3752 (accessed November 30, 2019).

[8] Tan AC, Ashley DM, López GY, Malinzak M, Friedman HS, Khasraw M. Management of glioblastoma: State of the art and future directions. CA Cancer J Clin 2020;70:299–312. https://doi.org/10.3322/caac.21613.

[9] Ostrom QT, Gittleman H, Xu J, Kromer C, Wolinsky Y, Kruchko C, et al. CBTRUS Statistical Report: Primary Brain and Other Central Nervous System Tumors Diagnosed in the United States in 2009–2013. Neuro Oncol 2016;18:v1–75. https://doi.org/10.1093/neuonc/now207.

[10] Laramy JK, Kim M, Parrish KE, Sarkaria JN, Elmquist WF. Pharmacokinetic assessment of cooperative efflux of the multitargeted kinase inhibitor ponatinib across the blood-brain barrier. J Pharmacol Exp Ther 2018;365:249–61. https://doi.org/10.1124/jpet.117.246116.

[11] Laramy JK, Kim M, Gupta SK, Parrish KE, Zhang S, Bakken KK, et al. Heterogeneous Binding and Central Nervous System Distribution of the Multitargeted Kinase Inhibitor Ponatinib Restrict Orthotopic Efficacy in a Patient-Derived Xenograft Model of Glioblastoma. J Pharmacol Exp Ther 2017;363:136–47. https://doi.org/10.1124/jpet.117.243477.

[12] Tan FH, Putoczki TL, Stylli SS, Luwor RB. Ponatinib: a novel multi-tyrosine kinase inhibitor against human malignancies. Onco Targets Ther 2019;Volume 12:635–45. https://doi.org/10.2147/OTT.S189391.

[13] DrugBank. Ponatinib: Uses, Interactions, Mechanism of Action n.d.

https://go.drugbank.com/drugs/DB08901 (accessed January 18, 2022).

[14] Alexander A, Agrawal M, Uddin A, Siddique S, Shehata AM, Shaker MA, et al. Recent expansions of novel strategies towards the drug targeting into the brain . Int J Nanomedicine 2019;Volume 14:5895–909. https://doi.org/10.2147/ijn.s210876.

[15] Mendiratta S, Hussein M, Nasser HA, Ali AAA. Multidisciplinary Role of Mesoporous Silica Nanoparticles in Brain Regeneration and Cancers: From Crossing the Blood–Brain Barrier to Treatment. Part Part Syst Charact 2019;36:1900195. https://doi.org/10.1002/ppsc.201900195.

[16] Teleanu DM, Negut I, Grumezescu V, Grumezescu AM, Teleanu RI. Nanomaterials for drug delivery to the central nervous system. Nanomaterials 2019;9. https://doi.org/10.3390/nano9030371.

[17] Lu CT, Zhao YZ, Wong HL, Cai J, Peng L, Tian XQ. Current approaches to enhance CNS delivery of drugs across the brain barriers. Int J Nanomedicine 2014;9:2241–57. https://doi.org/10.2147/IJN.S61288.

[18] Chen Y, Liu L. Modern methods for delivery of drugs across the blood-brain barrier. Adv Drug Deliv Rev 2012;64:640–65. https://doi.org/10.1016/j.addr.2011.11.010.

[19] Gabathuler R. Approaches to transport therapeutic drugs across the blood-brain barrier to treat brain diseases. Neurobiol Dis 2010;37:48–57. https://doi.org/10.1016/j.nbd.2009.07.028.

[20] Sánchez-Dengra B, González-Álvarez I, Bermejo M, González-Álvarez M. Nanomedicine in the Treatment of Pathologies of the Central Nervous System Advances in Nanomedicine. Adv. Nanomedicine, 2020.

[21] Ohtsuki S, Terasaki T. Contribution of Carrier-Mediated Transport Systems to the Blood–Brain Barrier as a Supporting and Protecting Interface for the Brain; Importance for CNS Drug Discovery and Development. Pharm Res 2007;24:1745–58. https://doi.org/10.1007/s11095-007-9374-5.

[22] Pulgar VM. Transcytosis to cross the blood brain barrier, new advancements and challenges. Front Neurosci 2019;13. https://doi.org/10.3389/fnins.2018.01019.

[23] He Q, Liu J, Liang J, Liu X, Li W, Liu Z, et al. Towards Improvements for Penetrating the Blood–Brain Barrier—Recent Progress from a Material and Pharmaceutical Perspective. Cells 2018;7:24. https://doi.org/10.3390/cells7040024.

[24] Sanità G, Carrese B, Lamberti A. Nanoparticle Surface Functionalization: How to Improve Biocompatibility and Cellular Internalization. Front Mol Biosci 2020;7:381. https://doi.org/10.3389/FMOLB.2020.587012/BIBTEX.

[25] Khan MM, Madni A, Filipczak N, Pan J, Rehman M, Rai N, et al. Folate targeted lipid chitosan hybrid nanoparticles for enhanced anti-tumor efficacy. Nanomedicine Nanotechnology, Biol Med 2020;28:102228. https://doi.org/10.1016/j.nano.2020.102228.

[26] Xu X, Li J, Han S, Tao C, Fang L, Sun Y, et al. A novel doxorubicin loaded folic acid conjugated

PAMAM modified with borneol, a nature dual-functional product of reducing PAMAM toxicity and boosting BBB penetration. Eur J Pharm Sci 2016;88:178–90. https://doi.org/10.1016/j.ejps.2016.02.015.

[27] González-Alvarez I, Vivancos V, Coll C, Sánchez-Dengra B, Aznar E, Ruiz-Picazo A, et al. pH-Dependent Molecular Gate Mesoporous Microparticles for Biological Control of Giardia intestinalis. Pharmaceutics 2021;13:94. https://doi.org/10.3390/pharmaceutics13010094.

[28] Shinde P, Prasad BL V. Amphifunctional Mesoporous Silica Nanoparticles with "Molecular Gates" for Controlled Drug Uptake and Release. Part Part Syst Charact 2021;38:2100185. https://doi.org/10.1002/ppsc.202100185.

[29] Saraiva C, Praça C, Ferreira R, Santos T, Ferreira L, Bernardino L. Nanoparticle-mediated brain drug delivery: Overcoming blood-brain barrier to treat neurodegenerative diseases. J Control Release 2016;235:34–47. https://doi.org/10.1016/j.jconrel.2016.05.044.

[30] Heggannavar GB, Hiremath CG, Achari DD, Pangarkar VG, Kariduraganavar MY. Development of Doxorubicin-Loaded Magnetic Silica-Pluronic F-127 Nanocarriers Conjugated with Transferrin for Treating Glioblastoma across the Blood-Brain Barrier Using an in Vitro Model. ACS Omega 2018;3:8017–26. https://doi.org/10.1021/acsomega.8b00152.

[31] Baghirov H, Karaman D, Viitala T, Duchanoy A, Lou Y-R, Mamaeva V, et al. Feasibility Study of the Permeability and Uptake of Mesoporous Silica Nanoparticles across the Blood-Brain Barrier. PLoS One 2016;11:e0160705. https://doi.org/10.1371/journal.pone.0160705.

[32] Ku S, Yan F, Wang Y, Sun Y, Yang N, Ye L. The blood–brain barrier penetration and distribution of PEGylated fluorescein-doped magnetic silica nanoparticles in rat brain. Biochem Biophys Res Commun 2010;394:871–6. https://doi.org/10.1016/j.bbrc.2010.03.006.

[33] Mo J, He L, Ma B, Chen T. Tailoring Particle Size of Mesoporous Silica Nanosystem to Antagonize Glioblastoma and Overcome Blood-Brain Barrier. ACS Appl Mater Interfaces 2016;8:6811–25. https://doi.org/10.1021/ACSAMI.5B11730/SUPPL_FILE/AM5B11730_SI_001.PDF.

[34] Sánchez-Cabezas S. Development of a reproducible and optimized synthetic protocol for the preparation of monodisperse core-shell-type magnetic mesoporous silica nanoparticles. Universidad Politécnica de Valencia, 2019.

[35] Sousa F, Dhaliwal HK, Gattacceca F, Sarmento B, Amiji MM. Enhanced anti-angiogenic effects of bevacizumab in glioblastoma treatment upon intranasal administration in polymeric nanoparticles. J Control Release 2019;309:37–47. https://doi.org/10.1016/j.jconrel.2019.07.033.

[36] Thommes M, Kaneko K, Neimark A V., Olivier JP, Rodriguez-Reinoso F, Rouquerol J, et al. Physisorption of gases, with special reference to the evaluation of surface area and pore size distribution (IUPAC Technical Report). Pure Appl Chem 2015;87:1051–69. https://doi.org/10.1515/PAC-2014-1117/PDF.

[37] Kong L, Zhang J, Zhou Q, Fang Z, Wang Y, Gao G, et al. The effects of ponatinib, a multi-targeted tyrosine kinase inhibitor, against human U87 malignant glioblastoma cells. Onco Targets Ther 2014;7:2013. https://doi.org/10.2147/OTT.S67556.

[38] Saunders NR, Dreifuss J-J, Dziegielewska KM, Johansson PA, Habgood MD, MÃ¸llgÃ¥rd K, et al. The rights and wrongs of blood-brain barrier permeability studies: a walk through 100 years of history. Front Neurosci 2014;8. https://doi.org/10.3389/fnins.2014.00404.

[39] Kwok AKH. Effects of trypan blue on cell viability and gene expression in human retinal pigment epithelial cells. Br J Ophthalmol 2004;88:1590–4. https://doi.org/10.1136/bjo.2004.044537.

[40] Awad D, Schrader I, Bartok M, Mohr A, Gabel D. Comparative Toxicology of Trypan Blue, Brilliant Blue G, and Their Combination Together with Polyethylene Glycol on Human Pigment Epithelial Cells. Investig Opthalmology Vis Sci 2011;52:4085. https://doi.org/10.1167/iovs.10-6336.

[41] Chemometec. Why Trypan Blue is Not a Good Idea And How It Effects Your Cell Counting n.d. https://chemometec.com/resources/mini-reviews/why-working-with-trypan-blue-is-not-a-good-idea/ (accessed December 31, 2021).

[42] Yang B, Lu Y, Du SY, Li PY, Zhang Y. Influences of molecular weight and particle size to intranasal drug delivery based on cell model of “nose-brain.” Chinese Tradit Herb Drugs 2020;51:5748–53. https://doi.org/10.7501/J.ISSN.0253-2670.2020.22.011.

AGRADECIMIENTOS - ACKNOWLEDGEMENTS

AGRADECIMIENTOS - ACKNOWLEDGEMENTS

Lo alcancé, el último apartado de la tesis, y parecía que nunca llegaría. No obstante, si eres como yo, puede que éste sea el primer apartado que consultes, ansioso por encontrar tu nombre o, simplemente, por conocer qué personas tienen un huequito en mi corazón y han contribuido de alguna manera a que ahora este libro esté entre tus manos. Pues bien, lo primero que voy a hacer es pedirte disculpas y darte las gracias, no sea que cuando termines de leer estos agradecimientos no encuentres tu nombre, ten claro que, si en estos cuatro años y cuarto te has cruzado en mi camino, aún si no encuentras tu nombre en estos agradecimientos, también formas parte de mi historia. Dicho esto, empiezo a agradecer de forma algo más concreta:

Gracias a mis directoras, Marival y Marta.

Marival, gracias por rodearme y guiarme con tu sabiduría, gracias por tu confianza y porque, gracias a ti, le he cogido el gusto a eso de sentarme delante del ordenador, a "hacer un piensing" (reflexionar sobre una cuestión, aclaración para aquellos que no estén familiarizados con el término), a modelar, a pelearme con los datos y, finalmente, disfrutar cuando la línea pasa por donde toca.

Marta, gracias por haberte fijado en mí en las clases de Galénica I y haberme escrito aquel email, allá por septiembre 2015, invitándome a hacer prácticas en vuestro laboratorio cuando aún era una estudiante de grado en 4º de Farmacia. Me abriste las puertas de un mundo fascinante.

Gracias a mi no-directora y tutora, Isabel (Isa). Gracias por las horas y horas en el laboratorio, por ayudarme a ganar más de mil batallas contra el HPLC, incluso aquellas que se libraban a horas intempestivas cuando ya hacía mucho que el sol se había ido y la luna era la que reinaba, por organizarte para acompañarme en los ensayos con células y con ratas y por cogerme el teléfono siempre que lo necesitaba, aunque tú estuvieses de vacaciones y yo de estancia. ¡Has sido una no-directora de 10!

Gracias a mi doctorando mayor por excelencia, Alejandro (Ale). Hemos pasado varios meses de mi tesis cruzando nuestros caminos, cuando uno venía el otro se iba, pero has sido un gran compañero de viaje. Primero, guiándome en los trámites del programa de doctorado y yendo juntos a seminarios y seguimientos, luego, compartiendo horas y risas en el laboratorio y, siempre, ayudándome en todo lo que necesitaba, especialmente, si había ratas de por medio.

Gracias al resto de doctorandos mayores que dejaron huella en mi camino, Isabel Lozoya y Mayte, que terminaban cuando empecé a hacer prácticas en el laboratorio, Nacho, con el que me inicié en R y, gracias a él, tengo unos gráficos preciosos en la tesis y José Manuel, cuya tesis me ha servido de modelo estético y de formato en la redacción de este libro.

Gracias a mis doctorandos pequeños, César, Alex e Irene, que, aunque llegaron al laboratorio en 2021, ya he compartido con ellos grandes momentos y no dudaron en colaborar en los últimos experimentos de mi tesis. Os deseo lo mejor, disfrutad mucho de esta etapa de vuestra vida que ahora comenzáis.

Gracias a todos y todas las TFGs y TFMs con los que he coincidido en el laboratorio y a todos los investigadores e investigadoras que nos han visitado durante estos años. No pongo todos los nombres porque seguro que me dejaba a alguien, pero todos habéis contribuido a hacer este camino más ameno.

Gracias a Emilio, por cuidar los detalles, tener todo listo y acompañarme en las primeras sesiones de prácticas que tuve que dar a los alumnos de Farmacia.

Gracias a Rebeca, la mejor limpiadora de la UMH, por siempre tener el laboratorio reluciente y una gran sonrisa de oreja a oreja que da ánimos cuando llegas al laboratorio de buena mañana.

Thank you very much to Professor Bruno Sarmento, from the University of Porto, where I spent 3 months of my thesis. Thank you, specially, to Flávia Sousa, who guided me there and to all the members of the Nanomedicines and Translational Drug Delivery research group (Ana Rita, Cláudia A, Cláudia M, Helena, Joana G, Joana M, Soraia, Vanessa and a long etc.) who made my time there really pleasant.

Gracias al profesor Ramón Martínez Máñez, de la Universidad Politécnica de Valencia, por acogerme en su grupo de investigación para hacer otra de las estancias de mi tesis. En este grupo conocí a otro montón de gente que hizo que, aunque tuve que alargar mi tiempo allí y hacer la estancia en dos tandas por culpa de la pandemia, ésta fuese muy agradable. Gracias por todo a Alejandra, Andrea B, Andrea E, Angy, Bea, Blanca, Elena, Elisa (aunque a Elisa la conocí cuando visitó nuestro laboratorio no en la UPV), Eva, Gonçalo (que también estaba de visita como yo), Paula, Serena y todos los demás, y, sobre todo, gracias a María, mi guía en el mundo de las nanopartículas mesoporosas durante esos meses.

Gracias a mis compañeras y amigas de la carrera, Sandra, Belén, Anca y Mayte. Nosotras somos el "Top Five" y con vosotras empezó todo, disfrutando de las sesiones de prácticas de la carrera. Gracias por darme ánimo y mostrar vuestro interés en mis proyectos durante este tiempo.

Acabo dando las gracias a las personas que más quiero, gracias a mi familia por aguantar mis nervios, compartir mis alegrías cuando los experimentos iban como tocaba y animarme cuando lo he necesitado. Gracias papá por ayudarme a rotular cuando los eppendorfs me salían por las orejas. Gracias mamá por acompañarme al laboratorio si tenía que ir a alguna hora poco convencional, horas de esas en las que llamaba a Isabel para que me ayudase con el HPLC. Gracias José María por venirte al laboratorio alguna que otra vez a hacerme compañía y echarme una mano. Gracias Alejandro (no confundir con los mencionados previamente), has llegado a mi vida en la fase final de mi tesis como un chute de energía. Gracias por quererme, por tu comprensión y por tus ánimos.

Gracias a todos, ¡os quiero mucho!